UNIVERSITY OF CALIFORNIA SAN DIEGO

Taming Carbene Copper(I)-Hydride Complexes

A dissertation submitted in partial satisfaction of the requirements for the degree of Doctor of Philosophy

in

Chemistry

by

Erik Anthony Romero

Committee in charge:

Professor Guy Bertrand, Chair
Professor Adah Almutairi
Professor Joshua Figueroa
Professor Arnold Rheingold
Professor Emmanuel Theodorakis

2018

The Dissertation of Erik Anthony Romero is approved, and it is acceptable in quality and form for publication on microfilm and electronically:

_____

_____

_____

_____

_____

Chair

University of California San Diego

2018

DEDICATION

This dissertation is dedicated to the three heroes of my life: my grandfather, José Campa Hernandez; my grandmother, Delia Vargas Hernandez; and my mother, Noemi Hernandez Chavez. To my grandparents, you looked after my brother and I as we grew up and showed us through action what it meant to be hard-working, trustworthy, and responsible adults. To my mother, words cannot describe the innumerable valuable lessons I learned from you throughout my life, but the most important of these are resilience and faith because without them, completion of this degree would be impossible.

TABLE OF CONTENTS

LIST OF ABBREVIATIONS

9-BBN: 9-borabicyclononane
AAC: azide-alkyne cycloaddition
Ar: aryl
BCF: trispentafluorophenylborane
Bn: benzyl
CAAC: cyclic (alkyl)(amino) carbene
cLP: classical Lewis pair
DBU: 1,8-Diazabicyclo[5.4.0]undec-7-ene
DFT: density functional theory
DCM: dichloromethane
DHBTA: dehydrogenative borylation of terminal alkynes
Dipp: 2,6-diisopropylphenyl
DPPP: diphenylphosphinopropane
DPPBZ: 1,2-bis(diphenylphosphino)benzene
DTBM-Segphos: (S)-(+)-5,5′-Bis[di(3,5-di-tert-butyl-4-methoxyphenyl)phosphino]-4,4′-bi-1,3-benzodioxole
Et: ethyl
FLP: frustrated Lewis pair
HBDan: 1,8-naphthalenediaminatoborane
HBPin: pinacolborane
***i*Pr:** isopropyl
IPr*: 1,3-bis(2,6-bis(diphenylmethyl)-4-methylphenyl)-imidazol-2-ylidene
IPr:** 1,3-bis[2,6-bis[di(4-tert-butylphenyl)methyl]-4-methylphenyl]imidazol-2-ylidene
KHMDS: potassium bis(trimethylsilyl)amide
KO*t*Bu: potassium tert-butoxide
LUT: 2,6-lutidine
Me: methyl
Mes: 2,4,6-trimethylphenyl
NaOH: sodium hydroxide
NEt_3: triethylamine
NHC: *N*-heterocyclic carbene
NMR: nuclear magnetic resonance
OPh: phenoxide
OTf: trifluoromethanesulfonate
Ph: phenyl
PhOH: phenol
PMHS: polymethylhydrosiloxane
PMP: pentamethylpiperidine
***t*Bu:** tert-butyl
TBD: 1,5,7-triazabicyclo[4.4.0]dec-5-ene
THF: tetrahydrofuran
TON: turnover number
Triphos: 1,1,1-tris(diphenylphosphinomethyl)ethane
Triflate: trifluoromethanesulfonate

LIST OF FIGURES

LIST OF SCHEMES

LIST OF TABLES

ACKNOWLEDGEMENTS

I would like to start out by acknowledging the time and effort put forth by my doctoral committee members: Prof. Arnold L. Rheingold, Prof. Joshua S. Figueroa, Prof. Emmanuel Theodorakis, and Prof. Adah Almutairi, for reading and commenting on this dissertation.

My greatest acknowledgement is to my advisor, Prof. Guy Bertrand for giving me a chance to be part of your research group. For the past four years, you have allowed me to follow my interests wherever they chose to take me, and you were always willing to show me how to refine my project ideas to make them the best they could be. I am most grateful for the time we would spend together discussing potential mechanisms and how we could best write our papers. Even though we didn't always see eye to eye about how to accomplish this task, you would take the time to hear me out, even when I was dead wrong. It was in these moments that I learned the most about how to develop a logical story and tell it in the most concise way possible. With the other graduate students in the lab, we would call this "Guy-ifying" a paper, and this is a skill that I will continue to refine throughout my time in chemistry. I also want to express my gratitude for your help in securing my future at UC Berkeley. I could not have gotten this postdoctoral position without your help. I am forever grateful to you, Guy.

My next biggest acknowledgement is to the guy with the shiniest head and cheesiest smile in the entire Chemistry and Biochemistry department, and maybe even San Diego, Dr. Rodolphe "Rudy" Jazzar. My friend, there is just too much to say for this one paragraph, but suffice it to say that without your help, I would not be where I am today. You came to San Diego during the middle of my first year as a Ph.D. student and we clicked immediately. I found out very quickly that we share the same outlook on life and family, the same sense of humor, and the same love of chemistry. During my time in the lab, I am grateful for the hours we would spend at the whiteboard

or at your desk combing through literature, compiling data, or writing a slew of different mechanisms for the sole purpose of being ready to discuss chemistry with Guy. You walked me through the ins and outs of writing publications and helped me when I started writing more complicated grant proposals. More than this though, you helped lighten the mood around the lab and provided so many laughs through your crazy stories and jokes. Along this line, I will also miss the hours that we would spend poking fun at the crazy vegan guy and making arguments with him just so see "El Professor" in action. Thank you, Rudy for all your guidance and for just being one hell of a friend. I look forward to the day that we can work together again.

I want to next give thanks to Mohand "Mo" Melaimi who taught me the fundamentals of handling air and moisture sensitive compounds. It was you that first showed me how to make CAAC, which essentially allowed me to handle most anything I would encounter in the Bertrand lab. Thanks for always being willing to help me when I had a question about literature precedent or something we had done previously in the group.

Thank you to Michele Soleilhavoup, who is the third and final CNRS member I had to pleasure to work around during my Ph.D. Thank you for all the time and energy you spent ordering chemicals and consumables to keep the lab running. It definitely did not go unnoticed! I am glad that we got to publish our work on the copper hydride together, and it is one of my favorite papers from my time in graduate school.

Transferring from UC Riverside to UC San Diego for graduate school came with a great slew of challenges but having good friends by your side can make any life changing event bearable. Pauline Olsen made this transition with me in 2014 after having known each other for a few years leading up to this point. In all these years together, we have had so many good times that I've lost count. I am thankful that we got to know each other even better over the past four years at UCSD

when we would go for our coffee walks and talk about life, love, and our respective pursuits of happiness. It seems that no matter how long we hang out or what we do, there is never a dull moment between us. I know that when I see you again down the road, we will just pick up where we left off as if no time had passed. Thanks for always being there for me, and for this, I will always consider you one of my dearest friends.

Being part of this wonderful group has allowed me to meet so many people from around the US and the world. Best wishes go out to all those awesome people I had the opportunity to meet: Adam, Bastien, Connor, Cory, Daniel "Jimmy", Delphine, Domenik "Baby Dom", Dominik "Big Dom", Desirée, Eder, Fatme, Janell, Jiaxiang, Lilja, Liqun, Liu, Luana, Mael, Max, Mazyar, Melinda, Ryo, Sebastian, Sima, Victor, and Xingbang.

Before I joined the lab, I was put into contact with David Ruiz, a graduate student in the lab at the time of my arrival. Once I entered the group, you were one of the few senior members of the lab with whom I felt comfortable talking about experiments, ideas, or San Diego life in general. You definitely made the transition into graduate school, and the Bertrand group, much easier. Outside of lab, we hung out and enjoyed the SD life by watching WWE and eating good food, which are still two things we do to this day. I wish you all the best in life and thank you for being a good friend.

The next person who had a profound impact on my time in San Diego was Jesse "El Professor" Peltier. Once you moved into my lab room, the volume level increased dramatically and never went down again, except when you were on holiday. I have thoroughly enjoyed all the conversations, laughs, and the lectures you would provide. For example, you just recently taught us that we are 25% more likely to have a heart attack after daylight savings time. I thoroughly enjoyed all the times we hung out outside of lab because you always brought with you a heaping

helping of mirth. Throughout the past 4 years, I would say that you have become one of my good friends, and I hope that we get to see each other down the road.

Glen Junor first came to the lab as a visiting student during the summer following my 2nd year in graduate school, and then joined the lab as a Ph.D. student during my final year. During this time, I got to know you very well and even had the pleasure of working directly with you for the better part of this year. I learned a lot about your life and your family, and I can say that your experiences have truly inspired me. I know that you are just beginning your time at UCSD, but I have known since I first met you that one day, you will be a successful graduate student, scientist, and human being. Keep up the excellent work and I wish you the best of luck for your future.

Xi Chen joined the group as an undergraduate researcher after taking a laboratory course with Glen, and since your arrival, I am convinced that you will be a superstar one day. There are very few undergraduate students who have the work ethic to rival graduate students, but you are one of them. More than that, you are an amazing person with a great personality that I thoroughly enjoyed being around. Thank you for putting up with our shenanigans and even participating in them a little bit. I hope that one day, we can see each other again, but until then, keep working hard and make a name for yourself.

François "Franzy V." Vermersch arrived from France in the summer of 2017 and we hit it off immediately. Upon your arrival to the lab, we started playing sport, and it was the best because I was still able to beat you, but alas, this didn't continue and now I can't win anymore haha. Thanks for always having a big smile on your face and lifting the mood in the lab, I really appreciate it. Keep working hard in lab. That being said, I know that you're already taking full advantage of that San Diego sunshine, mec. Tu seras toujours un très bon ami pour moi.

Next is Vianney Regnier. I first met Vianney during his 3-month trip to San Diego from Grenoble, France. You handled San Diego very well during your time here and were always down to hang out and enjoy the California lifestyle. We hung out quite a few times, and I got to know you well, and that makes me happy. Thank you so much for looking after me during my trip to France where I knew no one and was freaking out the whole flight over. I wrote this paragraph here in the office at the Université Grenoble-Alpes and you have walked by me a couple of times with no clue that I'm writing about you. You will see this eventually haha. Thanks for everything my bro, and I know that one day we will see each other again. If you ever come back to California, give me a call and I will meet you for a beer!

I never got to meet Dr. David Martin while he was a CNRS member in Guy's lab at San Diego, but I got to come to your home country and work in your lab for 3-months during the end of my Ph.D. I learned so much about electrochemistry and I expect to use this knowledge a lot during my independent research career (maybe we can collaborate at some point, too). That was a once in a lifetime experience, and I thank you so much for making it all happen. Thank you for hosting me for dinner at your home and introducing me to your beautiful family. I know that you will continue to be a successful researcher, and I hope that we can see each other again.

I want to thank my family for all the support they have given me during my undergraduate and graduate education. I could not have done it without you. I want to give an extra special thank you to David and Tina Hernandez as well as Armando Chavez for hosting me at your homes for various portions of my college years. It was nice having people I loved around during these first difficult years.

Finally, I want to thank my girlfriend, Kristen "Kai-Ting" Wang. We first became acquainted in September of 2014, which was my first official day as a Ph.D. student, and the first

day of instruction for Chem 143C. Although nothing would happen between us for another 2 years, I still remember your smile and overall joy from those early days. Over the next two years, I would see you around campus on occasion, and each time you would call out to me with a big wave and an even bigger smile on your face. Those moments meant so much to me during one of the most difficult times of my life and imparted upon me a connection to you that began with a simple smile. Fast forward to July of 2016, I had not seen you for many months, but we fatefully met up on the UCSD Mesa shuttle two days in a row, because one day simply wasn't enough time for me to get enough courage to ask you on a date. Excitingly you agreed, and three dates later on 20 July 2016 at 20h23, you agreed to be my girlfriend. Over the next two years, we went through so much together that it is impossible to talk about it all here. I want you to know that every moment we are together is the happiest moment of my life.

During the final two years of my Ph.D. you saw all the stress that I dealt with as well as the breakdowns that accompanied it, and you were always there. I am forever appreciative to you for that. Going through something as difficult as a Ph.D. was a lot easier once I had someone with whom to talk to about it. From our time together during the past few years, I know that you will always be there for me when I need you most, and I hope that I can return this support to you. I can honestly say that I never imagined someone could mean as much to me as you do, and for this reason, I want to close out my time in graduate school, by posing just one question to you. Kristen Wang, after sticking with me for the past two years, would you do me the great honor of sticking with me for the rest of my life, as my wife? Yes ☐ No ☐

Chapter 1 has been adapted from materials published in Romero, E. A.; Jazzar, R.; Bertrand, G., "Copper-Catalyzed Dehydrogenative Borylation of Terminal Alkynes with Pinacolborane", *Chem. Sci.* **2017**, *8*, 165 – 168 and Romero, E. A.; Jazzar, R.; Bertrand, G.,

"(CAAC)CuX-catalyzed hydroboration of terminal alkynes with pinacolborane directed by the x-ligand", *J. Organomet. Chem.* **2017**, *829*, 11 – 13. The dissertation author was the primary investigator of these publications.

Chapter 2 has been adapted from materials published in Romero, E. A.; Olsen, P. M.; Jazzar, R.; Soleilhavoup, M.; Gembicky, M.; Bertrand, G., "Spectroscopic Evidence for a Monomeric Copper(I) Hydride and Crystallographic Characterization of a Monomeric Silver(I) Hydride", *Angew. Chem. Int. Ed.* **2017**, *56*, 4024 – 4027 and Romero, E. A.; Zhao, T.; Nakano, R.; Hu, X.; Wu, Y.; Jazzar, R.; Bertrand, G., "Tandem Copper Hydride - Lewis Pair Catalyzed Reduction of Carbon Dioxide into Formate with Dihydrogen" *Nature Catalysis* **2018**, *1*, 743 – 747. The dissertation author was the primary investigator of the former publication and co-primary investigator of the latter publication.

Chapter 3 has been adapted from materials published in Romero, E. A.; Peltier, J. L.; Jazzar, R.; Bertrand, G., "Catalyst-Free Dehydrocoupling of Amines, Alcohols, and Thiols with Pinacol Borane and 9-Borabicyclononane (9-BBN)", *Chem. Commun.* **2016**, *52*, 165 – 168. The dissertation author was the primary investigator of this publication.

VITA

Education

Ph.D. in Chemistry	**2016 – 2018**
University of California San Diego (Prof. Guy Bertrand)	
M.S. in Chemistry	**2014 – 2016**
University of California San Diego (Prof. Guy Bertrand)	
B.S. in Chemistry with Honors	**2010 – 2014**
University of California Riverside	

Publications

1) Romero, E. A.; Zhao, T.; Nakano, R.; Hu, X.; Wu, Y.; Jazzar, R.; Bertrand, G., "Tandem Copper Hydride - Lewis Pair Catalyzed Reduction of Carbon Dioxide into Formate with Dihydrogen" *Nature Catalysis* **2018**, *1*, 743 – 747.
2) Mahoney, J. K.; Regnier, V.; Romero, E. A.; Molton, F.; Royal, G.; Jazzar, R.; Martin, D.; Bertrand, G., "The Serendipitous Discovery of a Readily Available Redox-Bistable Molecule Derived from Cyclic(alkyl)(amino)carbenes", *Org. Chem. Front.* **2018**, *5*, 2073 – 2078.
3) Romero, E. A.; Olsen, P. M.; Jazzar, R.; Soleilhavoup, M.; Gembicky, M.; Bertrand, G., "Spectroscopic Evidence for a Monomeric Copper(I) Hydride and Crystallographic Characterization of a Monomeric Silver(I) Hydride", *Angew. Chem. Int. Ed.* **2017**, *56*, 4024 – 4027.
4) Romero, E. A.; Jazzar, R.; Bertrand, G., "(CAAC)CuX-catalyzed hydroboration of terminal alkynes with pinacolborane directed by the x-ligand", *J. Organomet. Chem.* **2017**, *829*, 11 – 13.
5) Romero, E. A.; Jazzar, R.; Bertrand, G., "Copper-Catalyzed Dehydrogenative Borylation of Terminal Alkynes with Pinacolborane", *Chem. Sci.* **2017**, *8*, 165 – 168.
6) Romero, E. A.; Peltier, J. L.; Jazzar, R.; Bertrand, G., "Catalyst-Free Dehydrocoupling of Amines, Alcohols, and Thiols with Pinacol Borane and 9-Borabicyclononane (9-BBN)", *Chem. Commun.* **2016**, *52*, 165 – 168.
7) Jin, L.; Romero, E. A.; Melaimi, M.; Bertrand, G., "The Janus Face of the X Ligand in the Copper Catalyzed Azide Alkyne Cycloaddition", *J. Am. Chem. Soc.* **2015**, *137*, 15696 – 15698.

Presentations

1) Romero, E. A.; Olsen, P. M.; Jazzar, R.; Soleilhavoup, M.; Gembicky, M.; Bertrand, G., "Characterization of monomeric copper(I) and silver(I) hydrides", 256th National ACS Meeting, Boston, MA, August 2018, Oral Presentation.

2) Romero, E. A.; Jazzar, R.; Bertrand, G., "Cyclic (alkyl) (amino) carbene copper (I) catalyzed dehydrogenative borylation and β-hydroboration of terminal alkynes", 251st National ACS Meeting, San Diego, CA, March 2016, Oral Presentation.
3) Romero, E. A.; Jazzar, R.; Bertrand, G., "Cyclic (alkyl) (amino) carbene copper (I) catalyzed dehydrogenative borylation and β-hydroboration of terminal alkynes", University of California Symposium for Chemical Sciences, Lake Arrowhead, CA, March 2016, Oral Presentation.

Positions Held

1)	Visiting Research Scholar (Univ. of Grenoble-Alpes, France)	04/2018 – 07/2018
2)	Graduate Researcher (Univ. of Calif. San Diego)	09/2014 – 09/2018
3)	Graduate Teaching Assistant (Univ. of Calif. San Diego)	09/2014 – 06/2016
4)	Guest Researcher, Los Alamos National Laboratory (LANSCE)	07/2013 – 09/2013
5)	Undergraduate Researcher (Univ. of Calif., Riverside)	01/2012 – 06/2014

Technical Capabilities

1) Expert at synthesizing and handling air and moisture sensitive compounds using traditional Schlenk and drybox techniques.
2) Operation of both analytical and spectroscopic instruments, including multinuclear NMR (^{1}H, ^{13}C, ^{11}B, ^{19}F, ^{31}P), MS, IR, GC and a basic-intermediate understanding of Gaussian 09.
3) Expert in X-ray crystallographic analysis, which includes mounting and setting up data collections, structure refinements, detwinning, and modelling of positional disorder.

Honors and Awards

1) **ACS Division of Inorganic Chemistry Travel Grant**: A monetary award given to graduate students presenting their independent research at ACS national meetings. This award was comprised of a $450 cash prize to facilitate my travel to Boston, MA in FA '18.
2) **Graduate Assistance in Areas of National Need (GAANN) Fellow (Univ. of Calif. San Diego)**: A fellowship awarded to exceptional students in fields determined by the U.S. government as high need areas. The goal of this grant is to provide rigorous research and teaching experiences to students in preparation to assume post-graduate leadership roles in chemical research and education. This fellowship was comprised of an annual stipend of $29,000 as well as an additional $1,000 in travel and research support funds.
3) **2014 ACS Undergraduate Award in Inorganic Chemistry (Univ. of Calif. Riverside)**: Each ACS Certified Department nominates one student for this award. The student nominee will have demonstrated excellence in inorganic chemistry at the undergraduate level based on any combination of research, coursework, motivation, interest, and/or

dedication as defined by their nominating institution. The student is also expected to have future plans that involve a career in chemistry.

4) **Maximizing Access to Research Careers (MARC-U*) Fellow (Univ. of Calif. Riverside)**: A program that recognizes the exceptional abilities of undergraduate students in the sciences who wished to obtain Ph.D. degrees following graduation. This fellowship was comprised of an annual stipend of $12,000 as well as an additional $1,000 in travel and research support funds.
5) **University Honors program (Univ. of Calif. Riverside)**: Through rigorous coursework and extracurricular developmental activities, students are prepared for a future as leaders in their respective fields. As part of the program, all students are required to develop and write a capstone thesis project, which is housed in the University library post-graduation.

ABSTRACT OF THE DISSERTATION

Taming Carbene Copper(I)-Hydride Complexes

by

Erik Anthony Romero

Doctor of Philosophy in Chemistry

University of California San Diego, 2018

Professor Guy Bertrand, Chair

Although initially reported in 1844, copper(I)-hydrides were not widely studied until the isolation of "Stryker's reagent" in 1971. Following this development, researchers reported a myriad of chemical transformations employing other transient copper-hydride complexes as highly stereo-, regio-, and enantioselective catalysts. Each of these processes, however, rely on the ability of Cu-H bonds to insert into substrate π-bonds. By focusing on reactions involving this mechanistic step, chemists have limited the potential applications of copper-hydrides to reactions within this niche.

The first part of this manuscript discusses the ability of CAAC copper complexes to affect dehydrogenative borylation reactions of terminal acetylenes under mild conditions. Moreover,

during this study, we uncovered convincing evidence that points to the surprising involvement of a copper-hydride complex in the key dihydrogen extrusion step of the mechanistic cycle. We further show that more basic anions on copper switch the selectivity of the catalyst to favor formation of traditional anti-Markovnikov hydroboration products. Lastly, the active catalysts for both reactions were shown to tolerate a wide range of synthetically useful functional groups.

The second part of this manuscript describes our attempts to utilize extremely sterically encumbering NHC ligands to stabilize and characterize the first monomeric, monoligated copper(I)-hydride complex. Although this species exists as a dimer in the solid state, we confirmed the presence of an equilibrium in solution through variable temperature ^{1}H NMR experiments and extracted the kinetic and thermodynamic parameters for this dimerization process. We then applied our synthetic strategy to the isolation and crystallographic characterization of the first neutral monoligated silver(I)-hydride. Preliminary experiments indicate that its reactivity mirrors that of copper-hydrides as opposed to gold-hydrides. Refocusing on copper, we employed borane stabilized copper-hydride complexes as benchtop stable surrogates for their highly reactive LCu-H counterparts in the hydrogenation of CO_2 with H_2. Excitingly, we found that this process is enhanced by an *in situ* generated amino-borane co-catalyst, thereby affording a rare example of tandem catalysis involving both a transition-metal complex and a classical Lewis pair.

The final chapter discusses the uncatalyzed dehydrogenative coupling of alcohols, amines and thiols with pinacolborane and 9-borabicyclononane, a result which contrasts with literature precedent.

Chapter 0 : General Introduction

As scientists, we are trained to utilize previously established chemical concepts to formulate innovative hypotheses in an effort to further advance the limits of the current understanding of a field. This idea is well-exemplified by the research conducted over the past 150 years on the determination of the molecular structure and fundamental reactivity of copper(I)-hydrides. The first reported preparation of this fragment was in 1844 by the French chemist Adolphe Wurtz through the reaction of copper-sulfate with hypophosphorous acid (H_3PO_2).[1] Their potential, however, wasn't fully realized until the late 1980's when Stryker and coworkers employed the triphenylphosphine ligated Cu-H hexamer in conjugate addition reactions with α,β-unsaturated carbonyl compounds (Scheme 0.1).[2] Although first developed by Osborn *et al.*[3] in 1971, this reagent is commonly referred to as "Stryker's reagent" due to these early stoichiometric studies. It wasn't until 1998, however, that Lipshutz *et al.* discovered its ability to function selectively under catalytic conditions when in the presence of lithium chloride and phenylsilane.[4]

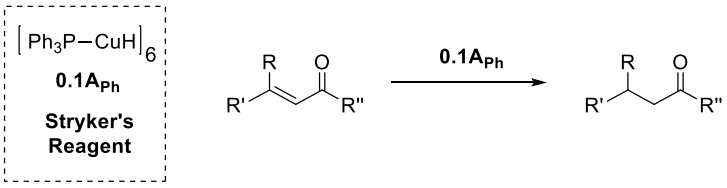

Scheme 0.1. General reaction for the conjugate addition reaction of α,β-unsaturated carbonyl compounds developed by Stryker and coworkers.

Since these pioneering works, many groups around the world have contributed to elucidating the reactivity of ligated copper-hydride complexes. Aside from generalizing this reaction to more synthetically useful substrates and enantioselective variants,[5,6] researchers also explored other novel transformations. To date, copper-hydride complexes have found applications in carbonyl reductions **A**,[7] alkene **B**[8] and alkyne **C**[9] hydrofunctionalization, alkyne semihydrogenation **D**,[10] alkyl-iodide/triflate reduction **E**,[11] CO_2 reduction **F**,[12] and others (Figure 0.1).

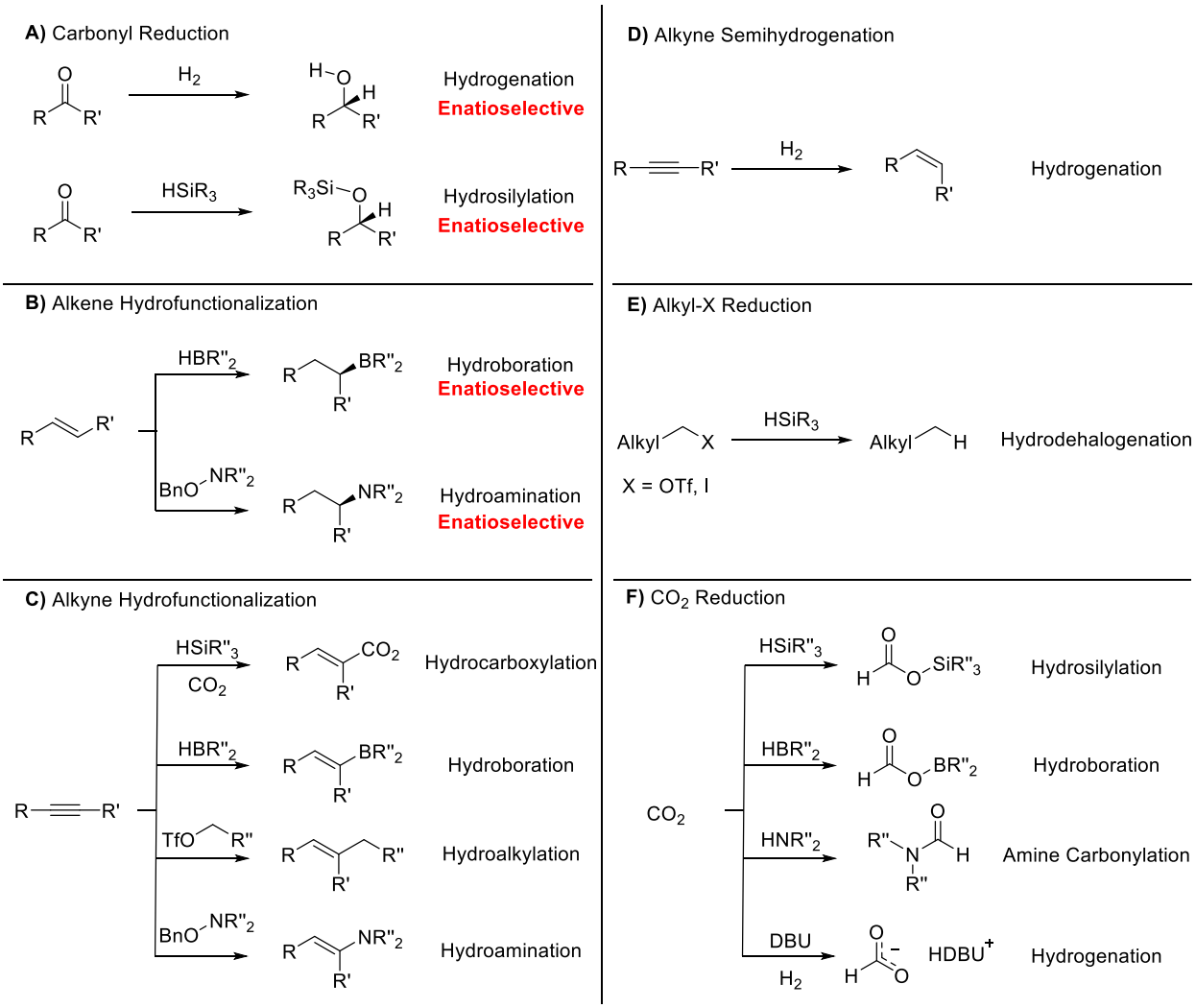

Figure 0.1. Selected subset of reactions known to involve copper-hydride complexes. This does not constitute an all-inclusive list.

For each of the reactions listed, the catalyst precursors were subjected to reaction conditions tailormade to generate copper-hydrides *in-situ*. For this reason, it is unsurprising that an (L_n)Cu-H species was involved in the catalytic mechanisms proposed by the researchers. Exploiting this method of *in-situ* Cu-H generation and reactivity has allowed researchers to make incredible strides in elucidating the fundamental reactivity of copper-hydride complexes; however, this way of thinking has ultimately limited their potential applications for catalytic transformations lying outside of this niche.

The first chapter of this dissertation details a novel copper-catalyzed C-H borylation reaction that proceeds under conditions that would not be expected to generate a copper-hydride. Interestingly our investigation into the mechanism uncovered convincing evidence pointing to the key involvement of this species lying along the preferred mechanistic pathway. Furthermore, this study brought an important question to my mind regarding this elusive species: why does the isolation and characterization of a monomeric monoligated copper-hydride (*e.g.* LCu-H) remain unaccomplished considering the major technological advancements of the past 150 years? Its isolation would allow chemists to further probe the fundamental reactivity of the Cu-H bond to apply it in reactions that scientists may have discounted due to the lack of reactivity of higher order oligomers.

Chapter 2 describes my attempts to build upon previously reported knowledge of copper-hydride dimerization in the hopes of isolating a discrete monomeric complex Following the seminal work of Osborn *et al.*[3] in 1971 and Caulton *et al.*[13] in 1981, chemists began using polydentate ligand scaffolds, presumably because they assumed that a greater degree of ligand coordination (*e.g.* L_nCu-H) would induce fragmentation of higher order copper-hydride aggregates to smaller cluster sizes. These studies employed ligands such as dppp,[14] triphos,[15] DTBM-Segphos,[16] and dppbz[17] and found that in at least several cases, this assumption was correct (Figure 0.2). Moreover, it was surprising that the hydride signal appeared in the *positive region of the ^{1}H NMR spectrum between δ 1.5 – 2.5 ppm for all of these complexes*. This is in marked contrast to other organometallic complexes containing an M-H bond, which are usually observed well upfield of δ 0.0 ppm in the negative region. Lastly, these Cu-H complexes are significantly upfield shifted as compared to monodentate phosphine ligated hexameric copper-hydride aggregates, whose hydride resonances appear between δ 2.5 – 3.5 ppm in ^{1}H NMR.[18]

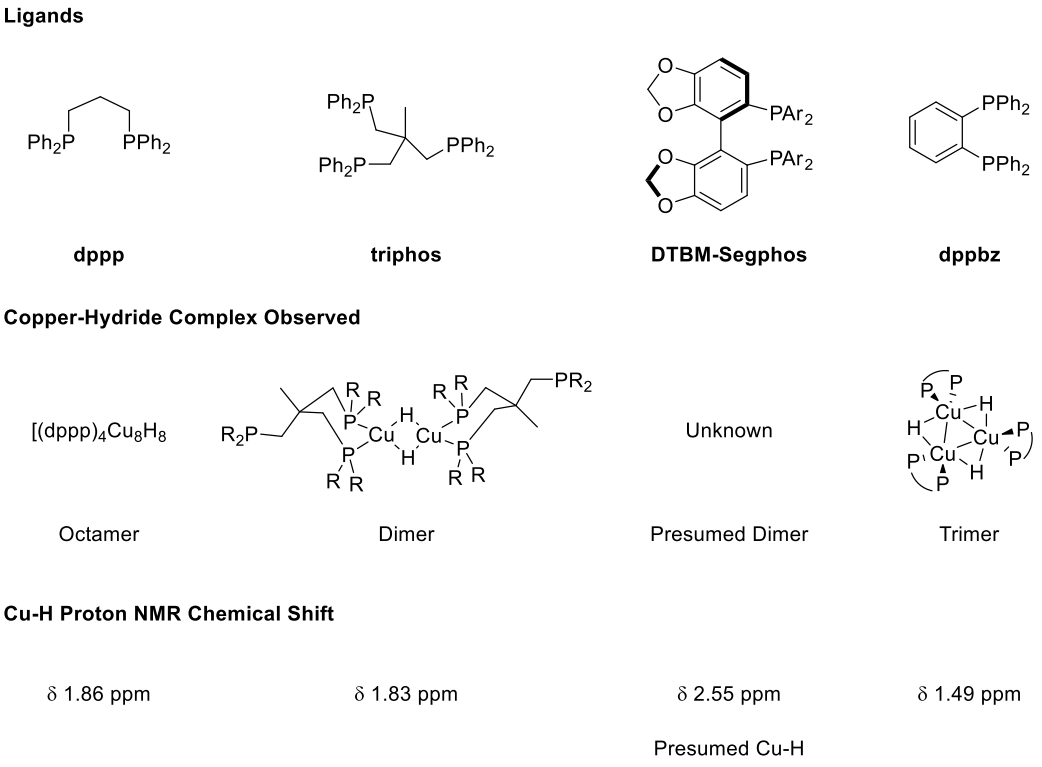

Figure 0.2. Multidentate phosphine ligands and their associated copper-hydride complexes. Each of these ligands were unable to stabilize a monomeric Cu-H, but its oligomer could be visualized by ^{1}H NMR spectroscopy and X-ray crystallography in most cases.

As these works with phosphine-based ligands was ongoing, the field of stable carbene chemistry was seeing an incredible rise to prominence following the seminal work of Bertrand *et al.*[19] in 1988 and the development of the *N*-heterocyclic carbene (NHC) by Arduengo *et al.* in 1991 (Figure 0.3, **NHC$_{Ad}$**).[20] In their short lifespan, NHCs have gone toe-to-toe with phosphines as ancillary ligands for organometallic complexes because they are known to generate robust and versatile catalysts. Moreover, they boast higher overall σ-donor capabilities as compared to phosphines and they contain readily modifiable steric protection properties. With respect to this latter point, it is well-known that the steric contribution of phosphines is best described as an away facing cone while that of the NHC faces the metal and can be substantially increased in size to "bury" the metal center within its protective pocket.[21] This difference in protecting ability is likely

the reason that monodentate phosphine copper-hydride complexes can generate such high nuclearity copper-hydride aggregates (*e.g.* Stryker's reagent).

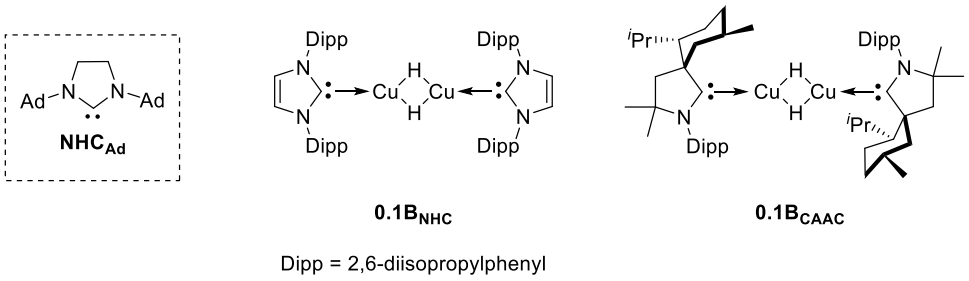

Figure 0.3. Arduengo's NHC (left), Sadighi's NHC stabilized Cu-H dimer **0.1B$_{NHC}$** (center), and Bertrand's CAAC dimer **0.1B$_{CAAC}$** (right).

For these reasons, Sadighi and coworkers surveyed the ability of NHCs to stabilize a copper-hydride complex in 2004 (Figure 0.3, **0.1B$_{NHC}$**).[22] Interestingly, in contrast to monodentate phosphine ligands bound to Cu-H, an X-ray crystallographic study unambiguously confirmed the dimeric nature of **0.1B$_{NHC}$**, suggesting that NHC ligands are better suited to stabilize monoligated copper-hydride complexes of low-nuclearity. Following these results, Dey and Elliot used quantum chemical density functional theory (DFT) calculations to investigate the thermodynamic parameters associated with the dimerization of two monomeric NHC ligated copper-hydride complexes.[23] In this study, the authors found that there is very little energetic cost to generate products of type **0.1B** from two monomeric (NHC)Cu-H complexes (ΔE = +5 kJ/mol). They further stated that this dimerization process is therefore, strongly dependent upon entropy. To put this latter result more simply, *more steric congestion should favor the dissociation of complexes **0.1B** into their constituent monomers.*

Although **0.1B$_{NHC}$** is unstable above -40 ^{o}C, the carbene copper-hydride dimer prepared using Bertrand's cyclic (alkyl)(amino) carbene (CAAC)[24] was reportedly stable at room temperature (Figure 0.3, **0.1B$_{CAAC}$**).[25] Surprisingly, these two carbene stabilized copper-hydride

complexes feature very different Cu-H vibrational bands by IR spectroscopy (981 cm^{-1} for **0.1B$_{CAAC}$** *vs* 881 cm^{-1} for **0.1B$_{NHC}$**), a difference which could be attributed to the increased steric hinderance imparted by the bulky CAAC ligand on the Cu-H core. Although the stretching frequency for a monomeric Cu-H is not known, the analogous monomeric gold congener of **0.1B$_{NHC}$** is reported to appear at 1976 cm^{-1}.[26] If we assume that a monomeric (carbene)Cu-H complex would exhibit a similar stretching frequency, the 100 cm^{-1} blue shift (toward higher wavenumber) of **0.1B$_{CAAC}$** as compared to **0.1B$_{NHC}$** could point towards the increased monomeric Cu-H character induced by the steric encumbrance of the former over the latter.

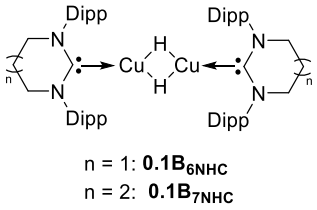

Figure 0.4. Room temperature stable 6- and 7-membered NHC ligated copper-hydride complexes.

It is well known that wider N-C-N carbene angles bring the flanking aryl substituents closer to the carbene center, which would in turn impart greater kinetic stabilization to whatever fragment is bound to the carbene carbon atom. The most recent copper-hydride complex reported was from Sadighi *et al.* in 2016. They found that 6- and 7-membered NHC ligands, in contrast to their 5-membered counterparts, could support the first room temperature stable (NHC)Cu-H complexes (Figure 0.4, **0.1B$_{6NHC}$** and **0.1B$_{7NHC}$** respectively).[27] In these cases, the complexes were isolated as their respective dimers and crystallographically characterized.

With all the work that has been done to isolate low nuclearity copper(I)-hydride oligomers, it is my opinion that carbene ligands are best suited to facilitate the stabilization of these highly reactive species as monomers. Furthermore, based on the computational results obtained by Dey and Elliot as well as the knowledge garnered from the work of Sadighi and Bertrand, it seems

logical to survey NHC ligands that boast incredible steric profiles. To this end, I will share with you my attempts to employ the NHCs reported by Marko *et al.*[28] and Straub *et al.*[29] in the isolation of a copper(I)-hydride monomer.

The research described henceforth is my attempt to stand on the shoulders of giants who came before and with their help, reach further than any of us could have dreamed to achieve alone.[30]

0.1 References

[1] Wurtz, A. "Sur l'Hydrure de Cuivre" *Ann. Chim. Phys.* **1844**, *11*, 250.

[2] (a) Brestensky, D. M.; Huseland, D. E.; McGettigan, C.; Stryker, J. M. "Simplified, "one-pot" procedure for the synthesis of $[(Ph_3P)CuH]_6$, a stable copper hydride for conjugate reductions" *Tetrahedron Lett.* **1988**, *29*, 3749. (b) Mahoney, W. S.; Brestensky, D. M.; Stryker, J. M. "Selective hydride-mediated conjugate reduction of α,β-unsaturated carbonyl compounds using $[(Ph_3P)CuH]_6$" *J. Am. Chem. Soc.* **1988**, *110*, 291. (c) Brestensky, D. M.; Stryker, J. M. "Regioselective conjugate reduction and reductive silylation of α,β-unsaturated" *Tetrahedron Lett.* **1989**, *30*, 5677. (d) Mahoney, W. S.; Stryker, J. M. "Hydride-mediated homogeneous catalysis. Catalytic reduction of α,β-unsaturated ketones using $[(Ph_3P)CuH]_6$ and H_2" *J. Am. Chem. Soc.* **1989**, *111*, 8818. (e) Koenig, T. M.; Daeuble, J. F.; Brestensky, D. M.; Stryker, J. M. "Conjugate reduction of polyfunctional α,β-unsaturated carbonyl compounds using $[(Ph_3P)CuH]_6$. Compatibility with halogen, sulfonate, and γ-oxygen and sulfur substituents" *Tetrahedron Lett.* **1990**, *31*, 3237.

[3] Bezman, S. A.; Churchill, M. R.; Osborn, J. A.; Wormald, J. "Preparation and crystallographic characterization of a hexameric triphenylphosphinecopper hydride cluster" *J. Am. Chem. Soc.* **1971**, *93*, 2063.

[4] Lipshutz, B. H.; Keith, J.; Papa, P.; Vivian, R. "A convenient, efficient method for conjugate reductions using catalytic quantities of Cu(I)" *Tetrahedron Lett.* **1998**, *39*, 4627.

[5] (a) Mori, A.; Fujita, A.; Nishihara, Y.; Hiyama, T. "Copper(I) salt mediated 1,4-reduction of α,β-unsaturated ketones using hydrosilanes" *Chem. Commun.* **1997**, 2159. (b) Mori, A.; Fujita, A.; Kajiro, H.; Nishihara, Y.; Hiyama, T. "Conjugate reduction of α,β-unsaturated ketones with hydrosilane mediated by copper(I) salt" *Tetrahedron* **1999**, *55*, 4573. (c) Ito, H.; Ishizuka, T.; Arimoto, K.; Miura, K.; Hosomi, A. "Generation of a reducing reagent from Copper(I) salt and hydrosilane. New practical method for conjugate reduction" *Tetrahedron Lett.* **1997**, *38*, 8887. (d) Lipshutz, B. H.; Ung, C. S.; Sengupta, S. "1,4-Reductions of α,β-Unsaturated Ketones and Aldehydes via in situ Generated Hydridocuprates" *Synlett* **1989**, *1989*, 64. (e) Lipshutz, B. H.; Keith, J.; Papa, P.; Vivian, R. "A convenient, efficient method for conjugate reductions using catalytic quantities of Cu(I)" *Tetrahedron Lett.* **1998**, *39*, 4627.

[6] (a) Appella, D. H.; Moritani, Y.; Shintani, R.; Ferreira, E. M.; Buchwald, S. L. "Asymmetric Conjugate Reduction of α,β-Unsaturated Esters Using a Chiral Phosphine−Copper Catalyst" *J. Am. Chem. Soc.* **1999**, *121*, 9473. (b) Moritani, Y.; Appella, D. H.; Jurkauskas, V.; Buchwald, S. L. "Synthesis of β-Alkyl Cyclopentanones in High Enantiomeric Excess via Copper-Catalyzed Asymmetric Conjugate Reduction" *J. Am.*

Chem. Soc. **2000**, *122*, 6797. (c) Hughes, G.; Kimura, M.; Buchwald, S. L. "Catalytic Enantioselective Conjugate Reduction of Lactones and Lactams" *J. Am. Chem. Soc.* **2003**, *125*, 11253.

7 Select examples of ketone and aldehyde hydrogenation/hydrosilylation: (a) Chen, J.-X.; Daeuble, J. F.; Brestensky, D. M.; Stryker, J. M. "Highly Chemoselective Catalytic Hydrogenation of Unsaturated Ketones and Aldehydes to Unsaturated Alcohols Using Phosphine-Stabilized Copper(I) Hydride Complexes" *Tetrahedron* **2000**, *56*, 2153. (b) Lipshutz, B. H.; Chrisman, W.; Noson, K. "Hydrosilylation of aldehydes and ketones catalyzed by $[Ph_3P(CuH)]_6$" *J. Organomet. Chem.* **2001**, *624*, 367. (c) Junge, K.; Wendt, B.; Addis, D.; Zhou, S.; Das, S.; Beller, M. "Copper-Catalyzed Enantioselective Hydrosilylation of Ketones by Using Monodentate Binaphthophosphepine Ligands" *Chem. Eur. J.* **2009**, *16*, 68. (d) Teci, M.; Lentz, N.; Brenner, E.; Matt, D.; Toupet, L. "Alkylfluorenyl substituted N-heterocyclic carbenes in copper(I) catalysed hydrosilylation of aldehydes and ketones" *Dalton Trans.* **2015**, *44*, 13991.

8 For hydroboration, see: (a) Noh, D.; Chea, H.; Ju, J.; Yun, J. "Highly Regio- and Enantioselective Copper-Catalyzed Hydroboration of Styrenes" *Angew. Chem. Int. Ed.* **2009**, *48*, 6062. (b) Xi, Y.; Hartwig, J. F. "Diverse Asymmetric Hydrofunctionalization of Aliphatic Internal Alkenes through Catalytic Regioselective Hydroboration" *J. Am. Chem. Soc.* **2016**, *138*, 6703. For Hydroamination, see: (c) Zhu, S.; Niljianskul, N.; Buchwald, S. L. "Enantio- and Regioselective CuH-Catalyzed Hydroamination of Alkenes" *J. Am. Chem. Soc.* **2013**, *135*, 15746. (d) Niljianskul, N.; Zhu, S.; Buchwald, S. L. "Enantioselective Synthesis of α-Aminosilanes by Copper-Catalyzed Hydroamination of Vinylsilanes" *Angew. Chem. Int. Ed.* **2014**, *54*, 1638. (e) Zhu, S.; Buchwald, S. L. "Enantioselective CuH-Catalyzed Anti-Markovnikov Hydroamination of 1,1-Disubstituted Alkenes" *J. Am. Chem. Soc.* **2014**, *136*, 15913.

9 For hydrocarboxylation, see: (a) Fujihara, T.; Xu, T.; Semba, K.; Terao, J.; Tsuji, Y. "Copper-Catalyzed Hydrocarboxylation of Alkynes Using Carbon Dioxide and Hydrosilanes" *Angew. Chem. Int. Ed.* **2010**, *50*, 523. For internal and terminal hydroboration respectively, see: (b) Lipshutz, B. H.; Bošković, Ž. V.; Aue, D. H. "Synthesis of Activated Alkenylboronates from Acetylenic Esters by CuH-Catalyzed 1,2-Addition/Transmetalation" *Angew. Chem. Int. Ed.* **2008**, *47*, 10183. (c) Jang, W. J.; Lee, W. L.; Moon, J. H.; Lee, J. Y.; Yun, J. "Copper-Catalyzed trans-Hydroboration of Terminal Aryl Alkynes: Stereodivergent Synthesis of Alkenylboron Compounds" *Org. Lett.* **2016**, *18*, 1390. For hydroalkylation, see: (d) Uehling, M. R.; Suess, A. M.; Lalic, G. "Copper-Catalyzed Hydroalkylation of Terminal Alkynes" *J. Am. Chem. Soc.* **2015**, *137*, 1424. For hydroamination, see: (e) Shi, S.-L.; Buchwald, S. L. "Copper-catalysed selective hydroamination reactions of alkynes" *Nat. Chem.* **2014**, *7*, 38.

[10] (a) Wakamatsu, T.; Nagao, K.; Ohmiya, H.; Sawamura, M. "Copper-Catalyzed Semihydrogenation of Internal Alkynes with Molecular Hydrogen" *Organometallics* **2016**, *35*, 1354.

[11] (a) Dang, H.; Cox, N.; Lalic, G. "Copper-Catalyzed Reduction of Alkyl Triflates and Iodides: An Efficient Method for the Deoxygenation of Primary and Secondary Alcohols" *Angew. Chem. Int. Ed.* **2013**, *53*, 752. (b) Cox, N.; Dang, H.; Whittaker, A. M.; Lalic, G. "NHC–copper hydrides as chemoselective reducing agents: catalytic reduction of alkynes, alkyl triflates, and alkyl halides" *Tetrahedron* **2014**, *70*, 4219.

[12] For hydrosilylation, see: (a) Motokura, K.; Kashiwame, D.; Miyaji, A.; Baba, T. "Copper-Catalyzed Formic Acid Synthesis from CO_2 with Hydrosilanes and H_2O" *Org. Lett.* **2012**, *14*, 2642. (b) Zhang, L.; Cheng, J.; Hou, Z. "Highly efficient catalytic hydrosilylation of carbon dioxide by an N-heterocyclic carbene copper catalyst" *Chem. Commun.* **2013**, *49*, 4782. For hydroboration, see: (c) Shintani, R.; Nozaki, K. "Copper-Catalyzed Hydroboration of Carbon Dioxide" *Organometallics* **2013**, *32*, 2459. For amine carbonylation, see: (d) Motokura, K.; Takahashi, N.; Kashiwame, D.; Yamaguchi, S.; Miyaji, A.; Baba, T. "Copper-diphosphine complex catalysts for N-formylation of amines under 1 atm of carbon dioxide with polymethylhydrosiloxane" *Catal. Sci. Technol.* **2013**, *3*, 2392. For CO_2 hydrogenation, see: (e) Zall, C. M.; Linehan, J. C.; Appel, A. M. "A Molecular Copper Catalyst for Hydrogenation of CO2 to Formate" *ACS Cat.* **2015**, *5*, 5301. (f) Zall, C. M.; Linehan, J. C.; Appel, A. M. "Triphosphine-Ligated Copper Hydrides for CO_2 Hydrogenation: Structure, Reactivity, and Thermodynamic Studies" *J. Am. Chem. Soc.* **2016**, *138*, 9968.

[13] Goeden, G. V.; Caulton, K. G. "Soluble copper hydrides: solution behavior and reactions related to carbon monoxide hydrogenation" *J. Am. Chem. Soc.* **1981**, *103*, 7354.

[14] Lemmen, T. H.; Folting, K.; Huffman, J. C.; Caulton, K. G. "Copper polyhydrides" *J. Am. Chem. Soc.* **1985**, *107*, 7774.

[15] Goeden, G. V.; Huffman, J. C.; Caulton, K. G. "A copper-(μ^2-hydrogen) bond can be stronger than an intramolecular phosphorus –> copper bond. Synthesis and structure of di-μ-hydridobis[η^2-1,1,1-tris(diphenylphosphinomethyl)ethane]dicopper" *Inorg. Chem.* **1986**, *25*, 2484.

[16] Lipshutz, B. H.; Frieman, B. A. "CuH in a Bottle: A Convenient Reagent for Asymmetric Hydrosilylations" *Angew. Chem. Int. Ed.* **2005**, *44*, 6345.

[17] For the initial complex formation, see: (a) Baker, B. A.; Bošković, Ž. V.; Lipshutz, B. H. "(BDP)CuH: A “Hot” Stryker's Reagent for Use in Achiral Conjugate Reductions" *Org. Lett.* **2008**, *10*, 289. For the X-ray crystallographic study, see: (b) Eberhart, M. S.; Norton,

J. R.; Zuzek, A.; Sattler, W.; Ruccolo, S. "Electron Transfer from Hexameric Copper Hydrides" *J. Am. Chem. Soc.* **2013**, *135*, 17262.

[18] (a) Goeden, G. V.; Caulton, K. G. "Soluble copper hydrides: solution behavior and reactions related to carbon monoxide hydrogenation" *J. Am. Chem. Soc.* **1981**, *103*, 7354. (b) Lemmen, T. H.; Folting, K.; Huffman, J. C.; Caulton, K. G. "Copper polyhydrides" *J. Am. Chem. Soc.* **1985**, *107*, 7774.

[19] Igau, A.; Grutzmacher, H.; Baceiredo, A.; Bertrand, G. "Analogous α,α'-bis-carbenoid, triply bonded species: synthesis of a stable λ^3-phosphino carbene-λ,λ^5-phosphaacetylene" *J. Am. Chem. Soc.* **1988**, *110*, 6463.

[20] Arduengo, A. J.; Harlow, R. L.; Kline, M. "A stable crystalline carbene" *J. Am. Chem. Soc.* **1991**, *113*, 361.

[21] Clavier, H.; Nolan, S. P. "Percent buried volume for phosphine and N-heterocyclic carbene ligands: steric properties in organometallic chemistry" *Chem. Commun.* **2010**, *46*, 841.

[22] Mankad, N. P.; Laitar, D. S.; Sadighi, J. P. "Synthesis, Structure, and Alkyne Reactivity of a Dimeric (Carbene)copper(I) Hydride" *Organometallics* **2004**, *23*, 3369.

[23] Dey, G.; Elliott, S. D. "Copper(I) carbene hydride complexes acting both as reducing agent and precursor for Cu ALD: a study through density functional theory" *Theor. Chem. Acc.* **2013**, *133*, 1416.

[24] Lavallo, V.; Canac, Y.; Präsang, C.; Donnadieu, B.; Bertrand, G. "Stable Cyclic (Alkyl)(Amino)Carbenes as Rigid or Flexible, Bulky, Electron-Rich Ligands for Transition-Metal Catalysts: A Quaternary Carbon Atom Makes the Difference" *Angew. Chem. Int. Ed.* **2005**, *44*, 5705.

[25] Frey, G. D.; Donnadieu, B.; Soleilhavoup, M.; Bertrand, G. "Synthesis of a Room-Temperature-Stable Dimeric Copper(I) Hydride" *Chem. Asian J.* **2011**, *6*, 402.

[26] Tsui, E. Y.; Müller, P.; Sadighi, J. P. "Reactions of a Stable Monomeric Gold(I) Hydride Complex" *Angew. Chem. Int. Ed.* **2008**, *47*, 8937.

[27] Jordan, A. J.; Wyss, C. M.; Bacsa, J.; Sadighi, J. P. "Synthesis and Reactivity of New Copper(I) Hydride Dimers" *Organometallics* **2016**, *35*, 613.

[28] Berthon-Gelloz, G.; Siegler, M. A.; Spek, A. L.; Tinant, B.; Reek, J. N. H.; Marko, I. E. "IPr* an easily accessible highly hindered N-heterocyclic carbene" *Dalton Trans.* **2010**, *39*, 1444.

[29] Weber, S. G.; Loos, C.; Rominger, F.; Straub, B. F. "Synthesis of an extremely stericall shielding *N*-heterocyclic carbene ligand" *Arkivok* **2012**, *iii*, 226.

[30] For in-depth discussions regarding the field of copper(I)-hydride chemistry including their history and reactivity, readers should refer to the following review articles: (a) Rendler, S.; Oestreich, M. "Polishing a Diamond in the Rough: “Cu-H” Catalysis with Silanes" *Angew. Chem. Int. Ed.* **2007**, *46*, 498. (b) Deutsch, C.; Krause, N.; Lipshutz, B. H. "CuH-Catalyzed Reactions" *Chem. Rev.* **2008**, *108*, 2916. (c) Jordan, A. J.; Lalic, G.; Sadighi, J. P. "Coinage Metal Hydrides: Synthesis, Characterization, and Reactivity" *Chem. Rev.* **2016**, *116*, 8318. (d) Pirnot, M. T.; Wang, Y.-M.; Buchwald, S. L. "Copper Hydride Catalyzed Hydroamination of Alkenes and Alkynes" *Angew. Chem. Int. Ed.* **2016**, *55*, 48. (e) Díez-González, S.; Nolan, S. P. "Copper, Silver, and Gold Complexes in Hydrosilylation Reactions" *Acc. Chem. Res.* **2008**, *41*, 349.

Chapter 1 : X-ligand Directed Borylation Reactions of Terminal Alkynes Using (CAAC)CuX Complexes

1.1 Introduction

Since their first isolation in 1988 by Bertrand and coworkers,[1] carbenes have gone from laboratory curiosity to a mainstay in the organometallic chemist's arsenal of ligands. The most well-known carbene is the *N*-heterocyclic carbene (NHC) developed by Arduengo *et al.* in 1991.[2] These strongly σ-donating ligands have become broadly applicable in transition metal catalyzed reactions, a field that was previously dominated by phosphines and cyclopentadienyl ligands.[3] Even more σ-donating ligands were then developed by Bertrand *et al.* in 2005, when they substituted one α-nitrogen atom with a quaternary carbon; they called this new NHC a cyclic (alkyl)(amino) carbene (CAAC).[4] Since their development,[5,6] CAACs have been useful in many applications, however, their claim to fame comes from their ability to stabilize highly reactive main-group[7] and organometallic compounds.[4,8] Aside from a few reports involving palladium, gold, and ruthenium, the broad usefulness of CAACs in catalysis has not yet been illustrated with more abundant base metals.[6c]

We sought to extend the reach of CAACs to catalytic processes such as the preparation of C-B bonds *via* dehydrogenative pathways. Organoboranes were popularized by the Suzuki-Miyaura cross-coupling reaction and are now regarded as key building blocks for compounds with applications ranging from materials to life sciences. Consequently, numerous methodologies have been developed to access these valuable substrates.[9] Following groundbreaking reports by Hartwig *et al.*,[10] and Smith *et al.*,[11] the catalytic dehydrogenative borylation of C(sp^3)- and C(sp^2)-H bonds are now well documented.[12] Conversely, for C(sp)-H bonds, there exist only a select few methodologies to access alkynylboronate esters **1.2B** (Scheme 1.1).

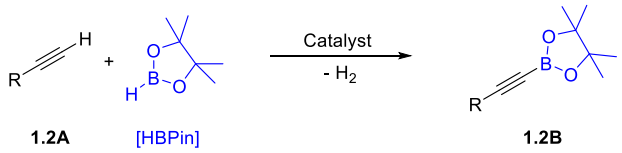

Scheme 1.1. Dehydrogenative borylation reaction between terminal alkynes **1.2A** and pinacolborane affording alkynylboronate esters **1.2B**.

In 2013, Ozerov *et al.* developed an efficient iridium catalyzed dehydrogenative C(sp)-H borylation reaction of terminal alkynes **1.2A** with pinacolborane.[13] Two years later, the same group published two additional reports, one using rhodium[14] and the other palladium.[15] These reports were quickly followed by Tsuchimoto and coworkers using zinc triflate; however, this method was only effective when the more reactive 1,8-naphthalenediaminatoborane (HBDan) was used as the boron partner.[16] It is worth noting that the major difficulty in accessing these alkynylboronate esters lies in the competing hydroboration reaction of the C-C triple bond, which leads to the production of the corresponding alkenylboronate esters **1.2C** (Scheme 1.2).[17]

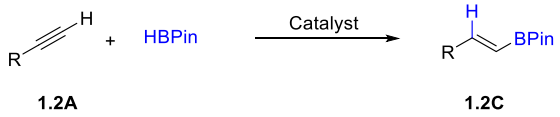

Scheme 1.2. Hydroboration reaction between terminal alkynes **1.2A** and pinacolborane affording alkenylboronate esters **1.2C**.

We were intrigued by the possibility of achieving catalytic C(sp)-H borylation with a catalyst that is cheaper and more abundant than Ozerov's noble-metal complexes all the while maintaining higher versatility than Tsuchimoto's zinc complex. To accomplish this task, we reasoned that protection of the C-C π-bond in **1.2A** should disfavor the competing hydroboration reaction and allow us to selectively perform the dehydrogenative borylation reaction. In 2015, we reported on the role of the X-ligand in the (CAAC)CuX (OTf = trifluoromethanesulfonate) catalyzed azide-alkyne cycloaddition reaction (CuAAC).[18] Therein, we found that (CAAC)CuOTf

(OTf = trifluoromethanesulfonate) complexes in the presence of triethylamine (NEt_3) and terminal alkynes reacted to give σ,π-biscopper acetylides **1.1C** (Scheme 1.3). These bimetallic complexes feature the proposed protection of the C-C triple bond and should therefore avoid traditional hydroboration.

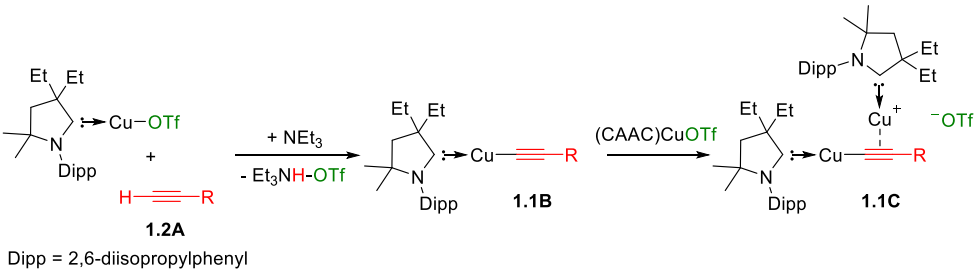

Scheme 1.3. Reaction of (CAAC)CuOTf with terminal alkynes **1.2A** in the presence of triethylamine yields σ,π-biscopper acetylide complexes **1.1C**.

Because of this protection, we predicted that the hydroborane would be forced to react with the highly polarized copper-acetylide bond to instead yield alkynylboronates **1.2B**. We further hypothesized that removal of the (CAAC)Cu^+ "protecting" group would change the chemoselectivity of the reaction to afford the anti-Markovnikov *trans*-hydroboration products **1.2C**.

1.2 Copper-Catalyzed Dehydrogenative Borylation of Terminal Alkynes (DHBTA) with Pinacolborane

1.2.1 Determining the Standard Reaction Conditions and Substrate Scope for the DHBTA Transformation

We began our investigation by confirming that no reaction occurs between pinacolborane and *p*-tolylacetylene **1.2AA** in the absence of catalyst (Table 1.1, entry 1). In the presence of 1 mol% of LCuOTf (L = ^{Et}CAAC), no significant reaction was observed either which likely stems from the difficulty of the triflate anion to deprotonate the alkyne (entry 2).[18] To facilitate alkyne

metalation, 1 mol% of TEA was added resulting in immediate hydrogen evolution as determined by the appearance of bubbles in the reaction mixture and a singlet at δ 4.47 ppm in ^{1}H NMR. In this case, the major product observed was the alkynylboronate **1.2BA** (48%); however, the alkenylboronate **1.2CA** (11%) and the styrene derivative **1.2DA** (7%) were also formed (entry 3). After confirming the necessity of the ligand (entry 4), we fully optimized the dehydrogenative borylation reaction leading selectively to **1.2BA**. We found that a two-fold excess of triethylamine with respect to LCuOTf was beneficial (entry 5). Furthermore, testing of various solvents (entries 5-8) and amine bases (Entries 9‑13) allowed us to identify benzene and TEA as most appropriate for this reaction. Increasing the catalyst loading to 2.5 mol% (Entries 14–16) and dilution of the reaction media to 0.1 mol/L (entry 17) allowed for quantitative formation of product **1.2BA** with excellent selectivity after two hours at room temperature. It is worth noting that substitution of the L ligand for the bulkier menthyl CAAC L_2 or the bis-2,6-diisopropylphenyl substituted NHC L_3 (IPr)[19] gave comparable conversions of **1.2AA** to **1.2BA** (entries 18 and 19, respectively).

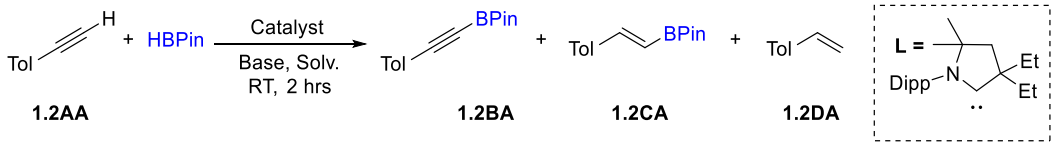

Scheme 1.4. Reaction conditions for the optimization of the copper catalyzed DHBTA reaction.

Table 1.1. Optimization of the dehydrogenative borylation reaction. Reactions were carried out in a test tube for 2 hrs at RT under an argon atmosphere using a 1:1 mixture (0.69 mmol) of *p*-tolylacetylene and pinacolborane. [a] Measured by ^{1}H NMR using 1,4-dioxane as an internal standard.

Entry	Cat. (mol%)	Base (mol%)	Solv.	Conc. (M)	1.2AA (%)[a]	1.2BA (%)[a]	1.2CA (%)[a]	1.2DA (%)[a]
1	-	-	C_6D_6	1.4	100	0	0	0
2	LCuOTf (1)	-	C_6D_6	1.4	86	0	6	6
3	LCuOTf (1)	Et_3N (1)	C_6D_6	1.4	14	48	11	7
4	CuOTf	Et_3N (1)	C_6D_6	1.4	100	0	0	0
5	LCuOTf (1)	Et_3N (2)	C_6D_6	1.4	1	70	14	12
6	LCuOTf (1)	Et_3N (2)	CD_2Cl_2	1.4	12	42	6	26
7	LCuOTf (1)	Et_3N (2)	THF-d_8	1.4	5	64	12	17
8	LCuOTf (1)	Et_3N (2)	CD_3CN	1.4	18	38	0	6
9	LCuOTf (1)	^{i}PrNH$_2$ (2)	C_6D_6	1.4	67	5	12	10
10	LCuOTf (1)	^{i}Pr$_2$NH (2)	C_6D_6	1.4	47	11	13	7
11	LCuOTf (1)	^{i}Pr$_2$NEt (2)	C_6D_6	1.4	10	28	45	3
12	LCuOTf (1)	BnNEt$_2$ (2)	C_6D_6	1.4	14	53	8	7
13	LCuOTf (1)	DABCO (2)	C_6D_6	1.4	18	60	1	7
14	LCuOTf (0.25)	Et_3N (0.5)	C_6D_6	1.4	37	36	15	6
15	LCuOTf (0.5)	Et_3N (1)	C_6D_6	1.4	20	54	15	9
16	LCuOTf (2.5)	Et_3N (5)	C_6D_6	1.4	4	83	4	7
17	**LCuOTf (2.5)**	**Et_3N (5)**	**C_6D_6**	**0.1**	**1**	**98**	**0**	**1**
18	L_2CuOTf (2.5)	Et_3N (5)	C_6D_6	0.1	0	96	0	4
19	L_3CuOTf (2.5)	Et_3N (5)	C_6D_6	0.1	0	92	0	8

The scope of the dehydrogenative borylation reaction was then studied at room temperature (Figure 1.1) using the following standard reaction conditions: 0.1 M benzene solution with a stoichiometric mixture of alkyne and borane (1.82 mmol), 5 mol% of NEt_3 and 2.5 mol% of LCuOTf. This methodology is applicable to a broad range of terminal alkynes bearing a range of synthetically useful functional groups such as OMe, CN, F, Cl, TMS and CO_2Me. It is important to note that electron-rich terminal alkynes require at least 12 hours for complete conversion (**1.2BJ-O**). Alkynylboronates **1.2BA-O** were isolated in good to excellent yields *via* simple filtration through a plug of dry neutral alumina using pentane as the eluent. This straightforward methodology can also be applied to multi-gram syntheses, as evidenced with **1.2BC**.

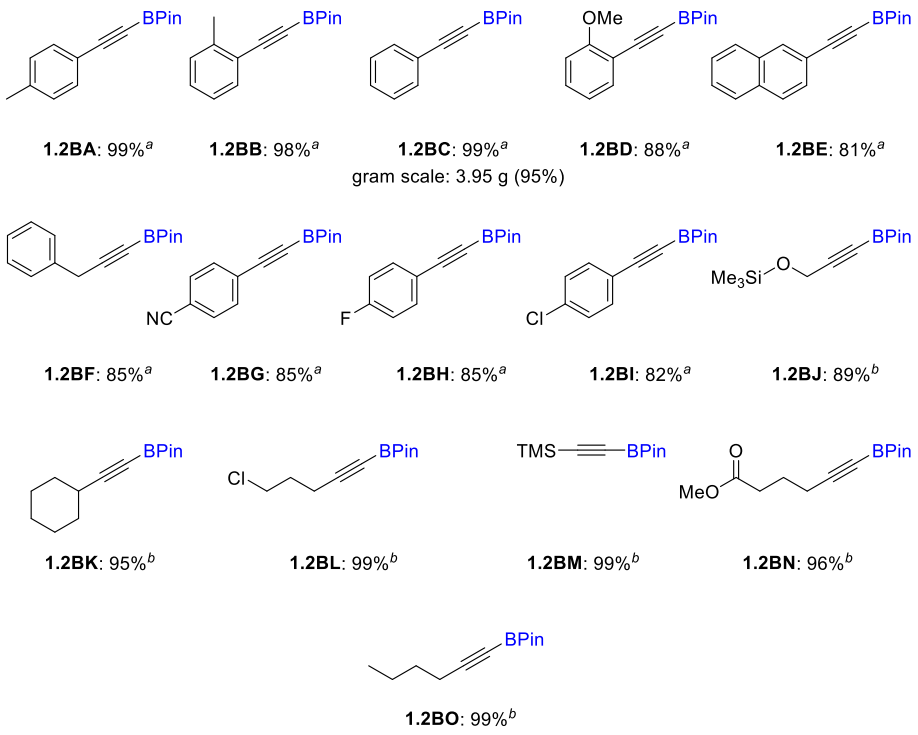

Figure 1.1. Scope of the dehydrogenative borylation of terminal alkynes. [a] Reaction time 2 h. [b] Reaction time 12 h.

1.2.2 Mechanistic Investigation

With these results in hand, we set out to determine the most likely mechanistic pathway of this transformation through a series of stoichiometric and catalytic reactions. As shown in Scheme 1.3, LCuOTf complexes form biscopper acetylides in the presence of terminal alkynes and NEt_3; however, formation of complex **1.1C** first requires the formation of monocopper acetylide **1.1B**. We sought confirmation that complexes **1.1B** do not sit within the preferred mechanistic pathway. To accomplish this task, we monitored the reaction of alkyne **1.2AC** with pinacolborane in the presence of a catalytic amount of complex **1.1BC** (Figure 1.2, a). ^{1}H NMR spectroscopy confirmed our hypothesis as we did not observe any formation of the desired dehydrogenative borylation product **1.2BC**.

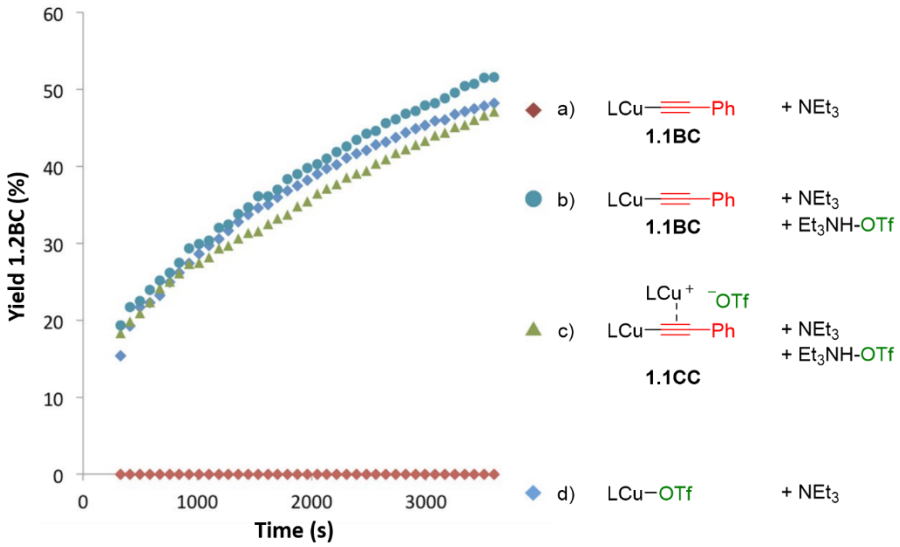

Figure 1.2. Experimental kinetic profiles of the formation of **1.2BC** using various catalytic systems. a) 2.5 mol% **1.1BC** and 5 mol% NEt_3. b) 2.5 mol% **1.1BC**, NEt_3, and Et_3NH-OTf. c) 2.5 mol% of **1.1CC**, 3.75 mol% NEt_3, and 1.25 mol% Et_3NH-OTf. d) 2.5 mol% LCuOTf and 5 mol% NEt_3.

Interestingly, addition of 2.5 mol% Et_3NH-OTf to the reaction of alkyne **1.2AC** with pinacolborane in the presence of **1.1BC** yielded selectively the dehydrogenative borylation product **1.2BC** (Figure 1.2, b). The kinetic profile obtained using conditions b was found to mirror that of

conditions c, which utilized the dinuclear copper acetylide complex **1.1C** as catalyst (Figure 1.2, c). It is important to note that both conditions b and c match the kinetic profile observed when using our standard catalytic conditions (Figure 1.2, d). Altogether, this data strongly implies a rearrangement of mononuclear copper acetylide complexes to biscopper acetylides in the presence of a proton source, a hypothesis that was confirmed by combining complex **1.1BC** with 0.5 equivalents of Et_3NH-OTf in a J-Young NMR tube (Scheme 1.5).

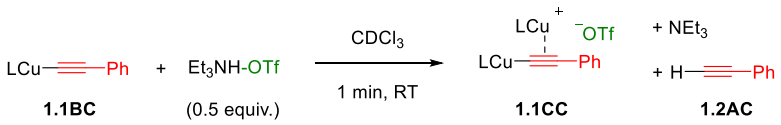

1.1BC **1.1CC** **1.2AC**

Scheme 1.5. Rearrangement of monocopper acetylide **1.1BC** to biscopper acetylide **1.1CC** in the presence of a proton source.

In this experiment, we immediately observed a 1:1:1 mixture of the biscopper acetylide **1.1CC**, free alkyne, and triethylamine by ^{1}H (Figure 1.3) and ^{13}C NMR spectroscopies (see Figure 1.12 in the appendix for the ^{13}C NMR spectrum). These experiments strongly suggest that dinuclear copper complexes **1.1C** are pivotal in selectively promoting the dehydrogenative borylation reaction.

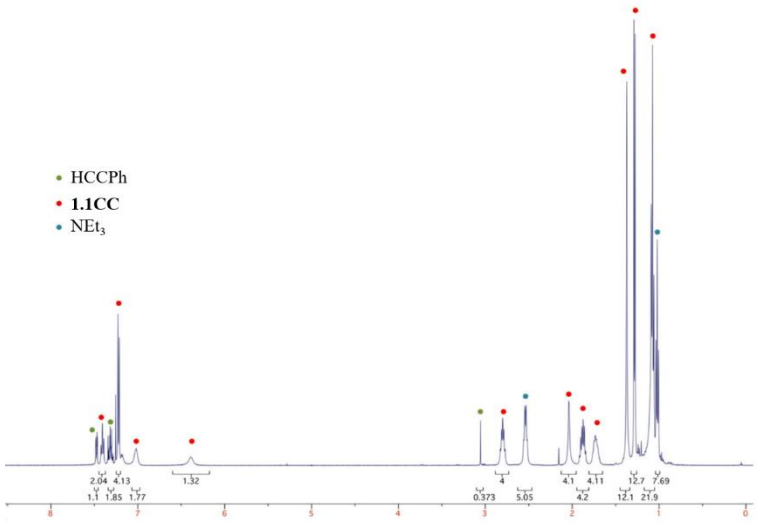

Figure 1.3. Reaction of complex **1.1BC** with Et_3NH-OTf yields free alkyne **1.2AC**, biscopper acetylide **1.1CC**, and NEt_3 by ^1H NMR spectroscopy.

Due to the small amounts of styrene formed in each of our reactions, we wondered whether it was possible that a transient copper-hydride was forming within the catalytic cycle. This copper-hydride could potentially arise from a σ-bond metathesis reaction of complexes **1.1C** with the hydroborane, as shown in Scheme 1.6 by transition state **1.2E**.

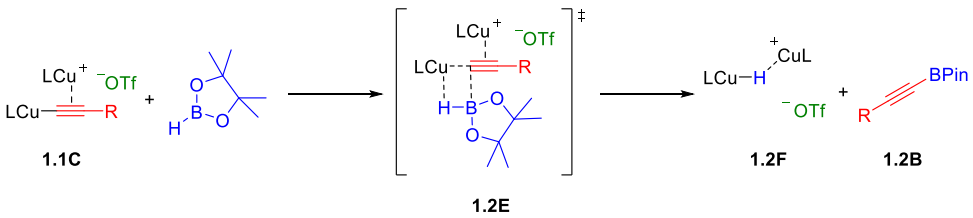

Scheme 1.6. Reaction of biscopper acetylide complexes **1.1C** with pinacolborane is hypothesized to form copper-hydride **1.2F** and alkynylboronate products **1.2B**.

Since their initial discovery in 1844 by Wurtz,[20] a monomeric copper-hydride has never been successfully isolated due to their incredible propensity to aggregate; however, credit is due to both CAAC[21] and NHC[22] ligands for their ability to stabilize low nuclearity copper-hydrides as dimers in the solid state. Interestingly, when using CAAC ligands to generate copper hydrides,[21] Bertrand *et al.* found that the increased π-acidity associated with CAACs as compared to NHCs

makes hydride migration to the carbene carbon more likely, a result which complicated our ability to isolate intermediate **1.2F** from the reaction mixture. Although we were unable to directly isolate this cationic copper-hydride, Sadighi and coworkers found that addition of pinacolborane to a solution of $[(IPr)Cu]_2(\mu\text{-}OSiMe_3)BF_4$ allowed for the isolation and X-ray crystallographic characterization of the NHC derivative of complex **1.2F**.[23] Furthermore, the authors determined that the ^1H NMR resonance of this hydride was significantly upfield shifted as compared to the corresponding neutral dimeric copper-hydride $[(IPr)CuH]_2$ (δ -4.13 ppm vs. δ 2.67[22a] ppm, respectively). Furthermore, the authors found that the reactivity of cationic bridging copper-hydrides mimic that of their neutral counterparts (*e.g.* insertion into CO_2, alkynes, and reaction with alcohols to release H_2). This study as well as the formation of styrene derivatives in our reaction mixtures lends strong support for our hypothesis that complex **1.2F** forms during the catalytic cycle. Although we did not isolate complex **1.2F** directly, we set out to prove the existence of this key intermediate by performing catalytic deuterium labelling studies. As noted above,[22,23] as well as by others,[21,24] copper-hydrides are well-known to undergo hydrocupration of alkynes to generate alkenes after protonolysis (Scheme 1.7).

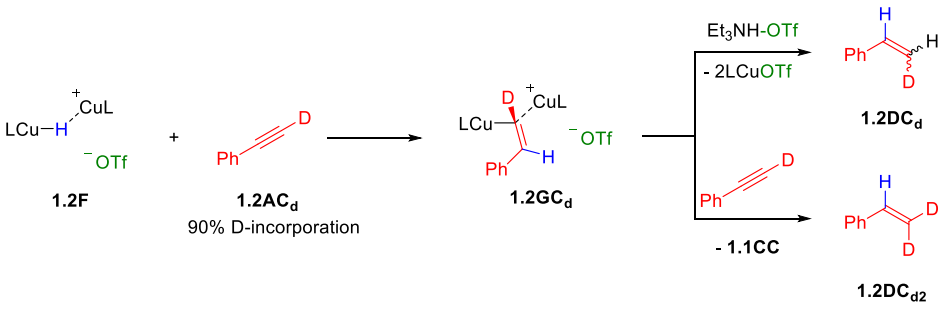

Scheme 1.7. Stoichiometric analysis exhibiting the insertion of a copper-hydride into deuterium labelled phenylacetylene. Presence of either mono- (**1.2DC$_d$**) or bis-deuterated (**1.2DC$_{d2}$**) styrene depends on the proton source for protodemetalation.

By employing the catalytic reaction conditions that gave the largest percentage of styrene (Table 1.1, entry 6), we could confirm the presence of a copper-hydride intermediate as well as determine what component could be responsible for inducing the demetalation of styrene derivatives **1.2D** from the copper (alkyne or the ammonium triflate salt). Using deuterium labelled phenylacetylene **1.2AC$_d$** (90% deuterium incorporation) with pinacolborane in the presence of 2.5 mol% LCuOTf and 5 mol% NEt_3, we observed the formation of the geminal bis-deuterated styrene **1.2DC$_{d2}$** by ^{1}H NMR with 75% incorporation of deuterium (Figure 1.4). This prevalence of the alkyne hydrocupration reaction is strongly indicative of the intermediacy of a transient copper-hydride in this reaction.

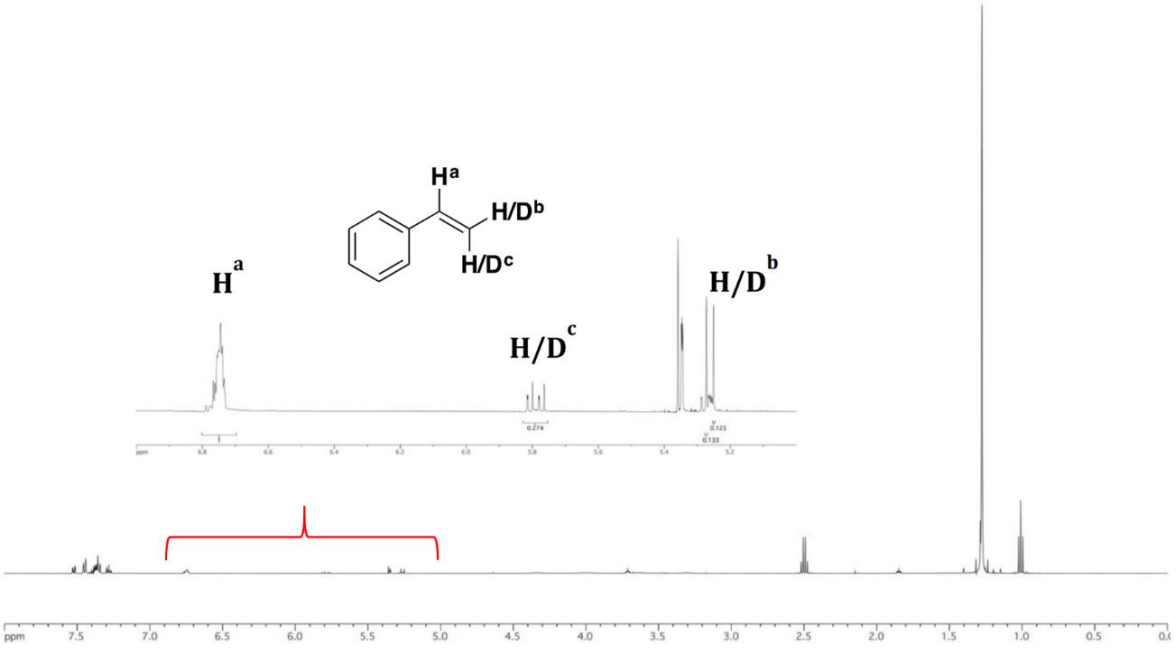

Figure 1.4. ^{1}H NMR spectrum of the catalytic dehydrogenative borylation reaction utilizing deuterium labelled phenylacetylene as the substrate in DCM shows the formation of *gem*-bis-deuterated styrene **1.2DC$_{d2}$**.

Since we know that terminal alkynes do not react with our transient copper-hydrides *via* dehydrogenation of the acetylide proton, we confirmed that the reaction of Et_3NH-OTf with the Cu-H bond is responsible for the extrusion of H_2 using the reaction depicted in Scheme 1.8.

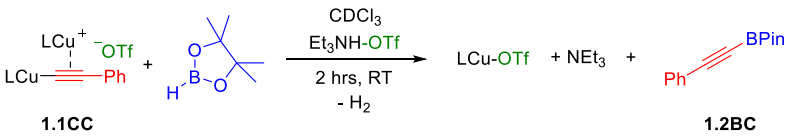

Scheme 1.8. Reaction of biscopper acetylide complexes **1.1CC** with pinacolborane and Et_3NH-OTf gives LCu-OTf, NEt_3, and the expected alkynylboronate **1.2BC**.

Reaction of a stoichiometric chloroform solution of biscopper acetylide **1.1CC** with pinacolborane in the presence of 1 equivalent of Et_3NH-OTf immediately produced bubbles, which were confirmed to be H_2 by ^1H NMR spectroscopy. After 2 hours at room temperature, multinuclear NMR spectroscopy confirmed the presence of LCuOTf, NEt_3, and alkynylboronate **1.2BC** in a 2:1:1 ratio.

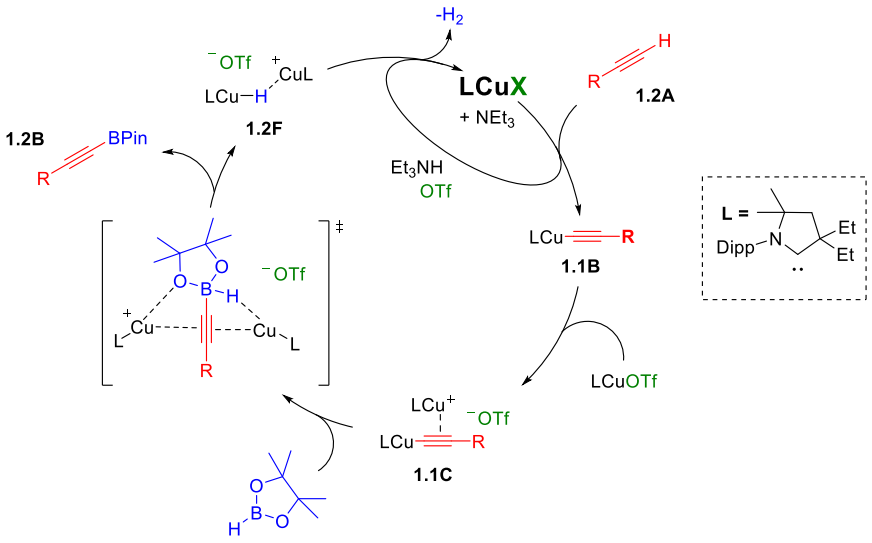

Figure 1.5. Experimentally determined mechanism for the dehydrogenative borylation reaction between terminal alkynes and pinacolborane.

In this section, we used a series of catalytic and stoichiometric reactions to support our hypothesized reaction mechanism for the (CAAC)Cu-OTf catalyzed dehydrogenative borylation reaction of terminal alkynes (Figure 1.5). We have also established the clear intermediacy of both biscopper acetylide complexes **1.1B** and copper-hydrides **1.2F** in this reaction. Confirmation of Cu-H participation in this reaction is important because none of the reaction conditions employed

are known to promote copper-hydride formation. Their participation further supports my initial hypothesis that these transient complexes can function as intermediates in catalytic reactions falling outside their traditional niche. Finally, to close the catalytic cycle, we have shown that the dehydrogenation step occurs by reaction of the copper-hydride **1.2F** with the Et_3NH-OTf that was generated upon terminal alkyne metalation.

1.3 Copper-Catalyzed (*E*)-β-Hydroboration of Terminal Alkynes with Pinacolborane

In Section 1.2, we showed that protection of the C-C triple bond of terminal alkynes eliminated the competing anti-Markovnikov hydroboration reaction. In the following section, we set out to prove that simple modification of the catalyst system used in Section 1.2 would allow for a switch in the reactivity of the active catalyst. More specifically, that changing the anion from triflate to a more basic alkoxide would allow us to selectively form anti-Markovnikov (*E*)-β-hydroboration products **1.2C**.

1.3.1 Determination of the Standard Reaction Conditions and Substrate Scope for the Hydroboration of Terminal Alkynes

Alkenylboronate esters have been prepared by both dehydrogenative borylation of styrenes[25] and transition metal-catalyzed hydroboration of the corresponding alkynes;[26] however, very few reports on these reactions employ inexpensive base-metals.[27,28] Using copper, Yun *et al.*[29] recently described the first example of an atom efficient methodology to selectively afford either (*E*)- or (*Z*)-β-hydroboration products of terminal alkynes using HBDan as the boron partner. Aside from this report, there were no extensive investigations detailing the hydroboration of terminal alkynes using pinacolborane and a copper catalyst to afford (*E*)-β-hydroboration products.

Since we previously noted the presence of these hydroboration products in Table 1.1, we set out to optimize the catalyst selectivity for this reaction. As mentioned in the introduction, we reported on the role of the X ligand in the mechanism of the CuAAC reaction,[18a] and in a follow-up report,[18b] we found that more basic anions favored monocopper acetylides **1.1B** rather than biscopper acetylides **1.1C**. These monocopper acetylide complexes no longer feature protection of the C-C π-bond and are therefore hypothesized to undergo rapid and selective hydroboration of the triple bond to afford (*E*)-β-hydroboration products **1.2C**.

We began our investigation by again confirming that there is no reaction between the alkyne and HBPin in the absence of catalyst (

Table 1.2, entry 1). Increasing the basicity of the X ligand increases the selectivity for the hydroboration reaction, with phenoxide ($^{-}$OPh) giving the best result (entries 2-4). Similarly, more polar solvents also increased the conversion and selectivity for the alkenylboronate product **1.2CC** (entries 5-6) with acetonitrile giving the best result at 94% conversion (entry 7). Decreasing the concentration of the reaction mixture (entries 8-9) or the catalyst loading (entries 10-11) had deleterious effects on the conversion, and therefore high reagent concentrations of 2.3 mol/L with 2.5 mol% catalyst loading was found to be ideal.

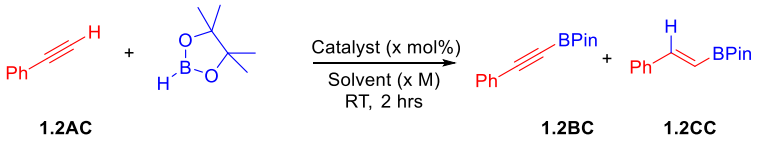

Scheme 1.9. Reaction conditions for the optimization of the copper catalyzed hydroboration reaction of terminal alkynes.

Table 1.2. Optimization of the hydroboration reaction of terminal alkynes with pinacolborane. The reactions were carried out at room temperature for 2 hours in a test tube under an argon atmosphere using 0.69 mmol of phenylacetylene and 0.71 mmol of pinacolborane. [a] Measured by ^{1}H NMR using CH_2Cl_2 or toluene as an internal standard.

Entry	Cat. (mol%)	Solvent	Conc. (M)	1.2BC (%)[a]	1.2CC (%)[a]
1	-	C_6D_6	2.3	0	0
2	LCuOBz (2.5)	C_6D_6	2.3	20	30
3	LCuOAc (2.5)	C_6D_6	2.3	10	40
4	LCuOPh (2.5)	C_6D_6	2.3	0	61
5	LCuOPh (2.5)	CD_2Cl_2	2.3	0	85
6	LCuOPh (2.5)	THF-d_8	2.3	0	79
7	**LCuOPh (2.5)**	**CD_3CN**	**2.3**	**0**	**94**
8	LCuOPh (2.5)	CD_3CN	1.6	0	91
9	LCuOPh (2.5)	CD_3CN	1.3	0	77
10	LCuOPh (1)	CD_3CN	2.3	0	81
11	LCuOPh (0.5)	CD_3CN	2.3	0	53

Using these optimized conditions, the scope of the hydroboration reaction was investigated at room temperature in acetonitrile (2.3 ± 0.1 M) using 3.65 mmol of alkyne and 3.74 mmol of borane in the presence of 2.5 mol% (^{Et}CAAC)CuOPh (Figure 1.6). This catalyst is compatible with a wide range of electronically diverse terminal alkynes. In most cases, the NMR spectra of the crude reaction mixture showed excellent selectivity, and the alkenylboronates **1.2CA-M** were isolated in good to excellent yields. Importantly, purification of products **1.2CA-M** is readily achieved in air by filtration of the crude reaction media through a short plug of silica using pentane as the eluent. This protocol is also applicable to gram-scale syntheses, as shown with **1.2CC**.

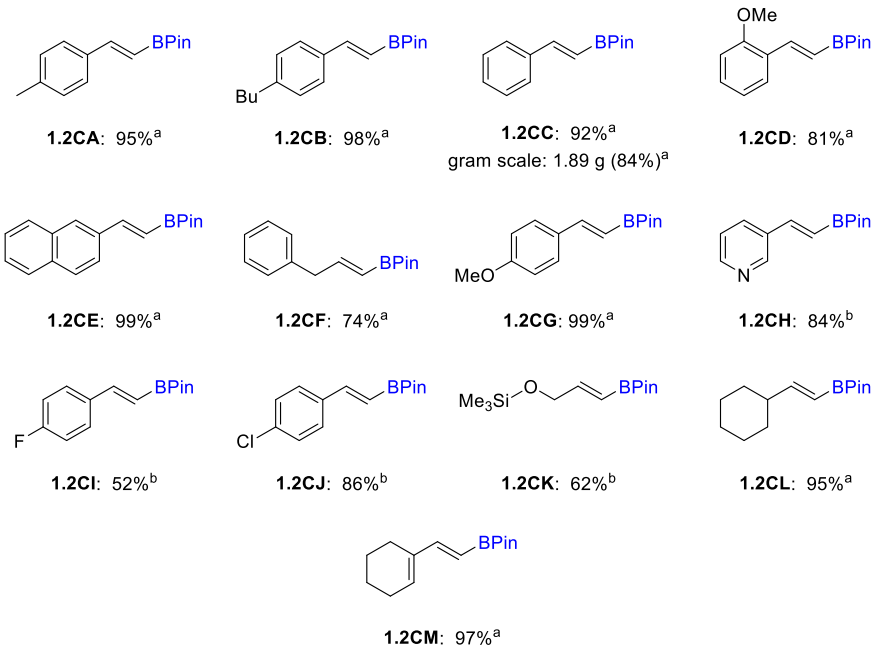

Figure 1.6. Substrate scope for the hydroboration reaction catalyzed by LCuOPh. [a] reaction time 2 hours. [b] reaction time 4 hours.

1.3.2 Elucidation of the Mechanism for the Hydroboration Reaction

Since the reaction of terminal alkynes with LCuOPh immediately forms monocopper acetylide complexes **1.1B** and phenol (PhOH), we confirmed the fate of this extruded PhOH by combining a stoichiometric mixture of phenol and pinacolborane. Upon addition of HBPin to a C_6D_6 solution of PhOH, we observed the immediate extrusion of gaseous H_2 and the formation of PhOBPin, which was determined to be catalytically inert (Scheme 1.10). This dehydrogenative coupling would further serve to drive the alkyne metalation to completion with no possibility of a reversible reaction.

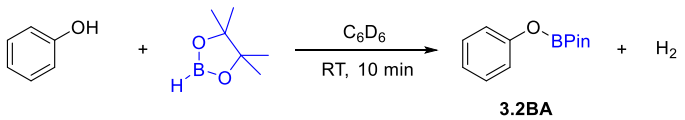

Scheme 1.10. Addition of pinacolborane to phenol immediately generates the dehydrogenatively coupled product **3.2BA**.

Starting from monocopper acetylide complexes **1.1B**, we set out to confirm our hypothesis that the unprotected triple bond would be susceptible to hydroboration and subsequently protonolysis to eliminate hydroboration products **1.2C**. This protonolysis step would regenerate the monocopper acetylide and close the catalytic cycle (Figure 1.7).

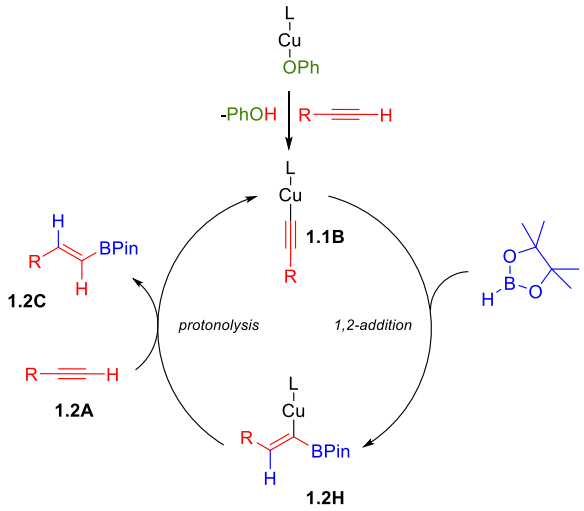

Figure 1.7. Proposed mechanism for the LCuOPh catalyzed hydroboration of terminal alkynes with pinacolborane.

For the 1, 2-addition step, Roesky and coworkers used density functional theory (DFT) to show that this hydroboration of pinacolborane onto a metal-acetylide C-C π-bond is thermodynamically favorable,[30] which implies that this transformation could be evoked as a potential elementary reaction step under our catalytic conditions. In this report, however, the authors did not make any attempts to experimentally confirm this result. We attempted the experimental preparation of vinyl-cuprate **1.2HC** by addition of pinacolborane to a benzene solution of **1.1BC**; however, we observed immediate deposition of black insoluble precipitate, which is indicative of decomposition of our copper complex. Subsequent alteration of the reaction conditions (solvent and temperature) did not change the experimental outcome.

This decomposition likely results from the instability of the copper-vinyl complex **1.2HC**. In an effort to confirm its presence in this reaction, we reasoned that it could be cleaved *in-situ* by

a different alkyne (Scheme 1.11). This reaction would then form a different copper-acetylide complex that could be confirmed by ^{1}H and ^{13}C NMR as well as the phenyl alkenylboronic ester product.

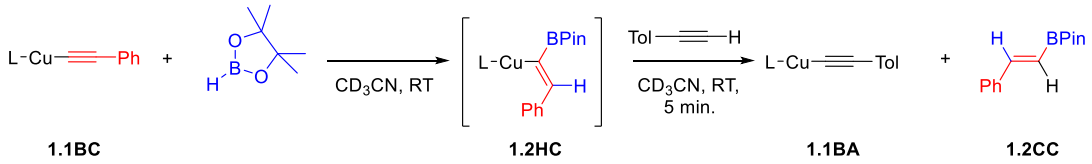

Scheme 1.11. This stoichiometric crossover experiment illustrates the potential intermediacy of **1.2HC** as well as the previously noted ability of terminal alkynes to cleave the copper-carbon bond of vinyl-cuprates to generate alkenylboronates **1.2CC**.

Excitingly, we found that addition of pinacolborane to a room temperature acetonitrile solution of monocopper phenylacetylide **1.1BC** and 3 equivalents of tolylacetylene **1.2AA** led to the quantitative formation of alkenylboronate **1.2CC** within 5 minutes. Evaporation of the volatiles and washing of the residue with pentane afforded monocopper tolylacetylide **1.1BA** as a white solid. This result strongly supports the intermediate formation of copper-vinyl complex **1.2HC** within the catalytic cycle and that it can be cleaved by a terminal alkyne C-H bond.

To further support its participation in this reaction, we reanalyzed the kinetic data from Figure 1.2 from the perspective of the hydroboration reaction and were excited to find that complex **1.2CC** preferentially catalyzes this process (Figure 1.8). This result, coupled with the stoichiometric crossover experiment, clearly indicate the high likelihood of monocopper acetylide complexes lying within the catalytic cycle for the anti-Markovnikov hydroboration reaction, and by extension, that the 1,2-addition of pinacolborane to the copper-acetylide C-C π-bond is plausible.

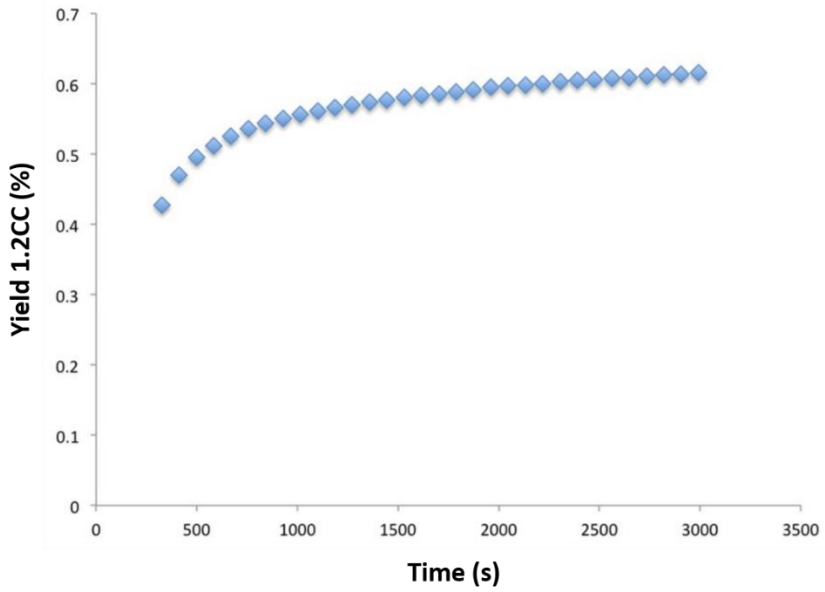

Figure 1.8. Kinetic profile of the formation of **1.2CC** using 2.5 mol% **1.1BC** as the catalyst with a 1:1 mixture of phenylacetylene and pinacolborane.

We next turned our attention to the final protonolysis step to liberate the free hydroboration products and regenerate the starting monocopper acetylide. As was shown previously,[18a] as well as in the DHBTA reaction, terminal alkynes are sufficiently acidic to cleave the copper-carbon bond of intermediary vinyl-cuprates, which was also displayed in Scheme 1.11. As a final proof of principle, we conducted a deuterium labeling experiment using deuterium labelled phenylacetylene **1.2AC$_d$** (Figure 1.9) and found a 90% incorporation of deuterium at the terminal position of product **1.2CC** by ^{1}H NMR spectroscopy (see appendix Figure 1.13).

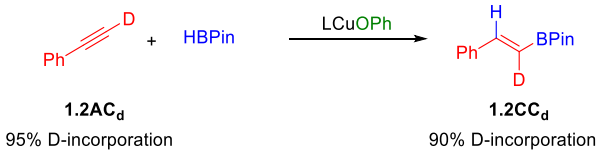

Figure 1.9. Deuterium labeling experiment supports the hypothesis that terminal alkynes are sufficiently acidic to cleave the copper-carbon bond.

1.4 Conclusions

In summary, we have disclosed the first examples of a highly selective dehydrogenative borylation reaction of terminal alkynes with pinacolborane that uses an inexpensive metal center supported by a readily accessible ligand. Furthermore, we have shown that replacement of the triflate anion with phenolate causes a switch in catalyst selectivity for (*E*)-β-hydroboration products. We have shown that these reactions are extremely accommodating to a wide range of substituents and electronic environments on the substrate scaffold. Furthermore, the exceptional selectivity of the catalyst made isolation of the products facile.

Through a series of stoichiometric and catalytic reactions, we have shown that the dehydrogenative borylation reaction must form σ,π-biscopper acetylide complexes as the key intermediate. Without formation of these complexes, the reaction was found to be unselective for alkynylboronates. Reaction of pinacolborane on these bimetallic intermediates leads to the generation of a transient copper hydride, whose existence was strongly supported through a deuterium labeling experiment. Finally, we were able to definitively show that dehydrogenation proceeds through the reaction of Et_3NH-OTf with this transiently generated copper-hydride, which closes the catalytic cycle.

During this investigation into the DHBTA reaction, we noted the ability of monocopper acetylide complexes to catalyze the hydroboration reaction.[31] We further found through a catalytic deuterium labeling study, coupled with a stoichiometric crossover experiment that terminal alkynes are sufficiently acidic to induce protonolysis of unstable vinyl-cuprates, which allows for the extrusion of alkenylboronate products and the reformation of the starting monocopper acetylide catalyst to close the cycle.

Chapter 1 has been adapted from materials published in Romero, E. A.; Jazzar, R.; Bertrand, G., "Copper-Catalyzed Dehydrogenative Borylation of Terminal Alkynes with Pinacolborane", *Chem. Sci.* **2017**, *8*, 165 – 168 and Romero, E. A.; Jazzar, R.; Bertrand, G., "(CAAC)CuX-catalyzed hydroboration of terminal alkynes with pinacolborane directed by the x-ligand", *J. Organomet. Chem.* **2017**, *829*, 11 – 13. The dissertation author was the primary investigator of these publications.

1.5 Appendix

1.5.1 General Considerations

All reactions were performed under an atmosphere of argon using standard Schlenk or dry box techniques; solvents were dried over Na metal, or CaH_2. Reagents of analytical grade were obtained from commercial suppliers, dried over 4Å molecular sieves and degassed before use. ^{1}H, ^{13}C, ^{11}B, and ^{19}F NMR spectra were obtained with a Bruker Advance 300 MHz, and a Varian INOVA 500 MHz spectrometer. Chemical shifts (δ) are reported in parts per million (ppm) relative to TMS and were referenced to the residual solvent peak. NMR multiplicities are abbreviated as follows: s = singlet, d = doublet, t = triplet, q = quartet, quin = quintet, sex = sextet, m = multiplet, br = broad signal. Complexes (Et_2CAAC)CuOTf (LCuOTf),[18a] (Et_2CAAC)CuOPh (LCuOPh),[18a] (Et_2CAAC)CuOAc (LCuOAc),[18a] (MenthylCAAC)CuOTf (L_2CuOTf),[18a] (Et_2CAAC)CuOBz (LCuOBz),[18b] and (IPr)CuOTf (L_3CuOTf)[32] were prepared following literature procedures.

1.5.2 Optimization Table Procedures

A) <u>General Procedure for Dehydrogenative Borylation Optimization:</u>

In a culture tube equipped with a magnetic stir bar were added cat. (x mol%) and *p*-tolylacetylene (0.087 ml, 0.69 mmol). y μL (determined according to the named concentration M)

of Solvent was added followed immediately by appropriate amount of base additive (z mol%). After 1-minute stirring, HBPin (0.100 ml, 0.69 mmol) was added in a single portion and the resulting solution was allowed to stir for 2 hours at room temperature. ^{1}H NMR yields were based on 1 equivalent addition of 1,4-dioxane after the 2-hour stirring period.

B) General Procedure for Hydroboration Optimization:

In a culture tube equipped with a magnetic stir bar were added LCuX (0.5, 1 or 2.6 mol%), phenylacetylene (0.69 mmol) and y μL of Solvent (determined according to the named concentration M) of Solvent. After 1-minute stirring, HBPin (0.71 mmol) was added in a single portion and the resulting solution was stirred for 2 hours at room temperature. 1H NMR yields were based on 1 equivalent addition of dichloromethane (entry 1-4 and 6-11) or toluene (entry 5) after the 2-hour stirring period.

1.5.3 Dehydrogenative Borylation Reaction Protocols

In a Schlenk tube under an argon atmosphere were added C_6H_6 (17 mL), the alkyne (1.82 mmol), pinacol borane (0.264 mL, 1.82 mmol), and triethylamine (0.012 mL, 0.091 mmol). Then, LCuOTf (0.024 g, 0.045 mmol%) was added to the mixture and the reaction was left stirring at room temperature until the reaction had completed. After completion, all the volatiles were evaporated under vacuum and 5 mL of pentane was added. The mixture was passed, under argon, through a short column packed with dry neutral alumina (3 cm diameter x 5 cm high) using 30 mL of pentane as eluent. Evaporation of the volatiles under vacuum afforded the corresponding products **1.2BA-O**.

1.5.4 Characterization of Products 1.2BA-O

1.2BA: White solid (m.p. 103-105 ^{o}C) 0.437 g (99% yield). ^{1}H NMR ($CDCl_3$, 500 MHz) δ = 1.27 (s, 12H), 2.29 (s, 3H), 7.07 (d, J = 8.0 Hz, 2H), 7.38 (d, J = 8.0 Hz, 2H) ppm. ^{13}C NMR ($CDCl_3$, 125.7 MHz) δ = 21.5, 24.6, 84.2, 102.0 (br), 118.6, 129.0, 132.5, 139.7 ppm.

1.2BB: Deliquescent solid 0.432 g (98% yield). ^{1}H NMR ($CDCl_3$, 500 MHz) δ = 1.03 (s, 12H), 2.35 (s, 3H), 6.75 (t, J = 8.0 Hz, 1H), 6.79 (d, J = 8.0 Hz, 1H), 6.89 (t, J = 8.0 Hz, 1H), 7.45 (d, J = 8.0 Hz, 2H) ppm. ^{13}C NMR ($CDCl_3$, 125.7 MHz) δ = 20.7, 24.7, 84.1, 101.0 (br), 122.6, 125.9, 129.4, 129.7, 133.3, 141.6 ppm.

1.2BC: Deliquescent solid 0.411 g (99% yield). ^{1}H NMR ($CDCl_3$, 500 MHz) δ = 1.22 (s, 12H), 7.23 (m, 3H), 7.41 (m, 2H) ppm. ^{13}C NMR ($CDCl_3$, 125.7 MHz) δ = 24.8, 84.6, 101.9 (br), 121.9, 128.4, 129.5, 132.7 ppm.

1.2BD: Deliquescent solid 0.413 g (88% yield). ^{1}H NMR (C_6H_6, 500 MHz) δ = 1.00 (s, 12H), 3.19 (s, 3H), 6.31 (d, J = 8.0 Hz, 1H), 6.55 (t, J = 8.0 Hz, 1H), 6.91 (t, J = 8.0 Hz, 1H), 7.44 (d, J = 8.0 Hz, 1H) ppm. ^{13}C NMR (C_6H_6, 125.7 MHz) δ = 24.7, 55.1, 83.9, 98.5 (br), 110.9, 112.3, 120.4, 130.7, 134.7, 160.6 ppm. HRMS analysis was unsuccessful.

1.2BE: Deliquescent solid 0.407 g (81% yield). ^{1}H NMR (C_6D_6, 500 MHz) δ = 1.06 (s, 12H), 7.12 (m, 2H), 7.32 (m, 1H), 7.34 (m, 1H), 7.40 (m, 1H), 7.43 (m, 1H), 7.85 (s, 1H) ppm. ^{13}C NMR (C_6D_6, 125.7 MHz) δ = 23.4, 82.8, 101.0 (br), 118.5, 125.4, 125.9, 127.2, 127.4, 131.8, 132.1, 132.3 ppm.

1.2BF: Deliquescent solid 0.374 g (85% yield). ^{1}H NMR (C_6D_6, 500 MHz) δ = 1.03 (s, 12H), 3.32 (s, 2H) 7.00-7.20 (m, 5H) ppm. ^{13}C NMR (C_6D_6, 125.7 MHz) δ = 24.7, 25.9, 83.8, 101.6 (br), 126.9, 128.2, 128.7, 135.9 ppm.

1.2BG: Deliquescent solid 0.392 g (85% yield). ^{1}H NMR (C_6D_6, 300 MHz) δ = 1.23 (s, 12H), 7.51 (s, 4H) ppm. ^{13}C NMR ($CDCl_3$, 125.7 MHz) δ = 24.7, 84.5, 99.5, 113.1, 118.2, 126.4, 131.9, 132.6 ppm.

1.2BH: Deliquescent solid 0.367 g (85% yield). ^{1}H NMR ($CDCl_3$, 500 MHz) δ = 1.31 (s, 12H), 7.0 (t, J = 8.7 Hz, 2H), 7.51 (m, 2H) ppm. ^{13}C NMR ($CDCl_3$, 125.7 MHz) δ = 24.7, 84.2, 100.7 (br), 115.5 (d, J = 22.1 Hz), 117.9 (d = 3.5 Hz), 134.7 (J = 8.5 Hz), 163.3 (J = 250.4 Hz) ppm.

1.2BI: Deliquescent solid 0.392 g (82% yield). ^{1}H NMR (C_6D_6, 500 MHz) δ = 1.02 (s, 12H), 6.75 (d, J = 8.5 Hz, 2H), 7.03 (d, J = 8.5 Hz, 2H) ppm. ^{13}C NMR (C_6D_6, 125.7 MHz) δ = 24.7, 84.2, 100.6 (br), 121.0, 129.0, 133.9, 135.5 ppm.

1.2BJ: Colorless oil 0.250 g (89% yield). ^{1}H NMR ($CDCl_3$, 300 MHz) δ = 0.07 (s, 9H), 1.17 (s, 12H), 4.12 (s, 2H) ppm. ^{13}C NMR (C_6D_6, 125.7 MHz) δ = 0.3, 24.7, 51.3, 84.3, 101.2 (br) ppm.

1.2BK: Deliquescent solid 0.405 g (95% yield). ^{1}H NMR (C_6D_6, 500 MHz) δ =1.26 (m, 16H), 1.00 (m, 13H), 1.19 (m, 1H) 1.38-1.64 (m, 8H), 2.25 (m, 1H) ppm. ^{13}C NMR (C_6D_6, 125.7 MHz) δ = 24.5, 24.6, 25.7, 29.7, 32.1, 83.5, 108.3 (br) ppm.

1.2BL: Colorless oil 0.437 g (99% yield). ^{1}H NMR (C_6D_6, 500 MHz) δ = 1.01, 1.410 (quint, J = 7.0 Hz, 2H), 1.99 (t, J = 7.0 Hz, 2H), 3.09 (t, J = 7.0 Hz, 2H) ppm. ^{13}C NMR (C_6D_6, 125.7 MHz) δ = 16.9, 24.7, 31.0, 43.3, 83.8, 102.3 (br) ppm.

1.2BM: Colorless oil 0.404 g (99% yield). ^{1}H NMR (C_6D_6, 500 MHz) δ = 0.05 (s, 9H), 0.93 ppm. ^{13}C NMR (C_6D_6, 125.7 MHz) δ = 0.51, 24.6, 84.0, 110.1 (br) ppm.

1.2BN: Colorless oil 0.441 g (96% yield). ^{1}H NMR (C_6D_6, 300 MHz) δ = 1.31 (s, 12H), 1.80 (quint, J = 6.0 Hz, 2H), 2.29 (t, J = 6.0 Hz, 2H), 2.40 (t, J = 6.0 Hz, 2H), 3.61 (s, 3H) ppm. ^{13}C NMR (C_6D_6, 125.7 MHz) δ = 18.9, 23.6, 24.7, 32.5, 51.0, 83.7, 103.2, 172.6 ppm.

1.2BO: Colorless oil 0.400 g (99% yield). ^{1}H NMR (C_6D_6, 500 MHz) δ = 0.67 (t, J = 7.5 Hz, 3H), 1.01 (s, 12H), 1.23 (sept, J = 7.5 Hz, 2H), 1.96 (t, J = 7.5 Hz, 2H) ppm. ^{13}C NMR (C_6D_6, 125.7 MHz) δ = 13.2, 19.0, 21.6, 24.3, 30.0, 83.2, 104.0 (br) ppm.

1.5.5 Dehydrogenative Borylation Mechanistic Investigation

A) Kinetic Experiments (Figure 1.2 & Figure 1.8)

All the kinetic measurements were performed in a J-Young NMR tube at room temperature on a Bruker 300MHz NMR machine using the multi_zgvd command. Conversions were measured by following the growth of the characteristic signals for **1.2BA** or **1.2CA** with respect to the depleting signals for **1.2AA**. In each kinetic run, 0.45 mmol (0.057 mL) of **1.2AA** and 0.45 mmol (0.066 mL) of pinacolborane were used in combination with 2.5 mol% of the catalyst (either LCuOTf: 6.8 mg or LCuCCPh: 5.4 mg), the corresponding amount of Et_3N (either 5 mol%: 0.0032 mL or 2.5 mol%: 0.0016 mL) and Et_3NH-OTf (1.4 mg, 2.5 mol%) when needed. At the end of these experiments, the reaction mixture was transferred to a Schlenk tube, the volatiles were evaporated under vacuum, and 5 mL of pentane was added. The mixture was passed through a short column packed with dry neutral alumina (3 cm diameter x 5 cm high) under an argon atmosphere, using pentane as eluent. Evaporation of the volatiles under vacuum afforded the corresponding product as white solids.

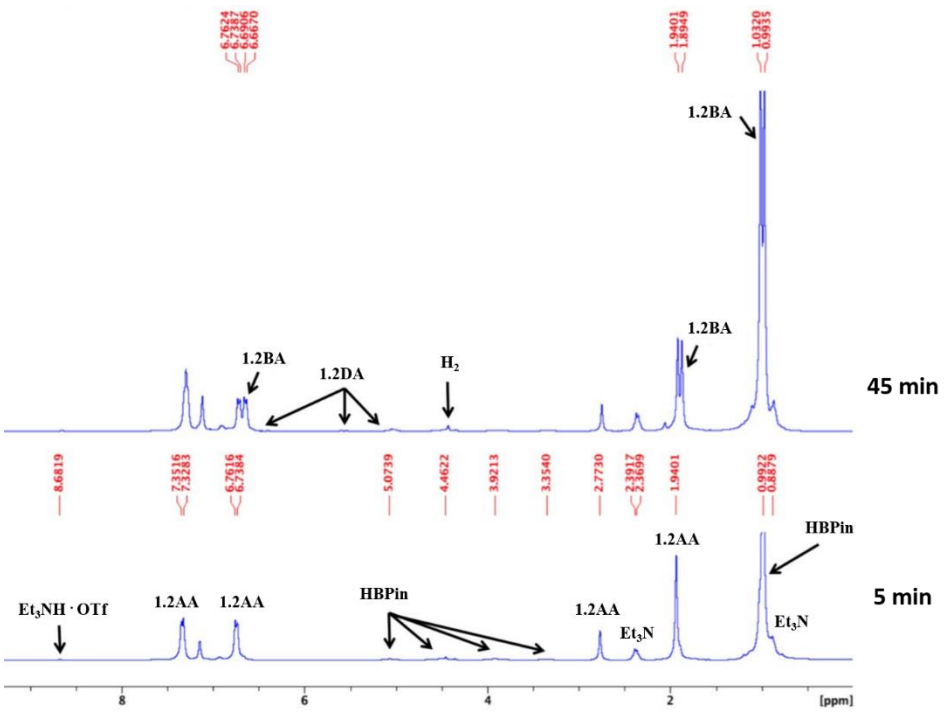

Figure 1.10. Selected spectra from the kinetic run using **Cat**: LCuCCPh + Et_3N (2.5 mol%) + Et_3NH-OTf (2.5 mol%).

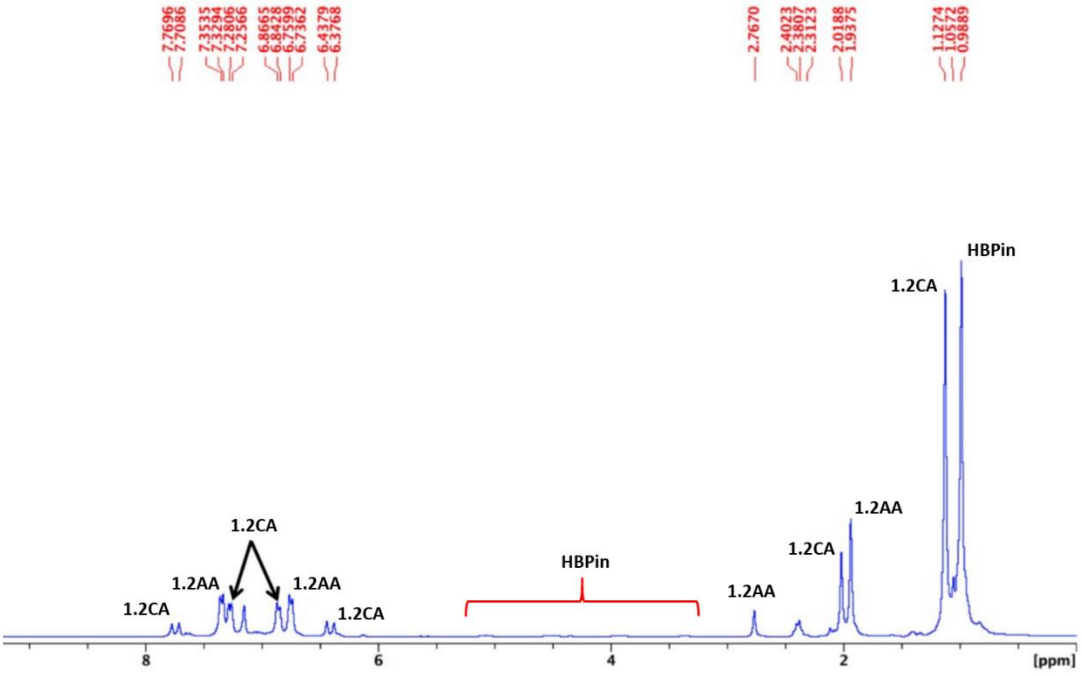

Figure 1.11. A selected spectrum taken 5 minutes after addition of HBPin during the kinetic run using **Cat**: LCuCCPh + Et_3N (5 mol%).

NMR of the isolated **1.2CA**, which was isolated at the end of the kinetic run using **Cat**: LCuCCPh + Et_3N (5 mol%). The reaction was complete within 30 minutes. Colorless oil: 95% yield. ^1H NMR ($CDCl_3$, 300 MHz): δ = 1.26 (s, 12H), 2.28 (s, 3H), 6.11 (d, J = 18.6 Hz, 1H), 7.10 (d, J = 7.9 Hz, 2H), 7.34 (d, J = 7.6 Hz, 2H), 7.38 (d, J = 19.5 Hz, 1H) ppm. ^{13}C NMR ($CDCl_3$, 75 MHz) δ = 21.3, 24.8, 83.2, 115.0 (br), 127.0, 129.3, 134.8, 138.8, 149.5 ppm.

B) Deuterium Labeling for the Dehydrogenative Transformation (Figure 1.4 & Scheme 1.7)

In a Schlenk tube fitted with a magnetic stir bar were added under an argon atmosphere CD_2Cl_2 (17 mL), phenylacetylene-d **1.2AC$_d$** (0.200 mL, 1.82 mmol), pinacolborane (0.264 mL, 1.82 mmol), and triethylamine (0.012 mL, 0.091 mmol). Then, LCuOTf (0.024 g, 0.045 mmol%) was added to the mixture and the reaction was left stirring at room temperature for three hours. After this time, ^1H NMR analysis of the reaction media showed the formation of a mixture of **1.2BA** and **1.2DA$_{d2}$**.

C) Evidence for the formation of **1.1CC** by proton mediated rearrangement of **1.1BC** using Et_3NH-OTf (Scheme 1.5 & Figure 1.3)

A J-Young NMR tube was charged with $CDCl_3$ (1 mL), **1.1BC** (20 mg), and Et_3NH-OTf (5.3 mg, 0.5 eq). The NMR spectra taken immediately after mixing the components together shows the clean formation of the biscopper acetylide complex **1.1CC** as well as the free alkyne **1.2AC** and triethylamine. The NMR spectra of complex **1.1CC** is in agreement with the literature.[18a] See the ^1H NMR spectrum in Figure 1.3. Reaction of complex **1.1BC** with Et_3NH-OTf yields free

alkyne **1.2AC**, biscopper acetylide **1.1CC**, and NEt_3 by ^1H NMR spectroscopy. and below for the ^{13}C NMR spectrum.

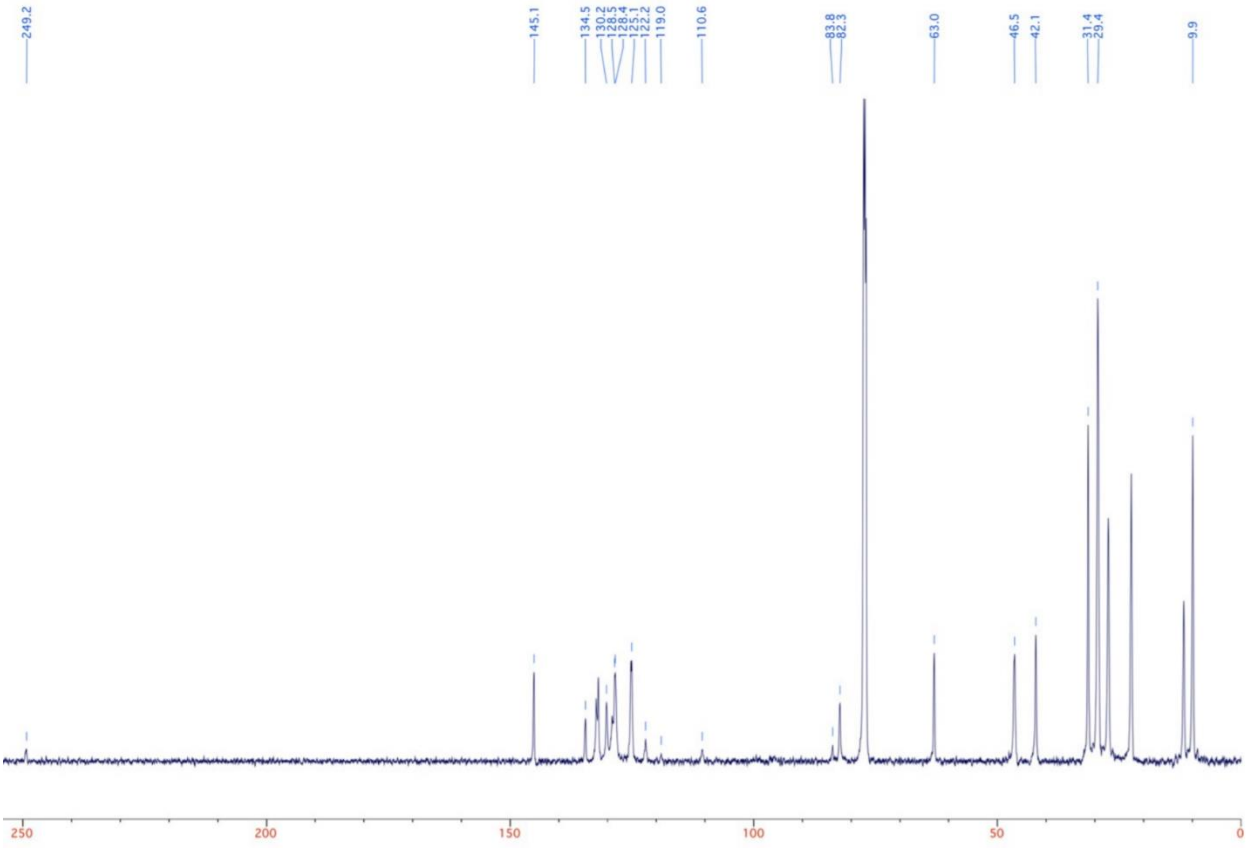

Figure 1.12. ^{13}C NMR spectrum of the reaction of complex **1.1BC** with Et_3NH-OTf.

1.5.6 Hydroboration Reaction Protocol

To a flame dried Schlenk was added LCuOPh (2.5 mol %) and a magnetic stir bar under an argon atmosphere. 0.097 mL freshly distilled MeCN was added to fully dissolve catalyst and yield a 2.3 ± 0.1 M solution depending on the nature of the alkyne. Alkyne (0.56 mmol, 1 eq.) was added followed immediately by pinacolborane (0.57 mmol, 1.025 eq). The resulting solution is stirred at room temperature for 2 hours. After this time, the volatiles were evaporated under vacuum. 10 mL pentane was added to residue. This solution was passed through a pad of silica (5

cm diameter x 5 cm high) to remove insoluble components. Elution with 2 x 10 mL of pentane, followed by evaporation under vacuum yielded pure products **1.2CA**-**M**.

1.5.7 Characterization of Products 1.2CA-M

1.2CA: Colorless oil 0.13 g (95% yield). ^{1}H NMR ($CDCl_3$, 300 MHz): δ = 1.26 (s, 12H), 2.28 (s, 3H), 6.11 (d, J = 18.6 Hz, 1H), 7.10 (d, J = 7.9 Hz, 2H), 7.34 (d, J = 7.6 Hz, 2H), 7.38 (d, J = 19.5 Hz, 1H) ppm; ^{13}C NMR ($CDCl_3$, 75 MHz) δ = 21.3, 24.8, 83.2, 115.0 (br), 127.0, 129.3, 134.8, 138.8, 149.5 ppm.

1.2CB: Colorless oil 0.16 g (98% yield). ^{1}H NMR ($CDCl_3$, 300 MHz): δ = 0.95 (t, J = 7.3 Hz, 3H), 1.33 (s, 12H), 1.36 (m, 2H), 1.62 (m, 2H), 2.62 (t, J = 7.8 Hz, 2H), 6.16 (d, J = 18.4 Hz, 1H), 7.17 (d, J = 8.0 Hz, 2H), 7.43 (d, J = 18.1 Hz, 1H), 7.44 (d, J = 8.4 Hz, 2H) ppm; ^{13}C NMR ($CDCl_3$, 75 MHz) δ = 14.0, 22.4, 24.9, 33.6, 35.6, 83.3, 127.1, 128.7, 135.1, 144.0, 149.6 ppm, C[B] was not detected.

1.2CC: Colorless oil 0.12 g (92% yield). ^{1}H NMR ($CDCl_3$, 300 MHz): δ = 1.33 (s, 12H), 6.22 (d, J = 18.4 Hz, 1H), 7.33 (m, 3H), 7.45 (d, J = 18.5 Hz, 1H), 7.51 (d, J = 7.2 Hz, 2H) ppm; ^{13}C NMR ($CDCl_3$, 75 MHz) δ = 24.9, 83.4, 127.2, 128.7, 129.0, 137.6, 149.6 ppm, C[B] was not detected.

1.2CD: Colorless oil 0.12 g (81% yield). ^{1}H NMR ($CDCl_3$, 300 MHz): δ = 1.34 (s, 12H), 3.88 (s, 3H), 6.22 (d, J = 18.7 Hz, 1H), 6.90(d, J = 8.6 Hz, 2H), 6.96 (t, J = 7.5 Hz, 1H), 7.29 (m, 1H), 7.58 (dd, J = 1.5 Hz, 7.7 Hz, 1H), 7.82 (d, J = 18.5, 1H) ppm; ^{13}C NMR ($CDCl_3$, 75 MHz) δ = 24.9, 55.5, 83.3, 111.0, 120.7, 127.2, 130.1, 144.2, 157.5 ppm, C[B] was not detected.

1.2CE: Yellow oil 0.15 g (99% yield). ^{1}H NMR ($CDCl_3$, 300 MHz): δ = 1.40 (s, 12H), 6.43 (d, J = 18.4 Hz, 1H), 7.49 (m, 2H), 7.71 (d, J = 18.3 Hz, 1H), 7.82 (m, 4H), 7.90 (s, 1H) ppm;

^{13}C NMR ($CDCl_3$, 75 MHz) δ = 24.8, 83.3, 116.7 (br), 123.3, 126.3, 126.4, 127.7, 128.0, 128.3, 128.4, 133.4, 133.7, 135.0, 149.6 ppm.

1.2CF: Colorless oil 0.10 g (74% yield). ^1H NMR ($CDCl_3$, 300 MHz): δ = 1.28 (s, 12H), 3.51 (d, J = 6.1 Hz, 2H), 5.49 (d, J = 17.7 Hz, 1H), 6.80 (dt, J = 6.2 Hz, 17.7 Hz, 1H), 7.21 (t, J = 7.5 Hz, 3H), 7.30 (m, 2H) ppm; ^{13}C NMR ($CDCl_3$, 75 MHz) δ = 24.9, 42.4, 83.2, 126.2, 128.5, 129.0, 139.1, 152.5 ppm, C[B] was not detected.

1.2CG: Colorless oil 0.14 g (99% yield). ^1H NMR ($CDCl_3$, 300 MHz): δ = 1.28 (s, 12H), 3.73 (s, 3H), 6.02 (d, J = 18.5 Hz, 1H), 6.82 (d, J = 9.1 Hz, 2H), 7.38 (d, J = 18.2 Hz, 1H), 7.42 (d, J = 8.8 Hz, 2H) ppm; ^{13}C NMR ($CDCl_3$, 75 MHz) δ = 24.7, 55.0, 83.0, 113.9, 128.4, 130.2, 149.1, 160.2 ppm, C[B] was not detected.

1.2CH: Colorless oil 0.11 g (84% yield). ^1H NMR ($CDCl_3$, 300 MHz): δ = 1.20 (s, 12H), 6.15 (d, J = 18.5 Hz, 1H), 7.16 (dd, J = 7.8 Hz, 8.0 Hz, 1H), 7.27 (d, J = 18.5 Hz, 1H), 7.68 (d, J = 8.2 Hz, 2H), 8.40 (d, J = 3.6 Hz, 1H), 8.58 (s, 1H) ppm; ^{13}C NMR ($CDCl_3$, 75 MHz) δ = 24.7, 83.5, 119.2 (br), 123.5, 133.1, 145.5, 148.9, 149.6 ppm.

1.2CI: Colorless oil 0.07 g (52% yield). ^1H NMR ($CDCl_3$, 300 MHz): δ = 1.31 (s, 12H), 6.08 (d, J = 18.7 Hz, 1H), 7.02 (t, J = 8.4 Hz, 2H), 7.36 (d, J = 18.8 Hz, 1H), 7.45 (m, 2H) ppm; ^{13}C NMR ($CDCl_3$, 75 MHz) δ = 24.9, 83.5, 115.7 (d, J = 21.6), 128.8 (d, J = 8.3), 148.3, 163.3 (d, J = 248.6) ppm, C[B] was not detected.

1.2CJ: Yellow Deliquescent solid 0.13 g (86% yield). ^1H NMR ($CDCl_3$, 300 MHz): δ = 1.31 (s, 12H), 6.15 (d, J = 18.3 Hz, 1H), 7.29 (d, J = 8.6 Hz, 2H), 7.35 (d, J = 18.6 Hz, 1H), 7.40 (d, J = 8.6 Hz, 2H) ppm; ^{13}C NMR ($CDCl_3$, 75 MHz) δ = 24.8, 83.4, 117.2 (br), 128.2, 128.8, 134.6, 136.0, 148.0 ppm.

1.2CK: Colorless oil 0.09 g (62% yield). ^{1}H NMR ($CDCl_3$, 300 MHz): δ = 0.08 (s, 9H), 1.23 (s, 12H), 4.17 (dd, J = 1.9 Hz, 3.9 Hz, 1H), 5.69 (broad dt, J = 1.6 Hz, 18.0 Hz, 1H), 6.64 (dt, J = 3.9 Hz, 18.2 Hz, 1H) ppm; ^{13}C NMR ($CDCl_3$, 75 MHz) δ = 0.4, 24.8, 64.2, 83.2, 151.9 ppm, C[B] was not detected.

1.2CL: Colorless oil 0.13 g (95% yield). ^{1}H NMR ($CDCl_3$, 300 MHz): δ = 1.07 (m, 3H), 1.24 (s, 12H), 1.71 (m, 7H), 2.00 (m, 1H, br), 5.35 (dd, J = 1.1 Hz, 18.2 Hz, 1H), 6.55 (dd, J = 6.2 Hz, 18.2 Hz, 1H) ppm; ^{13}C NMR ($CDCl_3$, 75 MHz) δ = 24.9, 26.1, 26.3, 32.0, 43.4, 83.0, 159.9 ppm, C[B] was not detected.

1.2CM: Colorless oil 0.13 g (97% yield). ^{1}H NMR ($CDCl_3$, 300 MHz): δ = 1.23 (s, 12H), 1.55-1.63 (m, 4H), 2.11 (s, 4H, br), 5.39 (d, J = 18.43 Hz, 1H), 5.92 (s, br, 1H), 6.98 (d, J = 18.27 Hz, 1H) ppm; ^{13}C NMR ($CDCl_3$, 75 MHz) δ = 22.4, 22.5, 23.8, 24.8, 26.20, 83.0, 112.4 (br), 134.2, 137.2, 153.3 ppm.

1.5.8 Hydroboration Mechanistic Investigation

A) Reaction of phenol with pinacolborane (Scheme 1.10)

Solid phenol (1.10 mmol, 1 eq.) was added to an NMR tube followed by 0.5 mL C_6D_6. Once fully dissolved, pinacolborane (0.95 eq., 1.05 mmol) was added in one portion. **N.B.:** vigorous gas evolution upon HBPin addition was observed. The NMR tube was capped and inverted to homogenize the solution and the cap removed immediately after to vent the pressure. Bubbles ceased after 10 min and the NMR spectra revealed quantitaive formation of PhOBPin. ^{1}H NMR (C_6D_6, 300 MHz): δ = 1.01 (s, 12H), 6.79 (m, 2H), 7.06 (t, J = 8.1 Hz, 2H), 7.21 (d, J = 7.8 Hz, 2H) ppm; ^{13}C NMR (C_6D_6, 75 MHz) δ = 24.5, 83.5, 115.7, 120.1, 123.4, 129.6, 154.3 ppm.

B) Deuterium Labeling for the Hydroboration Reaction (Figure 1.9)

A J-Young NMR tube was taken into an argon glovebox and loaded with LCuOPh (15 mg, 2 mol %), phenylacetylene-d **1.2AC$_d$** (200 µL, 1 eq.), and 322 µL CD_3CN. Pinacolborane (270 µL, 1.02 eq.) was added in one portion and the reaction was monitored by ^{1}H NMR until complete. All volatiles were evaporated under vacuum and 10 mL of pentane was added to residue. This solution was passed through a pad of silica (5 cm diameter x 5 cm high) to remove insoluble components. Elution with 2 x 10 mL of pentane, followed by evaporation under vacuum yielded 0.385 g of **1.2CC$_d$** (92 %).

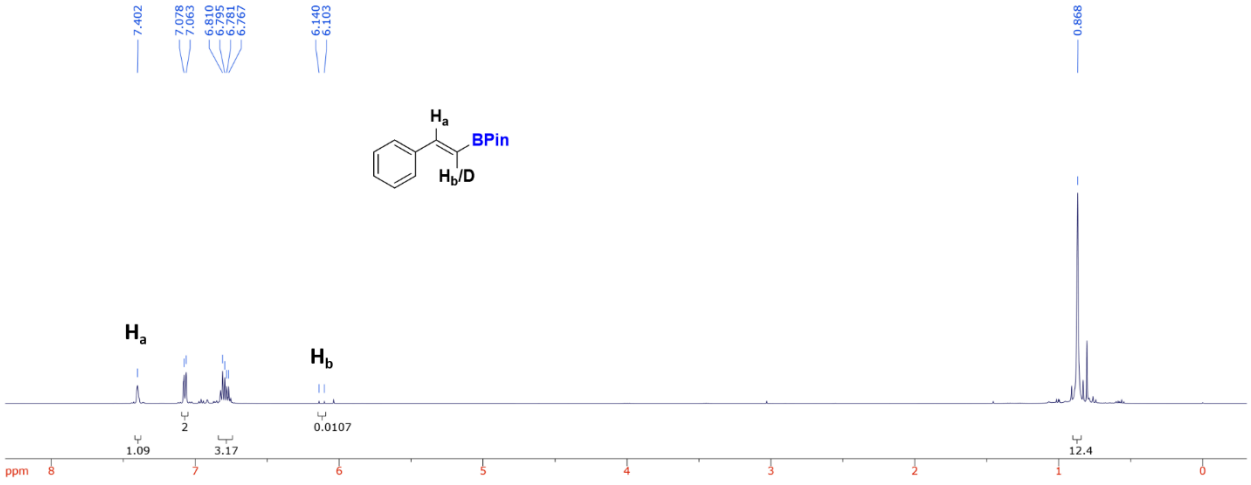

Figure 1.13. ^{1}H NMR spectrum of deuterated phenylalkenylboronate **1.2CC$_d$** depicting the presence of a deuterium atom at the terminal carbon atom.

C) Reaction of LCuCCPh **1.1BC** with HBPin in the presence of TolCCH **1.2AA** (Scheme 1.11)

A J-Young NMR tube was taken into an argon glovebox and loaded with 0.10 g of **1.1BC** (0.20 mmol) and 1.50 mL of CD_3CN. The tube was subsequently charged with 3 equiv. of TolCCH **1.2AA** (0.142 ml, 0.62 mmol) and HBPin (0.029 mL, 0.20 mmol). After 5 minutes, evaporation of the volatiles under vacuum and extraction of the residue with pentane afforded LCuCCTol

1.1BA as a white powder. Filtration and evaporation of the pentane solution under high vacuum afforded 41 mg of **1.2CC** (89% yield).

1.5.9 Gram Scale Reaction Protocols

Dehydrogenative Borylation Reaction: In a Schlenk tube under an argon atmosphere were added C_6H_6 (150 mL), phenylacetylene (2 mL, 18.2 mmol), pinacolborane (2.64 mL, 18.2 mmol), and triethylamine (0.12 mL, 0.91 mmol). Then, LCuOTf (0.24 g, 0.45 mmol%) was added to the mixture and the reaction was left stirring at room temperature until the reaction had completed (as confirmed by ^{11}B NMR). After completion, all the volatiles were evaporated under vacuum and 50 mL of pentane was added. The mixture was passed under argon through a short column packed with dry neutral alumina (3 cm diameter x 5 cm high) using 2 x 25 mL of pentane as eluent. Evaporation of the volatiles under vacuum afforded analytically pure **1.2BC** as a deliquescent solid in 3.952 g (95 %).

Hydroboration Reaction: To a flame dried schlenk flask under argon was added solid LCuOPh (2.5 mol%) and a magnetic stir bar. 1.7 mL anhydrous MeCN (distilled from CaH_2) was added to the catalyst and stirred until fully dissolved. Phenylacetylene (9.8 mmol) was added to the stirring solution and allowed to stir for 30 seconds. To this solution was added pinacolborane (10.1 mmol, 1.025 eq) and the resulting mixture was stirred at room temperature until complete (as determined by ^{11}B NMR). Volatiles were evaporated under vacuum at 50 °C for 1 hour. The flask was then cooled to room temperature and extracted with 3 x 10 mL of pentane. Organic extracts were passed through a silica pad (5 cm diameter x 10 cm high) and eluted with 2 x 25 mL pentane. Evaporation of the volatiles under vacuum yielding afforded 1.89 g of analytically pure **1.2CC** (84% yield).

1.6 References

[1] Igau, A.; Grutzmacher, H.; Baceiredo, A.; Bertrand, G. "Analogous α,α'-bis-carbenoid, triply bonded species: synthesis of a stable λ^3-phosphino carbene-λ,λ^5-phosphaacetylene" *J. Am. Chem. Soc.* **1988**, *110*, 6463.

[2] Arduengo, A. J.; Harlow, R. L.; Kline, M. "A stable crystalline carbene" *J. Am. Chem. Soc.* **1991**, *113*, 361.

[3] Díez-González, S.; Marion, N.; Nolan, S. P. "*N*-Heterocyclic Carbenes in Late Transition Metal Catalysis" *Chem. Rev.* **2009**, *109*, 3612.

[4] Lavallo, V.; Canac, Y.; Präsang, C.; Donnadieu, B.; Bertrand, G. "Stable Cyclic (Alkyl)(Amino)Carbenes as Rigid or Flexible, Bulky, Electron-Rich Ligands for Transition-Metal Catalysts: A Quaternary Carbon Atom Makes the Difference" *Angew. Chem. Int. Ed.* **2005**, *44*, 5705.

[5] For the synthesis of CAACs, see reference 4 along with the following: (a) Jazzar, R.; Dewhurst, R. D.; Bourg, J. B.; Donnadieu, B.; Canac, Y.; Bertrand, G. "Intramolecular "Hydroiminiumation" of Alkenes: Application to the Synthesis of Conjugate Acids of Cyclic Alkyl Amino Carbenes (CAACs)" *Angew. Chem. Int. Ed.* **2007**, *46*, 2899. (b) Jazzar, R.; Bourg, J. B.; Dewhurst, R. D.; Donnadieu, B.; Bertrand, G. "Intramolecular "Hydroiminiumation and -amidiniumation" of Alkenes: A Convenient, Flexible, and Scalable Route to Cyclic Iminium and Imidazolinium Salts" *J. Org. Chem.* **2007**, *72*, 3492.

[6] For reviews on CAACs, see: (a) Melaimi, M.; Soleilhavoup, M.; Bertrand, G. "Stable Cyclic Carbenes and Related Species beyond Diaminocarbenes" *Angew. Chem. Int. Ed.* **2010**, *49*, 8810. (b) Martin, D.; Melaimi, M.; Soleilhavoup, M.; Bertrand, G. "A Brief Survey of Our Contribution to Stable Carbene Chemistry" *Organometallics* **2011**, *30*, 5304. (c) Soleilhavoup, M.; Bertrand, G. "Cyclic (Alkyl)(Amino)Carbenes (CAACs): Stable Carbenes on the Rise" *Acc. Chem. Res.* **2015**, *48*, 256. (d) Melaimi, M.; Jazzar, R.; Soleilhavoup, M.; Bertrand, G. "Cyclic (Alkyl)(amino)carbenes (CAACs): Recent Developments" *Angew. Chem. Int. Ed.* **2017**, *56*, 10046.

[7] For select examples, see: (a) Ruiz, D. A.; Ung, G.; Melaimi, M.; Bertrand, G. "Deprotonation of a Borohydride: Synthesis of a Carbene-Stabilized Boryl Anion" *Angew. Chem. Int. Ed.* **2013**, *52*, 7590. (b) Back, O.; Celik, M. A.; Frenking, G.; Melaimi, M.; Donnadieu, B.; Bertrand, G. "A Crystalline Phosphinyl Radical Cation" *J. Am. Chem. Soc.* **2010**, *132*, 10262. (c) Kinjo, R.; Donnadieu, B.; Celik, M. A.; Frenking, G.; Bertrand, G. "Synthesis and Characterization of a Neutral Tricoordinate Organoboron Isoelectronic with Amines" *Science* **2011**, *333*, 610. (d) Mahoney, J. K.; Martin, D.; Moore, C. E.; Rheingold, A. L.; Bertrand, G. "Bottleable (Amino)(Carboxy) Radicals Derived from Cyclic

(Alkyl)(Amino) Carbenes" *J. Am. Chem. Soc.* **2013**, *135*, 18766. (e) Hansmann, M. M.; Melaimi, M.; Bertrand, G. "Crystalline Monomeric Allenyl/Propargyl Radical" *J. Am. Chem. Soc.* **2017**, *139*, 15620.

[8] For select examples, see: (a) Roy, S.; Mondal Kartik, C.; Meyer, J.; Niepötter, B.; Köhler, C.; Herbst‐Irmer, R.; Stalke, D.; Dittrich, B.; Andrada Diego, M.; Frenking, G.; Roesky Herbert, W. "Synthesis, Characterization, and Theoretical Investigation of Two‐Coordinate Palladium(0) and Platinum(0) Complexes Utilizing π‐Accepting Carbenes" *Chem. Eur. J.* **2015**, *21*, 9312. (b) Weinberger, D. S.; Amin Sk, N.; Mondal, K. C.; Melaimi, M.; Bertrand, G.; Stückl, A. C.; Roesky, H. W.; Dittrich, B.; Demeshko, S.; Schwederski, B.; Kaim, W.; Jerabek, P.; Frenking, G. "Isolation of Neutral Mononuclear Copper Complexes Stabilized by Two Cyclic (Alkyl)(amino)carbenes" *J. Am. Chem. Soc.* **2014**, *136*, 6235. (c) Ung, G.; Rittle, J.; Soleilhavoup, M.; Bertrand, G.; Peters Jonas, C. "Two‐Coordinate Fe^0 and Co^0 Complexes Supported by Cyclic (alkyl)(amino)carbenes" *Angew. Chem. Int. Ed.* **2014**, *53*, 8427. (d) Weinberger David, S.; Melaimi, M.; Moore Curtis, E.; Rheingold Arnold, L.; Frenking, G.; Jerabek, P.; Bertrand, G. "Isolation of Neutral Mono‐ and Dinuclear Gold Complexes of Cyclic (Alkyl)(amino)carbenes" *Angew. Chem. Int. Ed.* **2013**, *52*, 8964.

[9] (a) Hartwig, J. F. "Borylation and Silylation of C–H Bonds: A Platform for Diverse C–H Bond Functionalizations" *Acc. Chem. Res.* **2012**, *45*, 864. (b) Lennox, A. J.; Lloyd-Jones, G. C. "Selection of boron reagents for Suzuki-Miyaura coupling" *Chem. Soc. Rev.* **2014**, *43*, 412.

[10] Chen, H.; Schlecht, S.; Semple, T. C.; Hartwig, J. F. "Thermal, Catalytic, Regiospecific Functionalization of Alkanes" *Science* **2000**, *287*, 1995.

[11] Cho, J. -Y.; Tse, M. K.; Holmes, D.; Maleczka, R. E., Jr.; Smith III, M. R. "Remarkably Selective Iridium Catalysts for the Elaboration of Aromatic C-H Bonds" *Science* **2002**, *295*, 305.

[12] (a) Hartwig, J. F. "Regioselectivity of the borylation of alkanes and arenes" *Chem. Soc. Rev.* **2011**, *40*, 1992. (b) Mkhalid, I. A.; Barnard, J. H.; Marder, T. B.; Murphy, J. M.; Hartwig, J. F. "C−H Activation for the Construction of C−B Bonds" *Chem. Rev.* **2010**, *110*, 890.

[13] Lee, C.-I.; Zhou, J.; Ozerov, O. V. "Catalytic Dehydrogenative Borylation of Terminal Alkynes by a SiNN Pincer Complex of Iridium" *J. Am. Chem. Soc.* **2013**, *135*, 3560.

[14] Lee, C. I.; Hirscher, N. A.; Zhou, J.; Bhuvanesh, N.; Ozerov, O. V. "Adaptability of the SiNN Pincer Ligand in Iridium and Rhodium Complexes Relevant to Borylation Catalysis" *Organometallics* **2015**, *34*, 3099.

[15] Pell, C. J.; Ozerov, O. V. "Catalytic dehydrogenative borylation of terminal alkynes by POCOP-supported palladium complexes" *Inorg. Chem. Front.* **2015**, *2*, 720.

[16] Tsuchimoto, T.; Utsugi, H.; Sugiura, T.; Horio, S. "Alkynylboranes: A Practical Approach by Zinc-Catalyzed Dehydrogenative Coupling of Terminal Alkynes with 1,8-Naphthalenediaminatoborane" *Adv. Synth. Catal.* **2015**, *357*, 77.

[17] Barbeyron, R.; Benedetti, E.; Cossy, J.; Vasseur, J. J.; Arseniyadis, S.; Smietana, M. "Recent developments in alkyne borylations" *Tetrahedron* **2014**, *70*, 8431.

[18] (a) Jin, L.; Tolentino, D. R.; Melaimi, M.; Bertrand, G. "Isolation of bis(copper) key intermediates in Cu-catalyzed azide-alkyne "click reaction"" *Science Advances* **2015**, *1*, e1500304. (b) Jin, L.; Romero, E. A.; Melaimi, M.; Bertrand, G. "The Janus Face of the X Ligand in the Copper-Catalyzed Azide–Alkyne Cycloaddition" *J. Am. Chem. Soc.* **2015**, *137*, 15696.

[19] Arduengo, A. J.; Krafczyk, R.; Schmutzler, R. "Imidazolylidenes, imidazolinylidenes and imidazolidines" *Tetrahedron* **1999**, *55*, 14523.

[20] Wurtz, A. "Sur l'Hydrure de Cuivre" *Ann. Chim. Phys.* **1844**, *11*, 250.

[21] Frey, G. D.; Donnadieu, B.; Soleilhavoup, M.; Bertrand, G. "Synthesis of a Room-Temperature-Stable Dimeric Copper(I) Hydride" *Chem. Asian J.* **2011**, *6*, 402.

[22] (a) Mankad, N. P.; Laitar, D. S.; Sadighi, J. P. "Synthesis, Structure, and Alkyne Reactivity of a Dimeric (Carbene)copper(I) Hydride" *Organometallics* **2004**, *23*, 3369. (b) Jordan, A. J.; Wyss, C. M.; Bacsa, J.; Sadighi, J. P. "Synthesis and Reactivity of New Copper(I) Hydride Dimers" *Organometallics* **2016**, *35*, 613.

[23] Wyss, C. M.; Tate, B. K.; Bacsa, J.; Gray, T. G.; Sadighi, J. P. "Bonding and Reactivity of a μ-Hydrido Dicopper Cation" *Angew. Chem. Int. Ed.* **2013**, *52*, 12920.

[24] For representative examples, see: (a) Cox, N.; Dang, H.; Whittaker, A. M.; Lalic, G. "NHC–copper hydrides as chemoselective reducing agents: catalytic reduction of alkynes, alkyl triflates, and alkyl halides" *Tetrahedron* **2014**, *70*, 4219. (b) Uehling, M. R.; Rucker; R. P.; Lalic, G. "Catalytic Anti-Markovnikov Hydrobromination of Alkynes" *J. Am. Chem. Soc.* **2014**, *136*, 8799. (c) Suess, A. M.; Uehling, M. R.; Kaminsky, W.; Lalic, G. "Copper-Catalyzed Hydroalkylation of Terminal Alkynes" *J. Am. Chem. Soc.* **2015**, *137*, 7747. (d) Semba, K.; Fujihara, T.; Xu, T. H.; Terao, J.; Tsuji, Y. "Copper-Catalyzed Highly Selective Semihydrogenation of Non-Polar Carbon-Carbon Multiple Bonds using a Silane and an Alcohol" *Adv. Synth. Catal.* **2012**, *354*, 1542. (e) Suess, A. M.; Lalic, G. "Copper-Catalyzed Hydrofunctionalization of Alkynes" *Synlett* **2016**, *27*, 1165. (f) Collins, L. R.;

Riddlestone, I. M.; Mahon M. F.; Whittlesey, M. K. "A Comparison of the Stability and Reactivity of Diamido- and Diaminocarbene Copper Alkoxide and Hydride Complexes" *Chem. Eur. J.* **2015**, *21*, 14075.

[25] Borylation in these cases proceeds via migratory insertion/β-hydride elimination mechanisms rather than direct C-H activation. For representative examples of transition metal catalyzed dehydrogenative borylation with pinacolborane, see: (a) Jiang, S.; Quintero-Duque, S.; Roisnel, T.; Dorcet, V.; Grellier, M.; Sabo-Etienne, S.; Darcel, C.; Sortais, J.-B. "Direct synthesis of dicarbonyl PCP-iron hydride complexes and catalytic dehydrogenative borylation of styrene" *Dalton Trans.* **2016**, *45*, 11101. (b) Morimoto, M.; Miura, T.; Murakami, M. "Rhodium-Catalyzed Dehydrogenative Borylation of Aliphatic Terminal Alkenes with Pinacolborane" *Angew. Chem. Int. Ed.* **2015**, *54*, 12659. (c) Murata, M.; Kawakita, K.; Asana, T.; Watanabe, S.; Masuda, Y. "Rhodium- and Ruthenium-Catalyzed Dehydrogenative Borylation of Vinylarenes with Pinacolborane: Stereoselective Synthesis of Vinylboronates" *Bull. Chem. Soc. Jpn.* **2002**, *75*, 825.

[26] For representative examples of transition metal catalyzed hydroboration with pinacolborane, see: (a) Pereira, S.; Srebnik, M. "Hydroboration of Alkynes with Pinacolborane Catalyzed by $HZrCp_2Cl$" *Organometallics* **1995**, *14*, 3127. (b) Haberberger, M.; Enthaler, S. "Straightforward Iron-Catalyzed Synthesis of Vinylboronates by the Hydroboration of Alkynes" *Chem. Asian J.* **2013**, *8*, 50. (c) Lee, T.; Baik, C.; Jung, I.; Song, K. H.; Kim, S.; Kim, D.; Kang, S. O.; Ko, J. "Stereoselective Hydroboration of Diynes and Triyne to Give Products Containing Multiple Vinylene Bridges: A Versatile Application to Fluorescent Dyes and Light-Emitting Copolymers" *Organometallics* **2004**, *23*, 4569. (d) Khramov, D. M.; Rosen, E. L.; Er, J. A. V.; Vu, P. D.; Lynch, V. M.; Bielawski, C. W. "*N*-Heterocyclic carbenes: deducing σ- and π-contributions in Rh-catalyzed hydroboration and Pd-catalyzed coupling reactions" *Tetrahedron* **2008**, *64*, 6853. (e) Gunanathan, C.; Holscher, M.; Pan, F.; Leitner, W. "Ruthenium Catalyzed Hydroboration of Terminal Alkynes to Z-Vinylboronates" *J. Am. Chem. Soc.* **2012**, *134*, 14349. (f) Obligacion, J. V.; Neely, J. M.; Yazdani, A. N.; Pappas, I.; Chirik, P. J. "Cobalt Catalyzed Z-Selective Hydroboration of Terminal Alkynes and Elucidation of the Origin of Selectivity" *J. Am. Chem. Soc.* **2015**, *137*, 5855. (g) Ohmura, T.; Yamamoto, Y.; Miyaura, N. "Rhodium- or Iridium-Catalyzed trans-Hydroboration of Terminal Alkynes, Giving (Z)-1-Alkenylboron Compounds" *J. Am. Chem. Soc.* **2000**, *122*, 4990. (h) Wang, Y. D.; Kimball, G.; Prashad, A. S.; Wang, Y. "Zr-Mediated hydroboration: stereoselective synthesis of vinyl boronic esters" *Tetrahedron Lett.* **2015**, *46*, 8777.

[27] a) Jang, H.; Zhugralin, A. R.; Lee, Y.; Hoveyda, A. H. "Highly Selective Methods for Synthesis of Internal (α-) Vinylboronates through Efficient NHC–Cu-Catalyzed Hydroboration of Terminal Alkynes. Utility in Chemical Synthesis and Mechanistic Basis for Selectivity" *J. Am. Chem. Soc.* **2011**, *133*, 7859. (b) Bidal, Y. D.; Lazreg, F.; Cazin, C. S. J. "Copper-Catalyzed Regioselective Formation of Tri- and Tetrasubstituted Vinylboronates in Air" *ACS Catal.* **2014**, *4*, 1564. (c) Lazreg, F.; Nahra, F.; Cazin, C. S. J.

"Copper–NHC complexes in catalysis" *Coord. Chem. Rev.* **2015**, *293-294*, 48. (d) Yun, J. "Copper(I)-Catalyzed Boron Addition Reactions of Alkynes with Diboron Reagents" *Asian J. Org. Chem.* **2013**, *2*, 1016. (e) Kim, H. R.; Jung, I. G.; Yoo, K.; Jang, K.; Lee, E. S.; Yun, J.; Son, S. U. "Bis(imidazoline-2-thione)–copper(I) catalyzed regioselective boron addition to internal alkynes" *Chem. Commun.* **2010**, *46*, 758. (f) Lee, J. -E.; Kwon, J.; Yun, J. "Copper-catalyzed addition of diboron reagents to α,β-acetylenic esters: efficient synthesis of β-boryl-α,β-ethylenic esters" *Chem. Commun.* **2008**, 733.

[28] Examples of bis(hydroboration) reaction have been reported Lee, S.; Li, D.; Yun, J. "Copper-Catalyzed Synthesis of 1,1-Diborylalkanes through Regioselective Dihydroboration of Terminal Alkynes" *Chem. Asian J.* **2014**, *9*, 2440.

[29] Jang, W. J.; Lee, W. L.; Moon, J. H.; Lee, J. Y.; Yun, J. "Copper-Catalyzed trans-Hydroboration of Terminal Aryl Alkynes: Stereodivergent Synthesis of Alkenylboron Compounds" *Org. Lett.* **2016**, *18*, 1390.

[30] Yang, Z.; Zhong, M.; Ma, X.; Nijesh, K.; De, S.; Parameswaran, P.; Roesky, H. W. "An Aluminum Dihydride Working as a Catalyst in Hydroboration and Dehydrocoupling" *J. Am. Chem. Soc.* **2016**, *138*, 2548.

[31] Further investigation using computational methods indicates the high probability that copper-hydride complexes are key to affecting the hydroboration reaction of terminal alkynes. A more detailed report is forthcoming and therefore will not be discussed in this dissertation.

[32] Cheng, L.; Cordier, C. J. "Catalytic Nucleophilic Fluorination of Secondary and Tertiary Propargylic Electrophiles with a Copper–N-Heterocyclic Carbene Complex" *Angew. Chem. Int. Ed.* **2015**, *54*, 13734.

Chapter 2 : Spectroscopic Characterization and Reactivity Studies of Monomeric Copper(I)-Hydrides and Their Silver(I) Analogue

2.1 General Introduction

In this chapter, we will discuss our contributions to the field of copper- and silver-hydride chemistry. In the first section, our efforts to synthesize and characterize the first example of a monomeric copper(I)-hydride using extremely sterically encumbering *N*-heterocyclic carbene ligands are discussed. We will then focus our attention on the application of borane stabilized monomeric copper-hydrides to the reduction of CO_2 to formate using a rationally designed synergistic cooperation between copper-hydride complexes and classical amine-borane Lewis pairs (cLPs). In the final section, we will apply the synthetic methodology developed to obtain a monomeric copper-hydride to the preparation of the first neutral silver(I)-hydride. Finally, for the first time, we have preliminarily probed the reactivity of LAg(I)-H complexes and determined that its reactivity better mirrors its copper congener over its gold analogue.

2.2 Preparation and Characterization of a Monomeric Copper(I)-Hydride

Although copper(I)-hydrides were discovered by Wurtz[1] more than a century ago, their isolation in the solid-state as monomers has eluded the skills of synthetic chemists.[2] During this time, copper-hydrides were found to have a considerable propensity to aggregate, as evidenced by the widely studied Stryker's reagent $[(Ph_3P)CuH]_6$,[3] first described by Osborn *et al.* in 1971.[4] In 2004, using NHC ligands, Sadighi *et al.* reported the isolation and structural characterization of the first monoligated dimeric copper-hydride **2.2A**;[5] however, the authors noted slow decomposition even at -40 ^oC (Figure 2.1).

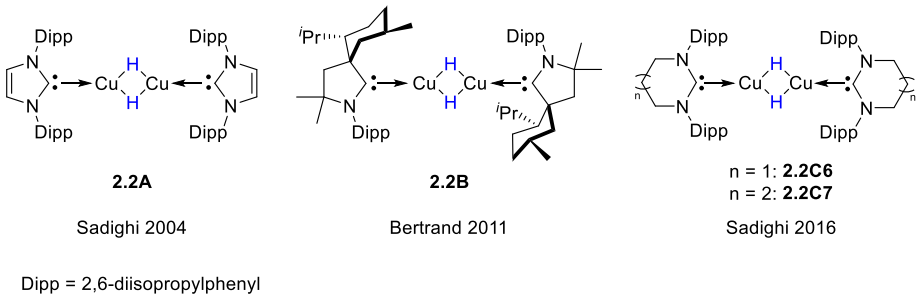

Figure 2.1. Structurally characterized carbene copper(I)-hydride dimers.

Using the more σ-donating and bulkier menthyl-CAAC ligand, our group was able to isolate the first room temperature stable monoligated copper-hydride dimer **2.2B** in 2011.[6] Recently, Sadighi and coworkers demonstrated that 6- and 7- membered NHC ligands were also capable of stabilizing the dimeric copper-hydrides [(6- and 7-NHC)CuH]$_2$ (**2.2C6** and **2.2C7**, respectively) at room temperature.[7] In these cases, the authors credited the added stability of expanded ring NHC ligated dimer complexes over that of **2.2A** to the increased N-C-N angle about the carbene carbon (*e.g.* 104^o for ^{5Mes}NHCAgX, 118^o for ^{6Mes}NHCAgX, and 119^o for ^{7Mes}NHCAgX).[8] This widened angle effectively brings the *N*-aryl substituents of the ligand closer to the metal center, thereby providing increased kinetic stabilization abilities. Interestingly, all three of these reports found the reactivity of the copper-hydride dimers to mimic what would be expected for their corresponding monomers;[2] however, there exists no experimental evidence to corroborate the hypothesis that polynuclear copper-hydride clusters (LCuH)$_n$ exist in solution-phase equilibrium with their corresponding monomers (LCuH).[9] For this reason, a monomeric copper-hydride has never been characterized in solution or in the solid state.

In a computational study conducted by Dey and Elliot,[10] *N*-phenyl substituted (NHC)Cu-H complexes present a low energy barrier for dimerization of two monomers; however, in this same report, the authors determined that this process is severely entropically dependent. To rephrase this incredibly important result in simpler terms, two copper-hydride complexes will

oligomerize when small supporting ligands are bound to the metal center, but when those ligands feature significant steric encumbrance, *destabilization of the copper-hydride dimer through steric repulsion can overcome the favorability of dimerization and produce two monomeric LCu-H complexes*. In line with this result as well as those from the groups of Sadighi and Bertrand, we reasoned that the significantly more sterically encumbering NHC ligands, 1,3-bis(2,6-bis(diphenylmethyl)-4-methylphenyl)-imidazol-2-ylidene (IPr*) described by Marko *et al.*[11] and even 1,3-bis[2,6-bis[di(4-tert-butylphenyl)methyl]-4-methylphenyl]imidazol-2-ylidene (IPr**) reported by Straub *et al.*,[12] should provide sufficient kinetic protection to destabilize a copper-hydride dimer and allow for the first example of a neutral monoligated monomeric copper-hydride for spectroscopic and solid-state crystallographic characterization.

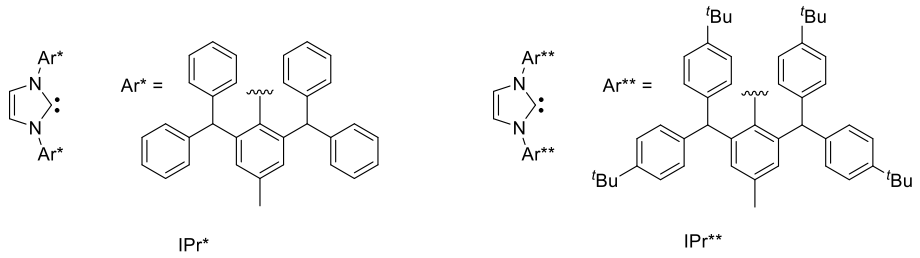

Figure 2.2. Structures of the two most sterically demanding NHC ligands, IPr* (left) and IPr** (right).

We[13] began our investigation by preparing (IPr*)CuOPh **2.2CA**, which was accomplished by a salt metathesis reaction between (IPr*)CuCl and potassium phenolate. Addition of 1 equivalent of pinacolborane to a THF solution of **2.2CA** resulted in the formation of a deep orange solution along with copious amounts of a bright yellow solid precipitate (Scheme 2.1).

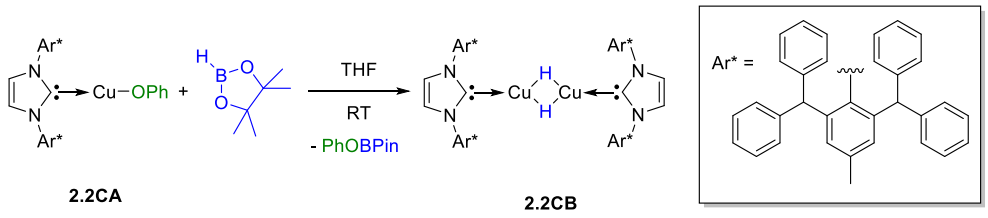

Scheme 2.1. Synthesis of $[(IPr^*)CuH]_2$ **2.2CB**.

This yellow solid was extremely moisture sensitive and even decomposed slightly upon removal of the supernatant if the filter paper was not thoroughly dried immediately prior to use. The $^{11}B\{^1H\}$ NMR spectrum of the supernatant revealed the presence of PhOBPin,[14] while the $^{13}C\{^1H\}$ NMR spectrum showed a distinctive shift of the carbene signal from δ 181.2 ppm (**2.2CA**) to δ 194.3 ppm (**2.2CB**). Based on the reported colors of previously reported carbene copper(I)-hydride dimers, our intense yellow color precipitate strongly implied a dimeric copper-hydride complex $[(IPr^*)CuH]_2$. To further support this hypothesis, we used proton-coupled ^{13}C NMR spectroscopy to observe the $^2J_{C\text{-}H}$ coupling of the hydride to the carbene carbon. Whitesides *et al.* showed that *cis* and *trans* hydrides display characteristically different coupling constants through a transition-metal center.[15] Excitingly, we found that the carbene carbon in complex **2.2CB** resolves as a triplet ($^2J_{C\text{-}H}$ = 6.4 Hz), strongly indicating its dimeric nature (Figure 2.3, left). To spectroscopically confirm our hypothesis, we employed ^1H-^{13}C HMBC NMR and observed a strong correlation between the carbene carbon atom in ^{13}C NMR with a singlet at δ 3.91 ppm on the ^1H NMR axis (Figure 2.3, right). It is worth noting that this resonance integrates 1:1 with the IPr* NHC.

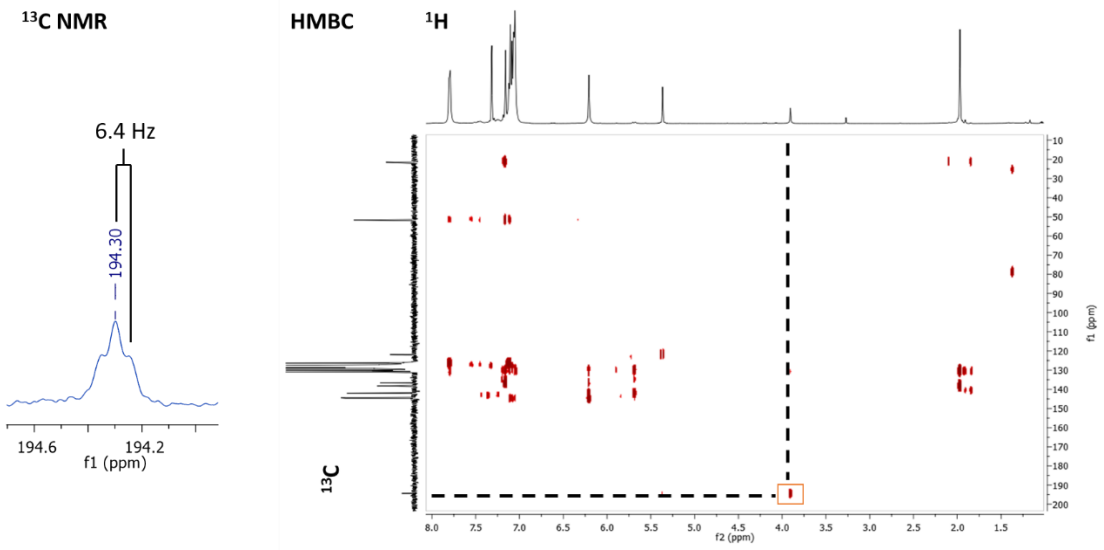

Figure 2.3. ^{13}C (left) and ^{1}H-^{13}C HMBC (right) NMR spectra for complex **2.2CB**.

Based on this HMBC NMR spectrum, we assigned the resonance at δ 3.91 ppm in the ^{1}H NMR as belonging to the bridging hydrides, which is significantly downfield shifted compared to the previously reported LCu(I)-H dimers **2.2A**-**2.2C**.[5,6,7] This shift is likely due to the strong anisotropic shielding of the aryl rings of the flanking NHC substituents, which was also noted in the most recent report by Sadighi.[7] Interestingly, contrary to the 5-membered NHC copper-hydride dimer **2.2A**,[5] this complex is stable in solution up to 80 ºC for several hours with no noticeable decomposition by ^{1}H NMR. A single crystal X-ray diffraction study unambiguously confirmed the structure of (IPr*)CuH dimer **2.2CB**, which were grown by diffusion of pentane into a saturated benzene solution at 5 ºC (Figure 2.4).

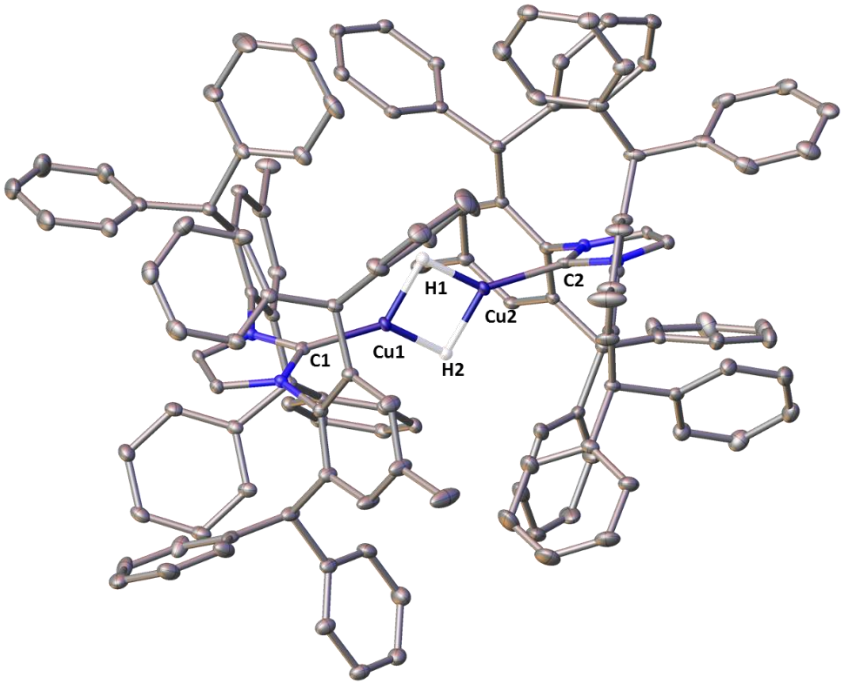

Figure 2.4. Molecular structure of **2.2CB** in the solid state. Ellipsoids are set at 25 % probability. Ligand hydrogen atoms and solvent molecules have been omitted for clarity. Selected distances [Å]: C1-Cu1 1.900(3); Cu1-H1 1.71(5); Cu1-H2 1.59(5); Cu1-Cu2 2.3144(10). Atoms Cu2, C2, and H2 are symmetry generated.

Complex **2.2CB** displays a nearly linear arrangement of the C1-Cu1-Cu2-C2 framework with non-coplanar NHC rings (torsion angle: 26.3 °) due to the steric hindrance of the Ar* rings. The Cu1-Cu2 (2.3144(10) Å) and C-Cu (1.900(3) Å) distances are comparable to those reported previously in the literature.[5,6,7]

As shown by Whittlesey *et al.* in 2016, dimeric $[IPrCuH]_2$ complex **2.2A** reacts with weak Lewis acids to form the monomeric copper-hydride boron adduct **2.2D** (Scheme 2.2, insert).[16] In this case, it is unclear whether this reaction proceeds from the dimer or the transiently dissociated monomer, however, we reasoned that the IPr* NHC ligand should be sufficiently large to shield the copper centers of **2.2CB** from bulky Lewis acids such as 9-borabicyclononane (9-BBN). We therefore concluded that any reaction between 9-BBN and complex **2.2CB** would suggest the

possibility of a rapid equilibrium occurring between complex **2.2CB** with its monomer **2.2CB$_{mono}$** (Scheme 2.2).

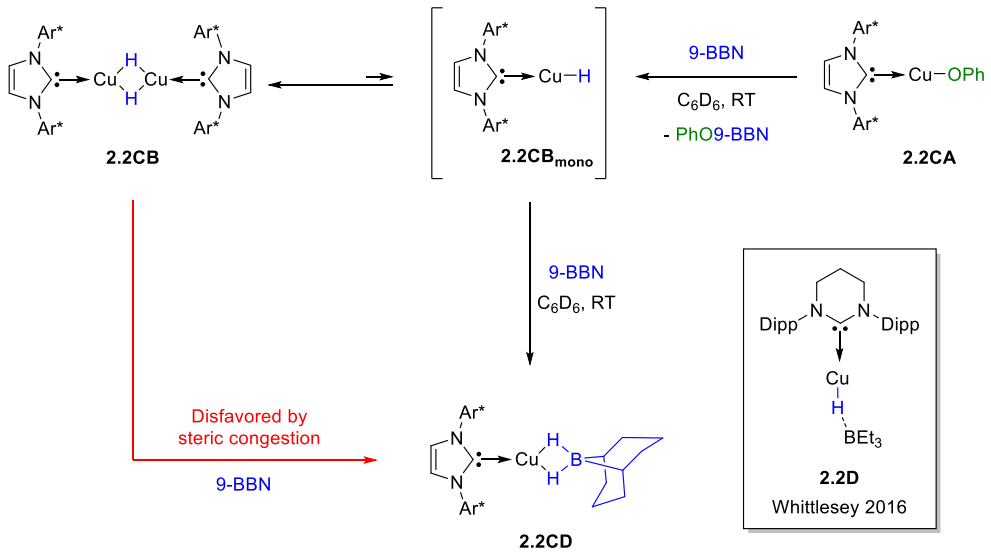

Scheme 2.2. Reactivity of (IPr*)CuH **2.2CB** with 9-BBN to give **2.2CD**.

To test this hypothesis, compound **2.2CB** was reacted with 1 equivalent of 9-BBN, which exists as a dimer. Within 10 minutes at room temperature, the solution changed from orange to colorless, and the ^{11}B NMR spectrum displayed a broad triplet at δ -10.4 ppm ($J_{B\text{-}H}$ = 52.7 Hz), which is consistent with the formation of the copper-hydride boron adduct **2.2CD**.[17] The same product was also obtained when reacting **2.2CA** with 1 equivalent of the 9-BBN dimer (93% isolated yield). A single crystal X-ray diffraction study of complex **2.2CD** (Figure 2.5) revealed the presence of a three-coordinate Cu center attached to a κ^2-H$_2$-9BBN moiety (the hydrogen atoms on boron were located and isotropically refined without restraint).

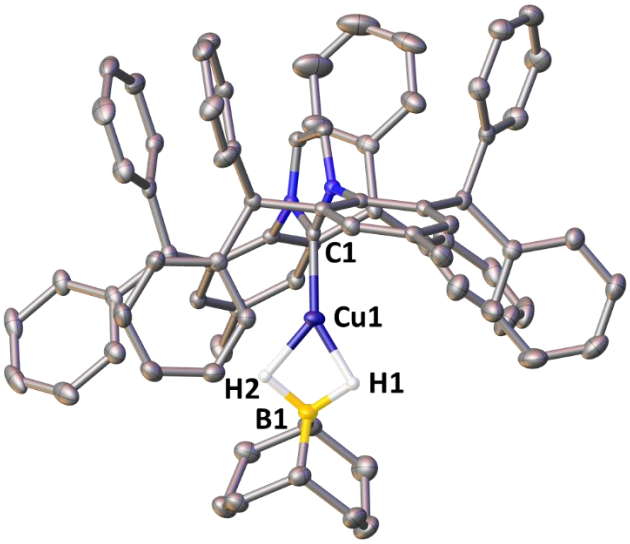

Figure 2.5. Molecular structure of **2.2CD** in the solid state. Ellipsoids are set at 50 % probability. Hydrogen atoms on the ligand and 9-BBN ring have been omitted for clarity. Selected distances [Å] and angles [°]: C1-Cu1 1.8764(16); Cu1-H1 1.6493(1); Cu1-H2 1.6517(1); Cu1-B1 2.0764(1); B1-H1 1.2258(1); B1-H2 1.2520(1); C1-Cu1-B1 164.64(8); C1-Cu1-H1 150.2004(10); C1-Cu1-H2 138.1162(7).

Having recently shown the superiority of the IPr** scaffold over that of IPr* for the kinetic protection of other highly reactive species,[18] we prepared the (IPr**)Cu-OPh complex **2.2DA** (Scheme 2.3). Addition of 1 equivalent of HBPin to a benzene solution of **2.2DA** yielded 33% conversion to a new product that gives 1 signal by ^{11}B NMR at δ -12.5 ppm that resolves as a broad quartet ($J_{B\text{-}H}$ = 81.5 Hz); however, addition of 3 equivalents of HBPin cleanly affords the same boron containing product (Scheme 2.3), which crystallizes out of solution overnight as colorless needles. X-ray crystallographic analysis of this species revealed the formation of complex **2.2DD** featuring the phenoxide group at boron (Figure 2.6). Although the mechanism of the reaction leading to **2.2DD** is not clear, this compound was isolated in nearly quantitative yield and represents a novel observation in the reactivity of copper-hydrides.

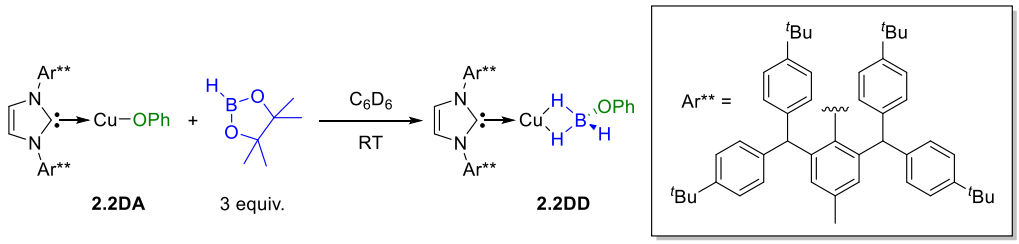

Scheme 2.3. Reaction of **2.2DA** with pinacolborane.

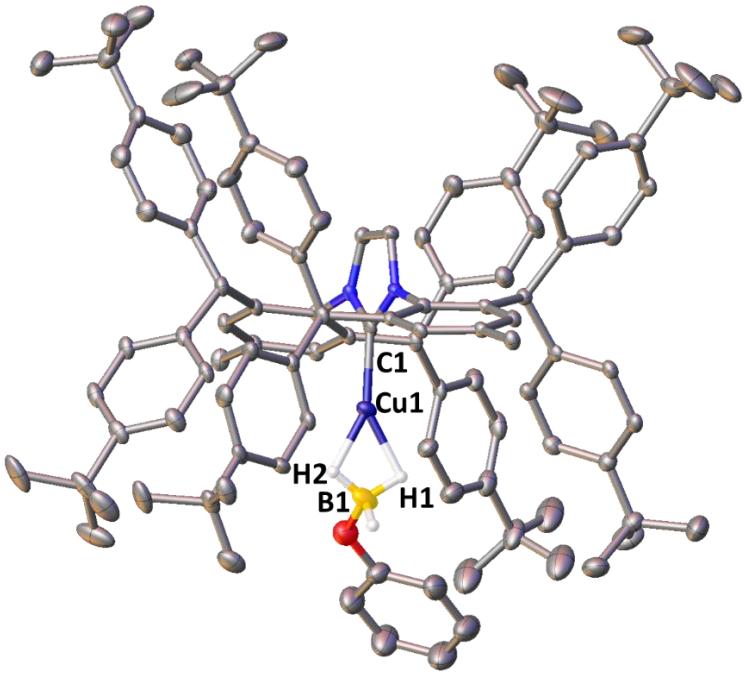

Figure 2.6. Molecular structure of **2.2DD** in the solid state. Hydrogen atoms other than those on boron have been omitted for clarity. Thermal ellipsoids are set at 25% probability. Selected distances [Å]: C1-Cu1 1.884(5); Cu1-B1 2.058(7); C1-Cu1-B1 178.6(3).

To mitigate this side reaction, we investigated other potential hydride sources that do not contain Lewis acidic components, such as polymethylhydrosiloxane (PMHS). Room temperature addition of one equivalent of PMHS to a benzene solution of **2.2DA** led to a light-yellow solution after 4 hours (Scheme 2.4).

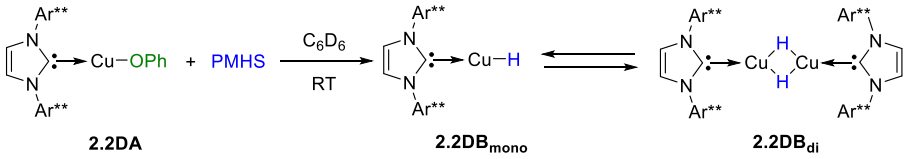

Scheme 2.4. Reaction of **2.2DA** with PMHS.

The $^{13}C\{^{1}H\}$ NMR spectrum showed the clean formation of two new carbene containing products at δ 185.8 and 192.8 ppm. In the ^{13}C proton coupled NMR, the signal at δ 192.8 ppm resolves as a triplet with a $^{2}J_{C\text{-}H}$ = 3.6 Hz, which is comparable to that of **2.2DB**, and was thus attributed to **2.2DB$_{di}$** (Figure 2.7).

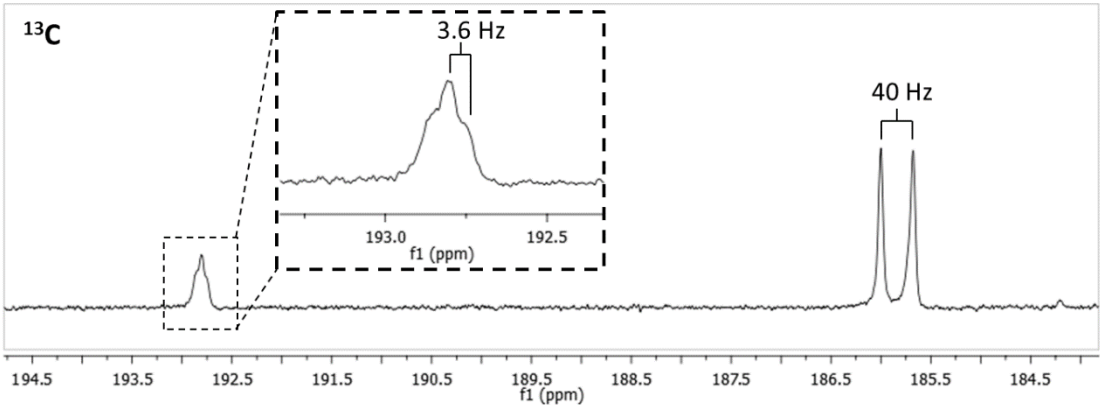

Figure 2.7. ^{13}C proton coupled NMR carbene signals of **2.2DB$_{mono}$** and **2.2DB$_{di}$** in C_6D_6.

In contrast, the signal at δ 185.8 ppm resolved as a doublet with a large coupling constant of 40 Hz and is consistent with a *trans*-hydride $^{2}J_{C\text{-}H}$ coupling.[15] We therefore tentatively assigned this resonance as the carbene signal for the desired monomeric copper hydride **2.2DB$_{mono}$**. The 2D-HMBC NMR spectrum correlated the carbene signals in ^{13}C NMR to distinctive proton signals at δ 4.26 ppm (**2.2DB$_{di}$**) and δ 2.14 ppm (**2.2DB$_{mono}$**) (Figure 2.8).

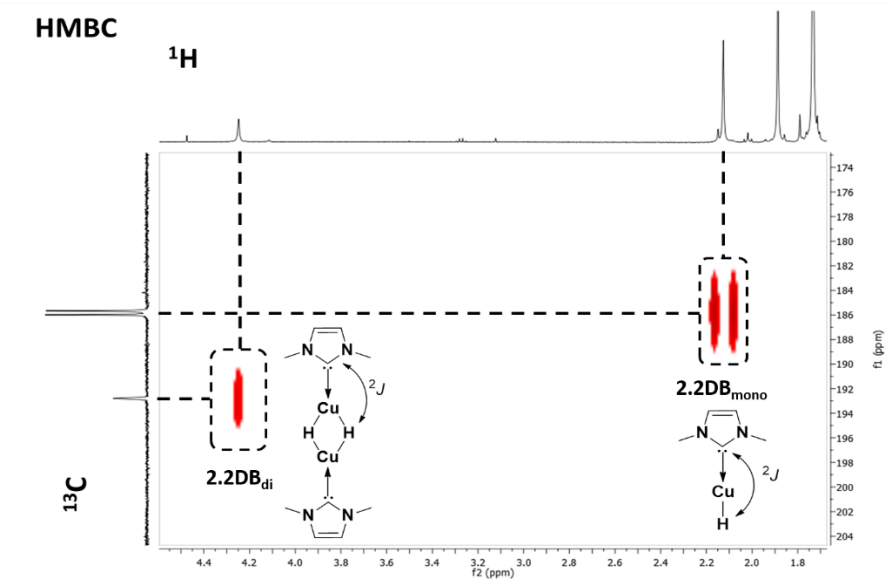

Figure 2.8. Selected region of the ^{1}H-^{13}C HMBC spectrum of **2.2DB$_{mono}$** and **2.2DB$_{di}$** in C_6D_6.

Evaporation of the solution afforded an oily residue that readily crystalized upon standing at -40 ^{o}C. The obtained crystals were yellow in color and were of a single crystal habit. Surprisingly, an X-ray diffraction study showed the dimeric (IPr**)CuH complex **2.2DB$_{di}$** (Figure 2.9).

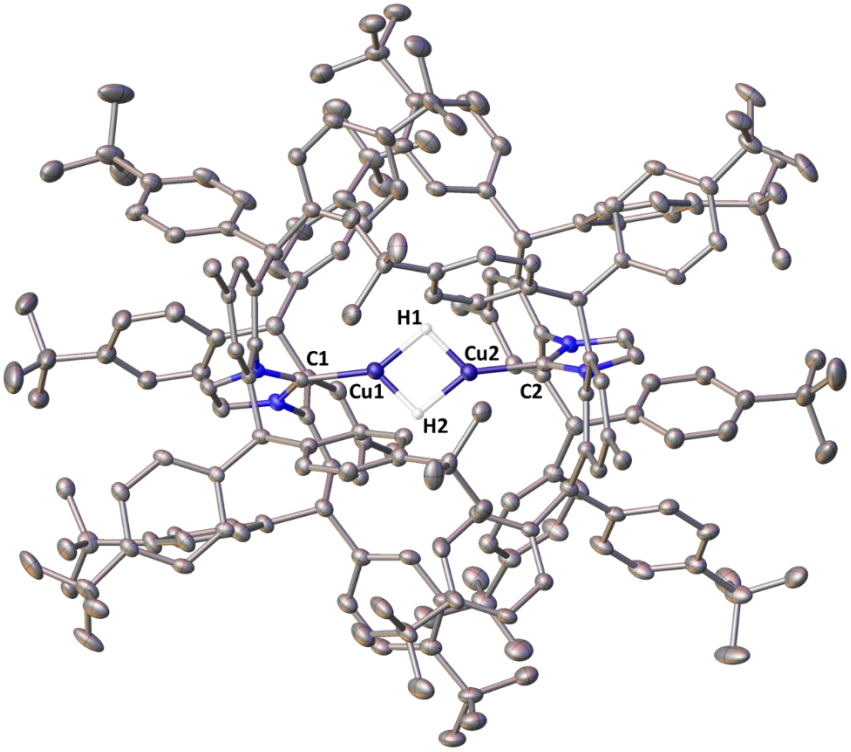

Figure 2.9. Molecular structure of **2.2DB$_{di}$** in the solid state. Hydrogen atoms other than the hydrides, solvent molecules, and positional disorder have been omitted for clarity. Thermal ellipsoids are set at 15% probability. Atoms Cu2, C2, and H2 are symmetry generated. Selected distances [Å]: C1-Cu1 1.89535(4); Cu1-H1 1.50400(6); Cu1-H2 1.63613(3); Cu1-Cu2 2.32432(4).

Interestingly, when crystals of **2.2DB$_{di}$** were dissolved in C_6D_6, a mixture of **2.2DB$_{di}$** and **2.2DB$_{mono}$** was observed by NMR, implying the possible existence of an equilibrium between the dimer **2.2DB$_{di}$** and its monomer **2.2DB$_{mono}$**. To further understand the nature of this equilibrium, a set of variable temperature NMR experiments were performed (Figure 2.10).

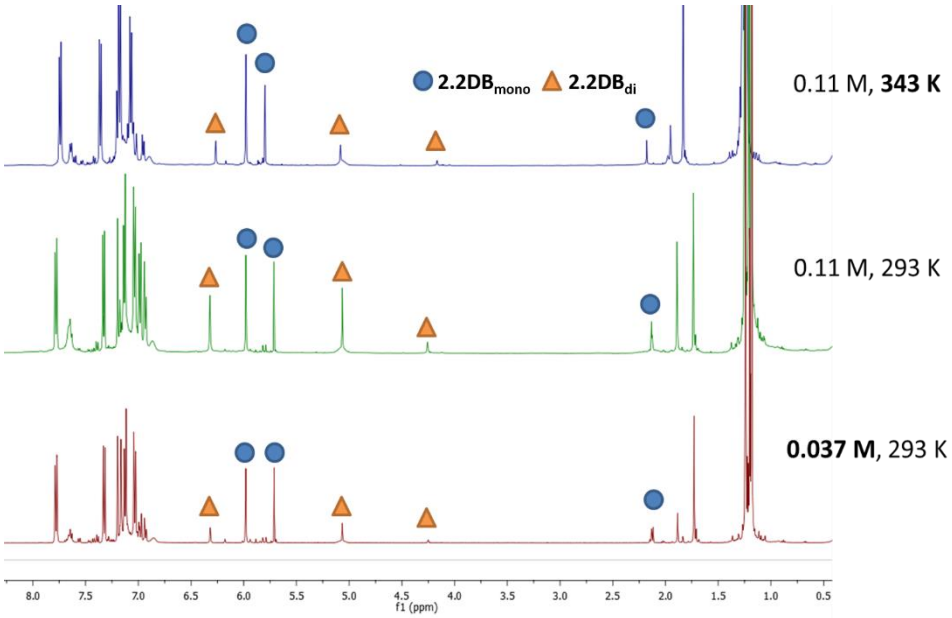

Figure 2.10. Select NMR spectra from a variable temperature NMR study depicting the equilibrium between **2.2DB$_{di}$** /**2.2DB$_{mono}$** in C_6D_6.

Under the standard conditions (0.11 M at 293 K, middle trace), we observe a larger prevalence of monomer **2.2DB$_{mono}$** as compared to its dimeric counterpart **2.2DB$_{di}$**. As expected for dimers containing large supporting ligands, increasing the temperature (top trace) shifts the equilibrium towards the monomer **2.2DB$_{mono}$**, which is due to the increased thermal motion and steric repulsion of the ligand. Along the same line, decreasing the concentration (bottom trace) of the mixture was found to display a similar effect as the monomeric components will have a greater mean free path between collisions. From the full set of these measurements (see appendix for more details), we calculated the equilibrium constant (K_{eq} = 4.04 ± 0.80 M^{-1}) as well as the enthalpy (ΔH = -6.15 ± 0.25 kcal.mol^{-1}), entropy (ΔS = -17.53 ± 1.36 cal.mol^{-1}.K^{-1}), and Gibbs free energy (ΔG = -0.84 ± 0.17 kcal.mol^{-1}) of the dimerization process at 30 ^{o}C. Based on these data, it is unsurprising that temperature and concentration have large effects on the ratio of monomer to dimer since this process was found to be entropically dependent by Dey and Elliot using computational methods.[10]

In conclusion, the bulky IPr* NHC ligand cannot support the monomeric copper(I)-hydride **2.2CB$_{mono}$** and therefore dimerizes immediately to form complex **2.2CB**; however, we found that addition of 9-BBN to this complex resulted in the rapid formation of the LCuH-borane adduct **2.2CD**, which suggests the possibility of an equilibrium in solution even for less sterically encumbering ligands. Using the larger IPr** scaffold, we have reported the first spectroscopic characterization of a monomeric LCu-H. Although this complex crystallizes as its dimer **2.2DB$_{di}$**, we discovered conclusive evidence that these two complexes exist in equilibrium in solution. Through a series of variable temperature NMR experiments, we were able to determine the thermodynamic parameters for this dimerization process. As a whole, this work strongly supports the hypothesis that copper hydride aggregates dissociate in solution and react as their corresponding monomers.[2b,9]

2.3 Copper(I)-Hydrides in the Catalytic Hydrogenation of CO_2 to Formate

Since their discovery, copper-hydrides have attracted considerable interest because of their role in a multitude of catalytic processes, some of which include: reduction of *α,β*-unsaturated carbonyl compounds,[19] ketone and imine hydrosilylation,[20] hydroamination of alkenes and alkynes,[21] dehydrogenative borylation of terminal alkynes,[22] and the reduction of CO_2 to formate.[23] This sequestration and conversion of CO_2 into useful products, such as formic acid, has drawn significant attention in recent years due to the ever-increasing atmospheric concentration of carbon dioxide, which emanates from the large-scale consumption of fossil fuels. In addition to reducing atmospheric CO_2 levels, hydrogenation of CO_2 to formic acid represents a valuable transformation due to the use of formic acid in various industrial applications (*e.g.* textiles and agriculture).[24] In 2016, more than 800,000 tons of formic acid were produced, which equates to upwards of $500

million in market value. Since the pioneering work of Inoue *et al.* in 1976,[25] the catalytic reduction of CO_2 with molecular hydrogen has been reported with a range of noble transition-metal complexes. These catalysts,[26] which include Ir,[27] Ru,[28] and Re,[29] have achieved turnover numbers (TONs) up to 3,500,000;[27] however, such high TONs have never been observed when catalysts employing abundant and inexpensive base metals such as Mn,[30] Fe,[31,32] Co,[33] Ni,[34] and Cu.[23]

With respect to copper, Haynes *et al.* reported the first hydrogenation of CO_2 with dihydrogen that was catalyzed by $(Ph_3P)_3CuCl$ in the presence of dimethylamine to form *N*,*N*-dimethylformamide with TONs reaching 900.[35] In 2015, Ikaraya and coworkers reported that the combination of $Cu(OAc)_2$ and 1,8-diazabicyclo(5.4.0)-undec-7-ene (DBU) could facilitate the production of the formate conjugate base with TONs of 167.[23a] Later that year, the process was further improved by Appel *et al.* (TON = 500) who relied on a triphosphine ligand to stabilize the *in-situ* generated copper-hydride catalyst **2.3AB** (Figure 2.11).[23b,c] However, in this report, the authors determined that their proposed copper-hydride intermediate still aggregates in solution, which is one possible explanation for the rapid deactivation of the catalyst. More importantly, from their follow-up report,[23c] it appears that while these L_nCuH complexes are prone to undergo facile CO_2 insertion at room temperature to give products **2.3AC**,[23b-c,36,37] the subsequent activation of H_2 to reform the copper-hydride is highly endergonic (**2.3AA** to **2.3AB**).

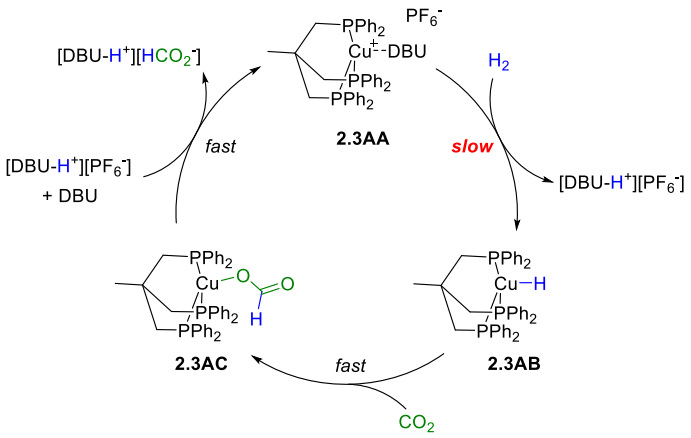

Figure 2.11. Hydrogenation of CO_2 with H_2 using the triphosphine ligated copper-hydride **2.3AB** as catalyst.

Although copper complexes have difficulty cleaving the enthalpically strong bond of H_2, frustrated Lewis pairs (FLPs) developed by Stephan and coworkers have no such problem.[38] Since their inception, both phosphine- and amine-borane based FLPs have been shown to react with dihydrogen at room temperature to afford the corresponding $[R_3P\text{-}H]^+$ or $[R_3N\text{-}H]^+$ $[H\text{-}BR_3]^-$ salts. Moreover, Stephan *et al.* recently showed that the FLP comprised of *N*,*N*-dimethylbenzylamine and $B(C_6F_5)_3$ (BCF) was not only capable of splitting H_2, but also inserting the resulting B-H bond into CO_2 to afford compound **2.3AE** (Figure 2.12).[39] O'Hare *et al.*, however, showed that this hydride insertion step is reversible above 80 ^oC.[40] Moreover, in the report by Stephan *et al.*,[39] the authors further noted that formic acid addition to the $[BnNMe_2][BCF]$ FLP resulted in the immediate formation of **2.3AE**. Altogether, these results strongly suggest that scission of the B-O bond in **2.3AE** has a higher activation energy than the non-catalytically productive hydride elimination from **2.3AE** and subsequent reformation of **2.3AD**. Based on this analysis, efficient catalytic reduction of CO_2 with dihydrogen using FLPs is unlikely given these data and other computational studies reported in the literature.[41]

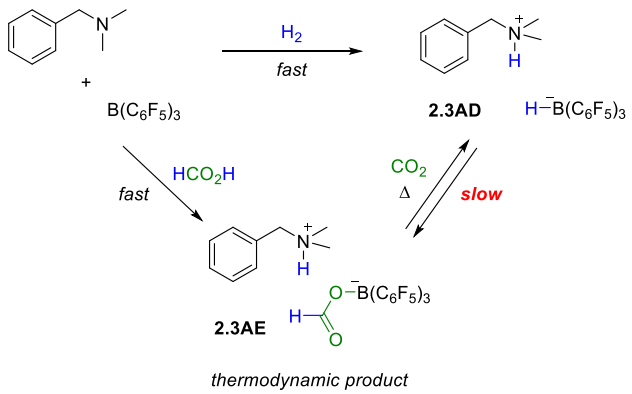

Figure 2.12. Stoichiometric hydrogenation of CO_2 using amine-borane based FLPs by Stephan and coworkers.

Due to the noted ability of copper-hydrides to readily reduce CO_2, and the ability of FLPs to activate H_2, we hypothesized that the combination of these two components as co-catalysts in CO_2 hydrogenation would facilitate an ideal synergy and allow for greater TONs than previously observed for each system individually.

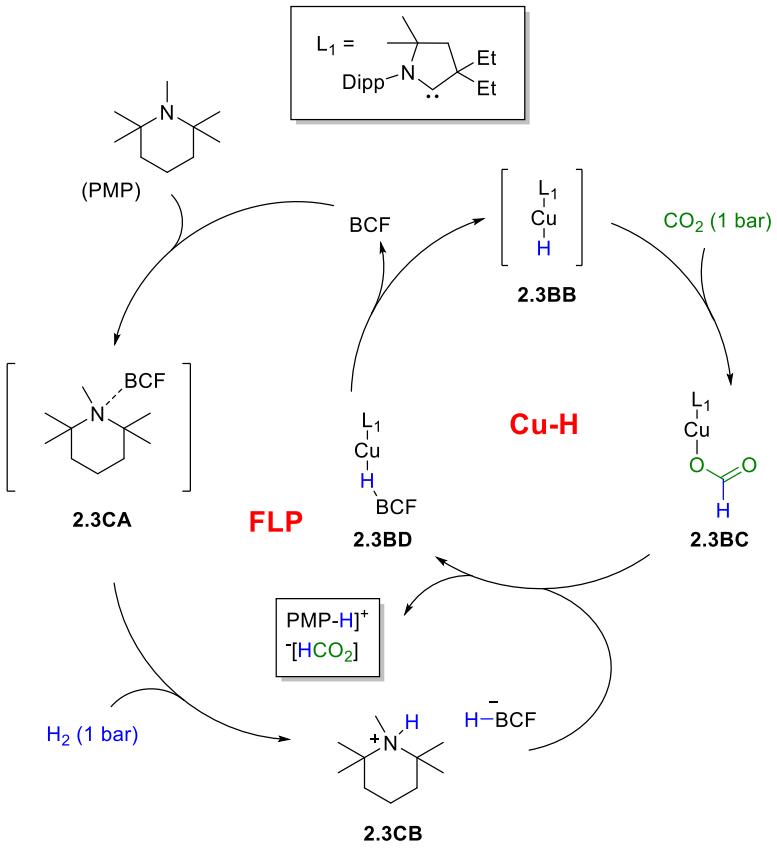

Scheme 2.5. Postulated mechanism for the synergystic cooperation between FLPs and copper-hydrides for the hydrogenation of carbon dioxide.

Scheme 2.5 depicts our proposed mechanism allowing for cooperation between copper-hydrides and FLPs in this reaction. Berke and coworkers reported the ability of the 1,2,2,6,6-pentamethylpiperidine (PMP)/BCF FLP **2.3CA** to generate the ammonium borohydride salt **2.3CB** under 1 bar of H_2.[42] We hypothesized that **2.3CB** would react with $(L_1)Cu\text{-}CO_2H$ **2.3BC** (L_1 = ^{Et}CAAC) through a salt metathesis reaction to form the desired [PMP-H][CO_2H] salt and the borane-stabilized copper-hydride adduct **2.3BD**. This reaction constitutes the most important step in our hypothesized catalytic cycle since it allows us to avoid the formation of any boron-oxygen bond containing intermediates. Finally, dissociation of the borane from **2.3BD** would regenerate our free transient copper-hydride and close the catalytic cycle.

Using the mechanism proposed in Scheme 2.5 as a guide, we wanted to first confirm the feasibility of conducting the salt metathesis reaction stoichiometrically. The first step in achieving this goal was the preparation of the two individual components, **2.3CB** and **2.3BC**. Using the method reported by Berke and coworkers,[42] we isolated the salt **2.3CB** in excellent yield. Since we propose that copper-hydride insertion into CO_2 constitutes the most likely mechanistic pathway for generation of complex **2.3BC**, we prepared the transient copper-hydride **2.3BB** under an atmosphere of CO_2 and found the immediate formation of complex **2.3BC** (Scheme 2.6). Complex **2.3BC** was isolated in excellent yield and its structure was further confirmed by a single crystal X-ray diffraction study (Figure 2.13).

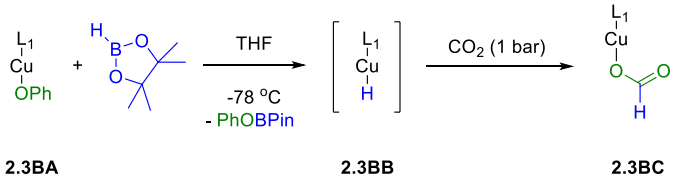

Scheme 2.6. Reduction of copper-phenoxide complex **2.3BA** with pinacolborane to afford the transient copper-hydride **2.3BB**. This complex readily inserts into CO_2 to afford the copper-formate complex **2.3BC**.

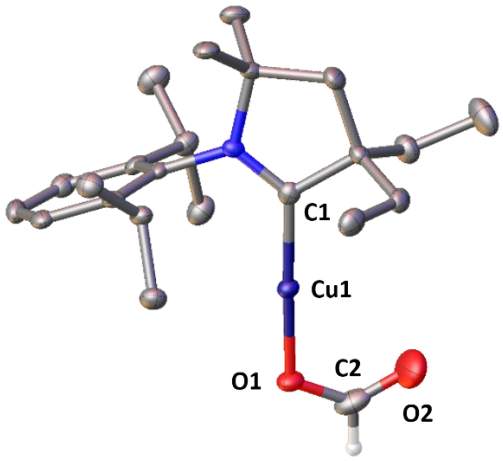

Figure 2.13. Solid-state structure of copper-formate **2.3BC**. Hydrogen atoms other than that bound to formate have been removed for clarity. Thermal ellipsoids are set at 50% probability. Selected distances [Å]: C1-Cu1 1.874(3), Cu1-O1 1.863(2), O1-C2 1.268(4), C2-O2 1.216(4).

Excitingly, we found that the equimolar reaction between **2.3CB** and **2.3BC** in THF at room temperature (Scheme 2.7) quantitatively forms the [PMP-H][CO_2H] salt along with a new carbene copper species displaying an $^{11}B\{^1H\}$ NMR signal at -25.6 ppm (Figure 2.14). We attributed this latter signal to the borane-stabilized monomeric (L_1)CuH-BCF adduct **2.3BD**, which was subsequently isolated and characterized by X-ray crystallography (Figure 2.15).

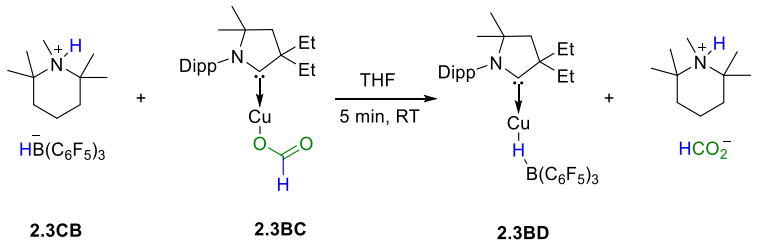

Scheme 2.7. Addition of **2.3CB** to copper-formate **2.3BC** immediately yields the borane-stabilized copper hydride **2.3BD** and the product formate.

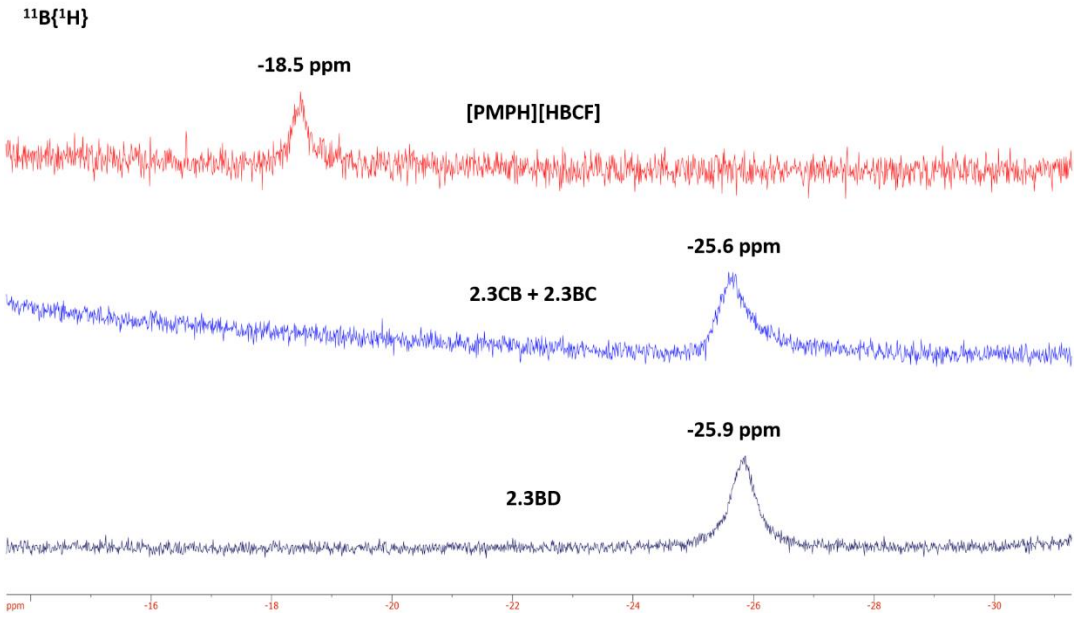

Figure 2.14. $^{11}B\{^1H\}$ NMR spectra for the previously reported [PMPH][HBCF] salt **2.3CB** (top), the crude reaction mixture described in Scheme 2.7 (middle), and the discretely prepared **2.3BD** (bottom).

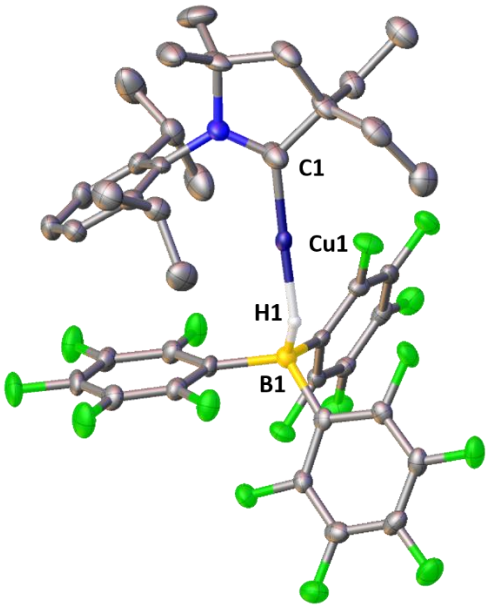

Figure 2.15. Solid-state structure of copper-formate **2.3BD**. Hydrogen atoms other than the hydride have been removed for clarity. Thermal ellipsoids are set at 50% probability. Selected distances [Å] and angles [°]: C1-Cu1 1.878(4); Cu1-H1 1.7661(12); H1-B1 0.999(4); C1- Cu1-H1 176.95(15); Cu1-H1-B1 147.5(2).

As expected, heating a THF solution of **2.3BD** to 100 °C led to complete decomposition of the complex over 24 hours, which is likely due to the formation and decomposition of the free copper-hydride **2.3BB**.[6] To avoid this decomposition, we performed the same reaction in the presence of PMP and 20 bar CO_2 to trap the intermediate copper-hydride complex **2.3BB**; however, in this case, we found the formation of a different carbene-copper complex. Upon isolation and further analysis, we confirmed the presence of the borane-capped copper-formate complex **2.3BE** (Scheme 2.8, left). It is important to note that this complex is also accessible by combining **2.3BC** with BCF in $CDCl_3$ (Scheme 2.8, right). The connectivity of complex **2.3BE** was unambiguously established by an X-ray diffraction study (Figure 2.16).

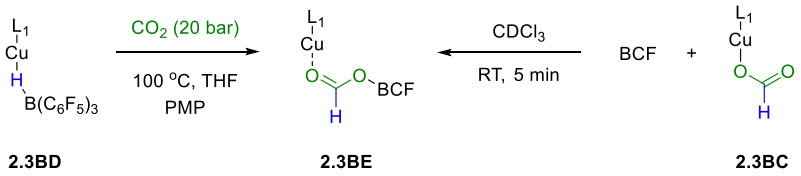

Scheme 2.8. Complex **2.3BE** can either be prepared via hydride insertion into CO_2 (left) or by addition of BCF to copper-formate complex **2.3BC** (right).

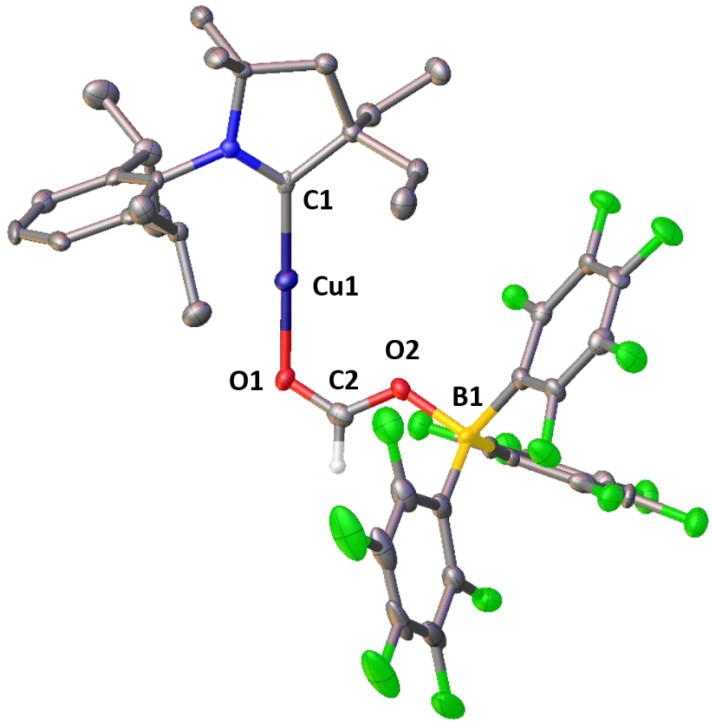

Figure 2.16. Solid state structure of copper-formate **2.3BE**. Hydrogen atoms other than the formate have been removed for clarity. Thermal ellipsoids are set at 50% probability. Selected distances [Å]: C1-Cu1 1.8667(4); Cu1-O1 1.8882(4); O1-C2 1.2178(2); C2-O2 1.28196(17); O2-B1 1.5498(3).

Having exhibited the feasibility of accomplishing each of the key reaction steps proposed in Scheme 2.5, we set out to identify a catalyst precursor that would function as a monomeric copper-hydride but be easily prepared and stored on multigram scales. Per these requirements, complex **2.3BD** is incompatible due to its extreme air sensitivity and the fact that it cannot be prepared on large scales. However, in 2014, our group developed the BH_3 derivative of complex **2.3BD** (**2.3BD^{H}**) which is accessible via a salt metathesis reaction between sodium borohydride and the corresponding (L_1)CuCl in THF (Scheme 2.9). Excitingly, initial testing of its reactivity

with CO_2 (10 bar at 80 °C is sufficient to cleanly generate copper-formate **2.3BC**) confirms that the Cu-H-B bond in complex **2.3BD^H** is more hydridic than it is in complex **2.3BD**. Moreover, with this complex, there does not appear to be any formation of the analogous borane capped copper-formate complex.

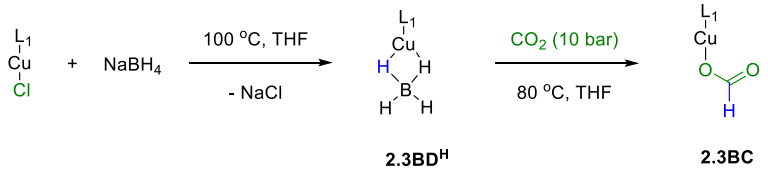

Scheme 2.9. Slightly modified preparation of complex **2.3BD^H** is followed by a more facile insertion reaction into CO_2 as compared to the HBCF complex **2.3BD**.

Using complex **2.3BD^H**, we set out to investigate the ability of FLPs and copper-hydrides to work in tandem under the catalytic conditions described in Table 1 (see appendix for more details). It is important to note that these catalytic studies were done in collaboration with a research group at Nanjing University in China who are well equipped to handle high pressure reaction conditions.[43] Surprisingly, we found that under these catalytic conditions, the combination of BCF/PMP is unable to work in tandem with the copper catalyst to hydrogenate CO_2 (entry 1). Even more surprisingly, we found that decreasing the steric hindrance of the base, and therefore going to a less frustrated and more classical Lewis pair (cLP), allowed the reaction to occur, with DBU giving the best result at 305 TON (entries 2-4). We next evaluated the influence of the borane partner and found that less Lewis acidic boranes give lower TONs, which is likely due to the greater difficulty in H_2 activation (entry 5). As expected for a tandem process, removal of the Lewis acidic borane additive shuts down the catalysis altogether (entry 6). We subsequently verified that the combination of $B(C_6F_5)_3$ and DBU is inefficient to effectively catalyze this process in the absence of a copper complex (entry 7). Excitingly, in the presence of DBU, both of our proposed catalytic intermediates $L_1CuH\text{-}B(C_6F_5)_3$ **2.3BD** (entry 8) and copper-formate complex

2.3BC with added $B(C_6F_5)_3$ (entry 9) can achieve CO_2 conversion to formate with TONs comparable to entry 4. As far as the L ligand is concerned, we tested $L_{1\text{-}4}$,[44,45,46] and confirmed that the best TON was obtained with L_1 (entries 4, 10-12). Furthermore, since we postulate that copper-hydrides are responsible for CO_2 sequestration, we tested the aforementioned IPr* and IPr** NHCs in this process (entries 13-14).[11,12] Likely due to the considerable steric encumbrance, these complexes failed to compete with **2.3BD^{H}** under our catalytic conditions. Lowering the reaction temperature also had a detrimental effect on the TON (entries 15-16). Finally, lowering the catalyst loading by orders of magnitude (entries 17-18) afforded TONs up to 1881.

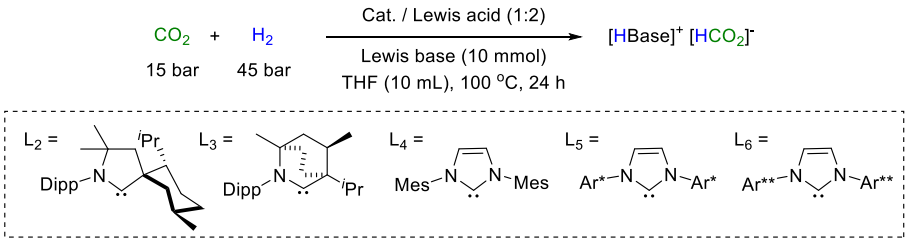

Scheme 2.10. Reaction conditions and associated ligands used for the optimization of the CO_2 hydrogenation reaction.

Table 2.1. Catalytic reduction of CO_2 with H_2.

Entry	Cat.	Cat. (mmol)	Lewis acid	Lewis base	Temp. (^oC)	TON
1	3.2BD^H	0.01	$B(C_6F_5)_3$	PMP	100	0
2	3.2BD^H	0.01	$B(C_6F_5)_3$	LUT	100	89
3	3.2BD^H	0.01	$B(C_6F_5)_3$	TBD	100	97
4	3.2BD^H	0.01	$B(C_6F_5)_3$	DBU	100	305
5	3.2BD^H	0.01	BPh_3	DBU	100	116
6	3.2BD^H	0.01	-	DBU	100	28
7	-	-	$B(C_6F_5)_3$	DBU	100	66
8	3.2BD	0.01	-	DBU	100	287
9	3.2BC	0.01	$B(C_6F_5)_3$	DBU	100	387
10	$L_2$3.2BD^H	0.01	$B(C_6F_5)_3$	DBU	100	264
11	$L_3$3.2BD^H	0.01	$B(C_6F_5)_3$	DBU	100	118
12	$L_4$3.2BD^H	0.01	$B(C_6F_5)_3$	DBU	100	154
13	$L_5$3.2BD^H	0.01	$B(C_6F_5)_3$	DBU	100	136
14	$L_6$3.2BD^H	0.01	$B(C_6F_5)_3$	DBU	100	122
15	3.2BD^H	0.01	$B(C_6F_5)_3$	DBU	80	131
16	3.2BD^H	0.01	$B(C_6F_5)_3$	DBU	60	54
17	3.2BD^H	0.005	$B(C_6F_5)_3$	DBU	100	340
18	**3.2BD^H**	**0.00025**	**$B(C_6F_5)_3$**	**DBU**	100	**1881**

During our optimization of the catalytic CO_2 hydrogenation reaction, we were unable to immediately rationalize why the combination of DBU/BCF far outperformed the true FLP PMP/BCF. To understand this result, we first analyzed the stoichiometric reaction between DBU and BCF. Unsurprisingly, addition of DBU to a dichloromethane solution of BCF quantitatively formed the cLP adduct **2.3LP**, which contains a distinctive $^{11}B\{^1H\}$ NMR signal at δ -7.6 ppm (Scheme 2.11). Adduct **2.3LP** was crystallized by slow cooling of a boiling acetonitrile solution to room temperature, which confirmed the presence of a discrete N-B bond by X-ray crystallography (Figure 2.17).

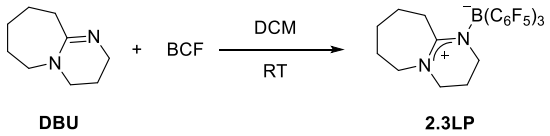

Scheme 2.11. Addition of DBU to BCF immediately forms Lewis pair **2.3LP**.

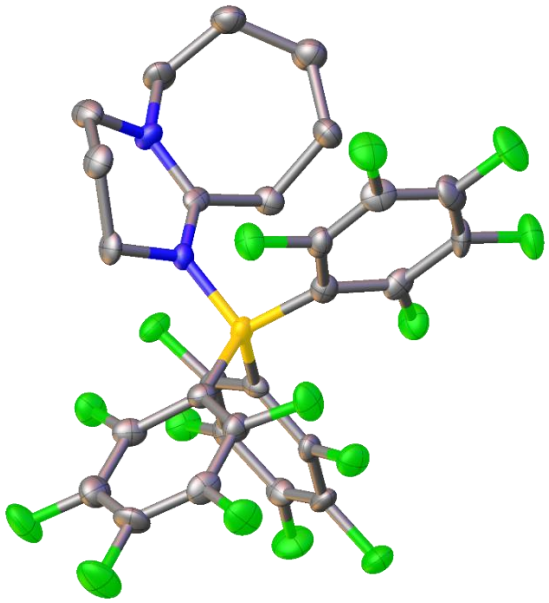

Figure 2.17. Solid state structure of the copper-formate **2.3LP**. Hydrogen atoms have been removed for clarity. Thermal ellipsoids are set at 50% probability. Selected distances [Å]: N-B 1.610(5).

It is worth noting that the N-B distance in **2.3LP** is 1.61 Å. Through a computational study, Stephan and coworkers discovered that 1.65 Å was the minimum distance for a Lewis pair to display FLP reactivity.[47] Therefore, it is unsurprising that activation of dihydrogen could not be observed at room temperature, even under 10 bar of H_2. Although the N-B distance of **2.3LP** falls below this minimum, it has been shown that elevated temperatures can promote FLP-like reactivity for other cLP adducts.[42,48] However, even under extremely forcing reaction conditions (10 bar of H_2 and up to 100 ^{o}C), the [HDBU][HBCF] salt could not be observed spectroscopically (Scheme 2.12, top). In an effort to confirm the FLP nature of **2.3LP** under our reaction conditions, we tested its reactivity in the presence of other reagents known to react with FLPs, such as CO_2 (Scheme 2.12, insert).[49]

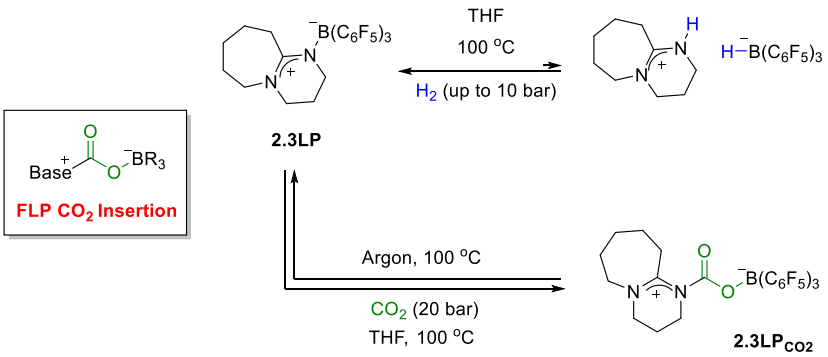

Scheme 2.12. Addition of H_2 to **2.3LP** gives no directly observable reaction; however, addition of CO_2 at 100 °C allows for the observation of CO_2 insertion product **2.3LP$_{CO2}$**.

To our delight, subjecting **2.3LP** to 20 bar of CO_2 at 100 °C in THF gives rise to a new species by ^{11}B NMR at δ -4.6 ppm. Interestingly, this reaction only converts 66% of **2.3LP** to this new product regardless of time, temperature, and pressure. This inability to drive the reaction to completion suggests a thermal equilibrium between **2.3LP** and this other product under our experimental reaction conditions. Multinuclear NMR analysis allowed us to confirm that this new compound was the CO_2 insertion product **2.3LP$_{CO2}$**, whose formation strongly supports our hypothesis of the FLP-like nature of **2.3LP** under the catalytic reaction conditions. As is also the case with true FLPs,[50] heating **2.3LP$_{CO2}$** under argon cleanly re-afforded **2.3LP**. From these results, we hypothesized that **2.3LP** and the [HDBU][HBCF] salt likely exist in equilibrium under the reaction conditions; however, formation of the latter is highly endergonic, and therefore should only exist in minute concentrations. Determined to confirm this hypothesis, we subjected a THF solution of **2.3LP** to 20 bar of H_2 at 80 °C in the presence of copper-formate complex **2.3BC** (Scheme 2.13). We postulated that any transient formation of the [HDBU][HBCF] salt would immediately react with the copper-formate as was previously exhibited in Scheme 2.7. From the reaction mixture, we confirmed the presence of the L_1Cu-HBCF complex **2.3BD** and the fomate salt $[HDBU]^+[HCO_2]^-$. This result, in conjunction with its reactivity with CO_2, confirms our hypothesis regarding the FLP-like behavior of **2.3LP** under the established reaction conditions.

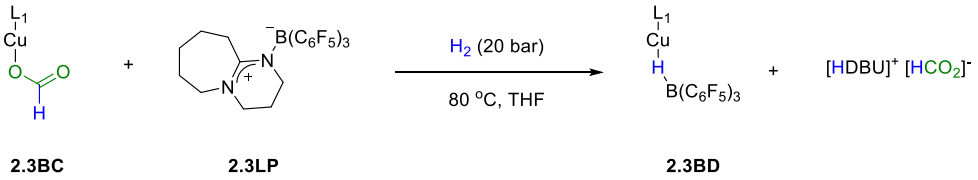

Scheme 2.13. Stoichiometric trapping reaction between **2.3BC**, **2.3LP**, and H_2 to generate the formate salt product and **2.3BD**.

Referring back to Scheme 2.8, we previously observed the insertion of the L_1CuH-BCF complex **2.3BD** into CO_2 to afford the borane capped copper-formate complex **2.3BE**. In that case, PMP did not appear involved in the reaction, which is likely due to its inability to form a true bond with boron. We wondered, however, if DBU would have any effect on this insertion reaction or the outcome of the reaction due to its proven ability to directly bind BCF. To further investigate this question, we performed the reaction of **2.3BD** with CO_2 in the presence of DBU and found that complex **2.3BE** was no longer formed. Instead, we observed the clean formation of the borane-free copper-formate complex **2.3BC** as well as a mixture of **2.3LP** and **2.3LP$_{CO2}$**.

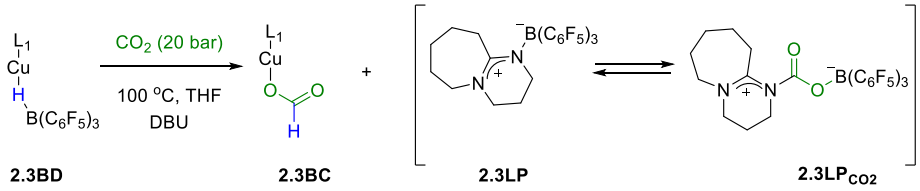

Scheme 2.14. Hydride insertion of **2.3BD** in the presence of DBU reforms the copper-formate complex **2.3BC** along with cLP **2.3LP**.

Although this result confirms the ability of DBU to sequester BCF and allow the formation of **2.3BC**, it does not allow us to definitively say that complex **2.3BE** does not form as a reactive intermediate. To test whether DBU is capable of cleaving the boron-oxygen bond in **2.3BE**, we combined complex **2.3BE** with a stoichiometric amount of DBU in an NMR tube and determined that borane abstraction was not observed. Instead, we spectroscopically confirmed that DBU displaces the formyl-BCF anion and coordinates itself to the copper center (Scheme 2.15, complex

2.3BF). Interestingly, this complex does not collapse to the copper-formate complex by elimination of the DBU-BCF adduct, even when the sample was heated to 100 °C in THF.

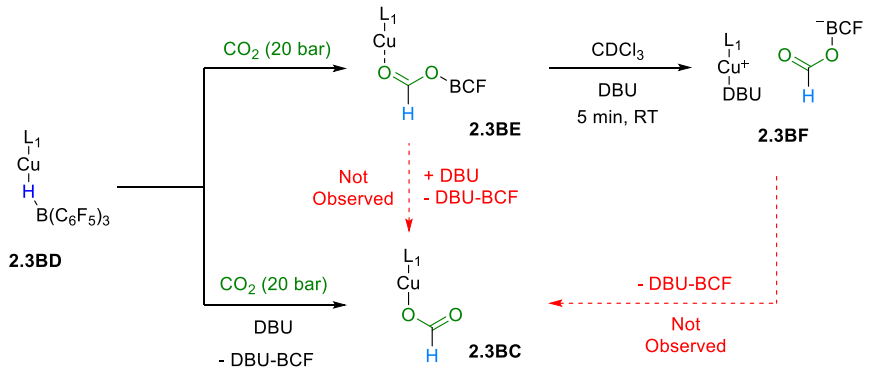

Scheme 2.15. Determining the likelihood of forming complex **2.3BE** within the catalytic cycle by assessing whether DCU can abstract BCF from the formate to generate **2.3BC** and **2.3LP**.

We believe that this result clearly explains why true FLPs such as **2.3AA** are ineffective under our catalytic reaction conditions (Table 2.1, entry 1). Since the cleavage of the boron-oxygen bond is enthalpically demanding and PMP cannot form a true bond with BCF, there is no driving force to turn over the catalytic cycle. Furthermore, as was noted by O'Hare and coworkers,[40] prolonged heating of formyl-BCF containing salts drives the hydride de-insertion reaction, which only serves to regenerate the H-BCF anion. This latter point would put the copper catalyst back at the pre-CO_2 insertion stage to repeat this process with no productive catalysis ever taking place.

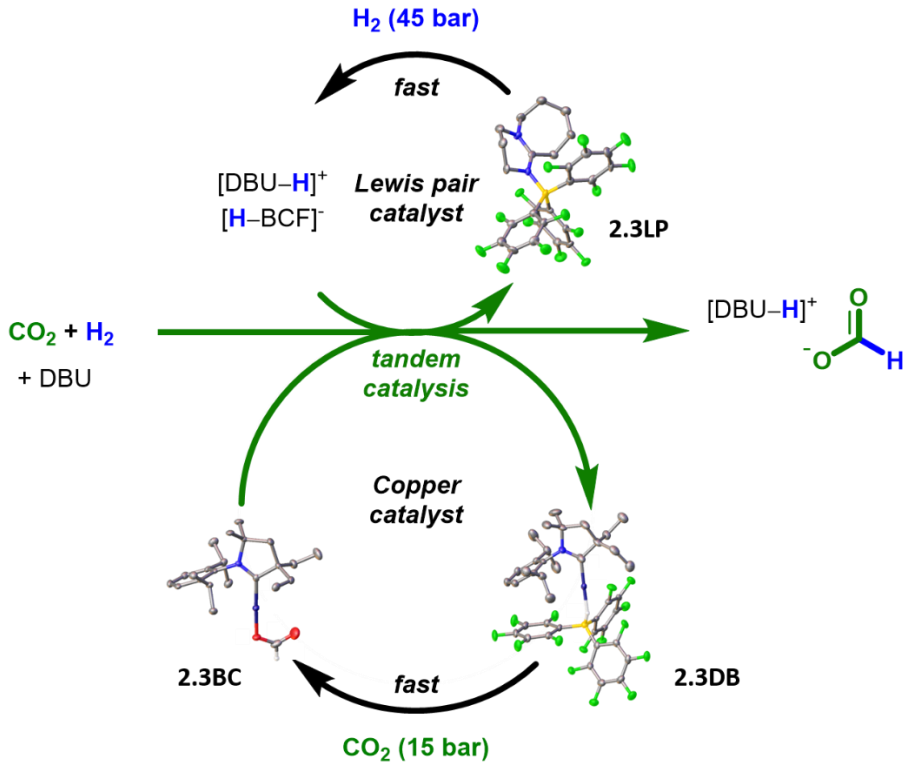

Scheme 2.16. Proposed mechanism for the hydrogenation of CO_2 to formate derived from extensive catalytic and stoichiometric reactions.

In summary, we have demonstrated the ability of copper complexes to work in tandem with cLPs and exemplified this cooperation in the reduction of CO_2 to formate using molecular hydrogen as the reductant. Through stoichiometric and catalytic reactions, we have shown that the likely mechanistic pathway involves the insertion of CO_2 into a copper-hydride bond to give a copper-formate (Scheme 2.16). The copper-oxygen bond of the latter is cleaved by H_2, which has been activated by the cLP, to give back the copper-hydride complex, and the product $[DBU\text{-}H]^+[CO_2H]^-$ salt. Despite the considerable advances that have been made by FLPs in catalysis,[38,39] our work suggests that cLPs should not be overlooked in tandem processes involving transition metals. For this reason, future research on synergistic processes should examine the application of cLPs working in tandem with different transition-metal complexes to facilitate other synthetically useful transformations.

2.4 Preparation of A Neutral Silver(I)-Hydride

In addition to the preparation, characterization, and reactivity studies of monomeric copper(I)-hydride complexes, the isolation, structural characterization, and reactivity of heavier silver and gold analogues have also intrigued chemists. In 2008, Sadighi *et al.* characterized the first example of a neutral monoligated gold(I)-hydride using the IPr NHC ligand (Figure 2.1, **2.4A**).[51] Interestingly, the necessity for steric protection to avoid oligomerization was a non-issue in this case as no evidence of nucleation occurred. Furthermore, the authors noted a greater solid-state resistance to hydrolysis for this gold-hydride as compared to the analogous copper dimer **2.2A** (>2 weeks vs. <5 seconds, respectively) as well as a lack of alkyne insertion chemistry with 3-hexyne or diphenylacetylene. These data suggest the significantly diminished hydricity of gold-hydrides as compared to their copper counterparts.

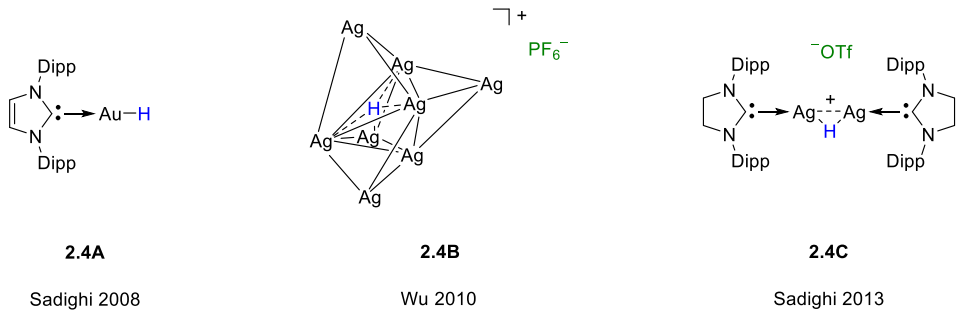

Figure 2.18. The first gold(I)-hydride complex **2.4A** and the only structurally characterized silver(I)-hydrides **2.4B** and **2.4C**. Note that the $Se_2[P(O^iPr)_2]$ ligands in the cluster **2.4B** have been omitted for clarity.

With respect to silver, there are no reported neutral monoligated silver(I)-hydride analogues, and consequently it is unknown whether the reactivity of this complex better mimics its copper(I) or gold(I) homologue. To date, the only known silver-hydride complexes are cationic in nature and are depicted in Figure 2.18. In 2010, Liu *et al.* isolated the cationic $[Ag_8(\mu_4{-}H)\{Se_2P(OR)_2\}_6]^+$ cluster **2.4B** containing Ag(I)-hydride bridges (Ag–μ-H–Ag).[52]

Following this report, Sadighi *et al*. described the dimeric silver-hydride cation **2.4C** in 2013, which constitutes the lowest nuclearity silver hydride complex to date.[53] Preliminary reactivity was conducted using **2.4C**, for which the authors report chemistry that is reminiscent of the analogous cationic copper-hydride.[37]

Using the same sterically encumbering NHC ligands described in Section 2.2, we set out to isolate and structurally characterize the first example of a neutral monoligated silver(I)-hydride complex. Due to the insolubility of AgCl in common organic solvents, preparation of (IPr**)AgCl was accomplished by reaction of silver(I) oxide with the imidazolium hydrochloride salt precursor. The subsequent salt metathesis reaction with potassium phenolate afforded (IPr**)AgOPh **2.4DA** in 92% isolated yield as a white solid. Addition of one equivalent of pinacolborane to a room temperature benzene solution led to an initially colorless solution, which began to turn purple within 1 hour at room temperature (Scheme 2.17, top). ^{1}H NMR analysis of this mixture showed only resonances associated with the free IPr** NHC while ^{11}B{^{1}H} NMR spectroscopy revealed the formation of PhOBPin.[14]

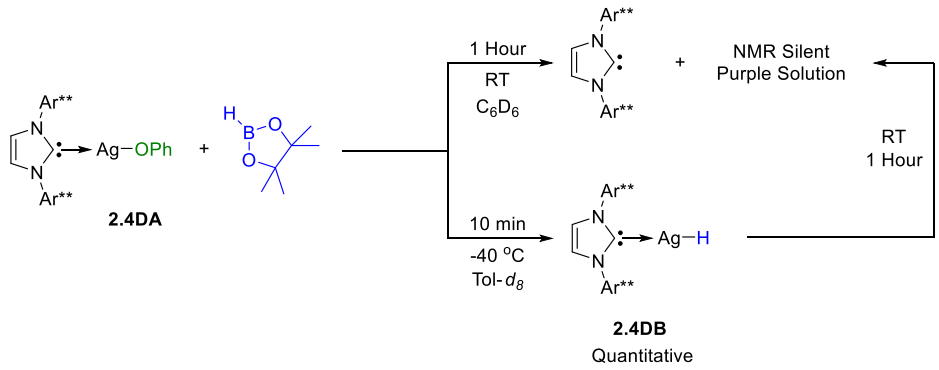

Scheme 2.17. Reaction of silver phenoxide **2.4DA** with pinacolborane affords the stable silver(I)-hydride **2.4DB** only at -40 °C.

Excitingly, in a -40 °C toluene-d_8 solution, addition of pinacolborane generates the same colorless solution; however, this reaction mixture remains colorless for at least a week at this

temperature (Scheme 2.17, bottom). Furthermore, the ^{1}H and ^{13}C{^{1}H} NMR spectra at -40 ^{o}C shows a pair of doublets [^{1}H: δ 3.87 ppm, $^{1}J(^{107}Ag\text{-}^{1}H)$ = 224.6 Hz and $^{1}J(^{109}Ag\text{-}^{1}H)$ = 260.6 Hz; ^{13}C: δ 193.2 ppm, $^{1}J(^{107}Ag\text{-}^{13}C)$ = 113.2 Hz and $^{1}J(^{109}Ag\text{-}^{13}C)$ = 126.6 Hz], which was expected for the monomeric silver(I)-hydride **2.4DB** (Figure 2.19). It should be noted that warming of this sample to room temperature generates the same purple solution and ^{1}H NMR spectrum that was obtained when the reaction was launched at ambient temperature.

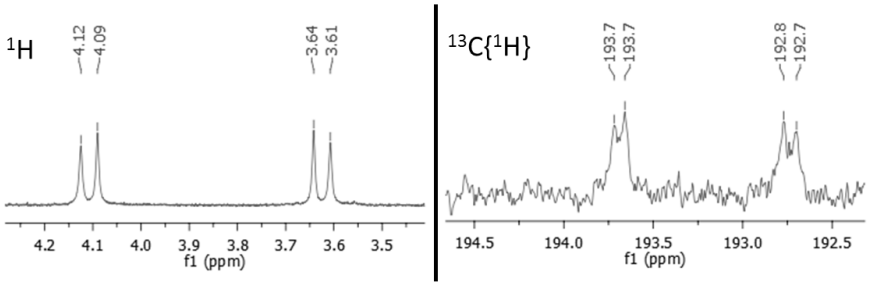

Figure 2.19. Hydride and carbene regions of the ^{1}H and ^{13}C{^{1}H} NMR spectra for monomeric silver hydride **2.4DB** at –40 ^{o}C.

Maintaining the solution at -40 ^{o}C overnight produced single crystals of hydride **2.4DB** as colorless needles. A single crystal X-ray diffraction study confirmed the monomeric nature of the (IPr**)Ag(I)-H **2.4DB** (Figure 2.20).

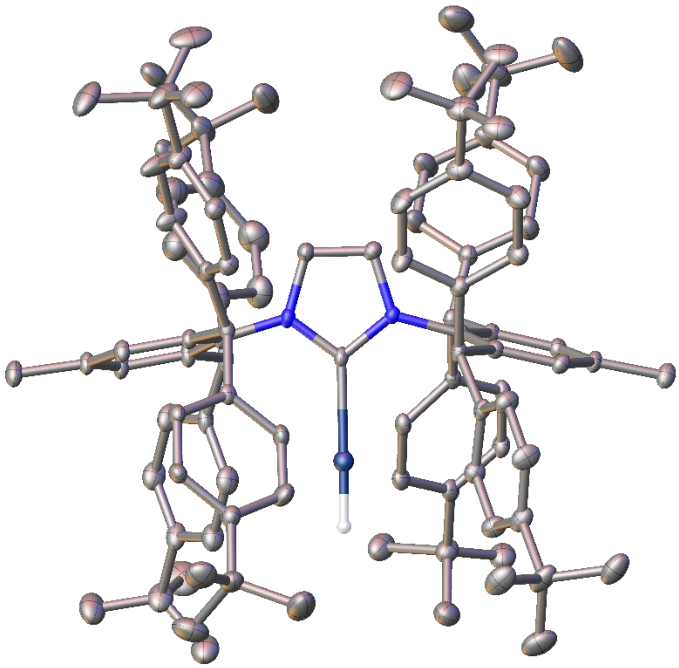

Figure 2.20. Molecular structure of **2.4DB** in the solid state. Thermal ellipsoids are set at 50% probability. Hydrogen atoms other than the hydride and solvent molecules are omitted for clarity. Selected distances [Å]: C1-Ag1 2.108(6).

Silver hydride **2.4DB** crystallizes in the chiral space group P^{-1} with 2 molecules in the asymmetric unit cell. Further analysis shows no interaction between neighboring silver atoms as they are separated by more than 3.5 Å. Due to the positional disorder of the silver atom, the hydride could not be located and was fixed in the molecular structure of **2.4DB**.

To gain insight into whether the reactivity of silver-hydride complex **2.4DB** better mimics that of its copper or gold analogues, we attempted the reaction of **2.4DB** with CO_2. As noted above, copper-hydrides readily insert into CO_2 to give copper-formate complexes;[23b-c,36,37] however, there are currently no examples of the analogous reaction with gold-hydrides. Following *in-situ* preparation of silver-hydride **2.4DB** in a J-Young NMR tube at -40 ^{o}C, the mixture was thoroughly degassed and backfilled with 1 bar of CO_2 and allowed to warm to room temperature. After 1 hour, the reaction mixture transitioned to purple and the ^{1}H NMR spectrum showed a mixture of free IPr** NHC and (IPr**)Ag-OC(O)H complex **2.4DC**. Conversely, maintaining the reaction

mixture at -40 °C for 6 hours in the presence of CO_2 results in quantitative formation of the silver-formate complex **2.4DC** as evidenced by ^{1}H and ^{13}C NMR spectroscopies (Scheme 2.18).

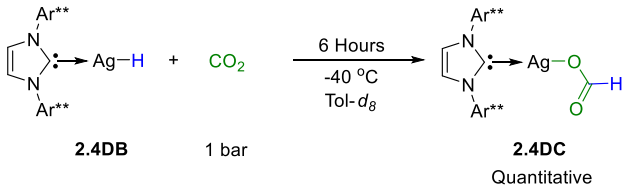

Scheme 2.18. Reaction of silver-hydride **2.4DB** with 1 bar of CO_2 proceed quantitatively at -40 °C within 6 hours to afford silver-formate complex **2.4DC**.

Copper-hydrides have also been shown by us and others to make adducts with Lewis acidic boranes, as exemplified in Sections 2.2 and 2.3 with the formation of complexes **2.2CD**, **2.2DD**, and **2.3BD** as well as by others.[16,54] Again, there are no such complexes known to be stable with gold-hydrides. If a similar complex could be isolated using silver-hydride **2.4DB**, this would strongly suggest that silver-hydrides contain a similar reactivity profile to their copper analogues rather than their gold counterparts. To test this hypothesis, one equivalent of BCF was added to a solution of **2.4DB** at -40 °C, which yielded the corresponding thermally stable (IPr**)Ag-H-$B(C_6F_5)_3$ adduct **2.4DD** within minutes (Scheme 2.19).

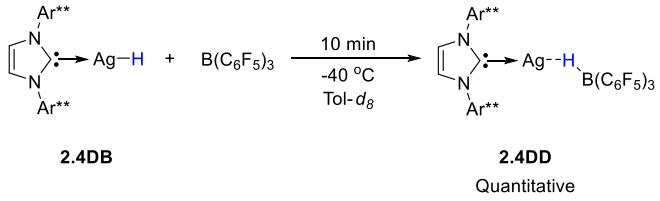

Scheme 2.19. Addition of BCF to a toluene solution of silver-hydride **2.4DB** at -40 °C affords the thermally stable Ag-H-BCF complex **2.4DD**.

Interestingly, ^{1}H NMR analysis does not show any Ag-H coupling as was observed for complex **2.4DB**; meanwhile, the boron resonance in ^{11}B NMR appears at -22.7 ppm, which is within range of other transition-metal H-BCF complexes.[16,55] A single crystal X-ray diffraction

study confirmed the connectivity proposed for complex **2.4DD**, and the hydride was located and isotropically refined without restraint (Figure 2.21).

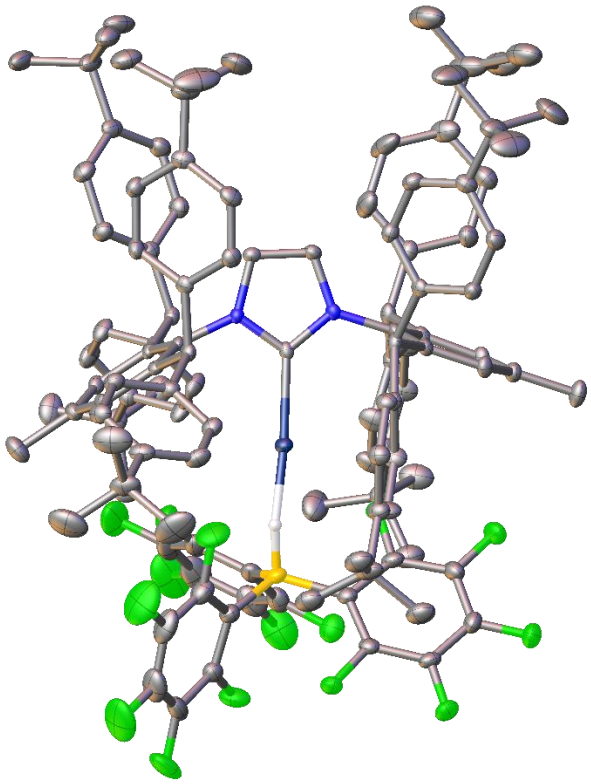

Figure 2.21. Molecular structure of **2.4DD** in the solid state. Thermal ellipsoids are set at 50% probability. Hydrogen atoms other than the hydride, and solvent molecules have been omitted for clarity. Selected distances [Å] and angles [°]: C1-Ag1 2.095(2); Ag1-H1 1.81(3); H1-B1 1.21(3); C1-Ag1-H1 173.5(9); Ag1-H1-B1 159.7(13).

Using the most sterically encumbering NHC ligand, we were able to synthesize and structurally characterize the only known example of a neutral, monoligated, and monomeric silver(I)-hydride. Although this complex was found to be unstable above -40 °C, we showed that its reactivity better mimics that of copper-hydrides. Future goals for neutral silver-hydride chemistry include the development of more readily accessible ligand frameworks that can stabilize a silver-hydride, potentially as a dimer, at room temperature so that its catalytic applications can be further investigated.

2.5 General Conclusion

In this chapter, we have shown that sterically encumbering *N*-heterocyclic carbene ligands can be used to kinetically stabilize highly reactive transition-metal complexes. More specifically, we have prepared a copper-hydride dimer that is stable in solution at temperatures up to 80 ^{o}C, as well as the only example of a characterizable monomeric copper-hydride complex. The latter was found to be in equilibrium with its dimer, which supported the longstanding hypothesis that copper-hydride aggregates dissociate in solution and react as their corresponding monomers. Using variable temperature NMR, we were able to determine the thermodynamic parameters associated with this dimerization event. Using the same bulky NHC, we were also able to prepare and structurally characterize the only known example of a neutral monomeric silver(I)-hydride complex. Based on preliminary experiments, reactivity for this complex better mirrors that of its copper counterparts rather than its gold analogues.

Transitioning away from bulky NHC ligands, we found that borane stabilized cyclic (alkyl)(amino) carbene copper-hydride monomers work well in tandem with classical Lewis pairs to affect the hydrogenation of carbon dioxide with H_2. The reaction was found to occur first by insertion of the Cu-H bond into CO_2 to generate a copper-formate. At the same time, hydrogen gas is cleaved by the classical Lewis pair, which was determined to become "frustrated" under the optimized reaction conditions. The resulting ammonium borohydride salt reacts with the copper-formate to release the formic acid conjugate base and regenerate the Cu-H-borane complex. It was determined that true FLPs are unable to function in this reaction and only serve to deactivate the tandem catalyst system.

Chapter 2 has been adapted from materials published in Romero, E. A.; Olsen, P. M.; Jazzar, R.; Soleilhavoup, M.; Gembicky, M.; Bertrand, G., "Spectroscopic Evidence for a

Monomeric Copper(I) Hydride and Crystallographic Characterization of a Monomeric Silver(I) Hydride" *Angew. Chem. Int. Ed.* **2017**, *56*, 4024 – 4027 and materials accepted for publication in Romero, E. A.; Zhao, T.; Nakano, R.; Hu, X.; Wu, Y.; Jazzar, R.; Bertrand, G., "Tandem Copper Hydride - Lewis Pair Catalyzed Reduction of Carbon Dioxide into Formate with Dihydrogen" *Nature Catalysis* **2018**, *1*, 743 – 747. The dissertation author was the primary investigator of the former publication and co-primary investigator of the latter publication.

2.6 Appendix

2.6.1 Preparation and Characterization of a Monomeric Copper(I)-Hydride

All reactions were performed under an atmosphere of argon using standard Schlenk or dry box techniques; all solvents were dried and degassed using standard procedures. Toluene, benzene, hexane, pentane, THF, and diethyl ether we distilled from sodium. C_6D_6 was distilled from sodium benzophenone and stored over a potassium mirror. Dichloromethane and chloroform were dried by distillation from CaH_2. Reagents of analytical grade were obtained from commercial suppliers, dried over 4Å molecular sieves and degassed before use. ^{1}H and ^{13}C and Variable temperature NMR spectra were obtained using a Varian Inova 500 MHz spectrometer. Chemical shifts (δ) are reported in parts per million (ppm) relative to TMS and were referenced to the residual solvent peak. NMR multiplicities are abbreviated as follows: s = singlet, d = doublet, t = triplet, q = quartet, pent = pentet, quin = quintet, sextet, dd = doublet of doublets, dt = doublet of triplets, qt = quartet of triplets, m = multiplet, br = broad signal. IPr*HCl[11] and IPr**HCl[12] imidazolium precursors were prepared according to literature procedures.

Synthesis of (IPr*)CuCl: A Schlenk tube was charged with IPr*HCl imidazolium (1.50 g, 1.58 mmol, 1 eq.), KOtBu (0.19 g, 1.66 mmol, 1.05 eq.), and CuCl (0.19 g, 1.90 mmol, 1.2 eq.).

5 mL anhydrous toluene was added, and the resulting solution was stirred for 24 hours at room temperature. The reaction was filtered over celite and the volatiles were evaporated under vacuum. The residue was washed with 3 x 5 mL portions of cold diethyl ether. The residue was again dried under vacuum yielding 1.57 g (98%) as a white solid. ^{1}H and ^{13}C NMR spectra match those reported in the literature.[56]

Synthesis of (IPr*)CuOPh (2.2CA): To a Schlenk tube charged with IPr*CuCl (2.20 g, 2.18 mmol, 1 eq.) was added KOPh (0.34 g, 2.61 mmol, 1.2 eq.). 10 mL anhydrous dichloromethane was added, and the resulting solution was stirred for 12 hours at room temperature. The reaction was filtrated over celite and the volatiles were evaporated under vacuum yielding 2.22 g of **2.2CA** as a white solid (87% yield). ^{1}H NMR (C_6D_6, 500 MHz): δ 1.77 (s, 6 H), 5.46 (s, 4 H), 5.57 (s, 2 H) 6.73 (t, J = 6.6 Hz, 1 H), 6.93-6.98 (m, 13 H), 6.99-7.03 (m, 20 H), 7.10 (t, J = 7.4 Hz, 10 H), 7.23 (d, J = 8.4 Hz, 8 H). ^{13}C{^{1}H} NMR (C_6D_6, 125 MHz): δ 181.2 (C_{carb}), 143.8, 142.8, 141.7, 140.7, 134.9, 130.8, 130.5, 130.1, 130.0, 129.8, 129.7, 129.44, 129.35, 129.0, 128.9, 128.6, 127.4, 127.1, 126.8, 123.6, 123.5, 51.9, 21.4, 21.3.

Synthesis of [(IPr*)CuH]$_2$ (2.2CB): IPr*CuOPh (0.330 g, 0.309 mmol, 1 eq.) was added to a flame dried Schlenk tube with a magnetic stir bar. 2 mL C_6H_6 was added followed by pinacolborane (47.1 μL, 0.325 mmol, 1.05 eq.). An intense deep orange color preceded the formation of copious amounts of yellow precipitate. The reaction was stirred for 2 hours at room temperature. 5 mL pentane was added to precipitate the remaining product in solution. The precipitate was filtrated, washed with 2 x 5 mL pentane, and dried under vacuum yielding 0.268 g of **2.2CB** as a yellow powder (89% yield). Crystals suitable for an X-ray diffraction study were grown from slow diffusion of pentane into a saturated solution of benzene at 5 ºC. M.P. 82.7 ºC dec. ^{1}H NMR (C_6D_6, 500 MHz): δ 1.97 (s, 6 H), 3.91 (s, 1 H, Cu*H*), 5.37 (s, 2 H) 6.21 (s, 4 H),

7.04-7.13 (m, 32 H), 7.32 (s, 4 H), 7.79 (s, 8 H). $^{13}C\{^{1}H\}$ NMR (C_6D_6, 125 MHz): δ 194.4 (C_{carb}), 144.7, 144.5, 142.0, 138.3, 136.7, 131.0, 130.3, 130.0, 129.0, 126.3, 121.9, 51.7, 21.5. ^{13}C NMR (C_6D_6, 125 MHz): δ 194.3 (C_{carb}, t, J = 6.4 Hz), 144.7 (q, J = 6.4 Hz), 144.5 (q, J = 6.3 Hz), 142.0 (d, J = 7.5 Hz), 138.3 (q, J = 6.2 Hz), 136.7 (m), 131.0 (q, J = 3.8 Hz), 130.3 (m), 130.0 (m), 129.0 (s), 126.3 (dt, J = 7.6 Hz, 158.6 Hz), 121.9 (dd, J = 12.6 Hz, 197.3 Hz), 51.7 (d, J = 127.1 Hz), 21.5 (qt, J = 5.3 Hz, 126.1 Hz).

Synthesis of (IPr*)Cu(κ²-H₂)9BBN (2.2CD): IPr*CuOPh (33 mg, 30.9 μmol, 1 eq.) was added to a flame dried schlenk tube with a magnetic stir bar. 1 mL C_6H_6 was added followed by 9-BBN dimer (8 mg, 32.5 μmol, 1.05 eq.). The reaction was stirred for 2 hours at room temperature. Volatiles were removed under vacuum and the residue was washed with 2 x 5 mL pentane. The residue was dried under vacuum giving a white powder in 93% yield (31.5 mg). Crystals suitable for an X-ray diffraction study were grown overnight from slow diffusion of pentane into a saturated solution of benzene at room temperature. M.P. 236.3 ºC dec. ^{1}H NMR (C_6D_6, 500 MHz): δ 1.34 (s, br, 2 H, B – *H*), 1.67 (s, 6 H), 2.07 (m, 2 H) 2.28 (m, 8 H), 2.45 (m, 2 H), 5.40 (s, 2 H), 5.57 (s, 4 H), 6.92 (m, 8 H), 6.99 (m, 12 H), 7.04 (t, J = 7.8 Hz, 4 H), 7.25 (t, J = 7.8 Hz, 8 H), 7.38 (d, J = 7.91 Hz, 8 H). $^{13}C\{^{1}H\}$ NMR (C_6D_6, 125 MHz): δ 183.5 (C_{carb}), 143.7, 143.4, 141.6, 140.5, 135.0, 130.4, 130.1, 129.9, 129.0, 128.6, 127.3, 126.8, 123.33, 123.27, 51.8, 36.1, 33.6, 26.5, 24.4, 21.3. ^{11}B NMR (C_6D_6, 160 MHz): δ -10.4 (t, J = 52.8 Hz).

Synthesis of (IPr)CuCl**: A Schlenk tube was charged with IPr**HCl imidazolium (2.21 g, 1.58 mmol, 1 eq.), KOtBu (0.19 g, 1.66 mmol, 1.05 eq.), and CuCl (0.19 g, 1.90 mmol, 1.2 eq.). 10 mL anhydrous toluene was added, and the resulting solution was stirred for 24 hours at room temperature. The reaction was filtered over celite and the volatiles were evaporated under vacuum. The residue was washed with 3 x 5 mL portions of cold diethyl ether. The residue was again dried

under vacuum yielding 2.10 g (91%) as an off-white solid. ^{1}H NMR ($CDCl_3$, 500 MHz): δ 1.18 (s, 72 H), 2.17 (s, 6 H), 5.21 (s, 4 H), 5.70 (s, 2 H) 6.72 (d, J = 7.0 Hz, 8 H), 6.80 (s, 4 H), 7.02 (d, J = 7.5 Hz, 8 H), 7.28 (d, J = 7.9 Hz, 8 H), 7.17 (d, J = 7.4 Hz, 8 H). ^{13}C{^{1}H} NMR ($CDCl_3$, 125 MHz): δ 180.1 (C_{carb}), 149.2, 149.1, 141.3, 140.1, 140.0, 139.7, 134.2, 130.1, 129.3, 129.1, 125.5, 125.1, 123.4, 50.4 (CHAr$_2$), 34.5 (ArCH$_3$), 31.5 (C(CH$_3$)$_3$), 22.0 (C(CH$_3$)$_3$).

Synthesis of (IPr)CuOPh (2.2DA)**: To a Schlenk tube charged with IPr**CuCl (3.18 g, 2.18 mmol, 1 eq.) was added KOPh (0.35 g, 2.61 mmol, 1.2 eq.). 10 mL anhydrous dichloromethane was added, and the resulting solution was stirred for overnight at room temperature. The reaction was filtered over celite. The celite was washed with 2 x 5 mL DCM and the combined organic extracts were evaporated under vacuum yielding 2.71 g of **2.2DA** as a white solid (82% yield). ^{1}H NMR (C_6D_6, 500 MHz): δ 1.20 (s, 36 H), 1.24 (s, 36 H), 1.75 (s, 6 H), 5.75 (s, 2 H), 5.82 (s, 4 H) 6.73 (t, J = 6.6 Hz, 1 H), 7.02 (d, J = 8.5 Hz, 10 H), 7.10 (d, J = 8.0 Hz, 8 H), 7.22 (s, 4 H), 7.28 (d, J = 8.4 Hz, 8 H), 7.55 (d, J = 8.0 Hz, 8 H). ^{13}C{^{1}H} NMR (C_6D_6, 125 MHz): δ 181.8 (C_{carb}), 149.5, 149.2, 141.9, 141.0, 140.7, 135.0, 130.6, 129.9, 129.6, 128.6, 126.2, 125.5, 123.7, 51.0 (CHAr$_2$), 34.5 (ArCH$_3$), 31.5 (C(CH$_3$)$_3$), 21.2 (C(CH$_3$)$_3$).

Synthesis of (IPr)Cu(κ²-H₂)B(H)OPh) (2.2DD)**: IPr**CuOPh (50 mg, 33.0 μmol, 1 eq.) was added to a J-Young NMR tube followed by 500 μL C_6D_6 and pinacol borane (14.3 μL, 98.9 μmol, 3 eq.). A deep yellow color was immediately observed. The tube was allowed to sit overnight at room temperature. Large colorless rods suitable for X-ray diffraction grew overnight. The crystals were filtrated, washed with 2 x 1 mL pentane, and dried under vacuum yielding 49.5 mg of **2.2DD** as colorless needles (98% yield). M.P. 222.9 ^{o}C dec. ^{1}H NMR (C_6D_6, 500 MHz): δ 1.19 (s, 36 H), 1.20 (s, 36 H), 1.62 (s, 3 H, ROBH_3), 1.65 (s, 6 H), 5.71 (s, 4 H), 5.77 (s, 2 H), 6.84 (t, J = 7.1 Hz, 1 H), 6.98 (d, J = 8.2 Hz, 8 H), 7.11 (d, J = 8.3 Hz, 8 H), 7.13 (s, 4 H), 7.24 (t, J =

8.45 Hz, 2 H), 7.30 (d, J = 8.2 Hz, 8 H), 7.42 (d, J = 8.6 Hz, 2 H), 7.44 (d, J = 8.4 Hz, 8 H). $^{13}C\{^{1}H\}$ NMR (C_6D_6, 125 MHz): δ 182.1 (C_{carb}), 149.7, 149.3, 141.9, 140.9, 140.8, 134.9, 129.9, 129.6, 129.3, 126.2, 125.5, 117.8, 117.7, 50.95, 34.6, 34.5, 31.6, 31.6, 31.5, 24.7. ^{11}B NMR (C_6D_6, 160 MHz): δ -12.5 (q, J = 81.5 Hz).

(IPr)CuH Monomer/Dimer (2.2DB$_{di}$/2.2DB$_{mono}$)**: IPr**CuOPh **2.2DA** (60 mg, 39.6 μmol, 1 eq.) was added to a J-Young NMR tube, followed by 500 μL C_6D_6 and PMHS (2.50 μL, 39.6 μmol, 1 eq.). The solution was shaken and left overnight at room temperature. Over time, an intense yellow solution appeared, however, no precipitate formed. The solution was analyzed as the crude mixture at room temperature. Crystals of **2.2DB$_{di}$** suitable for an X-ray diffraction study were grown from a pentane solution with 10 μL of toluene at -40 °C. Crystals of **2.2DB$_{mono}$** could not be grown. The following spectra are reported for a 1:2 mixture of **2.2DB$_{di}$**:**2.2DB$_{mono}$** at 25 °C and 0.089 M solution in C_6D_6:

2.2DB$_{di}$: ^{1}H NMR (C_6D_6, 500 MHz): δ 1.18 (s, 72 H), 1.20 (s, 72 H), 1.88 (s, 12 H), 4.26 (s, 2 H, Cu*H*), 5.06 (s, 4 H), 6.32 (s, 8 H), 6.93 (d, J = 7.7 Hz, 16 H), 6.97 (d, J = 8.3 Hz, 16 H), 6.99 (s, 8 H), 7.65 (s, br, 16 H). $^{13}C\{^{1}H\}$ NMR (C_6D_6, 125 MHz): δ 192.8 (C_{carb}), 148.4, 148.2, 142.6, 142.3, 140.1, 137.2, 136.8, 135.2, 130.8, 130.5, 130.0, 125.8, 125.0, 122.7, 121.8, 120.2, 50.9, 34.5, 34.4, 31.9, 31.6, 21.8. ^{13}C NMR (C_6D_6, 125 MHz): δ 192.8 (t, J = 6.4 Hz, C_{carb}), 148.4 (m), 148.2 (m), 142.6 (d, J = 7.7 Hz), 142.3 (q, J = 6.6 Hz), 140.1 (q, J = 6.2 Hz), 137.2 (q, J = 6.0 Hz), 136.8 (sept, J = 3.7 Hz), 135.2 (sept, J = 4.3 Hz), 130.8 (dd, J = 4.1 Hz, 6.9 Hz), 130.5 (m), 130.0 (dd, J = 4.3 Hz, 7.0 Hz), 125.9 (dd, J = 6.9 Hz, 107.5 Hz), 125.3 (m), 122.6 (d, J = 12.7 Hz), 122.6, 121.8 (m), 120.2 (dd, J = 8.1 Hz, 159.9 Hz), 50.9 (d, J = 129.6 Hz), 35.5 (m), 31.8 (qpent, J = 5.0 Hz, 124.8 Hz), 21.8 (qt, J = 4.7 Hz, 126.2 Hz).

2.2DB$_{mono}$: ^{1}H NMR (C_6D_6, 500 MHz): δ 1.18 (s, 36 H), 1.24 (s, 36 H), 1.72 (s, 6 H), 2.14 (s, 1 H, Cu*H*), 5.70 (s, 2 H), 5.98 (s, 4 H), 7.03 (d, J = 7.8 Hz, 8 H), 7.12 (d, J = 8.4 Hz, 8 H), 7.19 (s, 4 H), 7.32 (d, J = 7.8 Hz, 8 H), 7.78 (d, J = 8.4 Hz, 8 H). ^{13}C{^{1}H} NMR (C_6D_6, 125 MHz): δ 185.8 (C_{carb}), 149.3, 149.0, 141.9, 141.7, 140.6, 130.5, 129.6, 128.6, 125.9, 125.5, 123.2, 122.5, 120.3, 50.9, 34.50, 34.45, 31.6, 21.3. ^{13}C NMR (C_6D_6, 125 MHz): δ 185.8 (d, J = 40.0 Hz, C_{carb}), 149.3 (m), 149.0 (m), 141.9 (d, J = 7.7 Hz), 141.7 (q, J = 6.9 Hz), 140.6 (q, J = 8.5 Hz), 130.5 (m), 129.5 (m), 128.6 (m) 126.3 (dd, J = 6.8 Hz, 61.0 Hz), 125.1 (dd, J = 6.2 Hz, 61.0 Hz), 123.2 (t, J = 6.8 Hz), 122. 4 (d, 11.5 Hz), 120.2 (dd, J = 8.1 Hz, 159.9 Hz), 50.9 (d, J = 129.6 Hz), 35.5 (m), 31.5 (qm, J = 124.4 Hz), 21.3 (qt, J = 4.6 Hz, 125.9 Hz).

Determination of ΔG, ΔH, and ΔS of Dimerization:

(IPr)CuH Dimer – Monomer Equilibrium Variable Temperature NMR Experiment (2.2DB$_{di}$/2.2DB$_{mono}$)**: IPr**CuOPh (67 mg, 44.0 μmol, 1 eq.) was added to a J-Young NMR tube. 400 μL C_6D_6 was added to the NMR tube followed by PMHS (2.8 μL, 44.0 μmol, 1 eq.) to give a 0.11 M solution. The tube was shaken and left overnight at room temperature. Over time, an intense yellow solution appeared, however, no precipitate formed. The solution was analyzed as the crude mixture at 10 ^{o}C intervals between 20.7 ^{o}C and 70 ^{o}C on a Varian Inova 500 MHz spectrometer. Upon reaching each temperature, the tube was allowed to equilibrate at this temperature for 10 minutes before data collection. After the first collection, 10 additional minutes elapsed before collection of a second spectrum at the same temperature. This process was repeated for each temperature point collected and again when returning to room temperature for a total of 4 collections at each temperature. The integration values were averaged before use in subsequent calculations. The following figure depicts the an NMR spectrum at each temperature point.

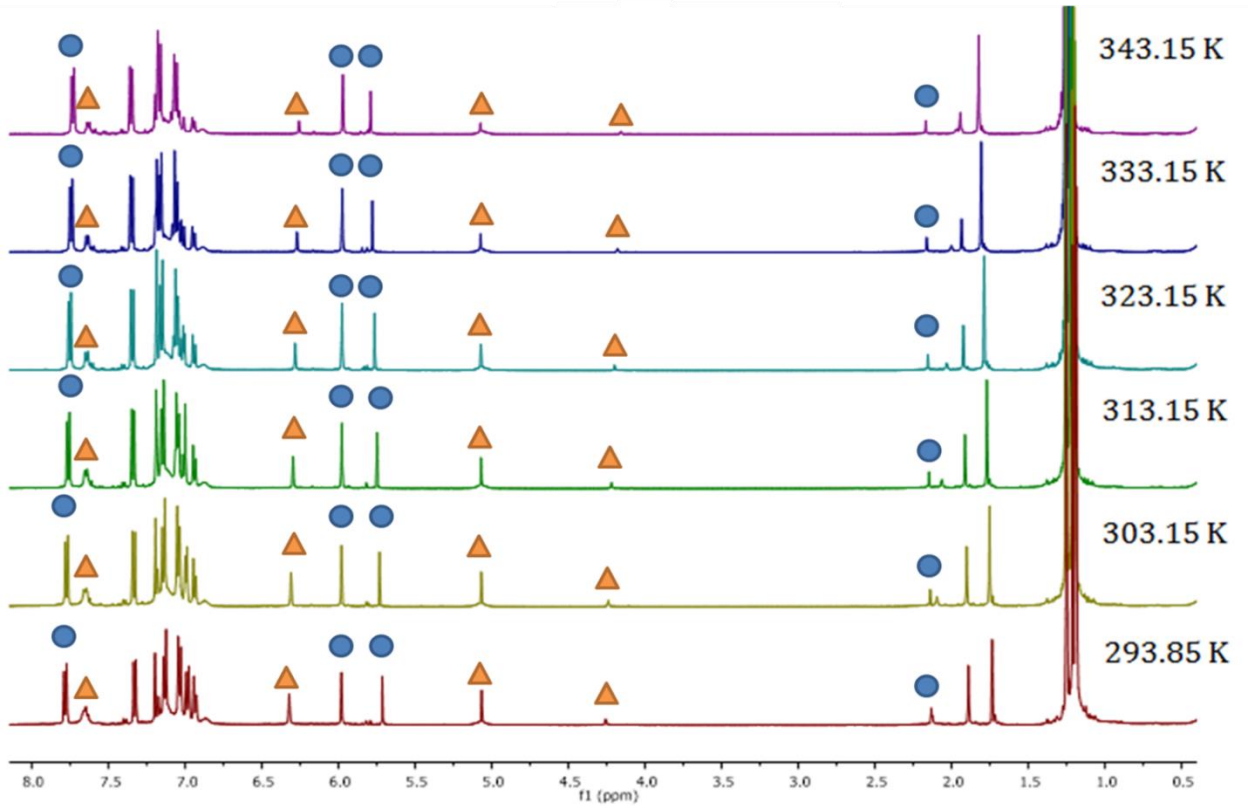

Figure 2.22. Sample VT ^{1}H NMR plot used to extrapolate the relative concentrations of **2.2DB$_{mono}$** and **2.2DB$_{di}$** which were subsequently used to calculate the thermal parameters for dimerization of monomeric copper hydrides. Blue circles correspond to **2.2DB$_{mono}$** and orange triangles denote **2.2DB$_{di}$**.

Relevent Equations:

1) $\Delta G = -RTln(K_{eq})$

2) $\frac{\Delta G}{T} = -Rln(K_{eq})$

3) $\Delta G = \Delta H - T\Delta S$

4) $\frac{\Delta G}{T} = \frac{\Delta H}{T} - \Delta S$

Plugging eq. 2 into eq. 4 gives the following:

5) $-Rln(K_{eq}) = \Delta H(\frac{1}{T}) - \Delta S$

Plotting –Rln(K_{eq}) vs. 1/T gives the Arrhenius plot shown below:

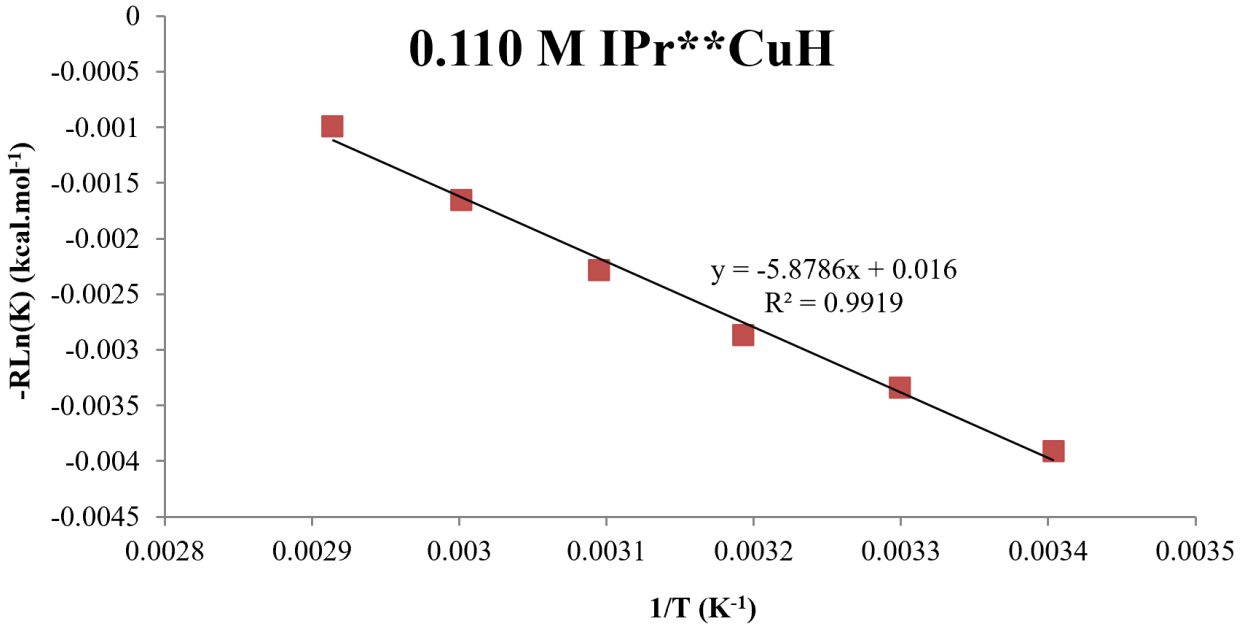

Figure 2.23. VT ^{1}H NMR plot at 0.11 M for the monomer:dimer ratios collected above. Using the equations described, the thermodynamic parameters can be extracted.

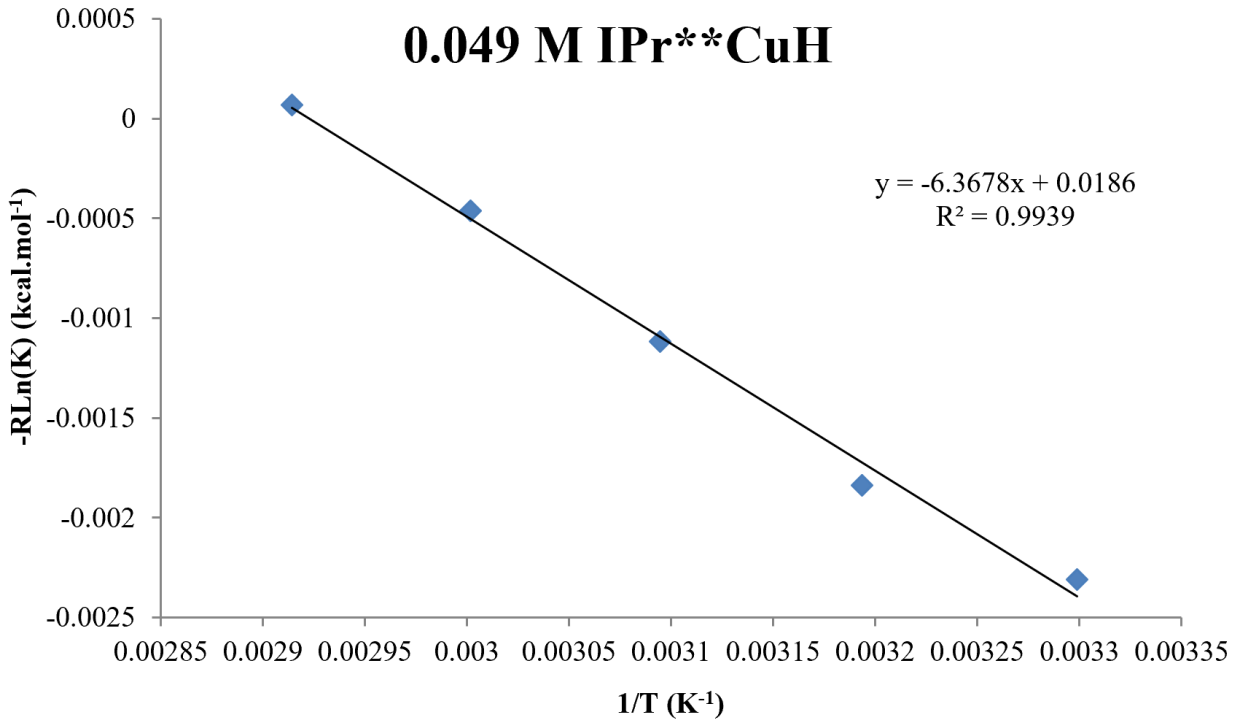

Figure 2.24. VT ^{1}H NMR plot at 0.049 M for the monomer:dimer ratios collected above. Using the equations described, the thermodynamic parameters can be extracted.

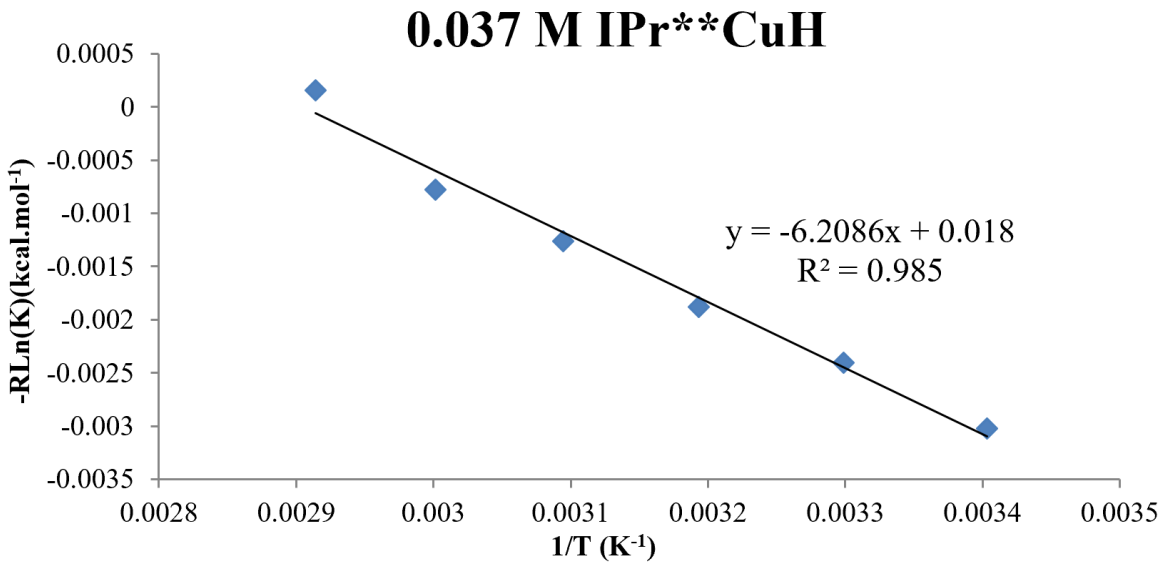

Figure 2.25. VT ^{1}H NMR plot at 0.037 M for the monomer:dimer ratios collected above. Using the equations described, the thermodynamic parameters can be extracted.

We can now extract ΔH and ΔS from each of the m and b terms respectively, and use eq. 3 to solve for ΔG at 303 K. The values reported in the main text correspond to the average of the three runs: 0.110 M, 0.049 M, and 0.037 M.

Crystal Structure Data:

Crystal data and structure refinement for 2.2CB.

Identification code	**2.2CB**
Empirical formula	$C_{162}H_{138}Cu_2N_4$
Formula weight	2267.84
Temperature/K	100.0
Crystal system	monoclinic
Space group	P2/c
a/Å	27.1295(8)
b/Å	14.4741(4)
c/Å	33.8823(10)
α/°	90
β/°	112.053(2)
γ/°	90
Volume/Å^3	12331.3(6)
Z	4
ρ_{calc}g/cm^3	1.222
μ/mm^{-1}	0.853
F(000)	4784.0
Crystal size/mm^3	0.1 × 0.1 × 0.01
Radiation	CuKα (λ = 1.54178)
2Θ range for data collection/°	3.514 to 133.448
Index ranges	$-32 \leq h \leq 32$, $-17 \leq k \leq 14$, $-40 \leq l \leq 40$
Reflections collected	38186
Independent reflections	21744 [R_{int} = 0.0199, R_{sigma} = 0.0295]
Data/restraints/parameters	21744/72/1524
Goodness-of-fit on F^2	1.117
Final R indexes [I>=2σ (I)]	R_1 = 0.0693, wR_2 = 0.1781
Final R indexes [all data]	R_1 = 0.0788, wR_2 = 0.1826
Largest diff. peak/hole / e Å^{-3}	1.13/-0.81

Crystal data and structure refinement for 2.2CD.

Identification code	**2.2CD**
Empirical formula	$C_{77}H_{72}BCuN_2$

Formula weight	1099.71
Temperature/K	100.0
Crystal system	monoclinic
Space group	$P2_1/n$
a/Å	13.4663(4)
b/Å	20.4463(7)
c/Å	22.1540(7)
α/°	90
β/°	104.0600(10)
γ/°	90
Volume/$Å^3$	5917.1(3)
Z	4
$\rho_{calc}g/cm^3$	1.234
μ/mm^{-1}	0.416
F(000)	2328.0
Crystal size/mm^3	0.1 × 0.1 × 0.1
Radiation	MoKα (λ = 0.71073)
2Θ range for data collection/°	3.232 to 52.802
Index ranges	$-11 \leq h \leq 16$, $-15 \leq k \leq 25$, $-27 \leq l \leq 27$
Reflections collected	41589
Independent reflections	12120 [R_{int} = 0.0303, R_{sigma} = 0.0331]
Data/restraints/parameters	12120/0/740
Goodness-of-fit on F^2	1.028
Final R indexes [I>=2σ (I)]	R_1 = 0.0379, wR_2 = 0.0906
Final R indexes [all data]	R_1 = 0.0515, wR_2 = 0.0974
Largest diff. peak/hole / e $Å^{-3}$	0.33/-0.34

Crystal data and structure refinement for 2.2DD.

Identification code	**2.2DD**
Empirical formula	$C_{107}H_{128}BCuN_2O$
Formula weight	1532.46
Temperature/K	100.0
Crystal system	triclinic
Space group	P-1
a/Å	19.0550(17)
b/Å	19.1118(16)
c/Å	20.6462(18)
α/°	87.796(6)
β/°	71.604(6)
γ/°	64.130(5)
Volume/$Å^3$	6376.1(10)

Z	2
ρ_{calc}g/cm^3	0.798
μ/mm^{-1}	0.498
F(000)	1652.0
Crystal size/mm^3	0.217 × 0.203 × 0.155
Radiation	CuKα (λ = 1.54178)
2Θ range for data collection/°	5.174 to 118.594
Index ranges	-21 ≤ h ≤ 20, -21 ≤ k ≤ 21, -21 ≤ l ≤ 22
Reflections collected	46084
Independent reflections	18129 [R_{int} = 0.0963, R_{sigma} = 0.1120]
Data/restraints/parameters	18129/0/1000
Goodness-of-fit on F^2	1.068
Final R indexes [I>=2σ (I)]	R_1 = 0.0941, wR_2 = 0.2410
Final R indexes [all data]	R_1 = 0.1488, wR_2 = 0.2760
Largest diff. peak/hole / e Å^{-3}	0.99/-0.65

Crystal data and structure refinement for 2.2DB$_{di}$.

Identification code	**2.2DB$_{di}$**
Empirical formula	$C_{101.04}H_{121}CuN_2$
Formula weight	1426.98
Temperature/K	100.0
Crystal system	tetragonal
Space group	$P4_32_12$
a/Å	30.1192(9)
b/Å	30.1192(9)
c/Å	21.0808(9)
α/°	90
β/°	90
γ/°	90
Volume/Å^3	19123.8(14)
Z	8
ρ_{calc}g/cm^3	0.991
μ/mm^{-1}	0.627
F(000)	6162.0
Crystal size/mm^3	0.2 × 0.1 × 0.1
Radiation	CuKα (λ = 1.54178)
2Θ range for data collection/°	4.148 to 114.466
Index ranges	-31 ≤ h ≤ 32, -18 ≤ k ≤ 32, -21 ≤ l ≤ 22
Reflections collected	87121
Independent reflections	12225 [R_{int} = 0.0316, R_{sigma} = 0.0222]
Data/restraints/parameters	12225/135/1155

Goodness-of-fit on F^2	1.078
Final R indexes [I>=2σ (I)]	R_1 = 0.0566, wR_2 = 0.1615
Final R indexes [all data]	R_1 = 0.0648, wR_2 = 0.1685
Largest diff. peak/hole / e $Å^{-3}$	0.47/-0.35
Flack parameter	0.017(5)

2.6.2 Copper(I)-Hydrides in the Catalytic Hydrogenation of CO_2 to Formate

All reactions were performed under an atmosphere of argon using standard Schlenk or dry box techniques unless otherwise noted; all solvents were dried and degassed using standard procedures. Toluene, benzene, hexane, pentane, THF, and diethyl ether were distilled from sodium. C_6D_6 was distilled from sodium benzophenone and stored over a potassium mirror. Dichloromethane and chloroform were dried by distillation from CaH_2. Reagents of analytical grade were obtained from commercial suppliers, dried over 4Å molecular sieves and degassed before use. ^1H, ^{13}C, ^{11}B and Variable temperature NMR spectra were obtained using a Varian Inova 500 MHz and ECA JEOL 500 MHz spectrometer. Chemical shifts (δ) are reported in parts per million (ppm) relative to TMS and were referenced to the residual solvent peak. NMR multiplicities are abbreviated as follows: s = singlet, d = doublet, t = triplet, q = quartet, pent = pentet, quin = quintet, sex = sextet, dd = doublet of doublets, dt = doublet of triplets, dm = doublet of multiplets, m = multiplet, br = broad signal. Preparation of (L_1)Cu-OPh[57] and (L_1)Cu-(κ^2-BH_4) [**2.3BD^{H}**][54] were prepared according to literature methods.

Synthesis of (L_1)Cu-OC(=O)H [2.3BC]: Under a CO_2 atmosphere, (L_1)Cu-OPh (230 mg, 490 µmol, 1 eq.) was dissolved in 5 mL THF. Pinacolborane (78 µL, 540 µmol, 1.1 eq.) was added dropwise to a vigorously stirred solution at -78 ^oC, at which point the solution becomes a bright yellow color. Stirring was continued at -78 ^oC for 1 hour before the solution was slowly warmed to room temperature over the course of 1 hour. Stirring was continued until solution was colorless.

All volatiles were removed under vacuum and the residue was stirred in 10 mL pentane for 30 min. After removal of all solvents under vacuum, the residue was washed with 2 x 5 mL of a 1:1 mixture of pentane and diethyl ether. The residue was then extracted with 2 x 5 mL dichloromethane yielding the **2.3BC** as an off-white solid in 83% yield (171 mg) after removal of dichloromethane. Single crystals suitable for an X-ray diffraction study were grown from a saturated Et_2O solution overnight at -40 ^oC. M.P. 141.1 ^oC dec. ^1H NMR ($CDCl_3$, 500 MHz): δ 1.09 (t, *J* = 7.45 Hz, 6H), 1.26 (d, *J* = 6.74 Hz, 6H), 1.30 (d, *J* = 6.81 Hz, 6H), 1.36 (s, 6H), 1.80 (m, 2H), 1.93 (m, 2H), 1.99 (s, 2H), 2.84 (sept, *J* = 6.50 Hz, 2H), 7.25 (d, *J* = 8.27 Hz, 2H), 7.39 (t, *J* = 7.75 Hz, 1H), 8.23 (s, 1H). $^{13}C\{^1H\}$ NMR ($CDCl_3$, 125 MHz): δ 9.7, 22.4, 27.2, 29.3, 29.4, 31.1, 42.7, 62.7, 77.4, 80.9, 124.8, 129.8, 134.1, 145.1, 168.3, 250.9 ($C_{Carbene}$). HRMS ESI-TOF+ could not find $[M + H]^+$ calculated for $[C_{23}H_{37}CuNO_2]^+$ = 422.2115.

Synthesis of (L_1)CuH-BCF [2.3BD]: A Schlenk tube was charged with (L_1)CuOPh (100 mg, 212 µmol, 1 eq.) and 5 mL Et_2O was added to dissolve the solid. HBPin (32.4 µL, 223 µmol, 1.05 eq.) was added at -78 ^oC forming a deep orange solution. Separately, BCF [tris(pentafluorophenyl)borane] (109 mg, 212 µmol, 1 eq.) was dissolved in 1 mL Et_2O and cooled to -78 ^oC. This solution was added to $[(L_1)CuH]_2$ via cannula. After addition, the orange color gave way to a light-yellow solution. The resulting solution warmed slowly to -40 ^oC. After stirring for 1 hour, all volatiles were evaporated under vacuum and the residue was washed with 2 x 1 mL of a 80:20 pentane:Et_2O mixture. Drying of the residue under vacuum yielded **2.3BD** as a white solid in 55 % yield. Single crystals were grown from a saturated toluene/pentane solution at -40 ^oC. M.P. 163.3-168.6 ^oC dec. ^1H NMR (C_6D_6, 500 MHz): δ 0.84 (t, *J* = 7.00 Hz, 6H), 0.86 (s, 6H), 1.02 (d, *J* = 6.72 Hz, 6H), 1.15 (d, *J* = 6.76 Hz, 6H), 1.40 (s, 2H), 1.49 (m, 2H), 1.56 (m, 2H), 2.23 (br, q, $^1J_{B\text{-}H}$ = 65.50 Hz, 6H), 2.61 (sept, *J* = 6.67 Hz, 2H), 6.87 (d, *J* = 7.79 Hz, 2H), 7.08 (t, *J* =

7.77 Hz, 1H). $^{13}C\{^{1}H\}$ NMR (C_6D_6, 125 MHz): δ 22.8, 22.8, 26.4, 26.4, 28.9, 29.0, 29.2, 31.2, 43.0, 62.3, 81.0, 117.3 (BCF_{ipso}, s, br), 125.2, 125.3, 130.1, 130.1, 135.4, 137.5 (dm, $^{1}J_{C\text{-}F}$ = 245.25 Hz), 140.6, 145.1, 148.3 (dm, $^{1}J_{C\text{-}F}$ = 241.50 Hz), 251.3 ($C_{Carbene}$). $^{11}B\{^{1}H\}$ NMR (C_6D_6, 160 MHz): δ -25.9 (br, s) ppm.

Synthesis of (L_1)Cu--O=C(O-BCF)H [2.3BE]: A quartz J-Young NMR tube was charged with **2.3BC** (25 mg, 59.2 µmol, 1 eq.) and BCF (30.6 mg, 59.2 µmol, 1 eq.). Addition of 500 µL $CDCl_3$ resulted in the clean and quantitative formation of **2.3BE** by NMR spectroscopy. Evaporation of all volatiles under vacuum yielded a colorless solid in quantitative yield. Single crystals were grown from a saturated $CHCl_3$/pentane solution at -40 °C. ^{1}H NMR ($CDCl_3$, 500 MHz): δ 1.03 (t, *J* = 7.46 Hz, 6H), 1.13 (d, *J* = 6.74 Hz, 6H), 1.31 (d, *J* = 6.80 Hz, 6H), 1.38 (s, 6H), 1.71 (m, 2H), 1.86 (m, 2H), 2.03 (s, 2H), 2.81 (sept, *J* = 6.50 Hz, 2H), 7.27 (d, *J* = 7.83 Hz, 2H), 7.43 (t, *J* = 7.78 Hz, 1H), 7.93 (s, 1H). $^{13}C\{^{1}H\}$ NMR ($CDCl_3$, 125 MHz): δ 9.4, 22.3, 22.3, 27.0, 27.0, 29.3, 29.3, 29.3, 29.4, 30.8, 42.7, 62.5, 77.3, 81.8, 118.7 (BCF_{ipso}, s, br), 125.1 (m), 130.3 (m), 134.6, 136.9 (dm, $^{1}J_{C\text{-}F}$ = 247.75 Hz), 139.8 (dm, $^{1}J_{C\text{-}F}$ = 248.13 Hz), 145.0, 147.9 (dm, $^{1}J_{C\text{-}F}$ = 235.13 Hz), 172.7, 248.5 ($C_{Carbene}$). $^{11}B\{^{1}H\}$ NMR ($CDCl_3$, 160 MHz): δ -2.51 (br, s) ppm.

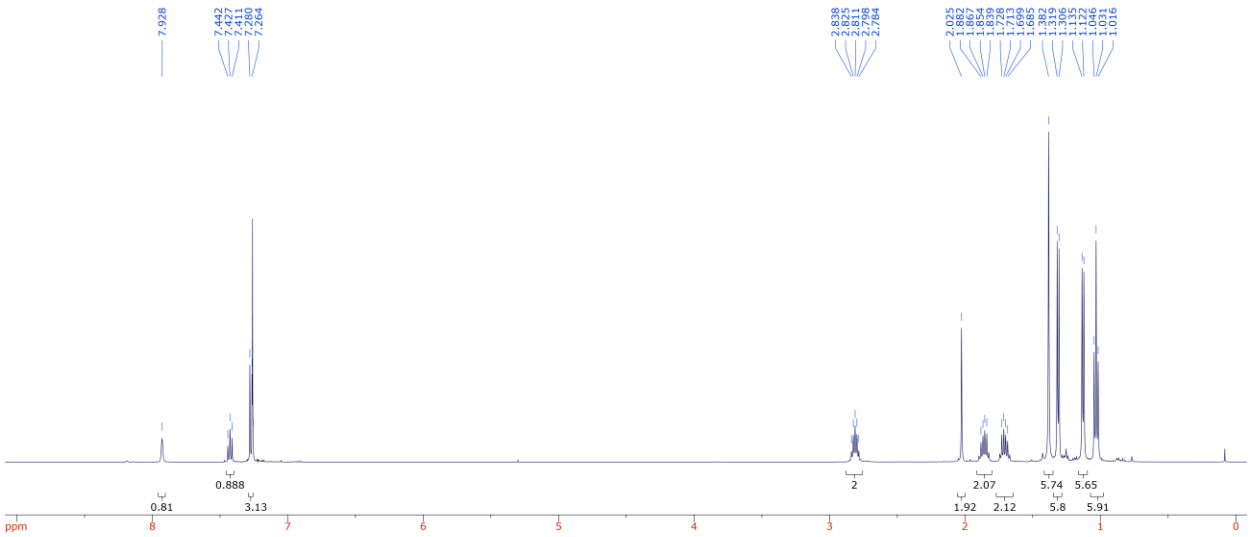

Figure 2.26. ^{1}H NMR spectrum of complex **2.3BE**.

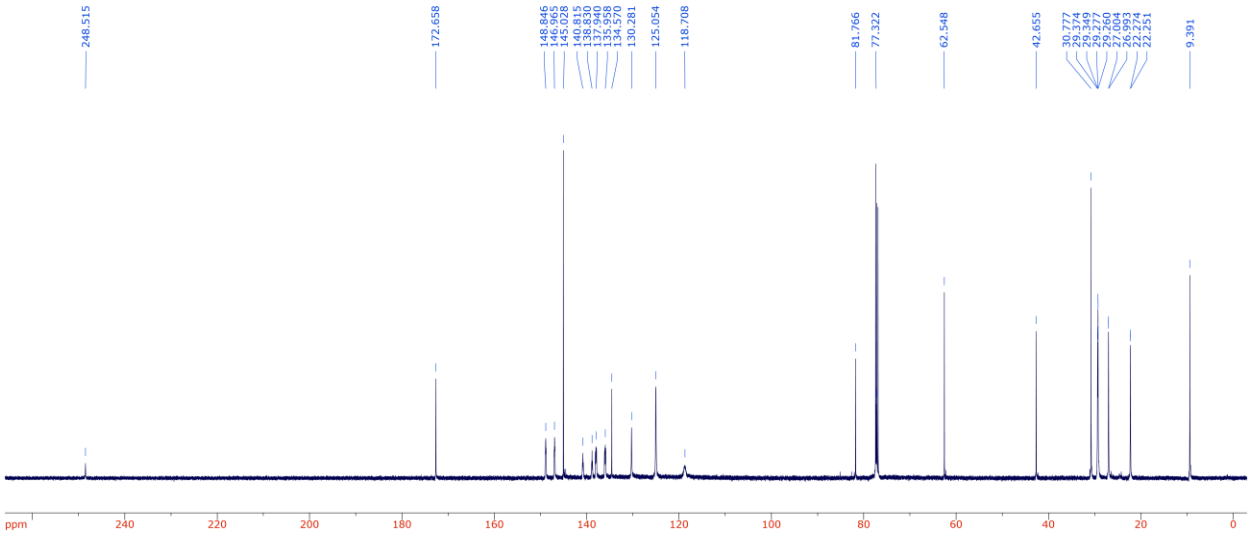

Figure 2.27. ^{13}C NMR spectrum of complex **2.3BE**.

Synthesis of [(L$_1$)Cu-DBU][O=C(O-BCF)H] [2.3BF]: A quartz J-Young NMR tube was charged with **2.3BE** (44.5 mg, 47.6 µmol, 1 eq.) and 500 µL $CDCl_3$. To this solution was added 1 equivalent of DBU (7.1 µL, 47.6 µmol, 1 eq.). Multinuclear NMR spectroscopy collected immediately following DBU addition clearly indicated formation of **2.3BF**. Evaporation of all volatiles under vacuum yielded a colorless deliquescent solid in quantitative yield. ^{1}H NMR ($CDCl_3$, 500 MHz): δ 1.07 (t, *J* = 7.50 Hz, 6H), 1.18 (d, *J* = 7.00 Hz, 6H), 1.31 (d, *J* = 7.00 Hz,

6H), 1.41 (s, 6H), 1.50 (m, 2H), 1.58 (m, 2H), 1.67 (m, 2H), 1.69 (m, 2H), 1.83 (m, 2H), 2.01 (d, J = 11.00 Hz, 2H), 2.04 (s, 2H), 2.82 (sept, *J* = 6.50 Hz, 2H), 2.86 (m, 2H), 3.16 (t, J = 6.50 Hz, 2H), 3.195 (m, 2H), 7.30 (d, *J* = 8.00 Hz, 2H), 7.43 (t, *J* = 8.00 Hz, 1H), 8.21 (s, 1H). $^{13}C\{^{1}H\}$ NMR ($CDCl_3$, 125 MHz): δ 9.4, 9.5, 21.0, 22.4, 22.5, 25.1, 26.8, 26.9, 27.1, 28.9, 29.1, 29.2, 29.3, 29.4, 31.1, 39.8, 43.2, 45.5, 47.9, 53.9, 62.2, 81.6, 121.8 (BCF_{ipso}, s, br), 125.2 (m), 130.2 (m), 135.4, 136.6 (dm, $^{1}J_{C\text{-}F}$ = 241.50 Hz), 139.0 (dm, $^{1}J_{C\text{-}F}$ = 245.25 Hz), 145.1, 148.0 (dm, $^{1}J_{C\text{-}F}$ = 235.75 Hz), 167.4, 250.1 ($C_{Carbene}$). $^{11}B\{^{1}H\}$ NMR ($CDCl_3$, 160 MHz): δ -4.84 (br, s) ppm.

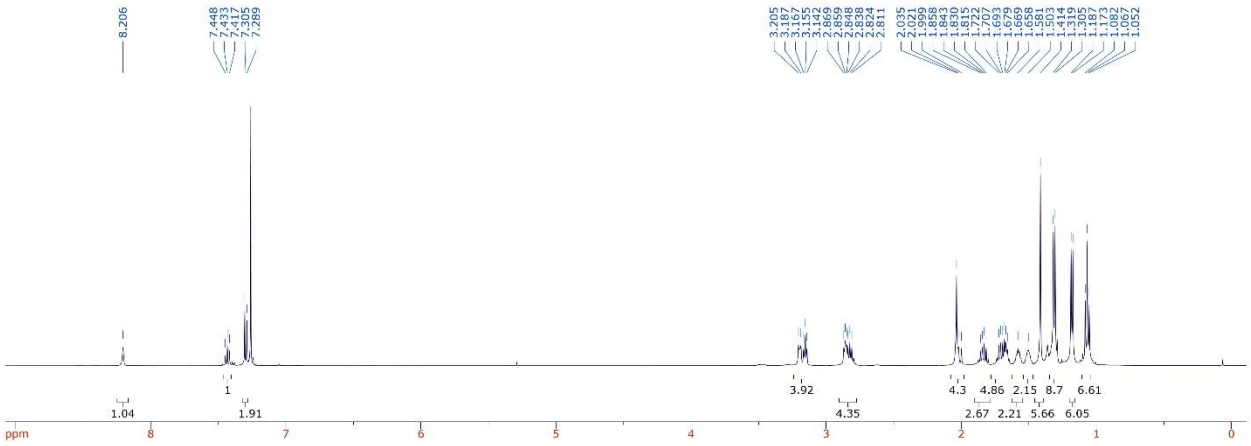

Figure 2.28. ^{1}H NMR of **2.3BF**.

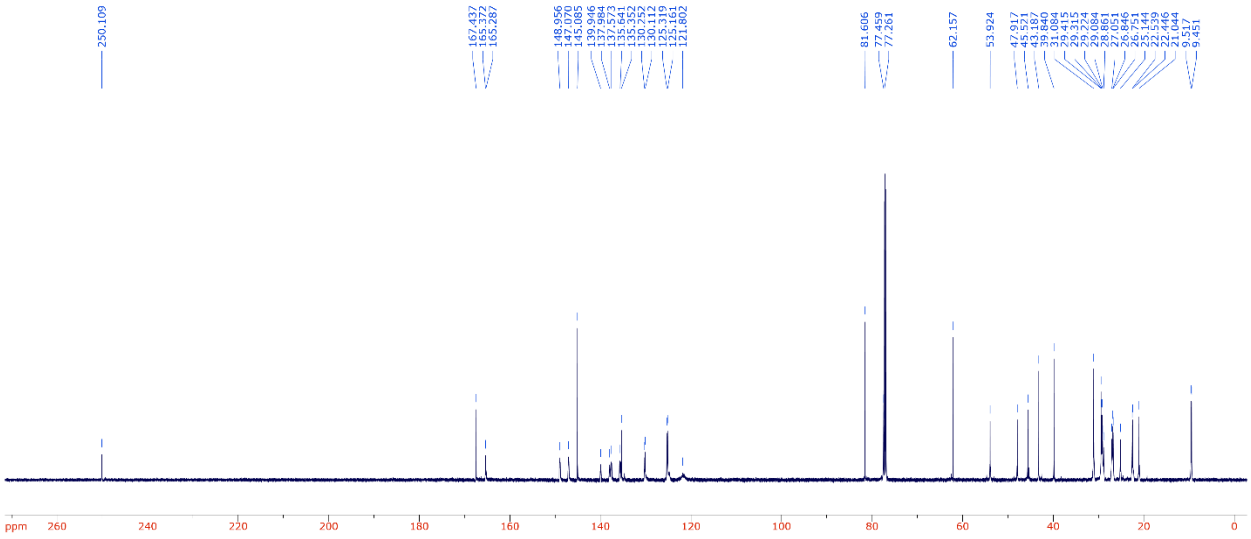

Figure 2.29. ^{13}C NMR spectrum of **2.3BF**.

Synthesis of (L$_2$)Cu-(κ^2-BH$_4$) [L$_2$2.3BD^H]: In a glove box, a 50 mL Schlenk flask was charged with (L$_2$)CuCl (240 mg, 0.5 mmol, 1 eq.) and NaBH$_4$ (75.6 mg, 2.0 mmol, 4 eq.) under nitrogen. Then, 10 mL of dry THF was added and the mixture was stirred for 24 hours at room temperature. The suspension was filtered under nitrogen. The solution was evaporated under vacuum and the residue was extracted with 3 x 10 mL C$_6$H$_6$, affording **L$_2$2.3BD^H** as a white solid in 57 % yield. M.P. 184.2-185.7 ºC. ^{1}H NMR (CDCl$_3$, 500 MHz): δ -0.34 (br, q, $^1J_{B\text{-}H}$ = 81.51 Hz, 4H), 0.91 (d, *J* = 6.44 Hz, 3H), 1.03 (d, *J* = 8.50 Hz, 6H), 1.25-1.10 (m, 2H), 1.32 (d, *J* = 8.50 Hz, 6H), 1.33 (d, *J* = 8.00 Hz, 3H), 1.39 (d, *J* = 8.29 Hz, 6H), 1.77 (d, *J* = 13.58 Hz, 1H), 1.83 (dq, *J* = 14.05, 3.40 Hz, 1H), 1.91-1.95 (m, 2H), 2.06-2.10 (m, 1H), 2.32 (d, *J* = 13.51 Hz, 1H), 2.54 (qd, *J* = 13.39, 3.40 Hz, 1H), 2.62-2.69 (m, 1H), 2.81-2.92 (m, 2H), 7.27 (m, 2H), 7.41 (t, *J* = 7.75 Hz, 1H). ^{13}C{^{1}H} NMR (CDCl$_3$, 125 MHz): δ 20.0, 23.1, 23.1, 23.2, 24.6, 25.1, 26.9, 27.7, 27.9, 29.0, 29.3, 29.7, 30.1, 31.0, 35.7, 48.6, 51.5, 52.7, 65.6, 77.6, 125.0, 125.1, 129.6, 135.6, 145.3, 145.8, 251.5 (C$_{Carbene}$). ^{11}B{^{1}H} NMR (CDCl$_3$, 160 MHz): δ -41.8 ppm.

Synthesis of (L_3)Cu-(κ^2-BH_4) [$L_3$2.3BD^H]: A teflon sealed pressure ampoule was charged with (L_3)CuCl (500 mg, 1.04 mmol, 1 eq.) and $NaBH_4$ (433 mg, 10.4 mmol, 1 eq.). ***N.B.*** *$NaBH_4$ cannot be anhydrous as the reaction will not work. It is likely that adventitious water aids in solubilizing the $NaBH_4$ for reaction with (L_3)CuCl.* After addition of 10 mL anhydrous THF, the ampoule was sealed and heated to 100 ^{o}C overnight. After cooling to room temperature, all volatiles were evaporated under vacuum and the residue was extracted with 3 x 10 mL C_6H_6. The organic layers evaporated under vacuum to give **$L_3$2.3BD^H** as a white solid in 96 % yield (458 mg). Single crystals suitable for an X-ray diffraction study were grown from a saturated C_6D_6/pentane solution at 30 ^{o}C. M.P. 182.1 ^{o}C dec. ^{1}H NMR (C_6D_6, 500 MHz): δ 0.54 (br, q, $^1J_{B\text{-}H}$ = 81.61 Hz, 4H), 0.63 (s, 3H), 0.74 (d, *J* = 6.79 Hz, 3H), 0.81 (d, *J* = 7.23 Hz, 3H), 1.03 (d, *J* = 6.93 Hz, 3H), 1.05-1.08 (m, 3H), 1.11 (d, *J* = 6.91 Hz, 3H), 1.19 (dt, *J* = 13.55, 4.52 Hz, 1H), 1.03 (d, *J* = 6.93 Hz, 3H), 1.30-1.33 (m, 1H), 1.31 (d, *J* = 6.82 Hz, 3H), 1.41 (apparent dd, *J* = 8.07, 6.83 Hz, 6H), 1.45 (dd, *J* = 13.52, 10.57 Hz, 1H), 1.67-1.74 (m, 1H), 2.46 (sept, *J* = 7.00 Hz, 1H), 2.83 (sept, *J* = 7.00 Hz, 1H), 2.92 (sept, *J* = 6.50 Hz, 1H), 7.00 (ddd, *J* = 11.35, 7.76, 1.50 Hz, 2H), 7.13 (t, *J* = 7.74 Hz, 1H). ^{13}C{^{1}H} NMR (C_6D_6, 125 MHz): δ 16.2, 19.3, 19.5, 20.9, 23.4, 23.5, 23.8, 25.1, 25.6, 28.6, 29.1, 31.9, 32.4, 33.4, 44.3, 54.0, 62.0, 125.2, 128.4 ,129.7, 142.2, 144.0, 144.7, 260.4 ($C_{Carbene}$). ^{11}B{^{1}H} NMR (C_6D_6, 160 MHz): δ -40.1 ppm.

Synthesis of (L_4)Cu-(κ^2-BH_4) [$L_4$2.3BD^H]: A teflon sealed pressure ampoule was charged with (**L_4**)CuCl (202 mg, 0.5 mmol, 1 eq.) and $NaBH_4$ (76 mg, 2.0 mmol, 4.0 eq.). ***N.B.*** *$NaBH_4$ cannot be anhydrous as the reaction will not work. It is likely that adventitious water aids in solubilizing the $NaBH_4$ for reaction with (L_4)CuCl.* After addition of 10 mL anhydrous THF, the ampoule was sealed and heated to 100 ^{o}C overnight. After cooling to room temperature, all volatiles were evaporated under vacuum and the residue was extracted with 3 x 10 mL C_6H_6. The

organic layers evaporated under vacuum to give **$L_4$2.3BD^H** as a white solid in 72 % yield (138 mg). ^{1}H NMR (500 MHz, $CDCl_3$) δ = 7.05 (s, 2H), 7.00 (s, 4H), 2.34 (s, 6H), 2.10 (s, 12H), -0.50 (quartet, $J_{B\text{-}H}$ = 20.6 Hz, 4H). ^{13}C NMR (125 MHz, $CDCl_3$) δ = 179.4 ($C_{carbene}$), 139.6, 135.2, 134.7, 129.6, 122.3, 21.2, 17.9. ^{11}B NMR (160 MHz, $CDCl_3$) δ = -40.7 (quint, $J_{B\text{-}H}$ = 82.2 Hz).

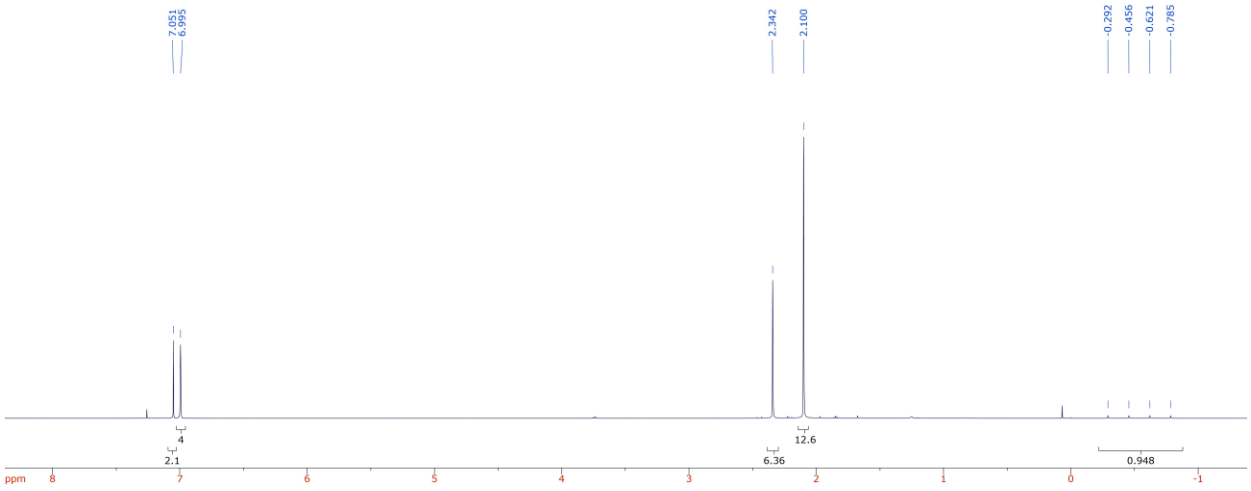

Figure 2.30. ^{1}H NMR spectrum of complex **$L_4$2.3BD^H**.

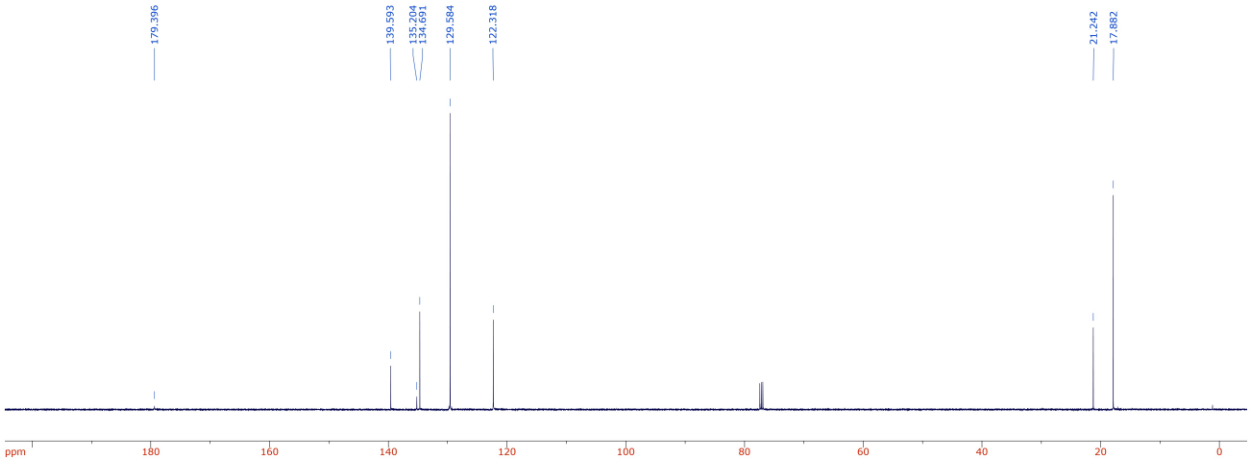

Figure 2.31. ^{13}C NMR spectrum of complex **$L_4$2.3BD^H**.

Synthesis of (L_5)Cu-(κ^2-BH_4) [$L_5$2.3BD^H]: A teflon sealed pressure ampoule was charged with (**L_5**)CuCl[58] (61 mg, 0.06 mmol, 1 eq.) and $NaBH_4$ (12 mg, 0.31 mmol, 5.2 eq.). ***N.B.*** *$NaBH_4$*

cannot be anhydrous as the reaction will not work. It is likely that adventitious water aids in solubilizing the $NaBH_4$ for reaction with ***(L5)****CuCl.* After addition of 10 mL anhydrous THF, the ampoule was sealed and heated to 100 ^{o}C overnight. After cooling to room temperature, all volatiles were evaporated under vacuum and the residue was extracted with 3 x 10 mL C_6H_6. The organic layers evaporated under vacuum to give **$L_5$2.3BD^{H}** as a white solid in 85 % yield (51 mg). ^{1}H NMR (400 MHz, $CDCl_3$) δ = 7.09 (m, 26H), 6.95-6.87 (m, 8H), 6.82 (m, 8H), 6.77 (s, 4H), 5.72 (s, 2H), 5.13 (s, 4H), 2.15 (s, 6H), -0.49 (quartet, J_{B-H} = Hz, 4H). ^{13}C NMR (100 MHz, $CDCl_3$) δ = 181.6 ($C_{carbene}$), 143.3, 142.6, 141.1, 140.0, 134.4, 130.3, 129.7, 129.6, 128.7, 128.6, 128.5, 126.8, 126.7, 123.2, 51.3, 22.0. ^{11}B NMR (128 MHz, $CDCl_3$) δ = -40.58 (quint, J_{B-H} = 82.9 Hz).

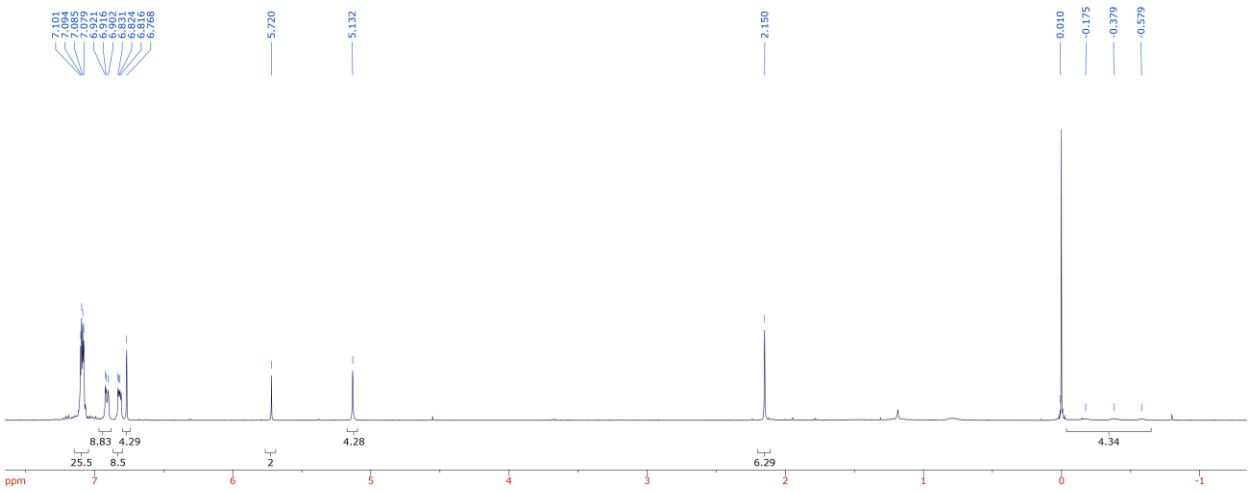

Figure 2.32.^{1}H NMR spectrum of complex **$L_5$2.3BD^{H}**.

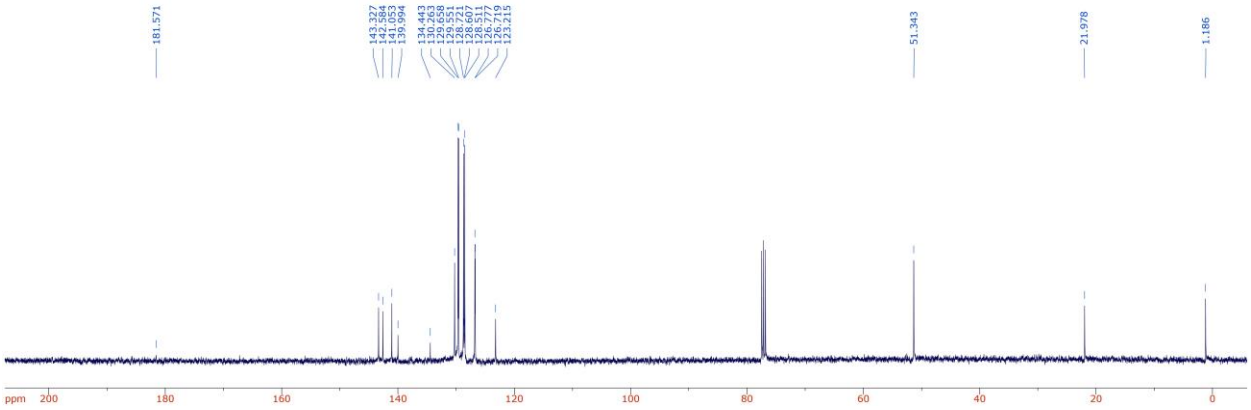

Figure 2.33. ^{13}C NMR spectrum of complex **$L_5$2.3BD^H**.

Synthesis of (L_6)Cu-(κ^2-BH_4) [$L_6$2.3BD^H]: A teflon sealed pressure ampoule was charged with (**L_6**)CuCl[58] (88 mg, 0.06 mmol, 1 eq.) and $NaBH_4$ (12 mg, 0.31 mmol, 5.2 eq.). ***N.B.*** *$NaBH_4$ cannot be anhydrous as the reaction will not work. It is likely that adventitious water aids in solubilizing the $NaBH_4$ for reaction with (**L_6**)CuCl.* After addition of 10 mL anhydrous THF, the ampoule was sealed and heated to 100 ^{o}C overnight. After cooling to room temperature, all volatiles were evaporated under vacuum and the residue was extracted with 3 x 10 mL C_6H_6. The organic layers evaporated under vacuum to give **$L_6$2.3BD^H** as a white solid in 82 % yield (71 mg). ^{1}H NMR (400 MHz, $CDCl_3$) δ = 7.21 (d, *J* = 8.5 Hz, 8H), 7.14 (d, *J* = 8.4 Hz, 8H), 7.03 (d, *J* = 8.2 Hz, 8H), 6.86 (s, 4H), 6.80 (d, *J* = 8.2 Hz, 8H), 5.75 (s, 2H), 5.25 (s, 4H), 2.23 (s, 6H), 1.25 (s, 72H), -0.14 (quartet, $J_{B\text{-}H}$ = 25.8 Hz, 4H). ^{13}C NMR (100 MHz, $CDCl_3$) δ ($C_{carbene}$) could not be located, 149.2, 149.1, 141.4, 140.2, 140.1, 139.5, 130.1, 129.3, 129.2, 125.4, 125.1, 123.2, 50.4, 34.5, 31.5, 22.0. ^{11}B NMR (128 MHz, $CDCl_3$) δ = -40.7 (quint, $J_{B\text{-}H}$ = 87.5 Hz).

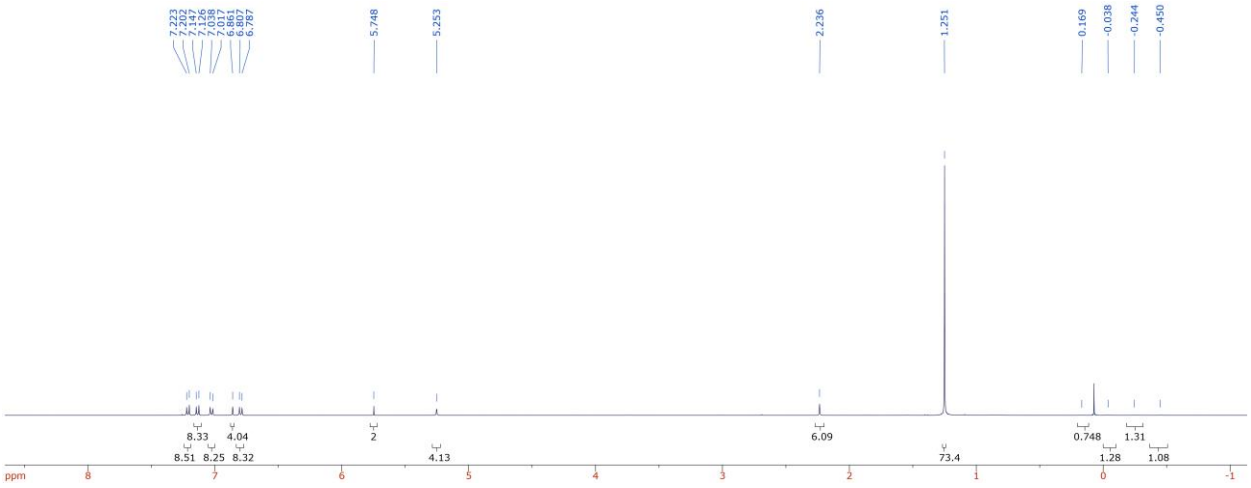

Figure 2.34. ^{1}H NMR spectrum of complex **L$_6$2.3BD^{H}**.

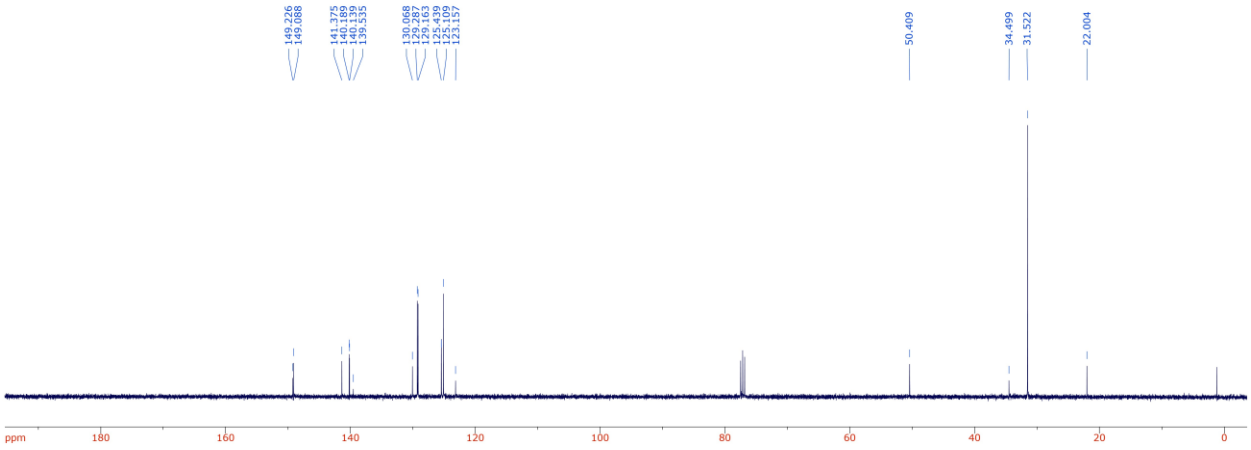

Figure 2.35. ^{13}C NMR spectrum of complex **L$_6$2.3BD^{H}**.

Stoichiometric Reactions:

Addition of 2.3CB to 2.3BC: A quartz J-Young NMR tube was charged with **2.3BC** (25 mg, 59.2 µmol, 1 eq.) and [PMPH][HBCF] **2.3CB**[42] (30.6 mg, 59.2 µmol, 1 eq.). To the solids was added 500 µL C_6D_6 and shaken to fully dissolve both reactants. A biphasic mixture forms immediately with the bottom layer being light yellow and the top colorless. ^{11}B NMR analysis after 5 minutes at room temperature showed a shift of the B-H resonances, which was attributed

to the formation of **2.3BD**. Isolation of the bottom phase revealed the formation of the [PMP-H^+][HCO_2^-]. See Figure 2.14 for ^{11}B NMR spectra analysis.

[PMPH^+][$^-$HBCF] (2.3CB): Prepared in a fashion similar to literature methods.[42] ^1H NMR (C_6D_6, 500 MHz): δ 0.14 (s, 6H), 0.57 (s, 6H), 0.72 (m, 4H), 1.08 (t, J = 13.00 Hz, 2H), 1.58 (s, 3H), 3.72 (q, br, $^1J_{B\text{-}H}$ = 98.00 Hz, 1H), 5.96 (s, br, 1H, N-*H*). $^{13}C\{^1H\}$ NMR (C_6D_6, 125 MHz): δ 15.2, 19.0, 28.8, 37.2, 64.9, 137.4 (dm, $^1J_{C\text{-}F}$ = 260.00 Hz), 148.6 (dm, $^1J_{C\text{-}F}$ = 240.00 Hz), 148.9 (dm, $^1J_{C\text{-}F}$ = 232.25 Hz). $^{11}B\{^1H\}$ NMR (C_6D_6, 160 MHz): δ -18.5 ppm.

[PMP-H^+][$HCOO^-$]: Product was isolated as a light-yellow oil in 89% yield. ^1H NMR ($CDCl_3$, 500 MHz): δ 1.38 (s, br, 12H), 1.70 (s, br, 4H), 2.13 (s, br, 2H), 2.72 (s, N-C*H*$_3$, 3H), 8.45 (s, 1H), 11.06 (s, br, N*H*, 1H). $^{13}C\{^1H\}$ NMR ($CDCl_3$, 125 MHz): δ 16.2, 21.0 (N-*C*H$_3$, br), 29.1, 37.2, 63.3, 168.1. ^{13}C NMR ($CDCl_3$, 125 MHz): δ 16.7 (tm, $^1J_{C\text{-}H}$ = 127.75 Hz), 21.1 (q, br, $^1J_{C\text{-}H}$ = 124.63 Hz), 29.1 (q, $^1J_{C\text{-}H}$ = 141.13 Hz), 36.7 (tm, $^1J_{C\text{-}H}$ = 128.63 Hz), 63.3 (s), 166.7 (d, $^1J_{C\text{-}H}$ = 200.13 Hz).

Insertion of 2.3BD into CO_2: A stainless steel 50 mL autoclave was charged with **2.3BD** (200 µmol, 178 mg) and 10 mL THF. The reactor was pressurized with 20 bar of CO_2 at room temperature. Then, it was heated and stirred at 100 ^oC for 24 h. After the reaction, the reactor was cooled to room temperature and the pressure was vented laxly. The solution was quickly transferred to a 25 mL Schlenk flask. The volatiles were removed in vacuo and the residue was extracted with 2 x 2 mL benzene and filtrated through a celite plug. After evaporation of solvent under reduced pressure, a mixture containing **2.3BE** was isolated as a white powder in 49 % yield.

Insertion of 2.3BD^H into CO_2: A stainless steel 50 mL autoclave was charged with **2.3BD^H** (0.5 mmol, 196 mg) and 10 mL THF. The reactor was pressurized with 10 bar of CO_2 at room temperature. Then, it was heated and stirred at 80 ^oC for 24 h. After the reaction, the reactor

was cooled to room temperature and the pressure was vented laxly. The solution was quickly transferred to a 25 mL Schlenk flask. The volatiles were removed in vacuo and the residue was extracted with 2 x 2 mL benzene and filtrated through a celite plug. After evaporation of solvent under reduced pressure, **2.3BC** was isolated as a white powder in 91 % yield (192 mg).

Addition of DBU to BCF giving Lewis acid-base adduct 2.3LP: $B(C_6F_5)_3$ (100 mg, 195 µmol, 1 eq.) was dissolved in 5 mL CH_2Cl_2 in a Schlenk tube. DBU (32.1 µL, 215 µmol, 1.1 eq.) was added to the solution and stirred for 1 hour at room temperature before evaporation of all volatiles under vacuum. The residue was washed with 2 x 5 mL of a 10% Et_2O in hexane solution and dried thoroughly under vacuum. The adduct 3 was isolated in 87% yield (113 mg) as a white powder. Crystals suitable for X-ray diffraction analysis were obtained from a saturated boiling acetonitrile solution upon slow cooling to room temperature. M.P. 258.6 ^oC dec. ^1H NMR ($CDCl_3$, 500 MHz): δ 0.01 (q, *J* = 12.0 Hz, 1H), 1.33-1.47 (m, 3H), 1.72-1.80 (m, 3H), 2.02-2.04 (m, 1H), 2.45 (t, *J* = 14.0 Hz, 1H), 3.15-3.21 (m, 2H), 3.31-3.34 (m, 1H), 3.40-3.45 (m, 2H), 3.67 (d, *J* = 13.5 Hz, 1H), 3.79 (dd, *J* = 4.0 Hz, 15.0 Hz, 1H. $^{13}C\{^1H\}$ NMR ($CDCl_3$, 125 MHz): δ 21.2, 22.8, 26.2, 28.8, 31.2, 45.3, 49.5, 54.3, 120.8 (BCF_{ipso}, d, br, *J* = 203.63 Hz), 136.8 (dm, $^1J_{C-F}$ = 247.50 Hz), 139.4 (dm, $^1J_{C-F}$ = 255.38 Hz), 139.8 (dm, $^1J_{C-F}$ = 249.00 Hz), 147.2 (dm, $^1J_{C-F}$ = 239.00 Hz), 147.9 (dm, $^1J_{C-F}$ = 240.75 Hz), 148.5 (dm, $^1J_{C-F}$ = 223.50 Hz), 150.9, 170.0 (d, J = 2.12 Hz). ^{11}B NMR ($CDCl_3$, 160 MHz): δ -7.6 (br, s) ppm. HRMS ESI-TOF+ could not locate $[M + H]^+$ calculated for $[C_{27}H_{17}BF_{15}N_2]^+$ 664.1167.

Reaction of 2.3LP with H_2: A stainless steel 50 mL autoclave was charged with **2.3LP** (133mg, 200 µmol, 1 eq.) and 5 mL THF. The reactor was pressurized with 20 bar of H_2 at room temperature. Then, it was heated and stirred at 100 ^oC for 24 h. After the reaction, the reactor was cooled to room temperature and the pressure was vented laxly. The solution was quickly

transferred to a 25 mL Schlenk flask. Multinuclear NMR analysis of the crude mixture only showed signals corresponding to those of **2.3LP**.

Insertion of CO_2 into 2.3LP yielding 2.3LP$_{CO2}$: A stainless steel 50 mL autoclave was charged with **2.3LP** (132 mg, 200 μmol, 1 eq.) in 5 mL THF. The reactor was pressurized with 20 bar of CO_2 at room temperature. Then, it was heated and stirred at 100 ºC for 24 hours. After the reaction, the reactor was cooled to room temperature and the pressure was vented laxly. The solution was quickly transferred to a 25 mL Schlenk flask. The volatiles were removed in vacuo and the residue was extracted with 3 x 3 mL benzene and filtrated through a celite plug. After evaporation of solvent under reduced pressure, product **2.3LP$_{CO2}$** was isolated as a white powder. ^{1}H, ^{13}C, and ^{11}B NMR spectroscopy showed a 66:33 ratio of **2.3LP$_{CO2}$**: **2.3LP**.

Elimination of CO_2 from 2.3LP$_{CO2}$ yielding 2.3LP: A J-Young NMR tube was charged with **2.3LP$_{CO2}$** in 500 μL C_6D_6 and heated to 100 ºC for 24 hours. ^{1}H and ^{11}B NMR analysis showed quantitative reformation of **2.3LP**.

Reaction of 2.3LP with 2.3BC and H_2: A 50 mL stainless autoclave was charged with compound **2.3BC** (85 mg, 0.20 mmol, 1 eq.) and **2.3LP** (133 mg, 0.20 mmol, 1 eq.) in 10 mL dry THF. The reactor was pressurized with 20 bar of H_2 at room temperature. Then, it was heated and stirred at 80 ºC for 24 h. After the reaction, the reactor was cooled to room temperature and the pressure was vented laxly. The solution was quickly transferred to a 25 mL Schlenk flask. The volatiles were removed in vacuo and the residue was extracted with 3 x 1 mL benzene. Drying of the remaining residue under vacuum afforded the DBU-H formate salt in 72 % yield (NMR matches product from catalytic reactions, vide infra). After evaporation of the benzene extracts under vacuum, the solid residue was washed sequentially with 1 mL Et_2O and 1 mL pentane, and

after drying under vacuum yielded **2.3BD** in 67 % yield as a white powder. The ^{1}H NMR of **2.3BD** matches that reported previously (vide supra).

Insertion of 2.3BD into CO_2 in the presence of DBU: A stainless steel 50 mL autoclave was charged with **2.3BD** (178 mg, 0.20 mmol, 1eq.), DBU (30.4 mg, 0.20 mmol, 1 eq.), and 10 mL THF. The reactor was pressurized with 20 bar of CO_2 at room temperature. Then, it was heated and stirred at 100 ^{o}C for 24 hours. After the reaction, the reactor was cooled to room temperature and the pressure was vented laxly. The solution was quickly transferred to a 25 mL Schlenk flask and the volatiles were removed in vacuo. Crude ^{11}B NMR analysis showed the formation of compounds **2.3LP** and **2.3LP$_{CO2}$**. Extraction of the residue with 2 x 2 mL of a 1:1 v/v mixture of C_6H_6/Et_2O and filtration through a plug of celite afforded **2.3BC** in 49 % yield as a white solid.

Establishing Catalytic Competency of **2.3BC** and **2.3BD**:

Conversion of CO_2 to Formate using 2.3BC as catalyst: A stainless steel 50 mL autoclave was charged with DBU (1.52 g, 10 mmol, eq.) and $B(C_6F_5)_3$ (10.2 mg, 0.02 mmol, 0.02 mol %) in 5 mL THF. This solution was stirred for 1 hour at room temperature to ensure formation of adduct **2.3LP**. Complex **2.3BC** (4.23 mg, 0.01 mmol, 0.01 mol %) was then added and the reactor was pressurized with 60 bar of a 3:1 of H_2:CO_2 at room temperature. Then, it was heated and stirred at 100 ^{o}C for 24 hours. After the reaction, the reactor was cooled to room temperature and the pressure was vented laxly. An aliquot (200 μL) of the reaction mixture was dissolved in 400 μL of D_2O, and 15 μL of DMF was added as an internal standard for an estimation of the yield by ^{1}H NMR spectroscopy. Using this method, we found that complex **2.3BC** is catalytically competent and gives 387 TON.

Conversion of CO_2 to Formate using 2.3BD as catalyst: A stainless steel 50 mL autoclave was charged with DBU (1.52 g, 10 mmol, 1 eq.) and complex **2.3BD** (8.9 mg, 0.01

mmol, 0.01 mol %) in 5 mL THF. The reactor was pressurized with 60 bar of a 3:1 of H_2:CO_2 at room temperature. Then, it was heated and stirred at 100 ^oC for 24 hours. After the reaction, the reactor was cooled to room temperature and the pressure was vented laxly. An aliquot (200 μL) of the reaction mixture was dissolved in 400 μL of D_2O, and 15 μL of DMF was added as an internal standard for an estimation of the yield by ^{1}H NMR spectroscopy. Using this method, we found that complex $\mathbf{C_1}^{C6F5}$ is catalytically competent and gives 287 TON.

Catalytic Hydrogenations of CO_2 with H_2:

A 50 mL stainless autoclave was charged with catalyst **2.3BD^H** as a stock solution in degassed dry THF (10 mL), DBU (1.52 g, 10 mmol, 1 eq.) and a corresponding amount of BCF additive [the stock solution of catalyst was made by dissolving **2.3BD^H** (98 mg, 0.25 mmol, 1 mM) in degassed dry THF (250 mL)]. The reactor was pressurized with 60 bar of a 3:1 of H_2:CO_2 mixture at ambient temperature. The reactor was then heated and stirred at 100 ^oC for 24 hours. After the reaction, the reactor was cooled, and the pressure was vented laxly. An aliquot (200 μL) of the reaction mixture was dissolved in 400 μL of D_2O, and 15 μL of DMF was added as an internal standard for an estimation of the yield by using ^{1}H NMR spectroscopy. Isolation of DBU-H formate was achieved by evaporation of all volatiles under vacuum followed by washing of the residue with Et_2O (10 × 3 mL). The residue was dried thoroughly under vacuum giving a white solid, which was identified as the pure [DBU-H$^+$][HCO_2^-].

[DBU-H$^+$][HCO_2^-]: ^{1}H NMR ($CDCl_3$, 500 MHz): δ 1.61 (m, 2H), 1.68 (m, 4H), 1.95 (pent, *J* = 5.87 Hz, 2H), 2.76 (m, 2H), 3.35 (t, *J* = 5.71 Hz, 2H) 3.41 (m, 4H), 8.62 (s, 1H), 12.86 (s, br, 1H). ^{13}C{^{1}H} NMR ($CDCl_3$, 125 MHz): δ 19.6, 20.1, 26.9, 29.0, 32.0, 37.9, 48.6, 54.2, 77.4, 165.9, 168.1.

Crystal Structure Data:

Crystal data and structure refinement for 2.3BC.

Identification code	2.3BC
Empirical formula	$C_{23}H_{36}CuNO_2$
Formula weight	422.07
Temperature/K	100
Crystal system	monoclinic
Space group	Cc
a/Å	10.1126(14)
b/Å	20.167(3)
c/Å	10.9530(17)
α/°	90
β/°	94.968(7)
γ/°	90
Volume/Å^3	2225.4(6)
Z	4
ρ_{calc}g/cm^3	1.260
μ/mm^{-1}	0.998
F(000)	904.0
Crystal size/mm^3	0.195 × 0.181 × 0.123
Radiation	MoKα (λ = 0.71073)
2Θ range for data collection/°	4.04 to 50.708
Index ranges	$-12 \leq h \leq 8$, $-24 \leq k \leq 24$, $-13 \leq l \leq 12$
Reflections collected	6723
Independent reflections	3044 [R_{int} = 0.0228, R_{sigma} = 0.0359]
Data/restraints/parameters	3044/2/252
Goodness-of-fit on F^2	1.009
Final R indexes [I>=2σ (I)]	R_1 = 0.0244, wR_2 = 0.0570
Final R indexes [all data]	R_1 = 0.0262, wR_2 = 0.0578
Largest diff. peak/hole / e Å^{-3}	0.33/-0.19
Flack parameter	0.104(8)

Crystal data and structure refinement for 2.3BD.

Identification code	2.3BD
Empirical formula	$C_{40}H_{36.55}BCu_{0.45}F_{15}N$
Formula weight	855.97
Temperature/K	100.0
Crystal system	monoclinic
Space group	$P2_1/n$
a/Å	11.9729(6)

b/Å	18.6985(10)
c/Å	16.5926(8)
α/°	90
β/°	96.7860(10)
γ/°	90
Volume/Å^3	3688.6(3)
Z	4
ρ_{calc}g/cm^3	1.541
μ/mm^{-1}	0.395
F(000)	1747.0
Crystal size/mm^3	0.25 × 0.1 × 0.1
Radiation	MoKα (λ = 0.71073)
2Θ range for data collection/°	3.294 to 52.808
Index ranges	-14 ≤ h ≤ 12, -23 ≤ k ≤ 23, -20 ≤ l ≤ 20
Reflections collected	35596
Independent reflections	7532 [R_{int} = 0.0600, R_{sigma} = 0.0622]
Data/restraints/parameters	7532/0/543
Goodness-of-fit on F^2	1.088
Final R indexes [I>=2σ (I)]	R_1 = 0.0635, wR_2 = 0.1215
Final R indexes [all data]	R_1 = 0.1028, wR_2 = 0.1342
Largest diff. peak/hole / e Å^{-3}	0.85/-0.26

Crystal data and structure refinement for 3.2BE.

Identification code	3.2BE
Empirical formula	$C_{41}H_{36}BCuF_{15}NO_2$
Formula weight	934.06
Temperature/K	100.0
Crystal system	triclinic
Space group	P-1
a/Å	9.350(2)
b/Å	14.635(3)
c/Å	16.597(3)
α/°	66.104(5)
β/°	79.074(5)
γ/°	73.704(6)
Volume/Å^3	1985.6(7)
Z	2
ρ_{calc}g/cm^3	1.562
μ/mm^{-1}	0.659
F(000)	948.0
Crystal size/mm^3	0.1 × 0.1 × 0.01

Radiation	MoKα (λ = 0.71073)
2Θ range for data collection/°	2.694 to 50.388
Index ranges	$-11 \leq h \leq 11$, $-17 \leq k \leq 17$, $-18 \leq l \leq 19$
Reflections collected	21118
Independent reflections	7140 [R_{int} = 0.0952, R_{sigma} = 0.1330]
Data/restraints/parameters	7140/0/558
Goodness-of-fit on F^2	0.983
Final R indexes [I>=2σ (I)]	R_1 = 0.0563, wR_2 = 0.0897
Final R indexes [all data]	R_1 = 0.1270, wR_2 = 0.1093
Largest diff. peak/hole / e $Å^{-3}$	0.93/-0.47

Crystal data and structure refinement for 2.3LP.

Identification code	2.3LP
Empirical formula	$C_{27}H_{16}BF_{15}N_2$
Formula weight	664.23
Temperature/K	100.0
Crystal system	monoclinic
Space group	$P2_1/c$
a/Å	20.107(4)
b/Å	17.209(3)
c/Å	15.486(3)
α/°	90
β/°	107.658(5)
γ/°	90
Volume/$Å^3$	5106.0(17)
Z	8
$\rho_{calc}g/cm^3$	1.728
μ/mm^{-1}	0.178
F(000)	2656.0
Crystal size/mm^3	0.1 × 0.1 × 0.01
Radiation	MoKα (λ = 0.71073)
2Θ range for data collection/°	3.636 to 50.776
Index ranges	$-24 \leq h \leq 24$, $-20 \leq k \leq 20$, $-18 \leq l \leq 18$
Reflections collected	48435
Independent reflections	9353 [R_{int} = 0.1177, R_{sigma} = 0.1043]
Data/restraints/parameters	9353/0/811
Goodness-of-fit on F^2	0.981
Final R indexes [I>=2σ (I)]	R_1 = 0.0513, wR_2 = 0.0957
Final R indexes [all data]	R_1 = 0.1128, wR_2 = 0.1192
Largest diff. peak/hole / e $Å^{-3}$	0.33/-0.40

Crystal data and structure refinement for $L_3$2.3BD^H.

Identification code	$L_3$2.3BD^H
Empirical formula	$C_{24}H_{39.96}B_{0.74}Cl_{0.26}CuN$
Formula weight	423.28
Temperature/K	100.0
Crystal system	monoclinic
Space group	$P2_1/n$
a/Å	9.7735(9)
b/Å	23.466(2)
c/Å	10.3053(9)
α/°	90
β/°	96.704(2)
γ/°	90
Volume/Å^3	2347.3(4)
Z	4
ρ_{calc}g/cm^3	1.198
μ/mm^{-1}	0.968
F(000)	912.0
Crystal size/mm^3	0.2 × 0.1 × 0.1
Radiation	MoKα (λ = 0.71073)
2Θ range for data collection/°	3.472 to 50.738
Index ranges	$-11 \leq h \leq 11$, $-28 \leq k \leq 28$, $-12 \leq l \leq 12$
Reflections collected	25524
Independent reflections	4302 [R_{int} = 0.0398, R_{sigma} = 0.0295]
Data/restraints/parameters	4302/6/278
Goodness-of-fit on F^2	1.064
Final R indexes [I>=2σ (I)]	R_1 = 0.0293, wR_2 = 0.0660
Final R indexes [all data]	R_1 = 0.0389, wR_2 = 0.0689
Largest diff. peak/hole / e Å^{-3}	0.32/-0.30

2.6.3 Preparation of the First Neutral Silver(I)-Hydride

Synthesis of (IPr)AgCl**: A Schlenk tube was charged with IPr**HCl imidazolium (1.00 g, 0.65 mmol, 2 eq.), Ag_2O (0.075 g, 0.325 mmol, 1 eq.), and $MgSO_4$ (0.325 g, 1 eq w/w). 10 mL anhydrous DCM was added, and the resulting solution was stirred for 24 hours at 40 °C. The reaction was filtered over a short pad of silica and the silica was washed with 3 x15 mL DCM. The volatiles were evaporated under vacuum yielding (IPr**)AgCl in 0.85 g (87%) as a white solid. M. P.: > 300 °C. ^{1}H NMR ($CDCl_3$, 500 MHz): δ 1.26 (pseudo-d, 72 H), 2.25 (s, 6 H), 5.20 (s, 4

H), 5.84 (s, 2 H), 6.80 (d, J = 7.8 Hz, 8 H), 6.86 (s, 4 H), 6.99 (d, J = 8.0 Hz, 8 H), 7.16 (d, J = 7.8 Hz, 8 H), 7.24 (d, J = 8.1 Hz, 8 H). $^{13}C\{^{1}H\}$ NMR ($CDCl_3$, 125 MHz): δ 183.9 (pseudo-dd, $^{1}J(^{13}C\text{-}^{107}Ag)$ = 232.3 Hz, $^{1}J(^{13}C\text{-}^{109}Ag)$ = 268.4 Hz, $C_{carbene}$-Ag), 149.3, 149.2, 141.2, 140.1, 139.8, 134.3, 130.2, 129.2, 129.1, 125.6, 125.1, 123.7, 123.6, 50.4 (CHAr$_2$), 34.50 (ArCH$_3$), 34.47 (ArCH$_3$), 31.50 (C(CH$_3$)$_3$), 31.48 (C(CH$_3$)$_3$), 22.0 (C(CH$_3$)$_3$). HRMS ESI-TOF+ found m/z 1467.8476, $[M - Cl]^+$ calculated for $[C_{101}H_{120}AgN_2]^+$ 1423.8742.

Synthesis of (IPr)AgOPh (2.4DA)**: To a Schlenk tube charged with IPr**AgCl (0.300 g, 0.199 mmol, 1 eq.) was added KOPh (0.029 g, 0.259 mmol, 1.3 eq.). 5 mL anhydrous DCM was added and the solution was stirred overnight at room temperature. The reaction was filtered over celite. The celite was washed with 3 x 5 mL DCM and the combined organic extracts were evaporated under vacuum yielding 0.286 g of **2.4DA** as an off-white solid (92% yield). M. P.: 175.6 – 182.5 ^{o}C ^{1}H NMR (C_6D_6, 500 MHz): δ 1.20 (s, 72 H), 1.71 (s, 6 H), 5.68 (s, 4 H), 5.83 (s, 2 H), 6.69 (t, J = 6.8 Hz, 1 H), 7.00 (d, J = 7.4 Hz, 10 H), 7.14 (m, 15 H), 7.27 (d, J = 7.8 Hz, 8 H), 7.39 (d, J = 7.8 Hz, 8 H). $^{13}C\{^{1}H\}$ NMR (C_6D_6, 125 MHz): δ 184.4 (pseudo-dd, $^{1}J(^{13}C\text{-}^{107}Ag)$ = 223.3 Hz, $^{1}J(^{13}C\text{-}^{109}Ag)$ = 243.4 Hz, $C_{carbene}$-Ag), 169.8 ($C_{carbene}$AgOC), 149.7, 149.4, 141.8, 140.8, 140.7, 140.6, 135.1, 130.6, 129.8, 129.6, 129.5, 126.3, 125.6, 124.12, 124.07, 120.2, 113.6, 51.0 (CHAr$_2$), 34.6 (ArCH$_3$), 34.5 (ArCH$_3$), 31.6 (C(CH$_3$)$_3$), 31.5 (C(CH$_3$)$_3$), 21.3 (C(CH$_3$)$_3$). HRMS ESI-TOF+ found m/z 1467.8483, $[M - OPh]^+$ calculated for $[C_{101}H_{120}AgN_2]^+$ 1467.8497.

Synthesis of (IPr)AgH (2.4DB)**: A J-Young NMR tube charged with IPr**AgOPh **2.4DA** (0.030 g, 0.019 mmol, 1 eq.) and 500 μL toluene-d_8 was cooled to -40 ^{o}C. Pinacolborane (2.8 μL, 0.019 mmol, 1 eq.) was added thus resulting in an immediate color change. The sample was taken to a pre-cooled NMR spectrometer at -40 ^{o}C. After collection of ^{1}H/^{13}C spectra, the sample was returned to the freezer overnight for crystallization. Clear colorless needles of **2.4DB**

grew overnight, which were suitable for X-ray crystallography. M. P.: >-10 °C dec. ^{1}H NMR (tol-d_8, 500 MHz): δ 1.19 (s, 36 H), 1.24 (s, 36 H), 1.66 (s, 6 H), 3.87 (pseudo-dd, $^{1}J(^{1}H\text{-}^{107}Ag)$ = 224.6 Hz, $^{1}J(^{1}H\text{-}^{109}Ag)$ = 260.6 Hz, Ag-*H*), 5.68 (s, 2 H), 5.86 (s, 4 H), 6.95 (d, J = 8.1 Hz, 8 H), 7.03 (d, J = 8.2 Hz, 8 H), 7.14 (s, 4 H), 7.27 (d, J = 7.5 Hz, 8 H) , 7.69 (d, J = 7.0 Hz, 8 H). ^{13}C{^{1}H} NMR (tol-d_8, 125 MHz): δ 193.2 (pseudo-dd, $^{1}J(^{13}C\text{-}^{107}Ag)$ = 113.2 Hz, $^{1}J(^{13}C\text{-}^{109}Ag)$ = 126.6 Hz, $C_{carbene}$-Ag), 149.3, 149.0, 141.9, 141.5, 140.7, 140.0, 135.4, 130.2, 129.6, 125.8, 125.4, 123.5, 123.4, 50.8 (*C*HAr$_2$), 50.7 (*C*HAr$_2$), 34.5 (Ar*C*H$_3$), 34.4 (Ar*C*H$_3$), 31.52 (C(*C*H$_3$)$_3$), 31.48 (C(*C*H$_3$)$_3$), 31.45 (C(*C*H$_3$)$_3$), 21.2 (*C*(CH$_3$)$_3$). HRMS ESI-TOF+ shows only [M - H]$^+$.

Synthesis of (IPr)AgOC(=O)H (2.4DC)**: A J-Young NMR tube charged with IPr**AgOPh **2.4DA** (0.030 g, 0.019 mmol, 1 eq.) and 500 μL toluene-d_8 was cooled to -40 °C. Pinacolborane (2.8 μL, 0.019 mmol, 1 eq.) was added thus resulting in an immediate color change. The sample was taken to a pre-cooled NMR spectrometer at -40 °C to ensure complete formation of **2.4DB**. The tube was subjected to 3 freeze-pump-thaw cycles and backfilled with 1 bar CO_2. The tube was left at -40 °C for 6 hours. ^{1}H NMR analysis showed complete conversion to product **2.4DC**. Concentration to ½ volume and cooling to -20 °C overnight deposited clear colorless needles. The crystals were collected by vacuum filtration, washed with 2 x 3 mL pentane, and dried under vacuum to yield complex **2.4DC** as a white powder in 96 % yield. ^{1}H NMR (C_6D_6, 500 MHz): δ 1.24 (s, 36 H), 1.27 (s, 36 H), 1.67 (s, 6 H), 5.77 (s, 4 H), 5.84 (s, 2 H), 7.04 (d, J = 8.2 Hz, 8 H), 7.15 (d, J = 8.2 Hz, 8 H), 7.16 (s, 4 H), 7.50 (d, J = 7.3 Hz, 8 H) , 7.61 (d, J = 8.3 Hz, 8 H), 9.12 (d, J = 16.0 Hz, 1 H). ^{13}C{^{1}H} NMR (tol-d_8, 125 MHz): δ 185.3 (pseudo-dd, $^{1}J(^{13}C\text{-}^{107}Ag)$ = 238.6 Hz, $^{1}J(^{13}C\text{-}^{109}Ag)$ = 274.4 Hz, $C_{carbene}$-Ag), 168.6 (d, $^{2}J_{Ag\text{-}C}$ = 5.4 Hz), 149.6, 149.2, 141.8, 141.0, 140.8, 140.6, 135.1, 130.6, 130.0, 129.6, 126.4, 125.5, 124.2, 124.1, 50.9 (*C*HAr$_2$), 34.6 (Ar*C*H$_3$), 34.5 (Ar*C*H$_3$), 31.6 (C(*C*H$_3$)$_3$), 31.5 (C(*C*H$_3$)$_3$), 21.2 (*C*(CH$_3$)$_3$).

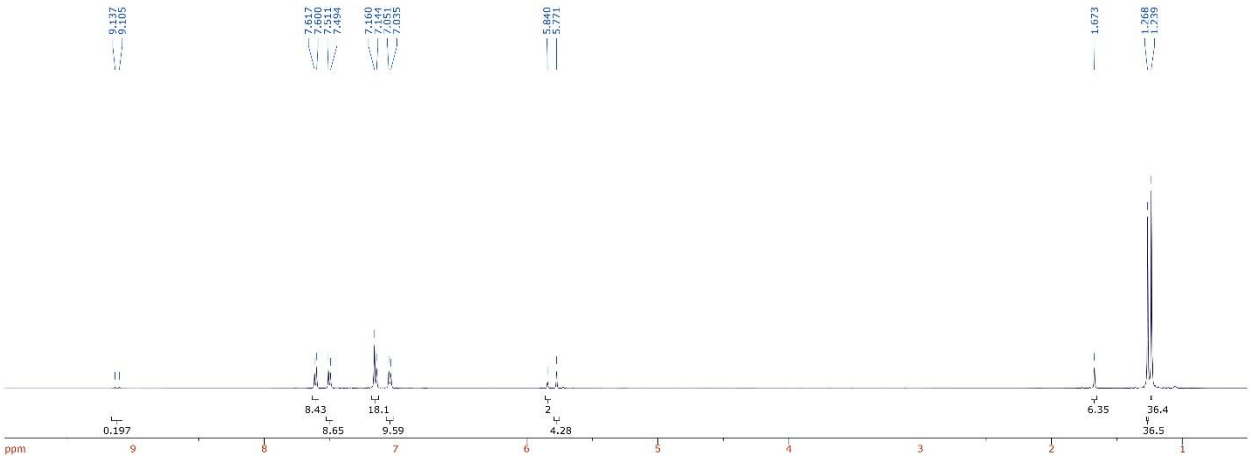

Figure 2.36. ^{1}H NMR spectrum for complex **2.4DC**.

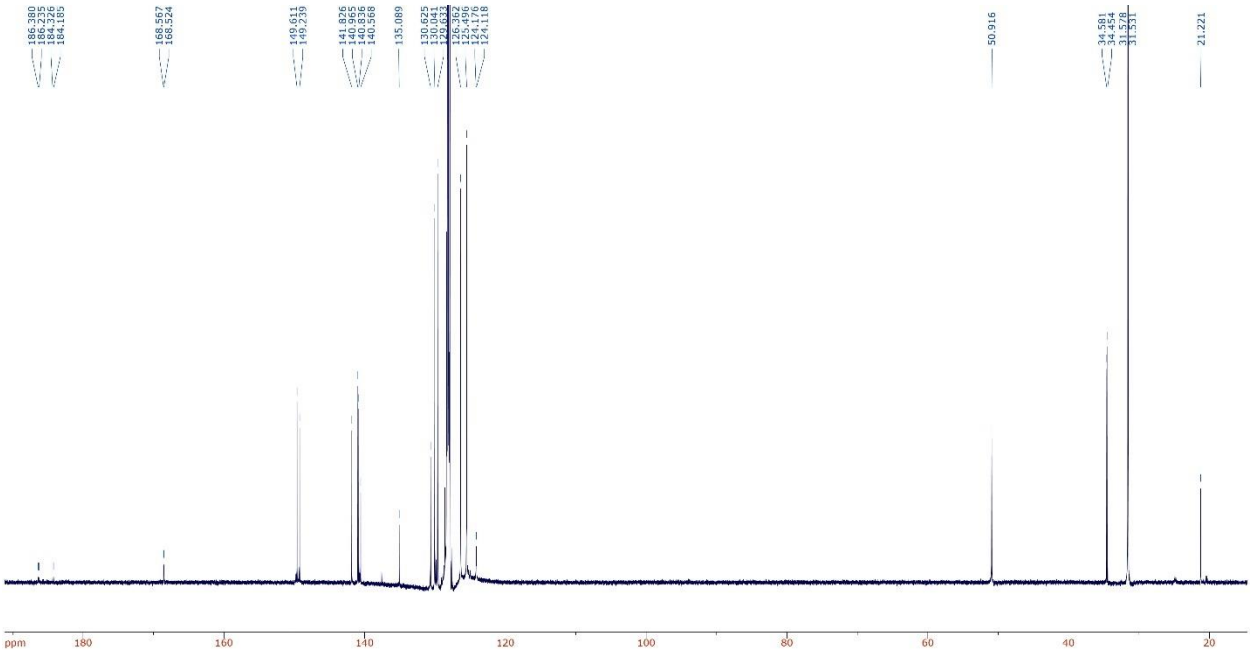

Figure 2.37. ^{13}C NMR spectrum for complex **2.4DC**.

Synthesis of (IPr)AgHBCF (2.4DD)**: To a J-Young NMR tube charged with IPr**AgOPh (0.060 g, 0.038 mmol, 1 eq.) and 600 μL tol-d_8 was added pinacolborane (5.6 μL, 0.038 mmol, 1 eq.) at -40 ^{o}C. After 15 minutes, solid BCF (0.020 g, 0.038 mmol, 1 eq.) was added in one portion and allowed to sit at -40 ^{o}C for 1 hour before being allowed to warm to room

temperature. The solution was concentrated under vacuum until ~ 50 μL toluene remained. Pentane was added to the NMR tube and left at room temperature overnight, during which time, X-ray quality crystals of **2.4DD** grew as colorless blocks. The white crystals were filtrated and dried under vacuum yielding 0.073 g (96 %) of **2.4DD**. M. P.: 271.8 ºC dec. ^{1}H NMR ($CDCl_3$, 500 MHz): δ 1.22 (s, 36 H), 1.26 (s, 36 H), 2.24 (s, 6 H), 5.31 (s, 4 H), 5.89 (s, 2 H), 6.84 (d, J = 8.1 Hz, 8 H), 6.90 (s, 4 H), 7.02 (d, J = 8.1 Hz, 8 H), 7.15 (d, J = 8.5 Hz, 8 H) , 7.16 (d, J = 8.5 Hz, 8 H). ^{13}C{^{1}H} NMR ($CDCl_3$, 125 MHz): δ 187.0 (pseudo-dd, $^{1}J(^{13}C\text{-}^{107}Ag)$ = 168.8 Hz, $^{1}J(^{13}C\text{-}^{109}Ag)$ = 189.0 Hz, $C_{carbene}$-Ag), 149.2, 149.1, 147.4, 147.2, 141.3, 140.2, 140.1, 139.6, 137.2, 135.2, 135.0, 134.4, 130.1, 130.0, 129.1, 125.5, 125.2, 125.0, 123.9, 123.7, 50.5 (CHAr$_2$), 50.4 (CHAr$_2$), 34.5 (ArCH$_3$), 34.4 (ArCH$_3$), 31.6 (C(CH$_3$)$_3$), 31.5 (C(CH$_3$)$_3$), 31.3 (C(CH$_3$)$_3$), 22.1 (C(CH$_3$)$_3$). ^{11}B NMR ($CDCl_3$, 96 MHz): δ -22.7 ppm.

Crystal Structure Data:

Crystal data and structure refinement for 2.4DB.

Identification code	**2.4DB**
Empirical formula	$C_{101}H_{120.5}AgN_2$
Formula weight	1474.39
Temperature/K	100.0
Crystal system	triclinic
Space group	P-1
a/Å	17.8877(4)
b/Å	20.6603(5)
c/Å	29.4115(8)
α/°	88.331(2)
β/°	86.405(2)
γ/°	71.350(2)
Volume/Å^3	10278.0(5)
Z	4
ρ_{calc}g/cm^3	0.953
μ/mm^{-1}	1.860
F(000)	3158.0
Crystal size/mm^3	0.3 × 0.1 × 0.1

Radiation	CuKα (λ = 1.54178)
2Θ range for data collection/°	4.514 to 109.018
Index ranges	$-18 \leq h \leq 18$, $-21 \leq k \leq 21$, $-31 \leq l \leq 31$
Reflections collected	89116
Independent reflections	25145 [R_{int} = 0.0861, R_{sigma} = 0.0916]
Data/restraints/parameters	25145/5/1979
Goodness-of-fit on F^2	1.028
Final R indexes [I>=2σ (I)]	R_1 = 0.0756, wR_2 = 0.1880
Final R indexes [all data]	R_1 = 0.1077, wR_2 = 0.2086
Largest diff. peak/hole / e $Å^{-3}$	0.92/-0.86

Crystal data and structure refinement for 2.4DD.

Identification code	**2.4DD**
Empirical formula	$C_{128}H_{130}AgBF_{15}N_2$
Formula weight	2100.01
Temperature/K	100.15
Crystal system	monoclinic
Space group	$P2_1/c$
a/Å	16.158(5)
b/Å	23.393(7)
c/Å	30.498(9)
α/°	90
β/°	95.659(7)
γ/°	90
Volume/$Å^3$	11472(6)
Z	4
ρ_{calc}g/cm^3	1.216
μ/mm^{-1}	0.249
F(000)	4396.0
Crystal size/mm^3	0.1 × 0.1 × 0.1
Radiation	MoKα (λ = 0.71073)
2Θ range for data collection/°	3.868 to 50.05
Index ranges	$-19 \leq h \leq 19$, $-23 \leq k \leq 27$, $-36 \leq l \leq 36$
Reflections collected	152716
Independent reflections	20236 [R_{int} = 0.0566, R_{sigma} = 0.0314]
Data/restraints/parameters	20236/12/1388
Goodness-of-fit on F^2	1.045
Final R indexes [I>=2σ (I)]	R_1 = 0.0391, wR_2 = 0.0946
Final R indexes [all data]	R_1 = 0.0530, wR_2 = 0.1051
Largest diff. peak/hole / e $Å^{-3}$	0.75/-0.51

2.7 References

[1] Wurtz, A. "Sur l'Hydrure de Cuivre" *Ann. Chim. Phys.* **1844**, *11*, 250.

[2] For reviews on copper(I)-hydrides, see: (a) Deutsch, C.; Krause, N.; Lipshutz, B. H. "CuH-Catalyzed Reactions" *Chem. Rev.* **2008**, *108*, 2916. (b) Jordan, A. J.; Lalic, G.; Sadighi, J. P. "Coinage Metal Hydrides: Synthesis, Characterization, and Reactivity" *Chem. Rev.* **2016**, *116*, 8318. (c) Cox, N.; Dang, H.; Whittaker, A. M.; Lalic, G. "NHC–copper hydrides as chemoselective reducing agents: catalytic reduction of alkynes, alkyl triflates, and alkyl halides" *Tetrahedron* **2014**, *27-28*, 4219.

[3] (a) Mahoney, W. S.; Brestensky, D. M.; Stryker, J. M. "Selective hydride-mediated conjugate reduction of α,β-unsaturated carbonyl compounds using $[(Ph_3P)CuH]_6$" *J. Am. Chem. Soc.* **1988**, *110*, 291. (b) Albert, C. F.; Healy, P. C.; Kildea, J. D.; Raston, C. L.; Skelton, B. W.; White, A. H. "Lewis-base adducts of Group 11 metal(I) compounds. 49. Structural characterization of hexameric and pentameric (triphenylphosphine)copper(I) hydrides" *Inorg. Chem.* **1989**, *28*, 1300.

[4] Bezman, S. A.; Churchill, M. R.; Osborn, J. A.; Wormald, J. "Preparation and crystallographic characterization of a hexameric triphenylphosphinecopper hydride cluster" *J. Am. Chem. Soc.* **1971**, *93*, 2063.

[5] Mankad, N. P.; Laitar, D. S.; Sadighi, J. P. "Synthesis, Structure, and Alkyne Reactivity of a Dimeric (Carbene)copper(I) Hydride" *Organometallics* **2004**, *23*, 3369.

[6] Frey, G. D.; Donnadieu, B.; Soleilhavoup, M.; Bertrand, G. "Synthesis of a Room-Temperature-Stable Dimeric Copper(I) Hydride" *Chem. Asian J.* **2011**, *6*, 402.

[7] Jordan, A. J.; Wyss, C. M.; Bacsa, J.; Sadighi, J. P. "Synthesis and Reactivity of New Copper(I) Hydride Dimers" *Organometallics* **2016**, *35*, 613.

[8] Lu, W. Y.; Cavell, K. J.; Wixey, J. S.; Kariuki, B. "First Examples of Structurally Imposing Eight-Membered-Ring (Diazocanylidene) N-Heterocyclic Carbenes: Salts, Free Carbenes, and Metal Complexes" *Organometallics* **2011**, *30*, 5649.

[9] (a) Vergote, T.; Nahra, F.; Merschaert, A.; Riant, O.; Peeters, D.; Leyssens, T. "Mechanistic Insight into the (NHC)copper(I)-Catalyzed Hydrosilylation of Ketones" *Organometallics* **2014**, *33*, 1953. (b) Schmid, S. C.; Van Hoveln, R.; Rigoli, J. W.; Schomaker, J. M. "Development of *N*-Heterocyclic Carbene–Copper Complexes for 1,3-Halogen Migration" *Organometallics* **2015**, *34*, 4164.

[10] Dey, G.; Elliott, S. D. "Copper(I) carbene hydride complexes acting both as reducing agent and precursor for Cu ALD: a study through density functional theory" *Theor. Chem. Acc.* **2013**, *133*, 1416.

[11] Berthon-Gelloz, G.; Siegler, M. A.; Spek, A. L.; Tinant, B.; Reek, J. N. H.; Marko, I. E. "IPr* an easily accessible highly hindered N-heterocyclic carbene" *Dalton Trans.* **2010**, *39*, 1444.

[12] Weber, S. G.; Loos, C.; Rominger, F.; Straub, B. F. "Synthesis of an extremely stericall shielding *N*-heterocyclic carbene ligand" *Arkivok* **2012**, *iii*, 226.

[13] Preliminary results leading to the potential existence of a monomer-dimer equilibrium were obtained by a former Master student in the group, Pauline M. Olsen. However, the full study including the isolation and characterization of all key copper-hydride complexes was accomplished by the dissertation author.

[14] Romero, E. A.; Peltier, J. L.; Jazzar, R.; Bertrand, G. "Catalyst-Free Dehydrocoupling of Amines, Alcohols, and Thiols with Pinacol Borane and 9-Borabicyclononane (9-BBN) " *Chem. Commun.* **2016**, *52*, 165.

[15] Whitesides, G. M.; Maglio, G. "Hydrogen-carbon-13 spin-spin coupling in transition metal hydride complexes" *J. Am. Chem. Soc.* **1969**, *91*, 4980.

[16] Collins, L. R.; Rajabi, N. A.; Macgregor, S. A.; Mahon, M. F.; Whittlesey, M. K. "Experimental and Computational Studies of the Copper Borate Complexes [(NHC)Cu(HBEt$_3$)] and [(NHC)Cu(HB(C$_6$F$_5$)$_3$)]" *Angew. Chem. Int. Ed.* **2016**, *55*, 15539.

[17] Chakraborty, S.; Zhang, J.; Patel, Y. J.; Krause, J. A.; Guan, H. "Pincer-Ligated Nickel Hydridoborate Complexes: the Dormant Species in Catalytic Reduction of Carbon Dioxide with Boranes" *Inorg. Chem.* **2013**, *52*, 37.

[18] Liu, L.; Ruiz, D. A.; Munz, D.; Bertrand, G. "A Singlet Phosphinidene Stable at Room Temperature" *Chem* **2016**, *1*, 147.

[19] (a) Brestensky, D. M.; Huseland, D. E.; McGettigan, C.; Stryker, J. M. "Direct synthesis of Stryker's reagent from a Cu(II) salt" *Tetrahedron Lett.* **1988**, *29*, 3749. (b) Brestensky, D. M.; Stryker, J. M. "Regioselective conjugate reduction and reductive silylation of α,β-unsaturated" *Tetrahedron Lett.* **1989**, *30*, 5677. (c) Koenig, T. M.; Daeuble, J. F.; Brestensky, D. M.; Stryker, J. M. "Conjugate reduction of polyfunctional α,β-unsaturated carbonyl compounds using [(Ph$_3$P)CuH]$_6$. Compatibility with halogen, sulfonate, and γ-oxygen and sulfur substituents" *Tetrahedron Lett.* **1990**, *31*, 3237. (d) Hughes, G.; Kimura, M.; Buchwald, S. L. "Catalytic Enantioselective Conjugate Reduction of Lactones and Lactams" *J. Am. Chem. Soc.* **2003**, *125*, 11253.

[20] (a) Lipshutz, B. H.; Caires, C. C.; Kuipers, P.; Chrisman, W. "Tweaking Copper Hydride (CuH) for Synthetic Gain. A Practical, One-Pot Conversion of Dialkyl Ketones to Reduced Trialkylsilyl Ether Derivatives" *Org. Lett.* **2003**, *5*, 3085. (b) Lipshutz, B. H.; Lower, A.; Noson, K. "Copper(I) Hydride-Catalyzed Asymmetric Hydrosilylation of Heteroaromatic Ketones" *Org. Lett.* **2002**, *4*, 4045. (c) Lipshutz, B. H.; Shimizu, H. "Copper(I)-Catalyzed Asymmetric Hydrosilylations of Imines at Ambient Temperatures" *Angew. Chem. Int. Ed.* **2004**, *43*, 2228.

[21] See the following minireview and all the references therein: Pirnot, M. T.; Wang, Y. -M.; Buchwald, S. L. " Copper Hydride Catalyzed Hydroamination of Alkenes and Alkynes" *Angew. Chem. Int. Ed.* **2016**, *55*, 48.

[22] Romero, E. A.; Jazzar, R.; Bertrand, G. "Copper-catalyzed dehydrogenative borylation of terminal alkynes with pinacolborane" *Chem. Sci.* **2017**, *8*, 165.

[23] (a) Watari, R.; Kayaki, Y.; Hirano, S. -I.; Matsumoto, N.; Ikariya, T. "Hydrogenation of carbon dioxide to formate catalyzed by a copper/1,8-diazabicyclo[5.4.0]undec-7-ene system" *Adv. Synth. Catal.* **2015**, *357*, 1369. (b) Zall, C. M.; Linehan, J. C.; Appel, A. M. "A molecular copper catalyst for hydrogenation of CO_2 to formate" *ACS Catal*. **2015**, *5*, 5301. (c) Zall, C. M.; Linehan, J. C.; Appel, A. M. "Triphosphine-ligated copper hydrides for CO_2 hydrogenation: Structure, reactivity, and thermodynamic studies" *J. Am. Chem. Soc.* **2016**, *138*, 9968.

[24] For recent reviews, see: (a) Goeppert, A.; Czaun, M.; Jones, J.; Prakash, G. K.; Olah, G. A. "Recycling of carbon dioxide to methanol and derived products – closing the loop" *Chem. Soc. Rev.* **2014**, *43*, 7995. (b) Aresta, M.; Dibenedetto, A.; Angelini, A. "Catalysis for the Valorization of Exhaust Carbon: from CO_2 to Chemicals, Materials, and Fuels. Technological Use of CO_2" *Chem. Rev.* **2014**, *114*, 1709. (c) Zhu, Q.; Xu, Q. "Liquid organic and inorganic chemical hydrides for high-capacity hydrogen storage" *Energy Environ. Sci*. **2015**, *8*, 478. (d) Wang, W.; Himeda, Y.; Muckerman, J. T.; Manbeck, G. F.; Fujita, E. "CO_2 Hydrogenation to Formate and Methanol as an Alternative to Photo- and Electrochemical CO_2 Reduction" *Chem. Rev.* **2015**, *115*, 12936. (e) Liu, Q.; Wu, L.; Jackstell, R.; Beller, M. "Using carbon dioxide as a building block in organic synthesis" *Nature Communications* **2015**, *6*, 5933. (f) Du, X.; Jiang, Z.; Su, D. S.; Wang, J. "Research Progress on the Indirect Hydrogenation of Carbon Dioxide to Methanol" *ChemSusChem* **2016**, *9*, 322. (g) Klankermayer, J.; Wesselbaum, S.; Beydoun, K.; Leitner, W. "Selective Catalytic Synthesis Using the Combination of Carbon Dioxide and Hydrogen: Catalytic Chess at the Interface of Energy and Chemistry" *Angew. Chem. Int. Ed.* **2016**, *55*, 7296. (h) Bernskoetter, W. H.; Hazari, N. "Reversible Hydrogenation of Carbon Dioxide to Formic Acid and Methanol: Lewis Acid Enhancement of Base Metal Catalysts" *Acc. Chem. Res.* **2017**, *50*, 1049.

[25] Inoue, Y.; Izumida, H.; Hashimoto, H. "Catalytic fixation of carbon dioxide to formic acid by transition metal complexes under mild conditions" *Chem. Lett.* **1976**, *5*, 863.

[26] Dong, K.; Razzaq, R.; Hu, Y.; Ding, K. "Homogeneous reduction of carbon dioxide with hydrogen" *Top. Curr. Chem.* **2017**, *375*, 1.

[27] Tanaka, R.; Yamashita, M.; Nozaki, K. "Catalytic hydrogenation of carbon dioxide using Ir(III)-pincer complexes" *J. Am. Chem. Soc.* **131**, 14168.

[28] Rezayee, N. M., Huff, C. A.; Sanford, M. S. "Tandem Amine and Ruthenium-Catalyzed Hydrogenation of CO_2 to Methanol" *J. Am. Chem. Soc.* **2015**, *137*, 1028.

[29] Jiang, Y.; Blacque, O.; Fox, T.; Berke, H. "Catalytic CO_2 Activation Assisted by Rhenium Hydride/$B(C_6F_5)_3$ Frustrated Lewis Pairs—Metal Hydrides Functioning as FLP Bases" *J. Am. Chem. Soc.* **2013**, *135*, 7751.

[30] Bertini, F.; Glatz, M.; Gorgas, N.; Stöger, B.; Peruzzini, M.; Veiros, L. F.; Kirchner, K.; Gonsalvi, L. "Carbon dioxide hydrogenation catalysed by well-defined Mn(I) PNP pincer hydride complexes" *Chem. Sci.* **2017**, *8*, 5024.

[31] Langer, R., et al. "Low-pressure hydrogenation of carbon dioxide catalyzed by an iron pincer complex exhibiting noble metal activity" *Angew. Chem. Int. Ed.* **2011**, *50*, 9948.

[32] Zhang, Y.; MacIntosh, A. D.; Wong, J. L.; Bielinsky, E. A.; Willard, P. G.; Mercado, B. Q.; Hazari, N.; Bernskoetter, W. H. "Iron catalyzed CO_2 hydrogenation to formate enhanced by Lewis acid co-catalysts" *Chem. Sci.* **2015**, *6*, 4291.

[33] Jeletic, M. S.; Mock, M. T.; Appel, A. M.; Linehan, J. C. "A Cobalt-based catalyst for the hydrogenation of CO_2 under ambient conditions" *J. Am. Chem. Soc.* **2013**, *135*, 11533.

[34] Vogt, C.; Groeneveld, E.; Kamsma, G.; Nachtegaal, M.; Lu, L.; Kiely, C. J.; Berben, P. H.; Meirer, F.; Weckhuysen, B. M. "Unraveling structure sensitivity in CO_2 hydrogenation over nickel" *Nature Catalysis* **2018**, *1*, 127.

[35] Haynes, P.; Slaugh, L. H.; Kohnle, J. F. "Formamides from carbon dioxide, amines and hydrogen in the presence of metal complexes" *Tetrahedron Lett.* **1970**, *11*, 365.

[36] Zhang, L.; Cheng, J.; Hou, Z. "Highly efficient catalytic hydrosilylation of carbon dioxide by an *N*-heterocyclic carbene copper catalyst" *Chem. Commun.* **2013**, *49*, 4782.

[37] Wyss, C. M.; Tate, B. K.; Bacsa, J.; Gray, T. G.; Sadighi, J. P. "Bonding and Reactivity of a μ-Hydrido Dicopper Cation" *Angew. Chem. Int. Ed.* **2013**, *52*, 12920.

[38] Reviews: (a) Stephan, D. W. "The broadening reach of frustrated Lewis pair chemistry" *Science* **2016**, *354*, aaf7229; (b) Stephan, D. W. "Frustrated Lewis Pairs" *J. Am. Chem. Soc.* **2015**, *137*, 10018. (c) Stephan, D. W. "'Frustrated Lewis pairs': a concept for new reactivity and catalysis" *Org. Biomol. Chem.* **2008**, 6, 1535. (c) Stephan, D. W.; Erker, G. "Frustrated Lewis Pairs: Metal-free Hydrogen Activation and More" *Angew. Chem. Int. Ed.* **2010**, *49*, 46.

[39] Courtemanche, M. -A.; Pulis, A. P.; Rochette, E.; Légaré, M. -A.; Stephan, D. W.; Fontaine, F. -G. "Intramolecular B/N frustrated Lewis pairs and the hydrogenation of carbon dioxide" *Chem. Commun.* **2015**, *51*, 9797.

[40] Ashley, A. E.; Thompson, A. L.; O'Hare, D. "Non-Metal-Mediated Homogeneous Hydrogenation of CO_2 to CH_3OH" *Angew. Chem. Int. Ed.* **2009**, *48*, 9839.

[41] (a) Liu, L.; Vankova, N.; Heine, T. "A kinetic study on the reduction of CO_2 by frustrated Lewis pairs: from understanding to rational design" *Phys. Chem. Chem. Phys.* **2016**, *18*, 3567. (b) Rokob, T. A.; Hamza, A.; Stirling, A.; Soós, T.; Pápai, I. "Turning Frustration into Bond Activation: A Theoretical Mechanistic Study on Heterolytic Hydrogen Splitting by Frustrated Lewis Pairs" *Angew. Chem. Int. Ed.* **2008**, *47*, 2435. (c) Wen, M.; Huang, F.; Lu, G.; Wang, Z. -X. "Density Functional Theory Mechanistic Study of the Reduction of CO_2 to CH_4 Catalyzed by an Ammonium Hydridoborate Ion Pair: CO_2 Activation via Formation of a Formic Acid Entity" *Inorg. Chem.* **2013**, *52*, 12098.

[42] Jiang, C.; Blacque, O.; Fox, T.; Berke, H. "Heterolytic cleavage of H_2 by frustrated B/N Lewis pairs" *Organometallics* **2011**, *30*, 2117.

[43] All reactions in this section that require high pressures of H_2 or CO_2 were performed by our collaborators at Nanjing University in China (T. Zhao, X. Hu, and Y. Wu). All the mechanistic investigative work was performed by the dissertation author.

[44] Mahoney, J. K.; Martin, D.; Moore, C. E.; Rheingold, A. L.; Bertrand, G. "Bottleable (amino)(carboxy) radicals derived from cyclic (alkyl)(amino)carbenes" *J. Am. Chem. Soc.* **2013**, *135*, 18766.

[45] Lavallo, V.; Canac, Y.; Prasang, C.; Donnadieu, B.; Bertrand, G. "Stable cyclic (alkyl)(amino)carbenes as rigid or flexible, bulky, electron-rich ligands for transition metal catalysts: A quaternary carbon makes the difference!" *Angew. Chem. Int. Ed.* **2005**, *44*, 5705.

[46] Tomás-Mendivil, E.; Hansmann, M. M.; Weinstein, C. M.; Jazzar, R.; Melaimi, M.; Bertrand, G. "Bicyclic (alkyl)(amino)carbenes (BICAACs): Stable carbenes more ambiphilic than CAACs" *J. Am. Chem. Soc.* **2017**, *139*, 7753.

[47] Geier, S. J.; Gille, A. L.; Gilbert, T. M.; Stephan, D. W. "From classical adducts to frustrated Lewis pairs: Steric effects in the interactions of pyridines and $B(C_6F_5)_3$" *Inorg. Chem*. **2009**, *48*, 10466.

[48] Johnstone, T. C.; Wee, G. N. J. H.; Stephan, D. W. "Accessing frustrated Lewis pair chemistry from a spectroscopically stable and classical Lewis acid-base adduct" *Angew. Chem. Int. Ed.* **2018**, *57*, 5881.

[49] Berkefeld, A.; Piers, W. E.; Parvez, M. "Tandem Frustrated Lewis Pair/Tris(pentafluorophenyl)borane-Catalyzed Deoxygenative Hydrosilylation of Carbon Dioxide" *J. Am. Chem. Soc.* **2010**, *132*, 10660.

[50] Mömming, C. M.; Otten, E.; Kehr, G.; Fröhlich, R.; Grimme, S.; Stephan, D. W.; Erker, G. "Reversible metal-free carbon dioxide binding by frustrated Lewis pairs" *Angew. Chem. Int. Ed.* **2009**, *48*, 6643.

[51] Tsui, E. Y.; Müller, P.; Sadighi, J. P. "Reactions of a Stable Monomeric Gold(I) Hydride Complex" *Angew. Chem. Int. Ed.* **2008**, *47*, 8937.

[52] Liu, C. W.; Chang, H. -W.; Sarkar, B.; Saillard, J. -Y.; Kahlal, S.; Wu, Y.-Y. "Stable Silver(I) Hydride Complexes Supported by Diselenophosphate Ligands" *Inorg. Chem.* **2010**, *49*, 468.

[53] Tate, B. K.; Wyss, C. M.; Bacsa, J.; Kluge, K.; Gelbaum, L.; Sadighi, J. P. "A dinuclear silver hydride and an umpolung reaction of CO_2" *Chem. Sci.* **2013**, *4*, 3068.

[54] Hu, X.; Soleilhavoup, M.; Melaimi, M.; Chu, J.; Bertrand, G. "Air-Stable (CAAC)CuCl and (CAAC)$CuBH_4$ Complexes as Catalysts for the Hydrolytic Dehydrogenation of BH_3NH_3" *Angew. Chem. Int. Ed.* **2015**, *54*, 6008.

[55] Choukroun, R.; Lorber, C.; Vendier, L.; Lepetit, C. "Vanadocene-Mediated Ionization of Water in the Aqua Species $[H_2O{\cdot}B(C_6F_5)_3]$: Structural Characterization of the Hydride and Hydroxide Complexes $[Cp_2V(\mu\text{-}H)B(C_6F_5)_3]$ and $[Cp_2V(\mu\text{-}OH)B(C_6F_5)_3]$" *Organometallics* **2006**, *25*, 1551.

[56] Gómez-Suárez, A.; Ramón, R. S.; Songis, O.; Slawin, A. M. Z.; Cazin, C. S. J.; Nolan, S. P. *Organometallics* **2011**, *30*, 5463.

[57] Jin, L.; Romero, E. A.; Melaimi, M.; Bertrand, G. "The Janus Face of the X Ligand in the Copper-Catalyzed Azide–Alkyne Cycloaddition" *J. Am. Chem. Soc.* **2015**, *137*, 15696.

[58] Romero, E. A.; Olsen, P. M.; Jazzar, R.; Soleilhavoup, M.; Gembicky, M.; Bertrand, G. "Spectroscopic Evidence for a Monomeric Copper(I) Hydride and Crystallographic Characterization of a Monomeric Silver(I) Hydride" *Angew. Chem. Int. Ed.* **2017**, *56*, 4024.

Chapter 3 : Dehydrocoupling of Primary and Secondary Amines, Alcohols, and Thiols with Pinacolborane and 9-BBN

3.1 Introduction

In Chapter 1, we discussed the ability of CAAC copper complexes to affect the dehydrogenative coupling reaction between terminal acetylenes and pinacolborane.[1] Processes that extrude dihydrogen as the sole byproduct are highly desirable due to their high atom economy. For this reason, we sought to develop cheap and sustainable dehydrogenative methodologies for other reactions that generate bonds to boron. A thorough survey of the literature revealed a handful of reports detailing the catalytic dehydrogenative coupling of alcohols, amines, and thiols with hydridoboranes. The first such report came from the laboratory of Nolan *et al.*[2] in 2013 using the ruthenium complex **3.1A** to couple thiols with both pinacol- and catecholboranes (Figure 3.1).

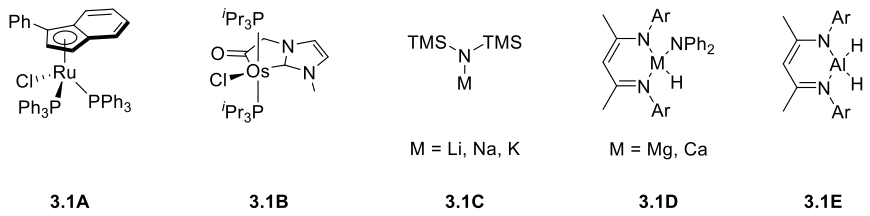

Figure 3.1. Catalysts reported for the dehydrocoupling of alcohols, amines, and thiols with pinacolborane, catecholborane, and/or 9-BBN.

Following this initial report, osmium (**3.1B**),[3] alkali metal (**3.1C**),[4] alkali earth metal (**3.1D**),[5] and aluminum (**3.1E**)[6] based catalysts were found to dehydrogenatively couple hydridoboranes with alcohols and amines. With respect to the osmium catalyzed alcoholysis of pinacolborane, the authors proposed that B-H bond activation occurs via cooperation between the transition-metal and the ligand to form an intermediate Os-H bond. Following this step, nucleophilic addition of the substrate alcohol facilitates elimination of the product alkoxy-borane and generates a transient $L_nOs(H_2)$ complex. Reductive dehydrogenation then reforms the starting osmium complex to close the cycle. Complexes **3.1C-E** are proposed to proceed through metal alkoxide, amide, or sulfide intermediates followed by a σ-bond metathesis into the hydridoborane

to generate the corresponding M-H bond. Interestingly, however, none of these reports investigate the background reaction between the starting E-H (E = NR and O) and B-H bond containing substrates. It is well-known that B-H bond containing compounds exhibit significant moisture sensitivity and must be stored under an inert atmosphere to prevent hydrolysis. For this reason, we set out to determine whether these dehydrogenative coupling reactions of boranes with amines, alcohols, and thiols could occur spontaneously without the need for a catalyst.

We hypothesized that the first step in an uncatalyzed process would be the formation of the Lewis acid-base adduct **3.1F** (Scheme 3.1). At this point, the reaction could proceed through either an intra- or intermolecular dehydrogenation pathway. In the former route, the B-H bond could be sufficiently hydridic to deprotonate the adjacent E-H bond to afford products **3.2**, while extruding H_2 in the process (Scheme 3.1, top).

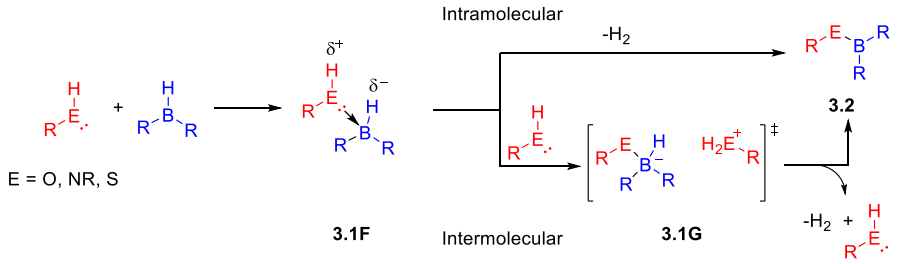

Scheme 3.1. The proposed mechanistic pathway proceeds via formation of Lewis acid-base adduct **3.1F** prior to intra- (top) or intermolecular (bottom) dehydrogenation affording products **3.2**.

The second possibility is intermolecular deprotonation of the E-H bond in **3.1F** by a second equivalent of RE-H to generate the transient charge separated salt **3.1G** (Scheme 3.1, bottom). In this species, the borohydride would be sufficiently hydridic to rapidly deprotonate the countercation R-EH_2^+ to extrude dihydrogen and form the dehydrocoupled products **3.2**.

Since their discovery in 1955 by Shore *et al.*,[7] aminoboranes have garnered notoriety primarily as molecular hydrogen storage compounds;[8] however, their uses in synthetic organic chemistry prior to 2016 is described in a handful of reports.

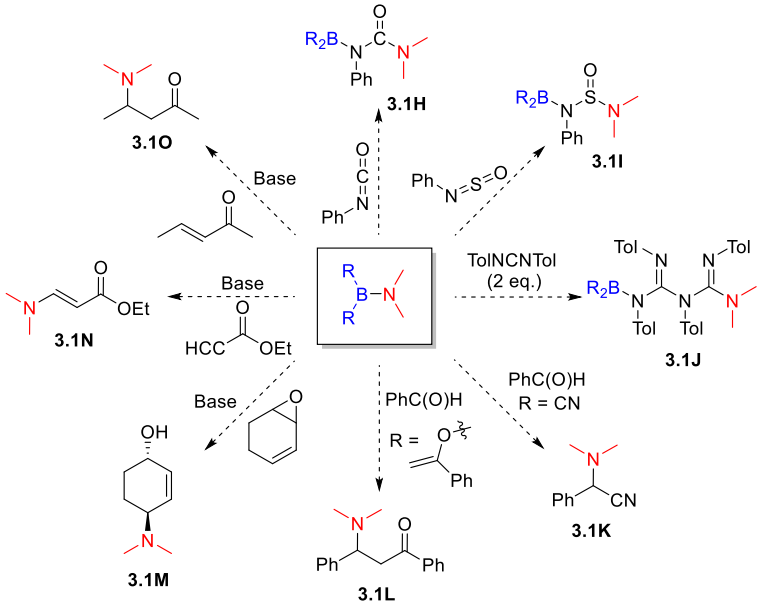

Scheme 3.2. Known reactions of aminoborane reagents with various organic substrates prior to **2016**.

In 1964, Tilley and coworkers[9] studied the reactivity of secondary aminoborane reagents with isocyanates and isothiocyanates to yield products **3.1H** and **3.1I**, respectively (Scheme 3.2). The same group then extended this methodology to carbodiimides allowing the formation of borylated guanidines **3.1J**.[10] In both accounts, the aminoborane was postulated to behave first as a nucleophile, despite boron being known primarily as a Lewis acid. In 2006, Suginome *et al.* utilized the traditional Lewis acidity of boron to perform both Strecker- and Mannich-type reactions of carbonyl compounds with aminoboranes (**3.1K** and **3.1L**, respectively).[11] More recently, Fernández *et al.*[12] demonstrated that secondary aminoboranes can be used in conjunction with Lewis basic alkoxides to affect the ring opening of alkenyl epoxides (**3.1M**), as well as conjugate addition reactions to ynones (**3.1N**) and Michael acceptors (**3.1O**). This reactivity was

attributed to the coordination of the base to the Lewis acidic boron center, which labilizes the B–N bond allowing nucleophilic addition of the amide fragment at the β-position.

The limited potential of E-B bond containing products as substrates in synthetically useful reactions is restricted by the difficulty in preparing products of this type efficiently and cheaply. For this reason, we set out to develop a simple and sustainable methodology for the preparation of E-B bond containing products in the hopes that we could subsequently develop useful applications.

3.2 Results and Discussion

3.2.1 Development of a Catalyst-Free Methodology for the Dehydrogenative Coupling of Amines, Alcohols, and Thiols with Pinacolborane and 9-BBN

We began our investigation into the catalyst-free dehydrocoupling reaction by examining the uncatalyzed reaction between amines and pinacolborane (Table 3.1). After 4 hours in benzene, ^{1}H NMR spectroscopy showed the selective formation of the aminoborane adduct **3.2AA** in 60% conversion (entry 1). **N.B.**: conversion was determined by comparison of the integrals of the product aminoborane to the starting aniline. Changing the solvent to THF or chloroform dramatically reduced the amount of product observed (entries 2-3) while acetonitrile gave the best conversion at 75% after 4 hours at room temperature (entry 4). We further found that increasing the concentration of the reactants increases the rate of the reaction (entries 5-7), with the fastest reaction occurring in the absence of solvent (entry 8). In this case, addition of pinacolborane to aniline resulted in the vigorous extrusion of H_2 gas, and after 25 minutes at room temperature, the reaction media solidified. Dissolution of the resulting solid in acetonitrile showed nearly quantitative formation of aminoborane **3.2AA** (94% conversion).

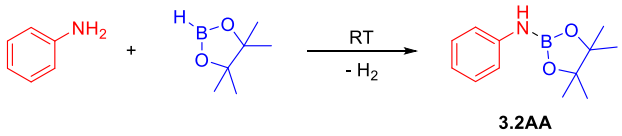

3.2AA

Scheme 3.3. Reaction diagram for the optimization of the dehydrocoupling reaction between amines and pinacolborane.

Table 3.1. Optimization of the dehydrocoupling reaction of aniline with pinacolborane. These reactions were carried out in a J-Young NMR tube at room temperature under an argon atmosphere using a 1:1 mixture of aniline (0.40 mmol) and pinacolborane (0.40 mmol).

Entry	Time (hr)	Solvent	Conc. (M)	Conv. (%)
1	4	C_6D_6	0.8	60
2	4	$CDCl_3$	0.8	22
3	4	THF-d_8	0.8	30
4	4	CD_3CN	0.8	75
5	0.5	CD_3CN	0.8	29
6	0.5	CD_3CN	1.2	49
7	0.5	CD_3CN	2.8	85
8	0.5	CD_3CN	-	94

The scope of the amine dehydrocoupling reaction with pinacolborane was studied in the absence of solvent, except when amines are solid at room temperature; in these cases, 0.151 mL of acetonitrile was used with 0.8 mmol of both reactants (Figure 3.2).

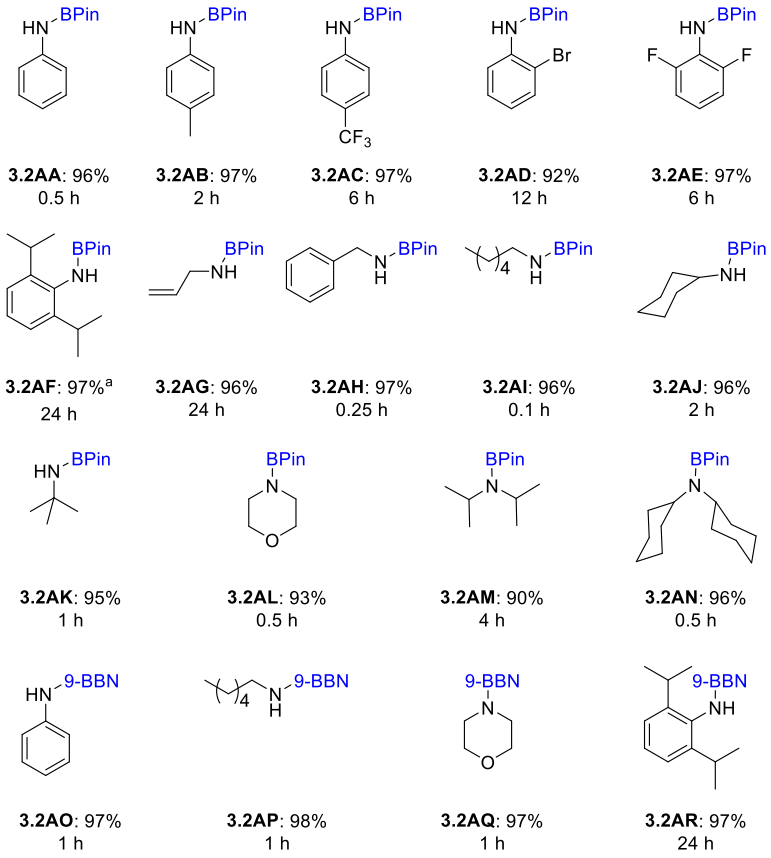

Figure 3.2. Substrate scope for the dehydrocoupling of pinacolborane and 9-BBN with amines at room temperature. Isolated yields and reaction times are reported for each product. [a]120 °C and 1 mol% NEt_3.

This reaction was applicable to both aliphatic and aromatic amines with various steric and electronic contributions. Due to the exceptional selectivity of this process, products **3.2AA-N** can be isolated in excellent yields and purity by simply removing all volatiles under vacuum. Interestingly, due to steric hinderance associated with 2,6-diisopropylaniline, formation of product **3.2AF** required the addition of a catalytic amount of NEt_3 and heating to 120 °C for complete conversion. Switching the borane partner to 9-BBN allowed the reaction to proceed under the standard reaction conditions for all substrates to obtain products **3.2AO-R**. Surprisingly, when 9-BBN is used as the boron partner, dilution of the reaction media to 0.8 mol/L does not affect the rate of the reaction, which was the case with pinacolborane (Table 3.1, entry 5).

To extend the scope of the catalyst-free dehydrocoupling reaction, we then used a broad range of alcohols and phenols as substrates. Using the standard experimental conditions developed for amines, we observed quantitative formation of the desired coupling products **3.2BA-S** within minutes at room temperature (Figure 3.3. Figure 3.3). Note that here too, catalytic triethylamine and heating was required when the bulky 2,6-ditertbutyl-4-methylphenol was used as the substrate (**3.2BL**). It is worth noting that there were no differences in reactivity between pinacolborane and 9-BBN as the boron partner (**3.2BT-W**).

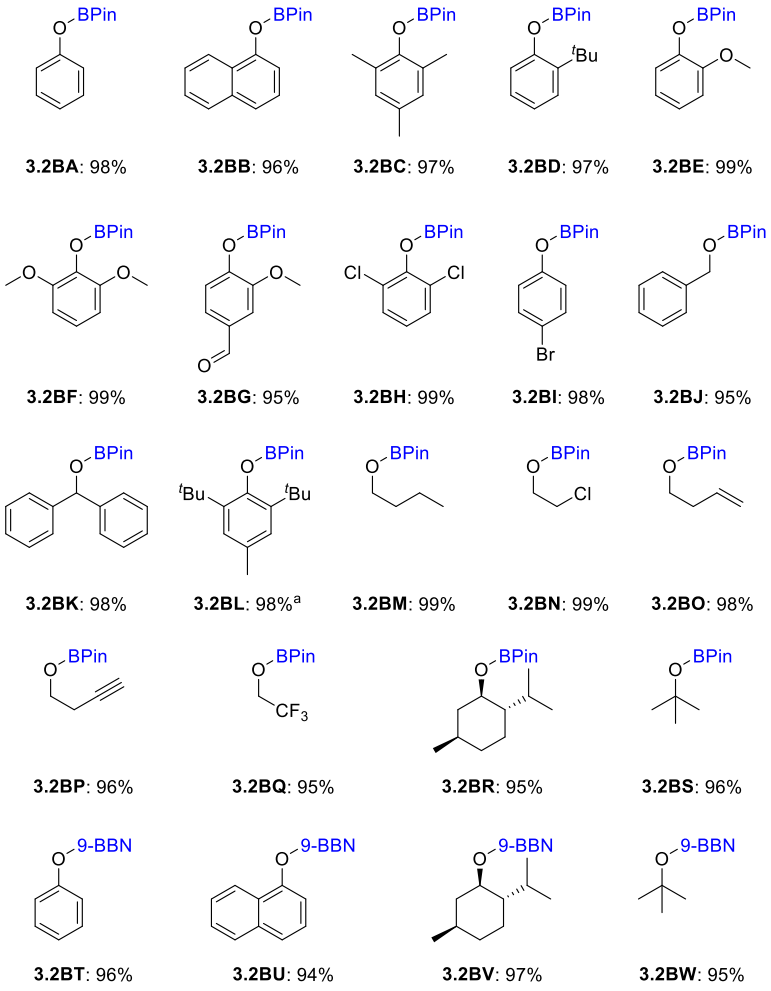

Figure 3.3. Substrate scope for the dehydrocoupling of pinacolborane and 9-BBN with alcohols and phenols at room temperature with isolated yields. [a]24 h at 120 °C with 1 mol% NEt_3.

In line with Nolan *et al.*[2] and Roesky *et al.*,[6] we found no reaction between thiols and pinacolborane under our standard reaction conditions. We hypothesized that the experimental conditions that allowed the formation of bulky products **3.2AF** and **3.2BL** would also facilitate the dehydrogenative coupling of thiols with pinacolborane. Excitingly, addition of catalytic triethylamine promoted the dehydrogenation reaction at 120 °C, albeit the reaction time exceeded 48 hours for complete conversion (Figure 3.4, **3.2CA** and **3.2CB**). As was the case with amines and alcohols, using 9-BBN as the boron partner eliminates the need for triethylamine as an additive (**3.2CC**-**D**); however, formation of **3.2CD** still required elevated temperatures to extrude H_2 from the starting materials.

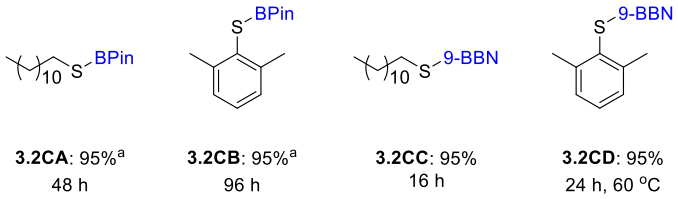

Figure 3.4. Substrate scope for the dehydrocoupling of pinacolborane and 9-BBN with thiols. Isolated yields and reaction times are reported for each product. [a]120 °C and 1 mol% NEt_3.

3.3 Mechanistic Investigation

Having in hand a viable catalyst-free methodology to couple amines, alcohols, and thiols with hydridoboranes, we set out to understand the elementary reaction steps through which this transformation proceeds as well as the role of triethylamine. We began by examining the ^{1}H and ^{11}B NMR spectrum of an equimolar mixture of Dipp-NH_2 with pinacolborane in the absence of NEt_3 in the hopes of observing resonances associated with the proposed reaction intermediates **3.1F** or **3.1G**; however, regardless of reaction duration and temperature, the only observable signals are those corresponding to the starting materials. Similarly, even amines and anilines that require multiple hours to completely form the aminoboranes do not exhibit any signals

corresponding to these proposed intermediates. Fortuitously, during the elucidation of the amine substrate scope in Figure 3.2, we found that addition of pinacolborane to allylamine immediately produced a white solid. Dissolution of this solid in acetonitrile and analysis by ^{1}H NMR, however, showed only signals corresponding to the starting allylamine and pinacolborane, which is in line with a labile B···N interaction. Based on the physical state of both reagents as liquids, we set out to prove that this white solid is the Lewis acid-base adduct **3.1FG**. Single crystals suitable for an X-ray diffraction study were grown from a supersaturated boiling acetonitrile solution (Figure 3.5), which unambiguously confirmed our hypothesis.

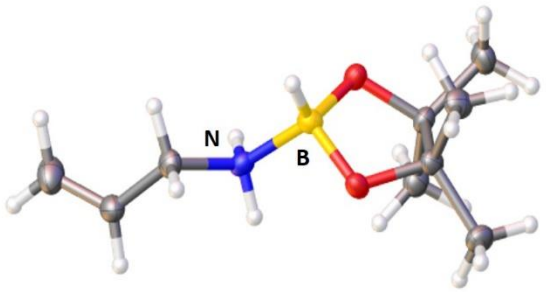

Figure 3.5. Solid-state structure of **3.1FG** at 50% probability thermal ellipsoids. Selected bond length: N–B = 1.61(7) Å.

From the solid-state structure, a boron-nitrogen bond was unambiguously established based on the tetrahedral geometries of both atoms and an N-B distance of 1.62 Å, which is within range of other R_3N-BR_3 compounds.[13] Analysis of the intermolecular interactions reveals the cause of the insolubility of **3.1FG** (Figure 3.6). Due to the strong polarity of the N-H bond in **3.1FG**, the acidic hydrogen atoms interact with the endocyclic dioxaborolane oxygen atoms with bond distances of 1.991 Å and 2.037 Å. Since we observe no ^{1}H or ^{11}B NMR resonances for this compound, we conclude that dissolution of the crystals likely severs these intermolecular contacts.

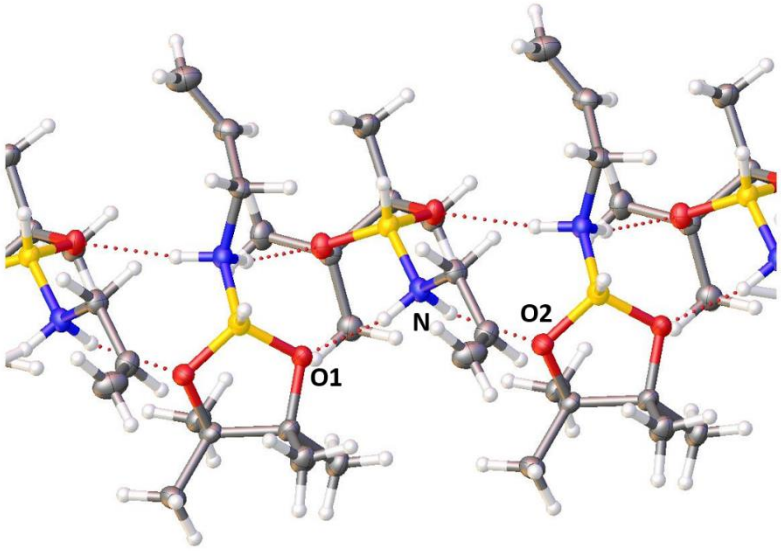

Figure 3.6. Intermolecular hydrogen bonding in the solid-state structure of **3.1FG** at 50% probability thermal ellipsoids. Selected bond lengths [Å]: N–O1 = 1.991 and N–O2 = 2.037.

Monitoring this acetonitrile mixture by ^{1}H NMR over the course of 24 hours at room temperature does not show the presence of any intermediates. Within 12 hours, we can assign resonances corresponding to product **3.2AG**, and after 24 hours, we observe complete conversion (Figure 3.7).

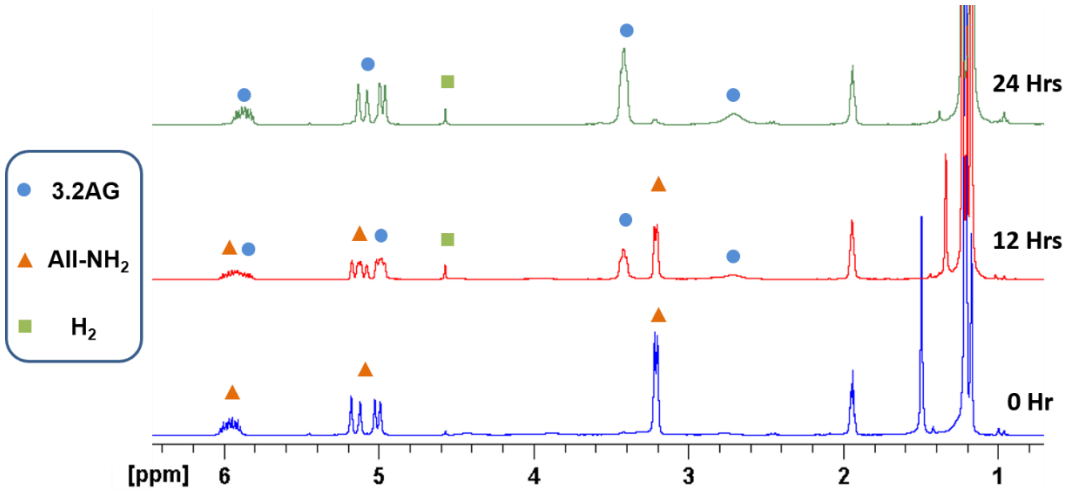

Figure 3.7. ^{1}H NMR spectra of allylamine and pinacolborane in acetonitrile at RT.

To support the intermediacy of a Lewis acid-base adduct in this process, we investigated whether proton acidity alone could promote a dehydrocoupling reaction. The test this hypothesis,

we reacted fluorene with pinacolborane at 120 °C. It is worth noting that the pKa of the benzylic C-H protons in DMSO were determined by Bordwell to be 22.6,[14] a value that is comparable to most anilines. Even in the presence of triethylamine, which allowed the formation of dehydrocoupling products with the most challenging substrates, we observed no reaction (Scheme 3.4).

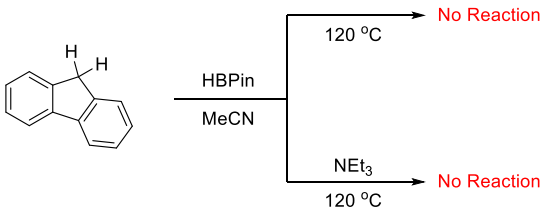

Scheme 3.4. Reaction of fluorene with pinacolborane at 120 °C in the absence of NEt_3 (top), and in the presence of NEt_3 (bottom).

In an effort to force the dehydrogenative coupling reaction to occur, we subjected pinacolborane to ethereal HCl at room temperature (Scheme 3.5); however, there remained no evidence of the expected coupling reaction, neither visually nor spectroscopically.

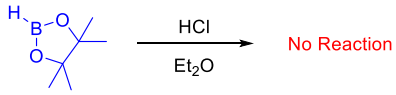

Scheme 3.5. Reaction of ethereal HCl with pinacolborane at room temperature.

The results presented in Scheme 3.4 and Scheme 3.5, coupled with the crystallographically characterized **3.1FG**, clearly highlight the intermediacy of the Lewis acid-base adduct in this reaction; however, the question of whether the dehydrogenation step is an intra- or intermolecular process still remains.

To answer this question, we will analyze the conditions for each of the three dehydrocoupling reactions reported starting with amines. Examining first the reaction of 2,6-diisopropylaniline with pinacolborane, we find that there is no reaction in the absence of

triethylamine. In the case of an intramolecular reaction, dehydrogenation would not be affected by steric hinderance; however, since we need a smaller Lewis basic additive, we can expect that NEt_3 is assisting the reaction by deprotonating the intermediate Lewis acid-base adduct of these substrates with pinacolborane. Additionally, in all the reactions involving amines and pinacolborane, we observe a strong concentration dependence, wherein high reactant concentrations dramatically increase the rate of the reaction – an effect that is consistent with intermolecular mechanistic pathways. Based on this analysis, we concluded that the dehydrocoupling reaction between amines with pinacolborane is an intermolecular process.

Turning our attention to alcohols, we find that similar limitations exist when the bulky 2,6-ditertbutyl-4-methylphenol is used as a substrate. For this reason, we can also conclude that bulky alcohols follow the same intermolecular dehydrogenative mechanism as amines. For non-sterically encumbered alcohols, we did not observe any concentration dependence, and all of the reactions occurred with very high rates. There are two possible explanations for these observations, both of which are centered around the heightened acidity of the O-H bond as compared to the N-H bond, especially within the confines of our proposed Lewis acid-base adduct. The first option is that this increased acidity allows for a more rapid intermolecular deprotonation step, while the second option is that the O-H is now acidic enough to be deprotonated intramolecularly by the B-H bond. Although both possibilities have merit, the extremely high rate of reaction limits our capability to probe the exact pathway by which this transformation occurs with small alcoholic substrates.

Finally, we turned our attention to the reaction of thiols with pinacolborane. More specifically, we find that the reaction of S-H bonds with pinacolborane do not proceed in the absence of triethylamine regardless of the substituent bound to sulfur. Furthermore, there are no reports of isolable Lewis acid-base adducts featuring an S-B bond, which indicates the weakness

of such an interaction. This likely arises from a significant difference in the HOMO and LUMO energies for the sulfur 3p and boron 2p orbitals, respectively. This weak interaction makes the S-H bond polarization within the transient Lewis adduct significantly weaker than its O-H and even N-H counterparts. From this simple bonding analysis, we can conclude that for all S-H bonds, the dehydrocoupling reaction with pinacolborane must be an intermolecular process.

Finally, we find that all reactions involving 9-BBN occur in the absence of NEt_3. This can be attributed to the heightened Lewis acidity of dialkylboranes as compared to dioxaborolanes. The resulting Lewis acid-base adducts involving 9-BBN likely feature extremely strong polarization of the E-H bond such that the hydricity of the B-H bond is sufficient to effect intramolecular dehydrogenation in all cases.

3.4 Application of Aminoborane Products to the Preparation of 2-chloro-4,4,5,5-tetramethyl-1,3,2-dioxaborolane

As noted in the introduction, synthetic organic applications for discretely prepared aminoborane reagents have remained underdeveloped due to the previous difficulty in their preparation. Using our facile preparative methodology, we set out to exhibit their usefulness by synthesizing the chlorinated derivative of pinacolborane, 2-chloro-4,4,5,5-tetramethyl-1,3,2-dioxaborolane (**3.4A**). Current methods used to prepare chloroborane **3.4A** are low yielding (< 40%) and produce a significant amount of diborane **3.4B** during the reaction (Scheme 3.6).[15]

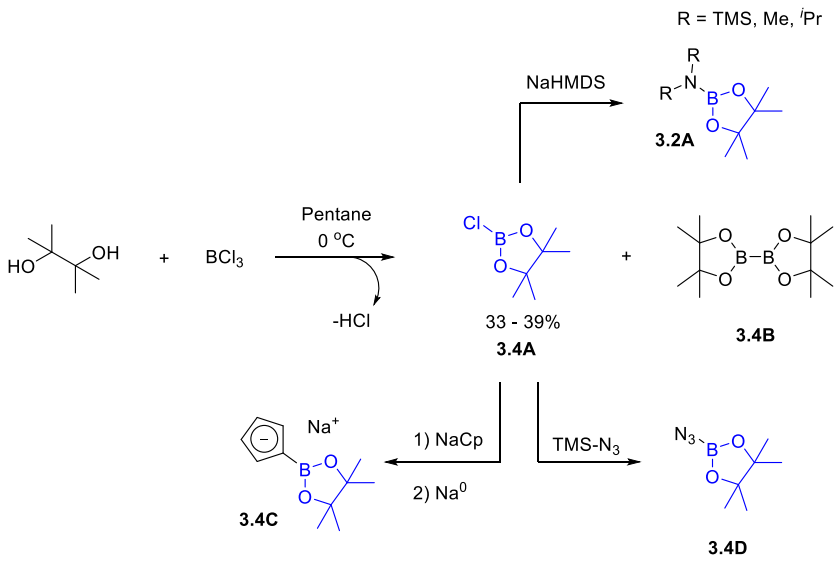

Scheme 3.6. Literature preparation of chloroborane derivative **3.4A** along with the major side product **3.4B**. Reaction of **3.4A** with various substrates to form borylated products (top and bottom arrows).

Compound **3.4A** has been used in several salt metathesis reactions to generate the corresponding aminoboranes **3.2A**[15b,16] and sodium borylcyclopentadienide **3.4C**.[16] Generally, salt metathesis reactions involving boron are rare due to its considerable Lewis acidity, and therefore, its reluctance to eliminate halides. In this case, the π-donation of the endocyclic oxygen atoms provide enough electron density to mitigate this effect. This donation by oxygen also allowed Bettinger *et al.* to react **3.4A** with trimethylsilylazide to form borylazide **3.4D**, which was then used stoichiometrically in alkane C-H amination reactions.[15a] These two reports constitute all the reactivity known with chloroborane **3.4A**, however, the fundamental reactions involved in these transformations should be applicable to the preparation of other more complex organic molecules and catalytic reactions pending further investigation.

To aid in this goal, we set out to develop a sustainable preparative strategy for compound **3.4A** by starting from aminoborane **3.2AA**. We hypothesized that protonation of aminoborane **3.2AA** by HCl would generate the chlorinated Lewis acid-base adduct **3.1F**$_{Cl}$ (Scheme 3.7). Adducts **3.1F** were shown above to rapidly dissociate in solution, a phenomenon that should also

occur with **3.1F$_{Cl}$**. Upon dissociation, the free aniline can be protonated a second time to form aniline-hydrochloride and chloroborane **3.4A**.

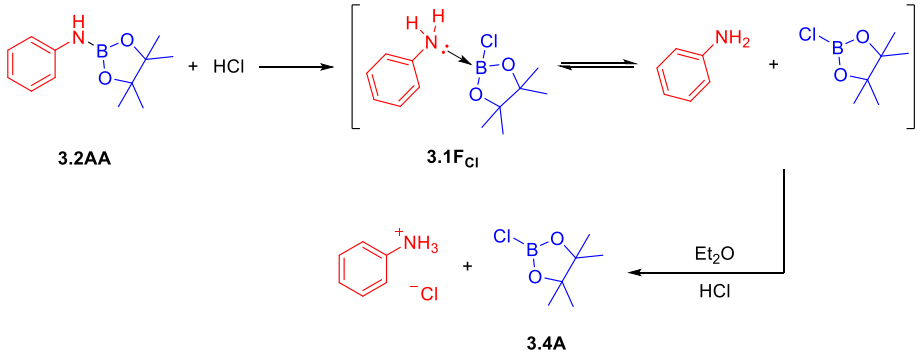

Scheme 3.7. Synthetic strategy for the formation of chlorinated pinacolborane derivative **3.4A** by HCl addition to aminoborane **3.2AA**.

We tested this hypothesis by reacting 1 equivalent of aminoborane **3.2AA** with 2 equivalents of anhydrous HCl in diethyl ether at room temperature for 1 hour. During this time, a white precipitate forms and ^{11}B NMR analysis of the supernatant confirms the quantitative formation of product **3.4A**.[15a] Isolation of the chloroborane was achieved by simple filtration of the solid precipitate via cannula and concentration of the resulting solution *in vacuo*. To recover the starting aniline for reuse, the solid residue was dissolved in aqueous 1M NaOH and extracted using Et_2O. Evaporation of the volatiles under rotary evaporation and distillation of the resulting oil afforded analytically pure aniline in near high yield.

3.5 Conclusion

In this chapter, we discussed the ability of amines, alcohols, and thiols to undergo dehydrogenative coupling reactions with pinacolborane and 9-BBN without the need for a catalyst. We then investigated the mechanism behind this reaction and found that the reaction must first proceed through an intermediate Lewis acid-base adduct of type **3.1F**. We then supported our

hypothesis that sterically encumbered alcohols along with amines and thiols proceed through an intermolecular dehydrogenative pathway with pinacolborane. With all substrates, this dehydrocoupling reaction was found to follow an intramolecular pathway when the more Lewis acidic 9-BBN is used as the boron partner. Finally, we have shown that aminoboranes can be used in the production of a halogenated derivative of pinacolborane by simple addition of hydrochloric acid. Encouraged by these findings, future directions will address the greater challenge of site-selective aminoborylation reactions, which would be highly desirable within the context of synthetic diversity and atom economy, thus allowing for rationally designed and highly modular synthetic methodologies.

Chapter 3 has been adapted from materials published in Romero, E. A.; Peltier, J. L.; Jazzar, R.; Bertrand, G., "Catalyst-Free Dehydrocoupling of Amines, Alcohols, and Thiols with Pinacol Borane and 9-Borabicyclononane (9-BBN)", *Chem. Commun.* **2016**, *52*, 165 – 168. The dissertation author was the primary investigator of this paper.

3.6 Appendix

3.6.1 General Information

All reactions were performed under an atmosphere of argon using standard Schlenk or dry box techniques; solvents were dried over Na metal, or CaH_2. Reagents of analytical grade were obtained from commercial suppliers and used without drying, degassing, or purification of any kind. New glassware and new stir bars were used to mitigate trace metal involvement. ^{1}H, ^{13}C, ^{11}B and ^{19}F NMR spectra were obtained using either a Bruker Avance 300 MHz, a Varian INOVA 500 MHz spectrometer or JOEL 500 MHz. Chemical shifts (δ) are reported in parts per million (ppm) relative to TMS and were referenced to the residual solvent peak. NMR multiplicities are

abbreviated as follows: s = singlet, d = doublet, t = triplet, q = quartet, quin = quintet, sex = sextet, sept = septet, m = multiplet, br = broad signal. NB: We were unable to obtain HRMS data analysis using the facility available at UCSD; Hence all substrates were submitted either low-resolution ESI (Micromass Quattro Ultima Triple Quadrupole MS) or to GCMS analysis (Agilent GCMS: 7820A). Corresponding LRMS are reported as obtained.

3.6.2 Dehydrocoupling Reaction Protocols

Protocol 1: Under an argon atmosphere, CD_3CN (if amine/alcohol/thiol is solid at RT to achieve 3 M solution), and the amine (0.8 mmol) were added to a 1-dram vial equipped with a magnetic stir bar. Then, pinacolborane (0.116 mL, 0.8 mmol) was added to the reaction mixture and the reaction was left stirring at room temperature until the reaction was complete. Evaporation of the volatiles under vacuum afforded the corresponding product.

Protocol 2: Under an argon atmosphere, C_6D_6 (0.5 mL) and 9-BBN (97.6 mg, 0.4 mmol) were added to a 1-dram vial equipped with a magnetic stir bar. Then, the amine or alcohol (0.8 mmol) was added to the reaction mixture, and the reaction was left stirring at room temperature until the reaction was complete. Evaporation of the volatiles under vacuum afforded the corresponding product.

Protocol 3: Under an argon atmosphere, CD_3CN (to achieve 3 M solution), the aniline or phenol (0.8 mmol), pinacolborane (0.8 mmol), and 1 mol % Et_3N were added to a J-Young NMR tube. The reaction was sealed and heated to 120 ^oC until the reaction was complete. Evaporation of the volatiles under vacuum afforded the corresponding product.

3.6.3 Characterization of Products 3.2AA-R

3.2AA: Protocol 1. White solid (96% yield). ^1H NMR ($CDCl_3$, 300 MHz) δ = 1.34 (s, 12H), 4.67 (s, br, 1H), 6.88 (t, J = 7.2 Hz, 1H), 7.11 (d, J = 7.2 Hz, 2H), 7.22 (d, J = 7.4 Hz, 2H) ppm.

^{13}C NMR ($CDCl_3$, 75 MHz) δ = 24.7, 82.9, 117.7, 120.2, 129.1, 143.4 ppm. ^{11}B NMR ($CDCl_3$, 96 MHz) δ = 23.9 ppm. GCMS (m/z : Calc : 219.1; Exp : 219.2).

3.2AB: Protocol 1. White solid (97% yield). ^{1}H NMR ($CDCl_3$, 300 MHz) δ = 1.36 (s, 12H), 2.34 (s, 3H), 4.67 (s, br, 1H), 7.05 (s, 4H) ppm. ^{13}C NMR ($CDCl_3$, 75 MHz) δ = 20.5, 24.6, 82.7, 117.6, 129.1, 129.5, 140.8 ppm. ^{11}B NMR ($CDCl_3$, 96 MHz) δ = 23.8 ppm. GCMS (m/z : Calc : 233.2; Exp : 233.2).

3.2AC: Protocol 1. Colorless oil (97% yield). ^{1}H NMR ($CDCl_3$, 300 MHz) δ = 1.32 (s, 12H), 4.85 (s, br, 1H), 7.15 (d, J = 8.8 Hz, 2H), 7.44 (d, J = 8.7 Hz, 2H) ppm. ^{13}C NMR ($CDCl_3$, 75 MHz) δ = 24.7, 83.4, 114.3, 117.4, 122.3, 126.4, 146.8 ppm. ^{11}B NMR ($CDCl_3$, 96 MHz) δ = 24.0 ppm. ^{19}F NMR ($CDCl_3$, 283 MHz) δ = -61.5 ppm. GCMS (m/z : Calc : 287.1; Exp : 287.1).

3.2AD: Protocol 1. White solid (92% yield). ^{1}H NMR ($CDCl_3$, 500 MHz) δ = 1.37 (s, 12H), 5.37 (s, br, 1H), 6.75 (m, 1H), 7.23 (m, 1H), 7.48 (dt, br, J = 1.4 Hz, 7.9 Hz, 1H), 7.71 (dt, br, J = 1.5 Hz, 8.2 Hz, 1H) ppm. ^{13}C NMR ($CDCl_3$, 125 MHz) δ = 24.8, 83.2, 112.5, 118.7, 121.1, 128.4, 132.3, 141.4 ppm. ^{11}B NMR ($CDCl_3$, 160 MHz) δ = 23.2 ppm. ESI-MS (M+K) (m/z : Calc : 336.0; Exp : 336.2).

3.2AE: Protocol 1. Colorless oil (97% yield). ^{1}H NMR ($CDCl_3$, 300 MHz) δ = 1.26 (s, 12H), 4.35 (s, 1H), 6.80-6.82 (m, 3H) ppm. ^{13}C NMR ($CDCl_3$, 75 MHz) δ = 24.4, 83.2, 111.3 (m), 120.0 (t, J_{C-F} = 15.9 Hz), 121.9 (t, J_{C-F} = 9.52 Hz), 156.0 (dd, J_{C-F} = 5.6 Hz, 246.4 Hz) ppm. ^{11}B NMR ($CDCl_3$, 96 MHz) δ = 23.9 ppm. ^{19}F NMR ($CDCl_3$, 283 MHz) δ = -122.9 ppm. GCMS (m/z : Calc : 255.1; Exp : 255.2).

3.2AF: Protocol 3. White solid (97% yield). ^{1}H NMR ($CDCl_3$, 300 MHz) δ = 1.23 (d, J = 6.8 Hz, 12H), 1.27 (s, 12H), 3.39 (m, 2H), 3.78 (s, br, 1H), 7.14 (m, 3H) ppm. ^{13}C NMR ($CDCl_3$,

75 MHz) δ = 23.7, 24.8, 28.4, 82.7, 123.1, 125.7, 135.5, 145.3 ppm. ^{11}B NMR ($CDCl_3$, 96 MHz) δ = 24.2 ppm. ESIMS (m/z : Calc : 304.3; Exp : 304.3).

3.2AG: Protocol 1. Deliquescent solid (96% yield). ^{1}H NMR (CD_3CN, 300 MHz) δ = 1.17 (s,12H), 2.71 (s, br, 1H), 3.42 (m, br, 2H), 4.98 (dd, J = 1.7 Hz, 10.4 Hz, 1H), 5.10 (dd, J = 1.9 Hz, 17.2 Hz, 1H), 5.87 (m, 1H) ppm. ^{13}C NMR (CD_3CN, 75 MHz) δ = 24.9, 44.1, 82.7, 113.2, 140.5 ppm. ^{11}B NMR (CD_3CN, 96 MHz) δ = 24.6 ppm. ESI-MS (m/z : Calc : 184.1; Exp : 184.1).

3.2AH: Protocol 1. Deliquescent solid (97% yield). ^{1}H NMR ($CDCl_3$, 300 MHz) δ = 1.22 (s, 12H), 2.52 (s, br, 1H), 4.08 (d, J = 7.9 Hz, 2H), 7.25 (m, 5H) ppm. ^{13}C NMR ($CDCl_3$, 75 MHz) δ = 24.6, 45.2, 82.2, 116.5, 126.7, 128.3, 142.3 ppm. ^{11}B NMR ($CDCl_3$, 96 MHz) δ = 24.5 ppm. GCMS (m/z : Calc : 233.2; Exp : 233.2).

3.2AI: Protocol 1. Deliquescent solid (96% yield). ^{1}H NMR ($CDCl_3$, 300 MHz) δ = 0.85 (t, J = 7.3 Hz, 3H), 1.19 (s, 12H), 1.22-1.41 (m, 8H) 2.13 (s, br, 1H), 2.84 (q, J = 6.6 Hz, 2H) ppm. ^{13}C NMR ($CDCl_3$, 75 MHz) δ = 14.1, 22.7, 24.6, 26.3, 31.7, 33.6, 41.1, 81.9 ppm. ^{11}B NMR ($CDCl_3$, 96 MHz) δ = 24.3 ppm. GCMS (m/z : Calc : 227.2; Exp : 227.2).

3.2AJ: Protocol 1. White Solid (96% yield). ^{1}H NMR ($CDCl_3$, 300 MHz) δ = 0.85-1.05 (m, 4H), 1.12 (s, 12H), 1.30-1.64 (m, 4H), 1.74 (dd (br), J = 3.0 Hz, 12.6 Hz, 2H), 2.09 (s, br, 1H), 2.81 (m, 1H) ppm. ^{13}C NMR ($CDCl_3$, 75 MHz) δ = 24.6, 25.3, 25.8, 37.2, 49.5, 81.8 ppm. ^{11}B NMR ($CDCl_3$, 96 MHz) δ = 24.6 ppm. GCMS (m/z : Calc : 225.2; Exp : 225.2).

3.2AK: Protocol 1. Deliquescent solid (95% yield). ^{1}H NMR ($CDCl_3$, 300 MHz) δ = 1.15 (s, 9H), 1.17 (s, 12H), 2.37 (s, br, 1H) ppm. ^{13}C NMR ($CDCl_3$, 75 MHz) δ = 24.6, 32.2, 47.8, 81.4 ppm. ^{11}B NMR ($CDCl_3$, 96 MHz) δ = 23.7 ppm. ESI-MS (m/z : Calc : 200.2; Exp : 200.2).

3.2AL: Protocol 1. White solid (93% yield). ^{1}H NMR ($CDCl_3$, 300 MHz) δ = 1.20 (s, 12H), 3.06 (t, J = 4.3 Hz, 4H), 3.55 (t, J = 4.6 Hz, 4H) ppm. ^{13}C NMR ($CDCl_3$, 75 MHz) δ = 24.7, 44.6, 68.5, 82.3 ppm. ^{11}B NMR ($CDCl_3$, 96 MHz) δ = 23.4 ppm. GC/ESI-MS could not be obtained.

3.2AM: Protocol 1. White solid (90% yield). ^{1}H NMR ($CDCl_3$, 500 MHz) δ =1.09 (d, 12H), 1.18 (s, 12H), 3.34 (m, 2H) ppm. ^{13}C NMR ($CDCl_3$, 125 MHz) δ = 23.3, 24.6, 44.6, 81.0 ppm. ^{11}B NMR ($CDCl_3$, 160 MHz) δ = 24.2 ppm. GCMS (m/z : Calc : 227.2; Exp : 227.1).

3.2AN: Protocol 1. White solid (96% yield). ^{1}H NMR ($CDCl_3$, 300 MHz) δ = 1.07 (m, 2H), 1.16 (s, 12H), 1.26 (m, 5H), 1.52 (m, 9H), 1.70 (m, 4H), 2.80 (m, 2H) ppm. ^{13}C NMR ($CDCl_3$, 75 MHz) δ = 24.6, 25.9, 26.7, 33.8, 54.1, 80.9 ppm. ^{11}B NMR ($CDCl_3$, 96 MHz) δ = 23.9 ppm. GCMS (m/z : Calc : 307.3; Exp : 307.4).

3.2AO: Protocol 2. Deliquescent solid (97% yield). ^{1}H NMR ($CDCl_3$, 300 MHz) δ = 1.07 (s, br, 2H), 1.40 (m, 4H), 1.79 (m, 8H), 6.05 (s, br, 1H), 7.00 (d, J = 8.1 Hz, 3H), 7.24 (t, J = 8.1 Hz, 2H) ppm. ^{13}C NMR ($CDCl_3$, 75 MHz) δ = 23.5, 33.0, 33.8, 122.4, 122.9, 129.0, 143.7 ppm. ^{11}B NMR ($CDCl_3$, 96 MHz) δ = 51.2 ppm. GC/ESI-MS could not be obtained.

3.2AP: Protocol 2. Deliquescent solid (98% yield). ^{1}H NMR ($CDCl_3$, 300 MHz) δ = 0.91 (s, br, 3H), 1.31 (s, 8H), 1.61-1.90 (m, 14H), 3.03 (q, J = 6.8 Hz, 2H), 3.92 (s, br, 1H) ppm. ^{13}C NMR ($CDCl_3$, 75 MHz) δ = 14.1, 22.8, 23.8, 26.5, 31.8, 33.1, 33.7, 33.9, 42.6 ppm. ^{11}B NMR ($CDCl_3$, 96 MHz) δ = 48.5 ppm. GC/ESI-MS could not be obtained.

3.2AQ: Protocol 2. White solid (97% yield). ^{1}H NMR ($CDCl_3$, 300 MHz) δ = 1.20-1.99 (m, br, 14H), 3.32 (t, J = 4.4 Hz, 2H), 3.60 (t, J = 4.4 Hz, 2H) ppm. ^{13}C NMR ($CDCl_3$, 75 MHz) δ = 23.5, 33.4, 47.6, 69.5 ppm, C[B] could not be detected. ^{11}B NMR ($CDCl_3$, 96 MHz) δ = 47.3 ppm. GC/ESIMS (m/z : Calc : 208.2; Exp : 208.1).

3.2AR: Protocol 2. Deliquescent solid (97% yield). ^{1}H NMR ($CDCl_3$, 300 MHz) δ = 1.29 (d, J = 6.6 Hz, 12H), 1.50 (m, br, 2H), 1.74 (m, 4H) 1.97 (m, br, 8H), 3.50 (m, 2H), 5.31 (s, br, 1H), 7.24 (m, 3H) ppm. ^{13}C NMR ($CDCl_3$, 75 MHz) δ = 22.6, 23.5, 28.0, 33.0, 33.8, 123.0, 125.9, 137.2, 145.2 ppm. ^{11}B NMR ($CDCl_3$, 96 MHz) δ = 50.5 ppm. GC/ESI-MS could not be obtained.

3.6.4 Characterization of Products 3.2BA-W

3.2BA: Protocol 1. White solid 0.169 g (98% yield). ^{1}H NMR ($CDCl_3$, 300 MHz) δ = 1.35 (s, 12H), 7.05-7.13 (m, 3H), 7.28-7.33 (m, 2H) ppm. ^{13}C NMR ($CDCl_3$, 75 MHz) δ = 25.3, 84.5, 116.4, 122.1, 133.0, 153.3 ppm. ^{11}B NMR ($CDCl_3$, 96 MHz) δ = 21.8 ppm. GCMS (m/z : Calc : 220.13 ; Exp : 220.1).

3.2BB: Protocol 1. White solid 0.211 g (96% yield). ^{1}H NMR ($CDCl_3$, 300 MHz) δ = 1.38 (s, 12 H), 7.31 (d, J = 9 Hz, 1H), 7.40-7.42 (m, 1H), 7.45-7.52 (m, 2H), 7.61 (d, J = 9 Hz, 1H), 7.85 (m, 1H), 8.22-8.23 (m, 1H) ppm. ^{13}C NMR ($CDCl_3$, 75 MHz) δ = 24.8, 83.8, 114.1, 122.2, 123.2, 125.7, 125.9, 126.4, 126.9, 127.8, 134.8, 149.4 ppm. ^{11}B NMR ($CDCl_3$, 96 MHz) δ = 22.2 ppm. GCMS (m/z : Calc : 270.14 ; Exp : 270.2).

3.2BC: Protocol 1. Colorless oil 0.203 g (97% yield). ^{1}H NMR ($CDCl_3$, 300 MHz) δ = 1.40 (s, 12H), 2.31 (s, 6H), 2.34 (s, 3H), 6.92 (s, 2H) ppm. ^{13}C NMR ($CDCl_3$, 75 MHz) δ = 16.4, 20.7, 24.5, 83.4, 127.9, 129.0, 132.4, 148.4 ppm. ^{11}B NMR ($CDCl_3$, 96 MHz) δ = 21.6 ppm. GCMS (m/z : Calc : 262.2 ; Exp : 262.2).

3.2BD: Protocol 1. Colorless oil 0.214 g (97% yield). ^{1}H NMR ($CDCl_3$, 300 MHz) δ = 1.39 (s, 12H), 1.48 (s, 9H), 7.08-7.11 (m, 2H), 7.19-7.22 (m, 1H), 7.38 (d, J = 9 Hz, 1H) ppm. ^{13}C NMR ($CDCl_3$, 75 MHz) δ = 24.7, 29.7, 30.1, 34.7, 83.6, 121.5, 123.3, 126.8, 127.0, 139.8, 152.2 ppm. ^{11}B NMR ($CDCl_3$, 96 MHz) δ = 21.9 ppm. GCMS (m/z : Calc : 276.2 ; Exp : 276.2).

3.2BE: Protocol 1. Colorless oil 10.98 g (99% yield). ^{1}H NMR ($CDCl_3$, 300 MHz) δ = 1.34 (s, 12H), 3.85 (s, 3H), 6.87-6.94 (m, 2H), 7.03-7.11 (m, 2H) ppm. ^{13}C NMR ($CDCl_3$, 75 MHz) δ = 24.5, 55.5, 83.4, 112.1, 120.4, 120.8, 123.8, 143.0, 150.1 ppm. ^{11}B NMR ($CDCl_3$, 96 MHz) δ = 22.0 ppm. GCMS (m/z : Calc : 250.1 ; Exp : 250.1).

3.2BF: Protocol 1. Colorless oil 0.221 g (99% yield). ^{1}H NMR ($CDCl_3$, 300 MHz) δ = 1.31 (s, 12H), 3.84 (s, 6H), 6.59 (d, J = 6 Hz, 2H), 6.96 (t, J = 9 Hz, 1H) ppm. ^{13}C NMR ($CDCl_3$, 75 MHz) δ = 24.6, 56.2, 83.5, 105.3, 122.9, 151.2 ppm. ^{11}B NMR ($CDCl_3$, 96 MHz) δ = 22.1 ppm. GCMS (m/z : Calc : 280.1 ; Exp : 280.1).

3.2BG: Protocol 1. Colorless oil 0.211 g (95% yield). ^{1}H NMR (C_6D_6, 500 MHz) δ = 1.01 (s, 12H), 3.29 (s, 3H), 6.41 (d, J = 9Hz, 1H), 7.29 (d, J= 0 Hz, 1H), 7.47 (s, 1H), 9.49 (s, 1H) ppm. ^{13}C NMR (C_6D_6, 125 MHz) δ = 24.6, 55.6, 83.8, 111.7, 121.0, 127.3, 130.5, 144.0, 155.7, 190.7 ppm. ^{11}B NMR ($CDCl_3$, 96 MHz) δ = 22.0 ppm. GCMS (m/z : Calc : 278.1 ; Exp : 278.1).

3.2BH: Protocol 1. White solid 0.228 g (99% yield). ^{1}H NMR ($CDCl_3$, 300 MHz) δ = 1.33 (s, 12H), 6.99 (t, J = 7.5 Hz, 1H), 7.30 (d, J = 9 Hz, 2H) ppm. ^{13}C NMR ($CDCl_3$, 75 MHz) δ = 24.6, 84.5, 124.6, 17.3, 128.6, 146.8 ppm. ^{11}B NMR ($CDCl_3$, 96 MHz) δ = 21.6 ppm. GCMS (m/z : Calc : 289.0 ; Exp : 289.0).

3.2BI: Protocol 1. White solid 0.234 g (98% yield). ^{1}H NMR ($CDCl_3$, 300 MHz) δ = 1.34 (s, 12H), 7.00 (d, J = 9 Hz, 2H), 7.39 (d, J = 6 Hz, 2H) ppm. ^{13}C NMR ($CDCl_3$, 75 MHz) δ = 24.7, 83.9, 115.8, 121.5, 132.4, 152.7 ppm. ^{11}B NMR ($CDCl_3$, 96 MHz) δ = 21.7 ppm. GCMS (m/z : Calc : 299.0 ; Exp : 299.0).

3.2BJ: Protocol 1. Colorless oil 0.178 g (95% yield). ^{1}H NMR ($CDCl_3$, 300 MHz) δ = 1.31 (s, 12H), 4.99 (s, 2H), 7.40 (m, 5H) ppm. ^{13}C NMR ($CDCl_3$, 75 MHz) δ = 24.7, 66.7, 83.0, 126.8,

127.4, 128.3, 139.3 ppm. ^{11}B NMR ($CDCl_3$, 96 MHz) δ = 22.5 ppm. GCMS (m/z : Calc : 234.1 ; Exp : 234.1).

3.2BK: Protocol 1. White solid 0.243 g (98% yield). ^{1}H NMR ($CDCl_3$, 300 MHz) δ = 1.28 (s, 12H), 6.29 (s, 1H), 7.30-7.49 (m, 10H) ppm. ^{13}C NMR ($CDCl_3$, 75 MHz) δ = 24.6, 83.1, 126.6, 127.4, 128.3, 143.2 ppm. ^{11}B NMR ($CDCl_3$, 96 MHz) δ = 22.5 ppm. GCMS (m/z : Calc : 310.2 ; Exp : 310.2).

3.2BL: Protocol 3. White solid 0.270 g (98% yield). ^{1}H NMR ($CDCl_3$, 300 MHz) δ = 1.29 (s, 12H), 1.42 (s, 18H), 2.29 (s, 3H), 7.04 (s, 2H) ppm. ^{13}C NMR ($CDCl_3$, 75 MHz) δ = 21.6, 25.4, 31.8, 35.3, 83.7, 126.5, 131.7, 140.7, 149.2 ppm. ^{11}B NMR ($CDCl_3$, 96 MHz) δ = 21.4 ppm. GCMS (m/z : Calc : 346.3 ; Exp : 346.3).

3.2BM: Protocol 1. Colorless oil 0.150 g (99% yield). ^{1}H NMR ($CDCl_3$, 300 MHz) δ = 0.87 (t, J = 7.5 Hz, 3H), 1.21 (s, 12H), 1.29-1.34 (m, 2H), 1.37-1.53 (m, 2H), 3.80 (t, J = 6 Hz, 2H) ppm. ^{13}C NMR ($CDCl_3$, 75 MHz) δ = 13.7, 18.8, 24.6, 33.6, 64.6, 82.6 ppm. ^{11}B NMR ($CDCl_3$, 96 MHz) δ = 22.0 ppm. GCMS (m/z : Calc : 200.2 ; Exp : 200.2).

3.2BN: Protocol 1. Colorless oil 0.163 g (99% yield). ^{1}H NMR ($CDCl_3$, 300 MHz) δ = 1.24 (s, 12H), 3.58 (t, J = 4.5 Hz, 2H), 4.05 (t, J = 4.5 Hz, 2H) ppm. ^{13}C NMR ($CDCl_3$, 75 MHz) δ = 24.6, 44.1, 64.9, 83.2 ppm. ^{11}B NMR ($CDCl_3$, 96 MHz) δ = 22.0 ppm. GCMS (m/z : Calc : 206.1 ; Exp : 206.1).

3.2BO: Protocol 1. Colorless oil 0.155 g (98% yield). ^{1}H NMR ($CDCl_3$, 300 MHz) δ = 1.22 (s, 12H), 2.29-2.31 (m, 2H), 3.86 (m, 2H), 4.99-5.09 (m, 2H), 5.77-5.79 (m, 1H) ppm. ^{13}C NMR ($CDCl_3$, 75 MHz) δ = 24.6, 36.0, 64.1, 82.7, 116.9, 134.7 ppm. ^{11}B NMR ($CDCl_3$, 96 MHz) δ = 22.0 ppm. GCMS (m/z : 182.1 Calc : ; Exp : 182.1).

3.2BP: Protocol 1. Colorless oil 0.150 g (96% yield). ^{1}H NMR ($CDCl_3$, 300 MHz) δ = 1.22, (s, 12H), 1.94 (s, 1H), 2.42 (m, 2H), 3.91 (t, J = 7.5 Hz, 2H) ppm. ^{13}C NMR ($CDCl_3$, 75 MHz) δ = 21.6, 24.6, 63.0, 69.7, 80.6, 83.0 ppm. ^{11}B NMR ($CDCl_3$, 96 MHz) δ = 22.1 ppm. GCMS (m/z : Calc : 196.1 ; Exp : 196.1).

3.2BQ: Protocol 1. Colorless oil 0.173 g (95% yield). ^{1}H NMR ($CDCl_3$, 300 MHz) δ = 1.28 (s, 12H), 4.18 (q, JH-F = 8 Hz, 2H) ppm. ^{13}C NMR ($CDCl_3$, 75 MHz) δ = 24.6, 62.8 (q, J_{C-F} = 35 Hz), 84.0, 123.8 (q, JC-F = 272.5 Hz) ppm. ^{11}B NMR ($CDCl_3$, 96 MHz) δ = 22.4 ppm. ^{19}F ($CDCl_3$, 96 MHz) δ = 76.57 ppm. GCMS (m/z : Calc : 226.1 ; Exp : 226.1).

3.2BR: Protocol 1. White solid 0.216 g (96% yield). ^{1}H NMR ($CDCl_3$, 300 MHz) δ = 0.75-1.08 (m, 12H), 1.22 (s, 12H), 1.43-1.64 (1.88-2.03 (m, 2H), 3.80 (q, J = 5 Hz, 1H) ppm. ^{13}C NMR ($CDCl_3$, 75 MHz) δ = 1.61, 21.1, 22.3, 23.0, 24.5, 24.7, 25.9, 31.5, 34.6, 43.8, 48.9, 74.3, 82.4 ppm. ^{11}B NMR ($CDCl_3$, 96 MHz) δ = 22.0 ppm. GCMS (m/z : Calc : 282.2 ; Exp : 282.2).

3.2BS: Protocol 1. Colorless oil 0.153 g (96% yield). ^{1}H NMR ($CDCl_3$, 300 MHz) δ = 1.17 (s, 12H), 1.28 (s, 9H) ppm. ^{13}C NMR ($CDCl_3$, 75 MHz) δ = 24.5, 29.9, 73.8, 81.9 ppm. ^{11}B NMR ($CDCl_3$, 96 MHz) δ = 21.2 ppm. GCMS (m/z : Calc : 200.1 ; Exp : 200.1).

3.2BT: Protocol 1. Colorless oil 0.152 g (96% yield). ^{1}H NMR ($CDCl_3$, 300 MHz) δ = 1.34 (m, 2H), 1.48-1.52 (m, 2H), 1.94 (m, br, 10H), 7.01 (d, J = 6 Hz, 2H), 7.17 (t, J = 6 Hz, 1H), 7.35 (t, J = 9 Hz, 2H) ppm. ^{13}C NMR ($CDCl_3$, 75 MHz) δ = 23.3, 24.6, 33.6, 120.4, 123.6, 129.5, 155.7 ppm. ^{11}B NMR ($CDCl_3$, 96 MHz) δ = 58.7 ppm. GCMS (m/z : Calc : 198.2 ; Exp : 198.2).

3.2BU: Protocol 1. White solid 0.186 g (94% yield). ^{1}H NMR ($CDCl_3$, 300 MHz) δ = 1.36 (m, br, 2H), 1.54 (m, br, 2H), 1.97 (m, br, 12H), 7.06 (d, br, J = 6 Hz, 1H), 7.48-7.69 (m, 4H), 7.93 (d, br, 1H), 8.13 (d, br, 1H) ppm. ^{13}C NMR ($CDCl_3$, 75 MHz) δ = 23.4, 24.8, 33.8, 115.1, 121.9,

123.6, 125.9, 126.0, 126.5, 127.1, 128.0, 134.9, 151.9 ppm. ^{11}B NMR ($CDCl_3$, 96 MHz) δ = 59.4 ppm. GCMS (m/z : Calc : 248.2 ; Exp : 248.2).

3.2BV: Protocol 1. White solid 0.201 g (97% yield). ^{1}H NMR ($CDCl_3$, 300 MHz) δ = 0.76-1.11 (m, 11H), 1.15-1.43 (m, 7H), 1.69-2.08 (m, 14H), 3.96 (m, 1H) ppm. ^{13}C NMR ($CDCl_3$, 75 MHz) δ = 16.1, 21.0, 22.3, 23.4, 24.5, 25.9, 31.7, 33.3, 33.6, 34.6, 44.9, 48.6, 75.2 ppm. ^{11}B NMR ($CDCl_3$, 96 MHz) δ = 55.9 ppm. GCMS (m/z : Calc : 248.2 ; Exp : 248.2).

3.2BW: Protocol 1. Colorless oil 0.134 g (95% yield). ^{1}H NMR ($CDCl_3$, 300 MHz) δ = 1.32 (m, br, 3H), 1.42 (s, 9H), 1.82-1.88 (m, br, 11H) ppm. ^{13}C NMR ($CDCl_3$, 75 MHz) δ = 23.2, 26.4, 31.2, 33.3, 74.9 ppm. ^{11}B NMR ($CDCl_3$, 96 MHz) δ = 55.6 ppm. GCMS (m/z : Calc : 178.1 ; Exp : 178.1).

3.6.5 Characterization of Products 3.2CA-D

3.2CA: Protocol 3. Colorless oil (95% yield). ^{1}H NMR (C_6D_6, 500 MHz) δ = 0.93 (t, J = 5 Hz, 3H), 1.02 (s, 12H), 1.17-1.39 (m, 19H), 1.41 (quint, J = 5 Hz, 19H), 2.22 (q, 5 Hz, 2 H) ppm. ^{13}C NMR (C_6D_6, 125 MHz) δ = 14.9, 23.7, 25.5, 29.3, 30.1, 30.4, 30.6, 30.7, 35.0, 83.7. ^{11}B NMR ($CDCl_3$, 96 MHz) δ = 33.5 ppm. GCMS (m/z : Calc : 328.3 ; Exp : 328.3).

3.2CB: Protocol 3. Colorless oil (95% yield). ^{1}H NMR (C_6D_6, 500 MHz) δ = 1.32 (s, 12 H), 2.53 (s, 6H), 7.16 (m, 3H) ppm. ^{13}C NMR (C_6D_6, 125 MHz) δ = 22.9, 24.5, 85.1, 127.5, 127.9, 142.2 ppm. ^{11}B NMR ($CDCl_3$, 96 MHz) δ = 32.4 ppm. GCMS (m/z : Calc : 264.1 ; Exp : 264.1).

3.2CC: Protocol 3. Colorless oil (95% yield). ^{1}H NMR (C_6D_6, 500 MHz) δ = 0.88 (bt, J = 5 Hz, 3H), 1.26 (s, 16H), 1.38 (m, 4H), 1.58 (m, 3H), 1.74 (m, 4H), 1.80-1.95 (m, 7H) ppm. ^{13}C NMR (C_6D_6, 125 MHz) δ = 14.3, 22.9, 23.3, 26.6, 28.7, 28.9, 29.4, 29.6, 29.7, 29.8, 29.8, 29.9, 32.1, 32.6, 33.5, 33.9 ppm. ^{11}B NMR ($CDCl_3$, 96 MHz) δ = 77.7 ppm. GCMS (m/z : Calc : 322.3 ; Exp : 322.3).

3.2CD: Protocol 3. White solid (95% yield). ^{1}H NMR (C_6D_6, 500 MHz) δ = 1.39 (m, 2H), 1.62 (m, 2H), 1.70 (m, 2H) 1.89-1.94 (m, 8H), 2.41 (s, 6H), 7.13 (s, 3H) ppm. ^{13}C NMR (C_6D_6, 125 MHz) δ = 22.9, 23.1, 27.4, 29.7, 33.5, 34.0, 127.5, 128.0, 132.4, 141.1 ppm. ^{11}B NMR ($CDCl_3$, 96 MHz) δ = 77.7 ppm. GCMS (m/z : Calc : 258.2 ; Exp : 258.2).

3.6.6 X-ray Crystallographic Data

Table 1 Crystal data and structure refinement for 3.1FG.

Identification code	3.1FG
Empirical formula	$C_9H_{20}BNO_2$
Formula weight	185.07
Temperature/K	100.0
Crystal system	orthorhombic
Space group	Iba2
a/Å	10.1195(6)
b/Å	29.385(2)
c/Å	7.4892(4)
α/°	90
β/°	90
γ/°	90
Volume/Å^3	2227.0(2)
Z	8
ρ_{calc}g/cm^3	1.104
μ/mm^{-1}	0.074
F(000)	816.0
Crystal size/mm^3	0.2 × 0.1 × 0.01
Radiation	MoKα (λ = 0.71073)
2Θ range for data collection/°	2.772 to 56.246
Index ranges	-13 ≤ h ≤ 13, -37 ≤ k ≤ 38, -9 ≤ l ≤ 9
Reflections collected	8760
Independent reflections	2442 [R_{int} = 0.0709, R_{sigma} = 0.0791]
Data/restraints/parameters	2442/1/130
Goodness-of-fit on F^2	1.005
Final R indexes [I>=2σ (I)]	R_1 = 0.0495, wR_2 = 0.0905
Final R indexes [all data]	R_1 = 0.0893, wR_2 = 0.1063
Largest diff. peak/hole / e Å^{-3}	0.19/-0.21
Flack parameter	0.5

3.7 References

[1] Romero, E. A.; Jazzar, R.; Bertrand, G. "Copper-catalyzed dehydrogenative borylation of terminal alkynes with pinacolborane" *Chem. Sci.* **2017**, *8*, 165.

[2] Fernandez-Salas, J. A.; Manzini, S.; Nolan, S. P. "Efficient ruthenium-catalysed S-S, S-Si and S-B bond forming reactions" *Chem. Commun.* **2013**, *49*, 5829.

[3] Bolaño, T.; Esteruelas, M. A.; Gay, M. P.; Oñate, E.; Pastor, I. M.; Yus, M. "An Acyl-NHC Osmium Cooperative System: Coordination of Small Molecules and Heterolytic B–H and O–H Bond Activation" *Organometallics* **2015**, *34*, 3902.

[4] Harinath, A.; Anga, S.; Panda, T. K. "Alkali metal catalyzed dehydro-coupling of boranes and amines leading to the formation of a B-N bond" *RSC Adv.* **2016**, *6*, 35648.

[5] Liptrot, D. J.; Hill, M. S.; Mahon, M. F.; Wilson, A. S. S. "Alkaline-Earth-Catalyzed Dehydrocoupling of Amines and Boranes" *Angew. Chem. Int. Ed.* **2015**, *54*, 13362.

[6] Yang, Z.; Zhong, M.; Ma, X.; Nijesh, K.; De, S.; Parameswaran, P.; Roesky, H. W. "An Aluminum Dihydride Working as a Catalyst in Hydroboration and Dehydrocoupling" *J. Am. Chem. Soc.* **2016**, *138*, 2548.

[7] Shore, S. G.; Parry, R. W. *J. Am. Chem. Soc.* **1955**, *77*, 6084.

[8] For representative examples on hydrogen storage and release using ammonia borane, see: (a) Rossin, A.; Peruzzini, M. "Ammonia–Borane and Amine–Borane Dehydrogenation Mediated by Complex Metal Hydrides" *Chem. Rev.* **2016**, *116*, 8848. (b) Peng, B.; Chen, J. "Ammonia borane as an efficient and lightweight hydrogen storage medium" *Energy Environ. Sci.* **2008**, *1*, 479. (c) Bluhm, M. E.; Bradley, M. G.; Butterick III, R.; Kusari, U.; Sneddon, L. G. "Amineborane-Based Chemical Hydrogen Storage: Enhanced Ammonia Borane Dehydrogenation in Ionic Liquids" *J. Am. Chem. Soc.* **2006**, *128*, 7748. (d) Müller, K.; Stark, K.; Müller, B.; Arlt, W. "Amine Borane Based Hydrogen Carriers: An Evaluation" *Energy Fuels* **2012**, *26*, 3691. (e) Wang, J. S.; Geanangel, R. A. "^{11}B NMR studies of the thermal decomposition of ammonia-borane in solution" *Inorg. Chim. Acta* **1988**, *148*, 185. (f) Gutowska, A.; Li, L. Y.; Shin, Y. S.; Wang, C. M. M.; Li, X. H. S.; Linehan, J. C.; Smith, R. S.; Kay, B. D.; Schmid, B.; Shaw, W.; Gutowski, M.; Autrey, T. "Nanoscaffold Mediates Hydrogen Release and the Reactivity of Ammonia Borane" *Angew. Chem. Int. Ed.* **2005**, *44*, 3578. (g) Denney, M. C.; Pons, V.; Hebden, T. J.; Heinekey, D. M.; Goldberg, K. I. "Efficient Catalysis of Ammonia Borane Dehydrogenation" *J. Am. Chem. Soc.* **2006**, *128*, 12048. (h) Chen, Y. S.; Fulton, J. L.; Linehan, J. C.; Autry, T. "In Situ XAFS and NMR Study of Rhodium-Catalyzed Dehydrogenation of Dimethylamine Borane" *J. Am. Chem. Soc.* **2005**, *127*, 3254.

[9] Cragg, R. H.; Lappert, M. F.; Tilley, B. P. "Chloroboration and allied reactions of unsaturated compounds. Part III. Aminoboration and alkoxyboration of isocyanates and isothiocyanates" *J. Chem. Soc.* **1964**, 2108.

[10] Jefferson, R.; Lappert, M. F.; Prokai, B.; Tilley, B. P. "Chloroboration and allied reactions of unsaturated compounds. Part IV. Boration of di-p-tolylcarbodi-imide" *J. Chem. Soc. A* **1966**, 1584.

[11] (a) Suginome, M.; Uehlin, L.; Murakami, M. "Aminoboranes as "Compatible" Iminium Ion Generators in Aminative C−C Bond Formations" *J. Am. Chem. Soc.* **2004**, *126*, 13196. (b) Suginome, M. "Aminoboranes as new iminium ion generators in amination reactions" *Pure Appl. Chem.* **2006**, *78*, 1377. (c) Tanaka, Y.; Hasui, T.; Suginome, M. "Acid-Free, Aminoborane-Mediated Ugi-Type Reaction Leading to General Utilization of Secondary Amines" *Org. Lett.* **2007**, *9*, 4407.

[12] (a) Sole, C.; Fernández, E. "Alkoxide activation of aminoboranes towards selective amination" *Angew. Chem. Int. Ed*. **2013**, *52*, 11351. (b) Civit, M. G.; Sanz, X.; Vogels, C. M.; Bo, C.; Wescott, S. A.; Fernández, E. "Ynones Merge Activation/Conjugate Addition of Chalcogenoborates ArE-Bpin (E=Se, S)" *Adv. Synth. Catal*. **2015**, *357*, 3098.

[13] For select examples, see: (a) Luo, W.; Campbell, P. G.; Zakharov, L. N.; Liu, S. -Y. "A Single-Component Liquid-Phase Hydrogen Storage Material" *J. Am. Chem. Soc.* **2011**, *133*, 19326. (b) Jang, H.; Romiti, F; Torker, S.; Hoveyda, A. H. "Catalytic diastereo- and enantioselective additions of versatile allyl groups to N–H ketimines" *Nature Chemistry* **2017**, *9*, 1269. (c) Reetz, M. T.; Niemeyer, C. M.; Hermes, M.; Goddard, R. "Molecular Recognition of Primary Amines by Three-Point Binding with Boron-Containing Host Molecules" *Angew. Chem. Int. Ed.* **1992**, *31*, 1017. (d) Sieber, J. D.; Morken, J. P. "Sequential Pd-Catalyzed Asymmetric Allene Diboration/α-Aminoallylation" *J. Am. Chem. Soc.* **2006**, *128*, 74.

[14] Bordwell, F. G. "Equilibrium acidities in dimethyl sulfoxide solution" *Acc. Chem. Res.* **1988**, *21*, 456.

[15] (a) Bettinger H. F.; Filthaus M.; Bornemann H.; Oppel, I. M. "Metal-Free Conversion of Methane and Cycloalkanes to Amines and Amides Employing a Single Nitrogen Center" *Angew. Chem. Int. Ed.* **2008**, *47*, 4744. (b) Cui, Y.; Sato, T.; Yamashita, Y.; Kobayashi, S. "Catalytic Use of Zinc Amide for Transmetalation with Allylboronates: General and Efficient Catalytic Allylation of Carbonyl Compounds, Imines, and Hydrazones" *Adv. Synth. Catal.* **2013**, *355*, 1193.

[16] Herberich, G. E.; Fischer, A. "Borylcyclopentadienides" *Organometallics* **1996**, *15*, 58.

Chapter 4 : Conclusions

Copper-hydride complexes developed in 1844 by Wurtz have seen a significant rise to prominence through the dedication of many great scientists over the past 150 years. During this time, this transient species was stabilized by P- and C-based ancillary ligands and used in synthetic organic chemical reactions. In the introduction, we mused about the possibility of using copper-hydride complexes outside of their well-developed niche and were excited to uncover a C-H functionalization reaction that was well proven to proceed through a copper-hydride intermediate (Scheme 4.1). Interestingly, at first glance, nothing about the reaction conditions suggested the possible intermediacy of a LCu-H complex; however, due to the appearance of products determined decades earlier to be caused by Cu-H reactivity with alkynes, we discovered that its participation lied within the dihydrogen extrusion step.

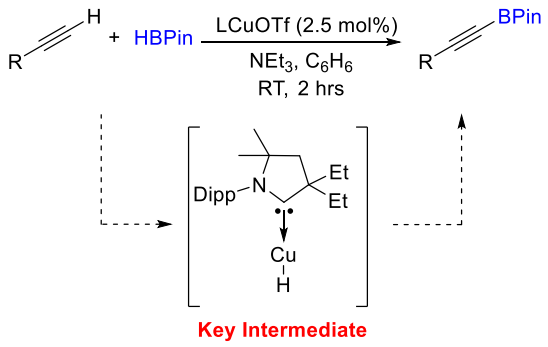

Scheme 4.1. Copper-catalyzed C-H borylation reaction that involves the transient formation of an LCu-H complex.

During our study, we noted the presence of the corresponding hydroboration product in trace quantities; however, we optimized the above catalyst system to selectively afford these β-hydroboration products of terminal alkynes with pinacolborane (Scheme 4.2). As with the DHBTA reaction, we used stoichiometric and catalytic reactions to provide evidence for a mechanism that is unique from others in the literature regarding similar reactions. Literature reported copper hydroboration is promoted by the insertion of a copper-hydride into the C-C multiple bond where

as we found convincing evidence that LCu-CCR complexes were key reaction intermediates as determined by kinetic ^{1}H NMR measurements.

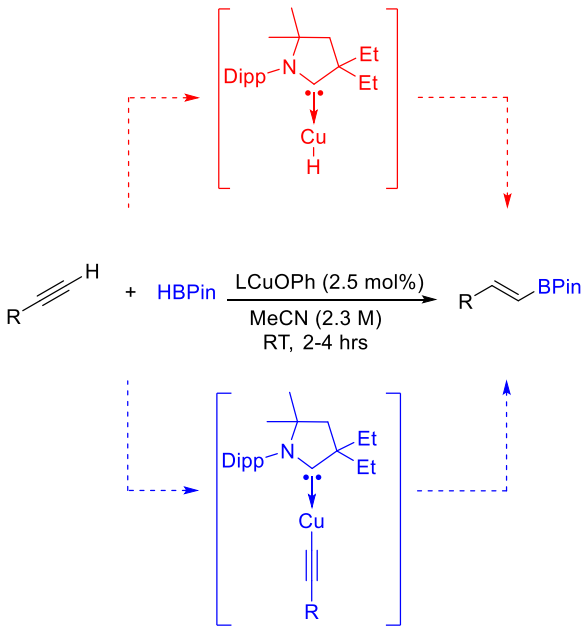

Scheme 4.2. The copper-catalyzed hydroboration reaction of terminal alkynes can proceed through two possible key intermediates: i) copper-hydride (top, red) and ii) copper-acetylide (blue, bottom).

Interestingly, recent results that will be published at a future date, strongly support our proposed mechanism for the DHBTA reaction, which includes the formation of a copper-hydride intermediate. Conversely, results of this study also indicate the unlikeliness of LCu-CCR being able to facilitate the hydroboration reaction (blue trace), and that a Cu-H mechanism is more likely (red trace). Further experiments are ongoing by the dissertation author and others in an effort to understand why kinetic measurements of LCu-CCR complexes mirror those obtained when using the established catalytic conditions.

Together, these results clearly exhibit the prevalence of copper-hydride complexes in organic transformations and highlight the fact that they can even be present when we would least expect them. To enhance our ability to predict what other reactions copper-hydrides could participate in, we set out to prepare and isolate the first monomeric monoligated copper-hydride

complex using NHCs as stabilizing entities. Although we were unsuccessful in isolating a true monomer in the solid state, as it exists in equilibrium with its dimer (Scheme 4.3, right), we found that we could see the ^{1}H NMR signals corresponding to the monomeric Cu-H fragment. This complex even features rearrangement reactivity that has never been observed for its dimeric counterpart, which further indicates that this monomeric copper-hydride can be used for new reaction discovery studies. Finally, we were able to take advantage of the knowledge we gained from this work and apply it to the preparation of the first neutral silver(I)-hydride (Scheme 4.3, left). This complex was found to be isolable as its corresponding monomer and does not seem inclined to dimerize. Furthermore, preliminary reactivity studies show that these Ag-H complexes better mirror the reactivity of their copper analogues as compared to their gold counterparts.

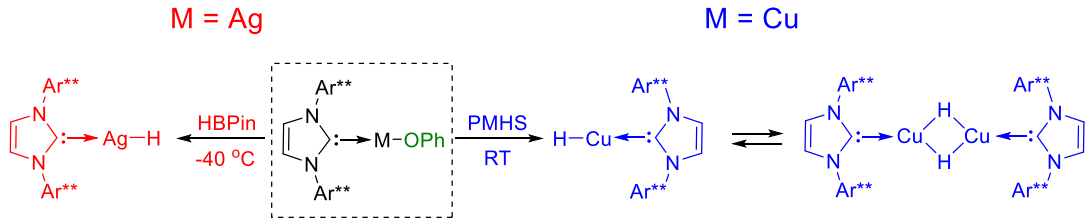

Scheme 4.3. Preparation of the first monomeric Cu-H complex, which exists in equilibrium with its dimer (blue). The only known neutral silver hydride complex (red).

In keeping with our initial direction of utilizing copper-hydrides in ways different from previous researchers, we set out to perform CO_2 hydrogenation with H_2 as the reductant. In our case, however, we sought to maximize the effect that our Cu-H catalyst could have by only asking it to perform what it's best at doing (*e.g.* sequestering CO_2 by Cu-H insertion). We hypothesized that utilizing the exceptional capabilities of FLPs to cleave H_2 would allow for the simple regeneration of the starting catalysts and extrude formic acid as its conjugate base. Even though FLPs fail to perform catalytically, we uncovered the ability of cLPs to function as exceptional

surrogates (Scheme 4.4). Using a combination of copper-hydrides and cLPs, we obtained significantly improved TONs as compared to those obtained for each system individually.

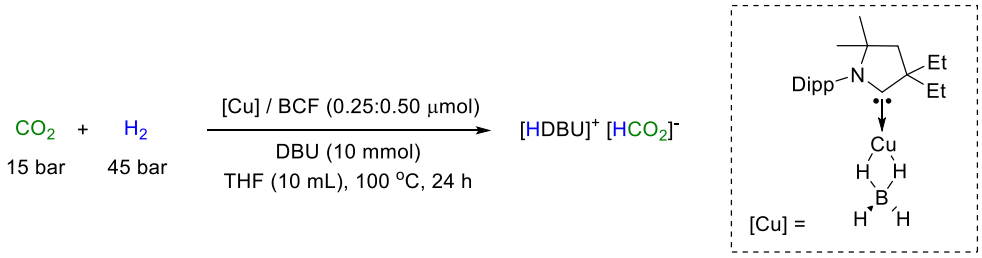

Scheme 4.4. General conditions for the tandem catalyzed hydrogenation of CO_2.

During this study, we were able to support our conclusion that each co-catalyst was performing only its own half of the reaction and that without the other half of the catalyst pair, the reaction fails to deliver significant TONs of product. It is important to stress that cLPs should not be overlooked in tandem catalytic processes since we have definitively shown that they can be successful even when their more popular competitors fail to perform. It will be interesting to see what other reactions can be improved by applying this type of tandem catalysis. It is my opinion that Haber-Bosh type ammonia production could be a suitable candidate for a future investigation into this topic using cLP co-catalysts.

In Chapter 3, we looked at a reaction that is simple on paper but is well misrepresented in the literature. This reaction, which couples alcohols, amines, and thiols with monohydridoboranes, proceeds by formation of a Lewis acid-base adduct and, after elimination of H_2, cleanly forms the dehydrocoupled products (Scheme 4.5). Interestingly, in marked contrast to other labs, we found that this reaction proceeds rapidly at room temperature with no catalyst necessary. We were even able to isolate the intermediary Lewis acid-base adduct in one case. Before our procedure was published, these compounds were difficult and low yielding to make, however, using this method, we can now begin to fully investigate the synthetic uses for these classes of compounds.

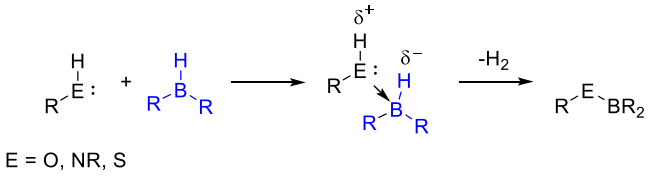

Scheme 4.5. Dehydrocoupling of alcohols, amines, and thiols with pinacolborane and 9-BBN. The reaction proceeds uncatalyzed at room temperature.

4.1 Future Directions

We began this dissertation with a discussion about some of the major developments surrounding the reactivity of copper(I)-hydride complexes over the past 150 years. During this analysis, I mentioned that scientists should begin considering reactivity studies that aren't tailormade to favor copper-hydride generation because it will allow us to expand the reach and utility of these reactive complexes beyond their current niche. To aid in this mission, we need to delve deeper into the fundamental reactivity profiles of true monomeric copper-hydride complexes. In Chapter 2 of this dissertation, we saw that copper-hydride monomers react in unprecedented ways that could be extrapolated to new catalytic transformations involving copper-hydride formation. This leads me into my final question for you: what will this next big copper(I)-hydride mediated reaction look like? It's my opinion that it is not an enantioselective variation of any reaction listed on the introductory table. No, I truly believe that the future of copper(I)-hydride chemistry lies in the utilization of basic Cu-H reactivity to perform reactions typically performed by expensive noble metals. For example, we know that low nuclearity Cu-H complexes contain significantly more reactive Cu-H bonds than their higher order oligomers. Using this knowledge, we should begin to investigate C-H functionalization reactions that proceed via deprotonation/metalation of the C-H bond to release dihydrogen. This reaction also lends itself to the development of extremely bulky chiral ligands to allow the elucidation of enantioselective

variations of these reactions. This constitutes just one example of a reaction that was deemed impossible for copper-hydrides to catalyze, but one that should be reinvestigated. By using the results in this dissertation as a new foundation, we can begin to rewrite the future of copper-hydride chemistry and show the world that cheap, abundant base metals can be noble too.